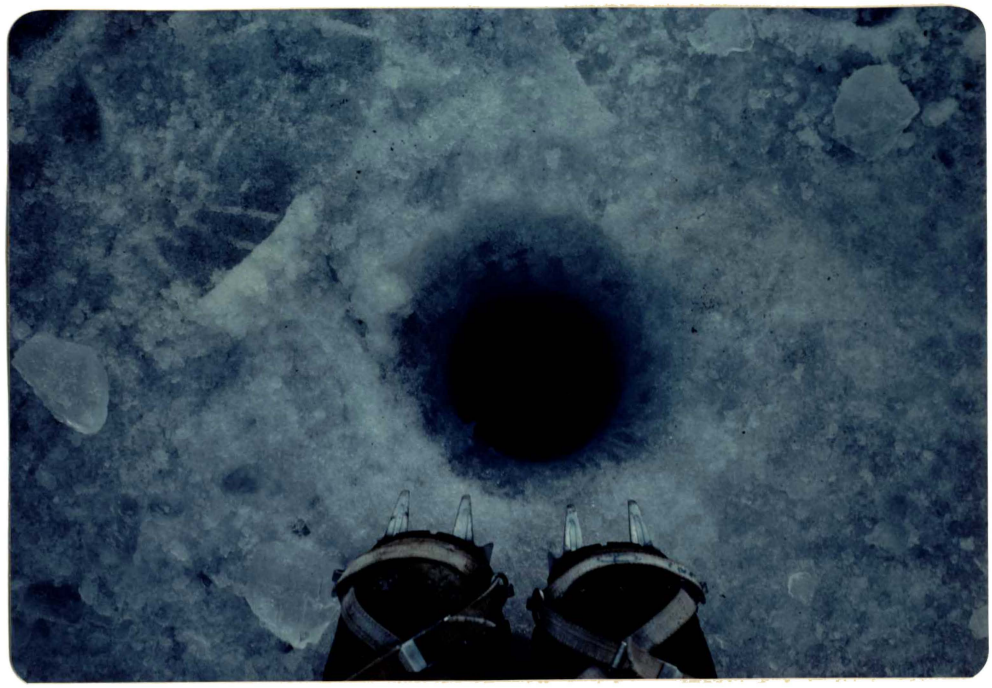

Frontispiece: Lake Fryxell icen gesamplehöllen
mit der gebootencrampons.

'Twixt the optimist and pessimist
The difference is droll:
The optimist sees the doughnut
But the pessimist sees the hole .....

(McLandburgh Wilson, 1915)

ORIGIN AND OCCURRENCE OF ANTARCTIC LACUSTRINE CARBONATES, WITH SPECIAL REFERENCE TO LAKE FRYXELL, TAYLOR VALLEY

A thesis

submitted in partial fulfilment

of the requirements for the degree

of

Master of Science in Earth Sciences

with a thesis in Chemistry

at the

University of Waikato

by

MARK JOHN FREDERICK LAWRENCE

University of Waikato

1982

ABSTRACT

Lake Fryxell is a permanently ice-covered 19 m deep lake located 15m a.s.l. in the lower Taylor Valley, Antarctica (75° 35'S, 163° 35'E). The lake occupies the lowest part of the Fryxell drainage basin and is surrounded by glacial tills with associated lacustrine carbonate and algal material of about Ross Sea I age. Lake Fryxell is a mesothermal, stratified, amictic lake with a euphotic (aerobic) zone above 10 m depth and an anaerobic (anoxic) zone below. The lake waters were derived from glacial meltwater into which upward diffusion of salts deposited in the basin or remnant brines occurred creating a gradient in density, which results in a physically stable lake. The so formed diffusion cell gave an estimated age of about 1000 years. Analysis of both lake water and lake bottom sediment cores show precipitation of $CaCO_3$ to have occurred both in the past and the present. Current carbonate precipitation is a biologically induced process occurring in the euphotic zone lake waters. Over deep waters, precipitated carbonates, in this case calcite, fall from suspension through the water column and form flakes on the lake bed. Where the lake bed is within the euphotic zone stromatolites occur. Dissolution processes predominate in Lake Fryxell bottom waters and account for the discontinuous carbonate record in the uppermost lithologic unit (unit E) of Lake Fryxell sediments. At the time of the Ross Sea I advance a calcareous mud (unit B) was deposited on top of fluvial-glacial sediments. The mud, a mixed calcite-aragonite deposit of up to 20 wt% $CaCO_3$ is C^{14} dated at about 20,000 yrs B.P., was deposited in a deep pro-glacial Lake Washburn. At this time the Ross Sea Ice occupied part of the Fryxell basin damming the lower Taylor Valley and supplying the lake with meltwater. In this ancient lake precipitation occurred in a similar manner to present Lake Fryxell except that aragonite was precipitated. Post-depositional change in the form of the

aragonite/calcite transformation caused the observed dual mineralogy. Retreat of the ice sheet caused the deposition of transitional unit C and an evaporite deposit (unit D). Unit D is a varve-like aragonite ∿10,000 years old, deposited in a lake of much reduced volume. The ice retreat from the drainage basin meant that the lake had an increased ablation surface enabling evaporation to exceed lake inputs resulting in brine concentration and subsequent precipitation of aragonite. Comparison of the Lake Fryxell carbonates with those of the Marshall Valley indicates that the Lake Fryxell depositional model, particularly evaporitic unit D, can adequately explain other Dry Valley carbonate deposits.

This thesis is dedicated to my parents
for their assistance, encouragement
and understanding.

ACKNOWLEDGEMENTS

I wish to express appreciation for the hospitality and assistance received from the staff of Scott Base, and help from the helicopter pilots of VXE-6 squadron, U.S. Navy.

I wish to thank my supervisors; Dr C.H. Hendy for assistance and advice in the field and laboratory and the provision of the Marshall Valley data, Dr C.S. Nelson for useful discussion of the manuscript, and Dr A.P.W. Hodder for his advice and proof reading the manuscript.

Thanks are extended to my colleagues in the field for their assistance, advice and encouragement: Dr T.G.A. Green, Dr C.G. Harfoot, Nev Rodgers, and Colin Rickard from Waikato University, and Dr W.F. Vincent from D.S.I.R., Ecology Division, Taupo. The assistance from Mr D. Rees from D.S.I.R., in collecting the cores is much appreciated. Mention must also be made of the ubiquitous skua whose capacity to devour food scraps, including sledge biscuits, whole chop bones, and one family block of cheese, alleviated a number of waste disposal problems.

The efforts of technical staff in various departments is much appreciated. Thanks go to Mike Vennard, Peter Codlin and Alan Brennan for putting up with continual harassment for bits of equipment. I wish to thank Allison Thomas for assistance in removing some of the tedium from A.A. work, and Wendy Schick for running the mass spectrometer. Frank Bailey receives due thanks for some of the draughting, as does Rex Julian for producing some of the photographs. Elaine Norton is thanked for her perserverance in producing an excellent typescript.

I wish to thank Dr C. Beltz for the S.E.M. work and Dr A.G. Hogg for ^{14}C dates. Dr R.A. Littler is acknowledged for his advice on the use of statistics. Mr T.J.H. Chinn from M.O.W.D., Christchurch, is

thanked for making the lake level data available. Mr K. Thompson and Sue Green are thanked for providing their stream analyses, as are George Denton and Mark Dragel, from the University of Maine for providing the Marshall Valley sections.

Mention must also be made of my fellow inmates in Ward E2.11 who did their best/worst to stave off/accelerate the incidious effects of incipient pseudo-insanity with the aid of rubber bungs, cries/screams of dispair, the sound of breaking glass/nerves, silly ethnic jokes, and the reassurance that one day I may know what reality is really like. The inmates include Nick "5 teabags per cup" Willet, the Rt. Hon. Ian Cameron of rubber bung fame; plus two escapees, Andrew "my brain hurts" Todd and Tony Phipps who spent most of his time on the lunatic fringe. Last, but by no means least, I thank my special friend Penny for her encouragement during construction of this work.

TABLE OF CONTENTS

LIST OF FIGURES

LIST OF TABLES

CHAPTER ONE

INTRODUCTION

1.1 AREA OF STUDY

This study deals primarily with Lake Fryxell and its deposits. Lake Fryxell is one of the lakes in the Taylor Valley, Dry Valleys, Antarctica (75^{o} 35'S, 163^{o} 35'E) (Fig. 1.1). In the Taylor Valley there are 4 major drainage basins, each containing permanently ice-covered lakes. These basins are the Pearce Valley, containing Lakes House and Joyce; the Bonney Basin, containing Lake Bonney and the Taylor Glacier terminus; the Hoare Basin, containing Lakes Chad and Hoare; and the Fryxell Basin, containing Lake Fryxell. The 230 km^2 Fryxell Drainage basin occupies the lower end of the Taylor Valley. Lake Fryxell lies between the Canada and Commonwealth Glaciers in the lowest portion of the basin, the surface of the lake being 15 m above sea level, and the lake bottom 4 m below sea level.

1.2 PREVIOUS WORK

The Taylor Valley was discovered by Scott in 1903 (Scott, 1905), and is probably the most visited part of the ice-free Dry Valleys (Murrell 1973). Scott recorded the presence of frozen lakes and glacial deposits. During the 1910-1913 *Terra Nova* Expedition the valley was visited by Taylor who briefly described the physiography and some of the geology (Taylor 1922).

Basement geology of the upper Taylor valley was later described by McKelvey and Webb (1959), and the lower Taylor Valley by Angino *et al.* (1962a). Haskell *et al.* (1965) described the lower and middle Taylor Valley geology (Section 2.1).

The first major description and correlation of glacial deposits was

Figure 1.1 Locality map for the Taylor Valley and Lake Fryxell. Other lakes and drainage basins are also shown. Str (east of the Commonwealth Glacier) = Commonwealth Stream.

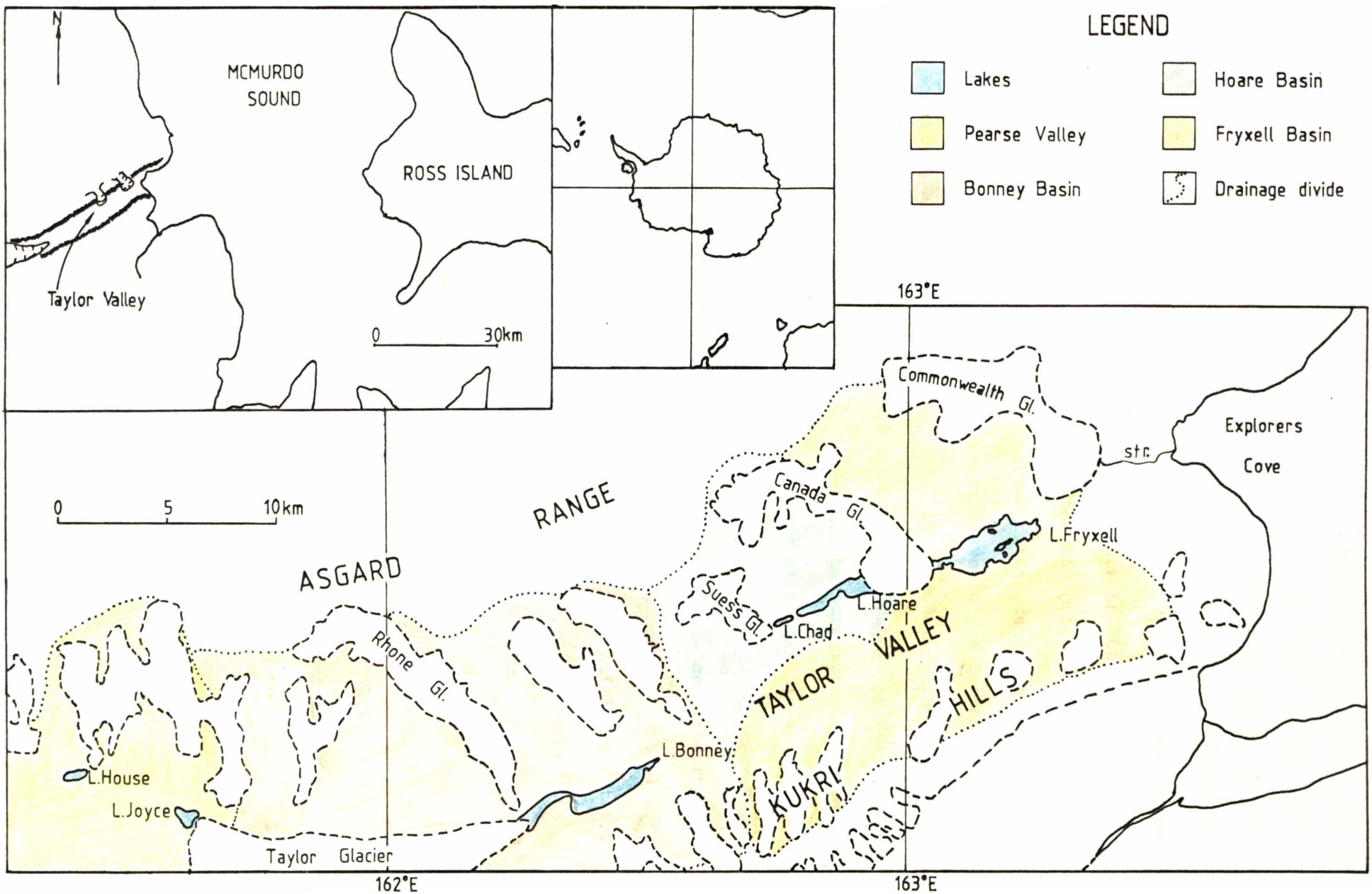
N
MCMURDO
SOUND
ROSS ISLAND
Taylor Valley
0 30km
LEGEND
Lakes
Pearse Valley
Bonney Basin
Hoare Basin
Fryxell Basin
Drainage divide
163°E
Commonwealth Gl.
str.
Explorers
Cove
0 5 10km
RANGE
ASGARD
Canada Gl.
L.Fryxell
Suess Gl.
L.Hoare
L.Chad
VALLEY
Rhone Gl.
TAYLOR
HILLS
L.Bonney
L.House
L.Joyce
KUKRI
Taylor Glacier
162°E
163°E

by Péwé (1960). This work attempted to correlate McMurdo Sound deposits, including those in the Taylor Valley, to produce an Antarctic glacial chronology. Comparisons were made between the then known New Zealand and North American glacial chronologies. Armstrong *et al.* (1968) produced evidence for Taylor Valley glaciations older than 2.7 myr. B.P. Denton *et al.* (1970, 1971) then produced from evidence in the Taylor and other valleys an overview of glacial events during the Quaternary (Section 2.1). This revised the work of Péwé and introduced the idea of non-synchronous Taylor Glacier and Ross Sea Ice advances. As evidence Denton *et al.* used the stratigraphic relations of the tills, interbedded volcanic deposits and lacustrine materials (algae and carbonates) included in tills. Subsequently Murrell (1973) attempted to detail the stratigraphy of Cenozoic deposits in the Lower Taylor Valley. Further stratigraphic work resulted from the DVDP programme (Chapman-Smith and Luckman, 1974; Chapman-Smith, 1975; McKelvey, 1976). By dating lacustrine carbonate deposits in tills, Hendy *et al.* (1979) revised the Taylor Glacial advance sequence of Denton *et al.* (1970, 1971). The most recent work on the glacial deposits is that of Stuiver *et al.* (1981). This is a detailed description of the last Ross Sea Ice advance and its deposits throughout the McMurdo Sound area (Section 2.1).

Microfaunal studies on Taylor Valley DVDP cores indicates the valley transformed from a deep marine fjord in the Miocene and early Pliocene to a terrestrial environment (Webb and Wren, 1976). Diatoms in perched deltas indicate the absence of seawater from the valley during the Ross Sea I advance (Kellog *et al.*, 1980).

Soils of the Taylor Valley region, as well as surface features have been described by McCraw (1962, 1967a, 1967b). Clay minerals were described by Claridge (1965). Most of the clays found were micas with some chlorite and vermiculite. Field (1975) studied the salts in saline dis-

charges and groundwaters in both the Taylor and Wright Valleys. Claridge and Campbell (1977) determined the distribution of salts in soils and their relationship to soil processes. Origins of these salts were discussed by Claridge and Campbell (1977) and also by Keys and Williams (1981) (Section 3.4.2). Jones and Faure (1978) studied Sr isotopes of Dry Valley lakes and soluble salts. They found that the $^{87}Sr/^{86}Sr$ ratio for Lake Fryxell waters is identical to seawater, and concluded that the $^{87}Sr/^{86}Sr$ ratios are representative of rocks underlying the basin. Thus the ratios in precipitated non-marine carbonates reflect changes in the geology of the drainage basin.

Much has been written about the saline lakes of the Dry Valleys (Burton 1981). General articles which include descriptions of Lake Fryxell are: Wilson (1967, 1970, 1981), and reviews by Burton (1981), and Heywood (1972, 1977 [cited Burton 1981]).

Work on the physical properties of Lake Fryxell show the relationship between the temperature profile and incident solar radiation (Hoare *et al.*, 1965; House *et al.*, 1966). Ablation rate studies on Lake Fryxell (Henderson *et al.*, 1966) were used to calculate ice budgets for the nearby Canada and Commonwealth Glaciers. Regular lake level recordings are made by the Ministry of Works, Water and Soil Conservation Organisation, e.g. Anderton and Fenwick, 1976.

The first detailed description of the chemistry of Lake Fryxell waters was by Angino *et al.* (1962b). They attempted to determine the origin of the solutes and lake stratification but could only conclude that no single origin exists. Further studies of the chemistry of Dry Valley lakes including Lake Fryxell followed (Boswell *et al.*, 1967a, 1967b; Yamagata *et al.*, 1967; Yoshida *et al.*, 1975; Torii *et al.*, 1975; Torii and Yamagata 1981). Much of this work is descriptive, though Boswell *et al.* (1967a, 1967b) suggest that Lake Fryxell may have once contained

seawater. Torii *et al.* (1975) paid particular attention to nutrient elements and Torii and Yamagata (1981) concentrated more on the origins and evolution of waters in the lakes. Hendy (in prep.) briefly describes the chemical characteristics of the lakes, including Fryxell, plus the glacial chronologic implications of the lakes deposits.

Until recently there have been few biological studies on Lake Fryxell. An outline of primary productivity in Antarctic lakes was carried out by Goldman (1964; cited Burton 1981). Wilson (1965) showed the mechanism by which algae can escape from lakes. The recent studies which include Lake Fryxell concentrate predominantly on algae (Seaburg *et al.*, 1981; Parker and Simmons, 1981; Parker *et al.*, 1981; Vincent, 1981; Wharton *et al.*, 1982). Vincent (1981) dealt with algal production strategies in the Lake Fryxell euphotic zone. Seaburg *et al.*, (1981) investigated growth responses of algae and found that of the 35 taxa studied only 4 were obligately cold adapted. Parker and Simmons, (1981), Parker *et al.*, (1981), and Wharton *et al.*, (1982) investigated the existence of stromatolites (Section 3.6).

1.3 AIMS AND OBJECTIVES

The present state of knowledge on Lake Fryxell consists of information about its chemical, physical and some of its biological characteristics. Glacial chronology of the area depends on the dating of materials such as algal mats and calcium carbonate horizons which are recognized to be of lacustrine origin. Therefore the aim of this study is to determine the relationship between the lake water characteristics and the carbonate deposits in Lake Fryxell. A depositional model is developed and used to explain similar carbonates in other Dry Valleys.

CHAPTER TWO

PHYSICAL CHARACTERISTICS OF THE LAKE FRYXELL BASIN AND SURROUNDING AREA

2.1 GEOLOGY AND SOILS

In the Lake Fryxell area the basement rocks of the valley floors are mantled by glacial debris. Bedrock exposures occur only in valley walls (Fig. 2.1). The northern valley wall is formed in the Larsen Granodiorite with an Irizar Granite intrusive, both of pre-Cambrian to early Palaeozoic age (Haskell *et al.*, 1965). The southern valley wall includes similar rocks as well as some schist and marble of the Skelton Group. The diorites are described as coarsely foliated, consisting of mainly oligoclase, orthoclase and quartz. Biotite is the dominant ferromagnesium mineral and is commonly altered to chlorite. Accessory minerals are magnetite, allanite, sphene and apatite. The Irizar Granite (Fig. 2.1) is a medium to coarse grained, pink porphyritic rock containing perthite, oligoclase and quartz along with some microcline-microperthite, orthoclase, hornblende and biotite. Accessory minerals are apatite and magnetite. Intrusive dyke complexes in the region are of early Paleozoic age (Haskell *et al.*, 1965). Angino *et al.*, (1962) suggest that a major strike-slip fault follows the axis of the valley and that movement along the fault has been of the order of several kilometres, possibly in the Tertiary or even Pleistocene. This faulting apparently focussed the glacial movement which created the valley. However the presence of Miocene glacial marine sediments within the valley suggests such movement would have been at least Oligocene in age.

The glacial sediments lying unconformably on the Paleozoic rocks record a number of ice advances and recessions during the late Cenozoic

LEGEND

PHYSIOGRAPHIC FEATURES

- Ice-showing flow direction
- Ross Sea
- Lakes
- Paleo-lake strandlines

GEOLOGY

- Ross Sea I Drift
- Alpine Moraine
- Overridden Moraine
- Pre-Ross Sea I Drift

Quaternary

Tertiary-Quaternary

- Dykes-undifferentiated

Silurian

- Irizar Granite
- Theseus Granodiorite
- Larsen Granodiorite
- Olympus Granite Gneiss

Ordovician

- Skelton Group

PreCambrian-Cambrian

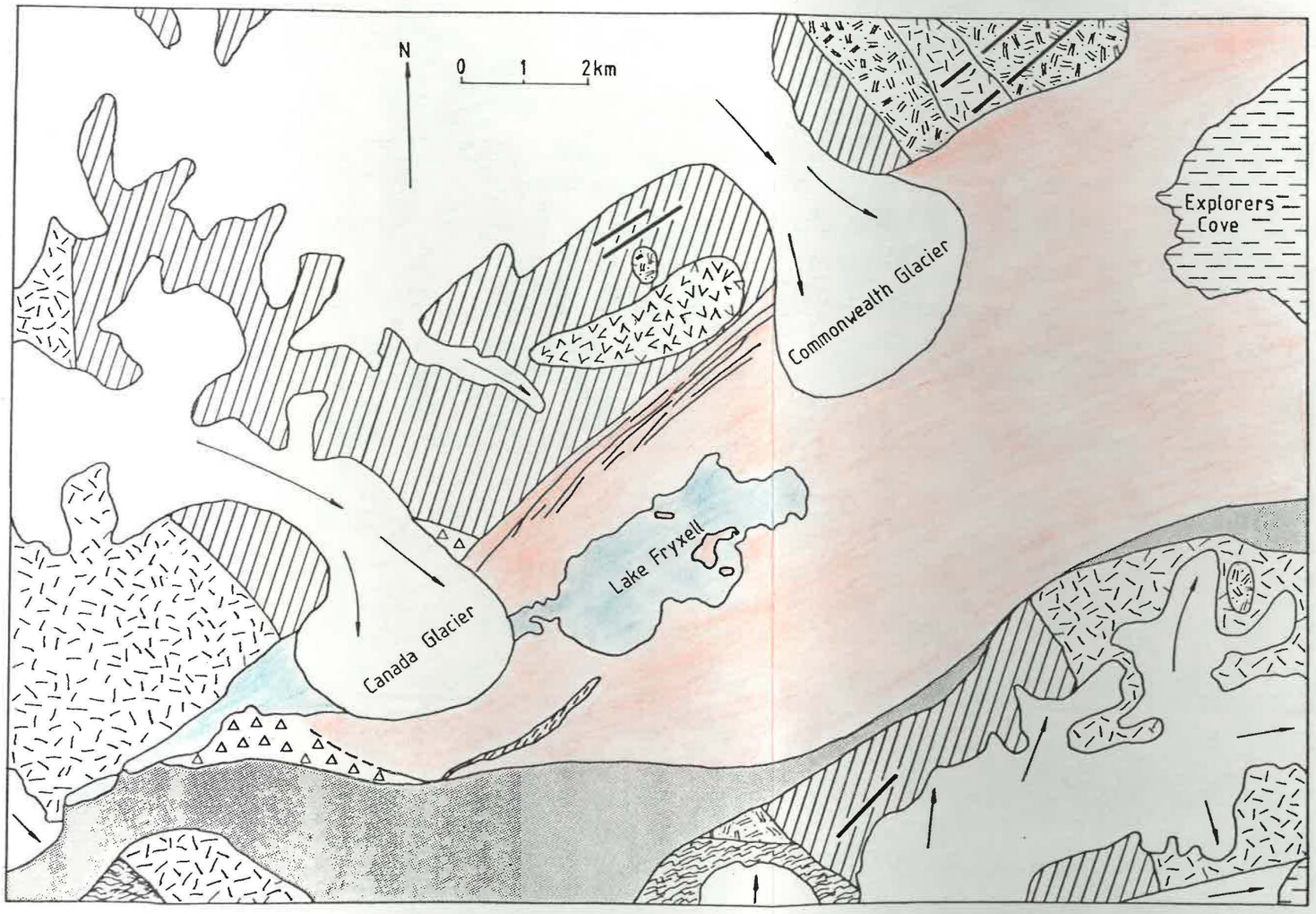

Figure 2.1 Geology of the lower Taylor Valley (From Haskell *et al.*, 1965; Stuiver *et al.*, 1981).

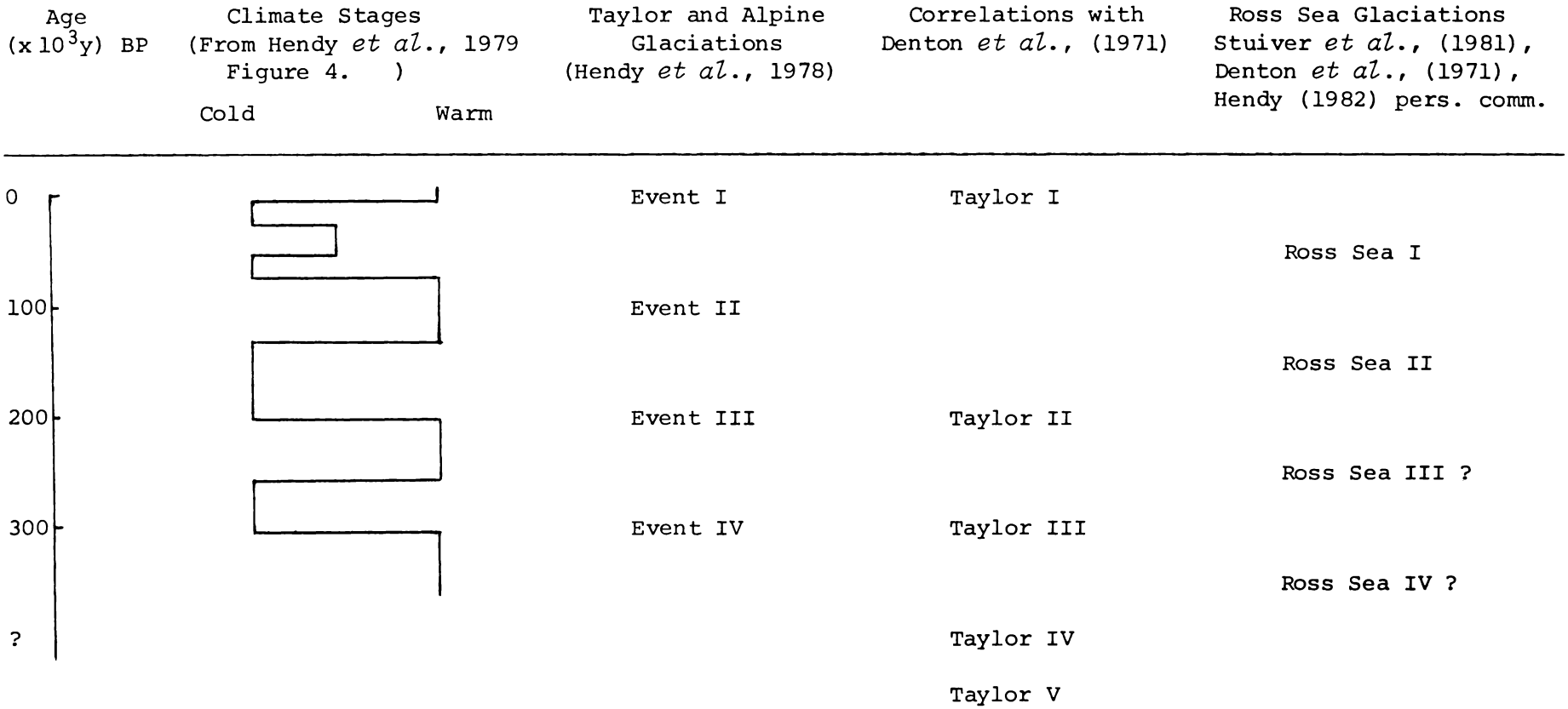

Figure 2.2 Nomogram of ice advances in the Taylor Valley and their chronological relationship to each other and climatic stages. (Modified from Hendy *et al.*, 1979).

(Fig. 2.2). In the Upper Taylor Valley at least 5 advances of the Taylor Glacier occurred, each of successively lesser extent (Denton *et al.*, 1971). Lava flows between the Taylor V and IV advances have ages of 3.5 - 2.7 m.y. BP. Taylor IV and the next advance, Taylor III, are separated by flows dated from 2.1 - 1.6 m.y. BP (Denton *et al.*, 1971). Subsequent work by Hendy *et al.* (1979) dated events which correspond to Taylor III (Denton *et al.*, 1971). The age of this deposit is 300,000 ± 20,000 yrs BP and is derived from dating lake deposits interbedded with till of apparent Taylor III age. Event III (Taylor II; Denton *et al.*, 1971) is marked by higher lake levels and is dated at 210,000 - 190,000 yrs BP. The Taylor I glaciation is the present Taylor glacial situation (Denton *et al.*, 1971) and corresponds to Event I of Hendy *et al.*, (1979). Between the Taylor I and II advances Hendy *et al.*, (1979) have dated deposits of a restricted Taylor advance at 90,000 yrs BP. Both Hendy *et al.*, (1979) and Denton *et al.*, (1971), suggest alpine glaciations were synchronous with Taylor glaciations.

From the seaward end of the valley at least 4 incursions of Ross Sea ice occurred (Denton *et al.*, 1971a). No firm dates for the Ross Sea III and IV are available. The age of the second to last advance (Ross Sea II) is approximately 180,000 - 130,000 yrs BP (Hendy pers. comm., 1982). The last Ross Sea advance, Ross Sea I, is the most important, and therefore will be described in more detail.

The Ross Sea I drift covers most of the floor of the lower Taylor Valley (Stuiver *et al.*, 1981) and surrounds the Lake Fryxell drainage basin (Fig. 2.1). The ice advance dammed the lower end of the valley, forming a large proglacial lake, "Glacial Lake Washburn" (Péwé, 1960). Subglacial meltwater plus some meltwater from the top of the ice sheet filled the lake, resulting in a high lake level (Fig. 2.3). Algal material deposited in the lake during the maximum extent of this advance

ranges in age from 21,200 to 17,000 yrs BP (Stuiver *et al.*, 1981). Stuiver *et al.* infer a rapid lake level drop after 17,000 yrs. Ice recession and minor readvances caused fluctuating levels until about 12,000 - 9200 yrs BP (Fig. 2.3) (Stuiver *et al.*, 1981). The latter date probably marks the last occupation of the valley by Ross Sea.

The Ross Sea I Drift is characterized by "numerous minor moraines and well preserved segments of lateral moraine" (Stuiver *et al.*, 1981). Pre-Ross Sea I tills have more subdued relief and lack minor moraines. Valley floor exposures of the Ross Sea Drift show stratified sediments and dropstones. Kenyte erratics are common (Stuiver *et al.*, 1981). Exposures in the bank of the Commonwealth Stream (Fig. 1.1) show several till units. The western limit of the Ross Sea I Drift extends beneath the present Canada Glacier and some adjacent alpine moraines (Fig. 2.1) Some alpine moraines were overrun near this glacier however (Stuiver *et al.*, 1981).

Soils developed on the glacial deposits have little clay and little variation in colour and texture (Stuiver *et al.*, 1981; McCraw, 1967b). Textures are gravelly sand or less commonly gravelly loamy sand (Stuiver *et al.*, 1981). In the Lake Fryxell area calcium carbonate or gypsum accumulation zones occur as either horizons or surface crusts (McCraw, 1962, 1967b). Salt effloresences also occur (Field, 1975; Keys and Williams, 1981). Topsoils around Lake Fryxell are slightly cemented, possibly by calcium carbonates or other salts, and have a strongly developed, fine platy structure. The subsoils consist of spherical or slightly elongated pellets of sandy silt (McCraw, 1967b). The platy structure of the topsoils is a function of wetting and drying and the spherical structure of the subsoils is a freeze-and-thaw phenomenon (McCraw, 1967b).

Figure 2.3 Lake level curve of glacial lake Washburn in the Lake Fryxell area derived from ^{14}C-dated algal material in deltas and tills (From Stuiver *et al.* 1981). The curve shows the major lake level build-up at about 20,000 yrs. B.P., and major lake level drops after 17,000 yrs. B.P. and again after 11,000 yrs. B.P.

LF = Lake Fryxell
LB = Lake Bonney
TE = Basin divide near Explorers cove (Fig. 1.1)
TS = Basin divide between the Hoare and Bonney Basins (Fig. 1.1)
US = Uppermost lacustrine strandlines near the Rhône and Canada glaciers.

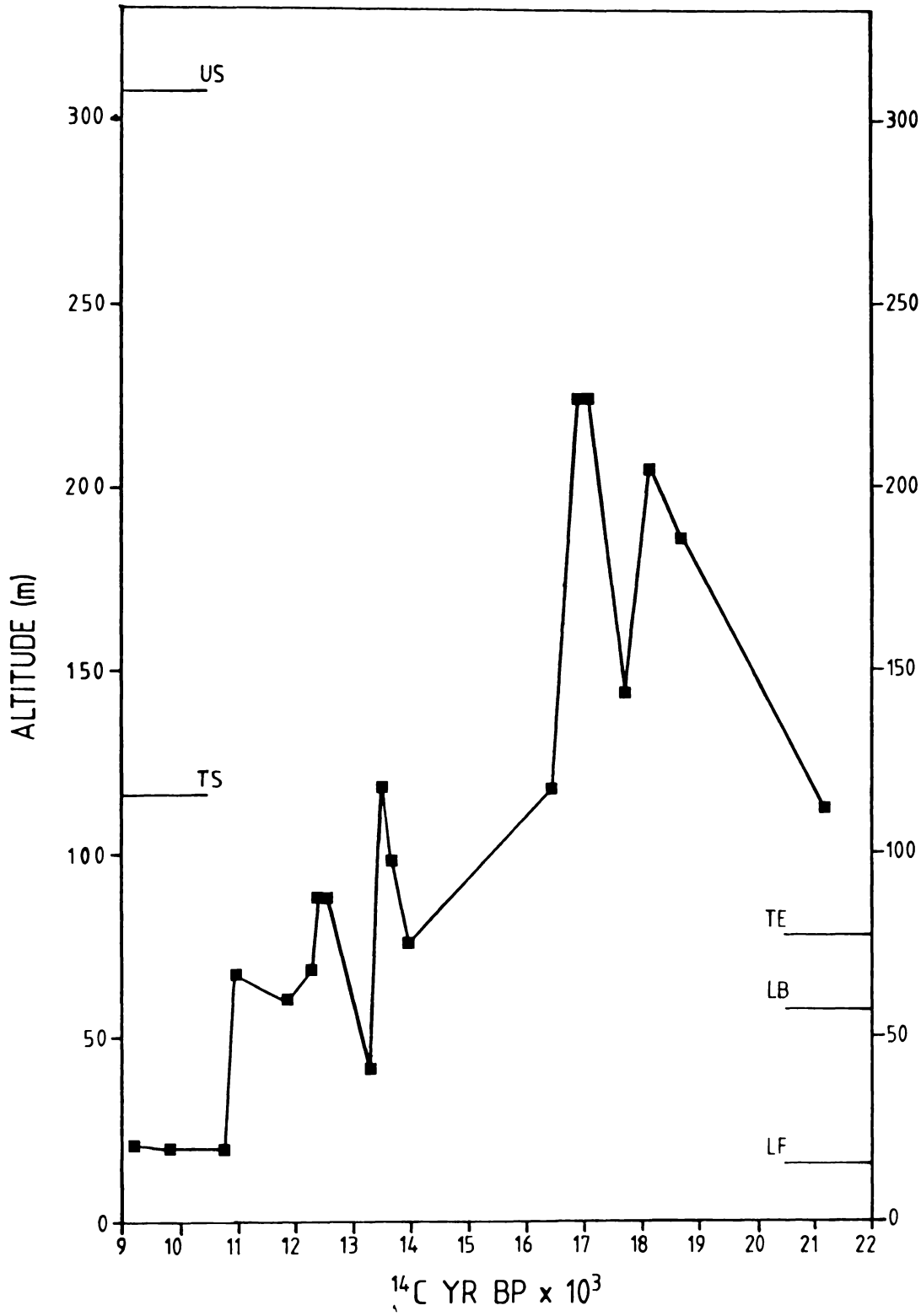
US
TS
TE
LB
LF
300
250
200
150
100
50
0
ALTITUDE (m)
9
10
11
12
13
14
15
16
17
18
19
20
21
22
^{14}C YR BP x 10^3

2.2 PHYSIOGRAPHY

The lower valley topography consists of tills, eskers, moraines, fans and perched deltas which have been modified by frost action, wind riving and in some cases water flow (Fig. 2.4). Older surfaces have more subdued relief and lateral moraines which slope down into the Taylor Valley. The Ross Sea I Drift has a complex system of eskers and minor moraines. Eskers range in length from 2000 - 200 m and are 1 - 5 m high; they are either bifurcate, continuous, or beaded (Stuiver *et al.*, 1981). The material is often mantled with cobble and boulder erratics some of which are striated and some display incipient cavernous weathering (Stuiver *et al.*, 1981). Cryogenic processes have left their imprint on these deposits in the form of patterned ground.

Meltwater streams from alpine glaciers have been able to cut down into the tills to some extent. Along the stream beds are arcuate deltas built up where meltwaters entered former lakes. The deltas and associated strandlines mark old lake levels (Fig. 2.4) and can be observed on both sides of the valley. In some cases river terraces are also present. The dating of algal mats buried within the deltas has provided much of the evidence for the Ross Sea I ice shelf chronology (Section 2.1).

2.3 CLIMATE

No long-term climate records are available for the Lake Fryxell area. However, regular meteorological readings were taken by the University of Waikato Antarctic Research Unit at Lake Fryxell during the summers of 1979/80, 1980/81. Results are summarized in Table 2.1.

For the 1979/80 data were recorded from 12/11/79 to 13/1/80. Three readings per day were taken: morning readings included all the parameters in Table 2.1, midday and evening readings included temperature at observation time, wind speed and direction, and cloud cover. A gap in

Figure 2.4 View looking sourth across the lower Taylor Valley. Lake Fryxell is in the middle distance. The deposits surrounding the lake are Ross Sea tills. Note the old strandlines on the valley walls and deltas along stream beds. Photo - C.H. Hendy.

Table 2.1 Summary of Lake Fryxell climatological data.

TABLE 2.1

	November 1979	December 1979	January 1980	1980/81
TEMPERATURE AT OBS. TIME (°C)				
Nos. observations	49	84	30	104
Mean	-3.6	-1.0	-0.4	-2.7
Std. Dev.	2.9	2.1	2.5	4.1
Highest temperature	+2.5 (30/11/79)	+2.7 (29/12/79)	+4.5 (5/1/80)	+5.5 (31/12/80)
Lowest temperature	-10.2 (14/11/79)	-5.6 (30/12/79)	-6 5 (11/1/80)	-12.7 (16/11/80)
DAILY MINIMUM (°C)				
Nos. observations	18	32	13	60
Mean	-8.1	-4.9	-4.2	-5.4
Std. Dev.	3.0	2.0	2.0	3.7
Extreme minimum	-13.6 (14/11/79)	-10.0 (16/12/79)	-7.2 (1/1/80)	-14.7 (16/11/80)
DAILY MAXIMUM (°C)				
Nos. observations	19	21	13	59
Mean	-0.6	+2.5	2.1	+0.5
Std. Dev.	3.0	1.8	2.3	4.1
Extreme maximum	+3.8 (30/11/79)	+6.0 (13/12/79)	+6.9 (6/1/80)	+6.8 (31/12/80)
MEAN				
T = ½ (mean max. + mean min.) (°C)	-2.2	-1.2	-2.6	-2.5
WIND				
Nos. observations	48	82	31	107
Easterly	34	75	30	95
Westerly	9	5	0	7
Calm	5	2	1	5
Mean velocity (knots)	8.6	6.2	42	-
Max. velocity (") (Direction)	35 (E)	21 (W)	10 (E)	25 (W)
CLOUD COVER				
Nos. observations	40	83	28	107
Clear	11	18	14	20
1/8 - 4/8	23	24	7	34
5/8 - 7/8	10	25	5	27
Overcast	4	16	2	26
SNOWFALL	1 light snowfall	2 light snowfalls 1 cm snowfall (19/12/79)	-	8 light snowfalls 1 accumulation 2 cm.

the maximum temperature record occurs from the 13/12/79 owing to a broken thermometer which took 11 days to replace. The summary for 1980/81 was supplied by the N.Z. Meteorological Service, for which only 2 readings per day were taken.

On some occasions small-scale circulation occurred when down-valley winds displaced the predominant easterlies. Generally the area experienced low precipitation, low humidity, and relatively low mean cloud cover.

2.4 BATHYMETRIC AND HYDROLOGIC CHARACTERISTICS

The lake bathymetry is shown in Fig. 2.5. Morphometric data are listed in Table 2.2.

Table 2.2 Some morphometric characteristics of Lake Fryxell

Maximum depth	18.2 m
Maximum length (L)	5570 m
Width	2000 m
Mean width ($^{A}/_{L}$)	1268 m
Surface area (A)	7.06 km^2
Lake volume	47 x 10^6 m^3

Lake Fryxell is typical of most Dry Valley lakes. It has a permanent ice cover and is thermally and chemically stratified. The lake lies within an enclosed drainage basin which is separated from the sea by an eroded ridge of Miocene and Pliocene glacial marine sediments. The western end of the lake is occupied by the Canada Glacier (Fig. 2.5) which also dams nearby Lake Hoare (Fig. 1.1), thus preventing flow into the Fryxell basin from meltwaters further to the west. The only

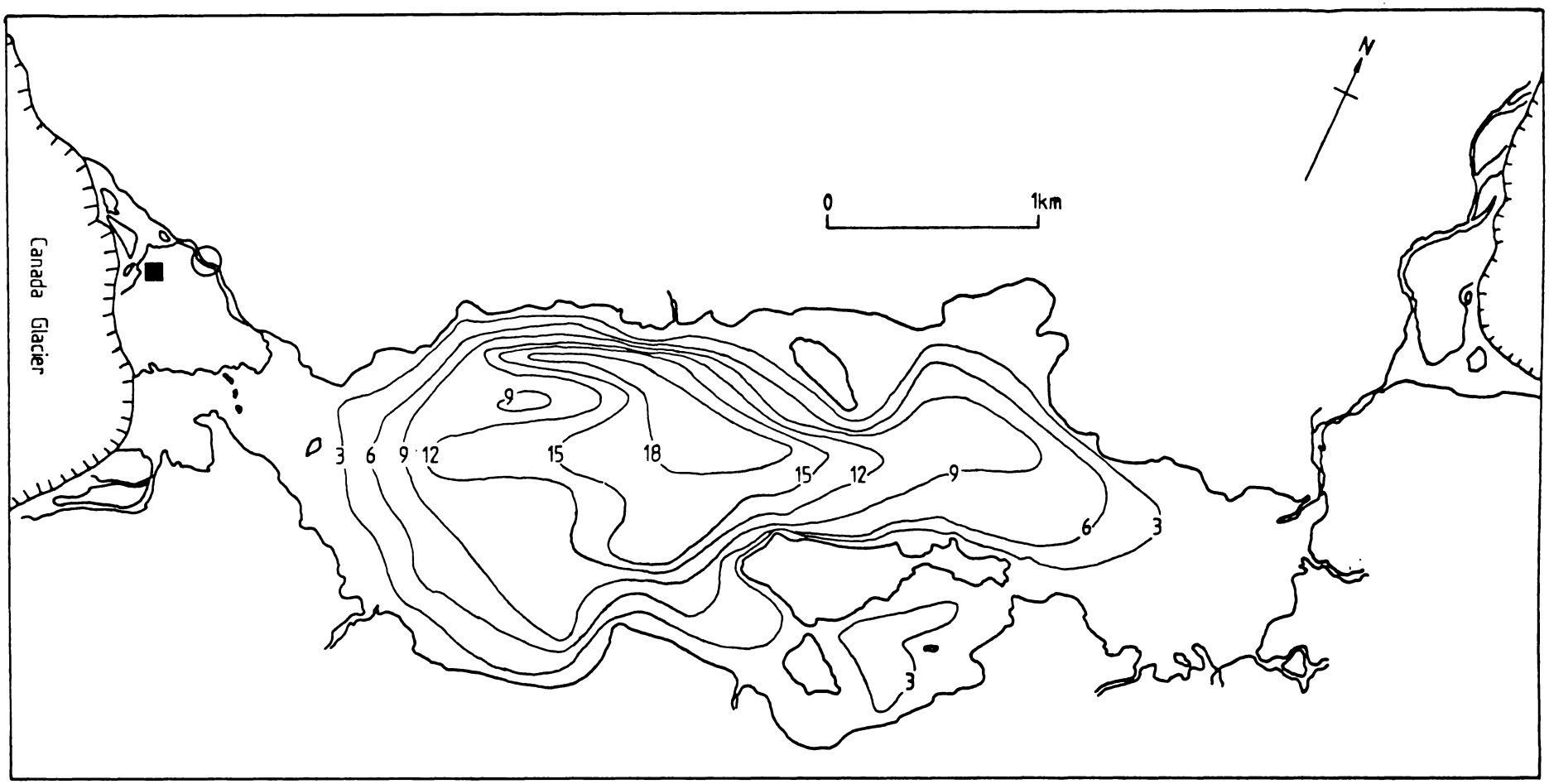

Figure 2.5 Lake Fryxell bathymetry surveyed by the University of Waikato Antarctic Research Unit (Depth in metres). The black square near the Canada Glacier indicates the position of the campsite. The position of the weir, installed during the 1981/82 season, is circled.

source of water for Lake Fryxell is from summer meltwater runoff originating from surrounding alpine glaciers, especially the Canada and Commonwealth Glaciers, as well as those of the southern valley walls.

The lake ice cover varies in thickness from 3.8 to 4.5 m, and appears to change little from year to year (Henderson *et al.*, 1966). A similar ice thickness was observed during the summer of 1979/80. The ice surface consists of two distinct ablation platforms. These platforms arise from dust patches on the ice which melt and pits that subsequently intersect the water table (see Fig. 3.1 for definition of the water table). The water then freezes during winter and is preserved as a platform. Surface ablation and addition of ice from the bottom of the ice column cause elevation of the platforms (Henderson *et al.*, 1966). During summer months a moat usually forms around the lake margins, although in the summer of 1980/81 this did not occur (T.G.A. Green, pers. comm. 1981). It is caused by warmer summer temperatures melting marginal ice and to some extent by warmer inflowing stream water ($\sim 10^{o}C$). The latter mechanism is indicated by the greater extent of ice-free water adjacent to stream mouths. Usually the moat extends 20 - 30 m from the lake shore.

Meltwater inputs appear to vary considerably. During 1979/80 summer the flow in the stream bypassing the campsite (Fig. 2.6) began on 20/11/79 and was still flowing on 14/1/80. In the following summer virtually no flow occurred at all (T.G.A. Green, pers. comm. 1981). During the 1981/82 season a weir was installed (Fig. 2.5). Flow data is shown in Fig. 2.6.

Lake levels also fluctuate (Fig. 2.7) and in general appear to increase. Air photographs taken in 1972 show that the large islands near the southern shores of the lake (Fig. 2.5), were, at that time, a single peninsula.

Figure 2.6 Stream discharge and the weir site. Recordings commenced on 20.11.1981 and ended 19 days later when the weir was washed away. (K. Thompson, S. Green, pers. comm.).

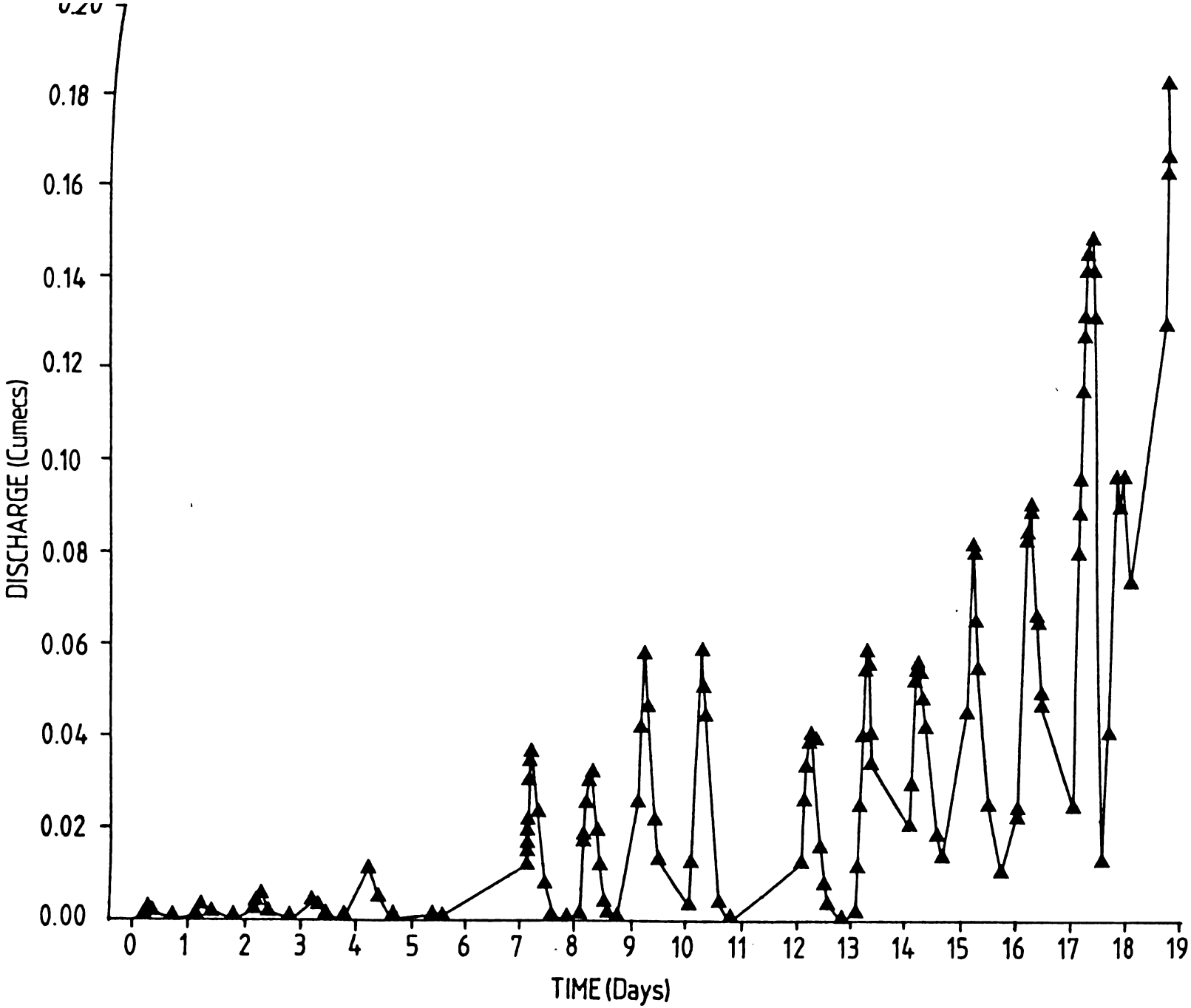
0.20
0.18
0.16
0.14
0.12
0.10
0.08
0.06
0.04
0.02
0.00
DISCHARGE (Cumecs)
0 1 2 3 4 5 6 7 8 9 10 11 12 13 14 15 16 17 18 19
TIME (Days)

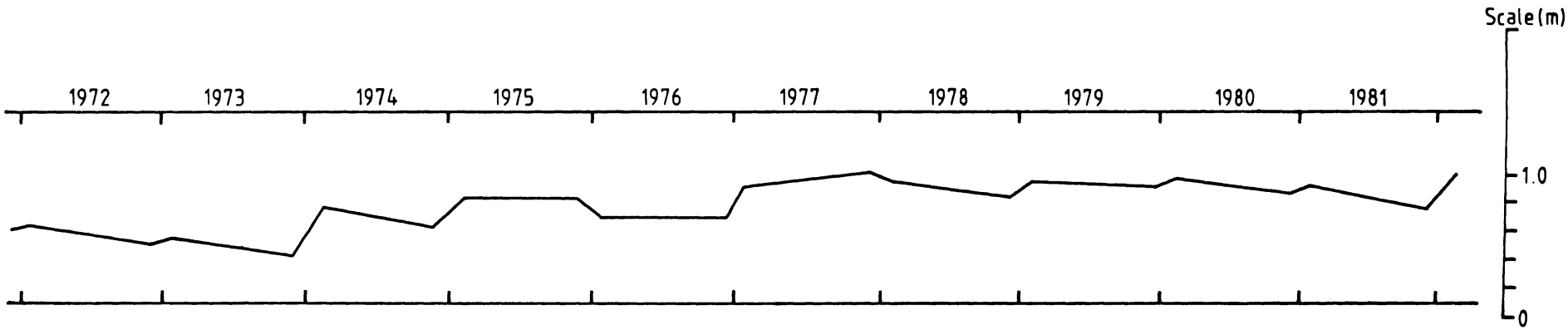

Figure 2.7 Lake level curve for Lake Fryxell from 1972 to 1982 (from Anderton and Fenwick, 1976; T.J.H. Chinn, per. somm.). The curve shows an overall increase of about 0.4 m in the last 10 years.

CHAPTER THREE

THE WATER COLUMN AND PRESENT CARBONATE DEPOSITIONAL SYSTEM

3.1 INTRODUCTION

This chapter describes sampling and analytical methods, and the chemical and physical characteristics of the water column in an attempt to describe the origins of the waters, their solutes, and the processes operating therein. Particular attention is paid to the carbonate system, including presently forming carbonate deposits on the lake bed.

3.2 METHODS

3.2.1 *FIELD WORK*

The field work was carried out in the 1979/80 austral summer field season: water samples were collected for laboratory analysis, and field measurements were made of pH, P_{CO_2}, ΣCO_2, temperature, P_{O_2} and water turbidity.

Sampling

To facilitate sampling the lake, the ice cover was drilled using a SIPRE Auger which produces a 10 cm diameter hole. Water samples were obtained using a bilge pump with an attached heavy rubber hose. Attached to the hose was a line marked at 0.5 m intervals. The hose was lowered and a wire used to raise the intake to the required depth (House *et al.*, 1966). The water depth was measured from the water table (Fig. 3.1). Water was pumped through to thoroughly flush the system. Plastic sample bottles were then rinsed at least 3 times with the sample solution before a sample was taken. The bottles were tightly capped and taken back to the campsite for analysis.

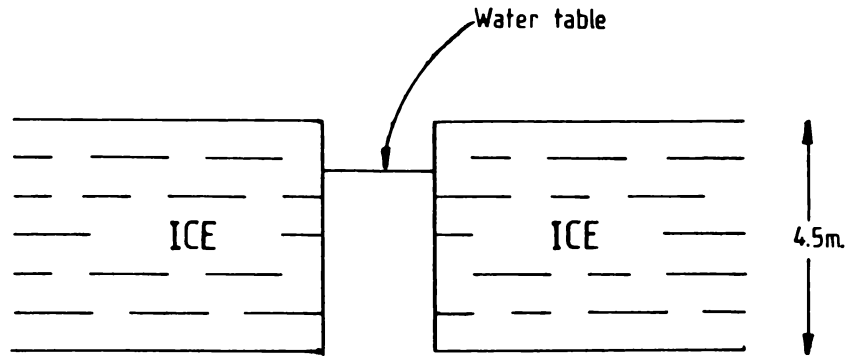

Figure 3.1 Pictorial definition of the water table. All depths are measured from the water table.

Three main sampling runs took place: early season sampling from 20 - 28/11/79, mid-season sampling from 7 - 14/12/79, and late-season sampling from 2 - 8/1/80. These plus samples for laboratory analysis collected on 11/1/80, were obtained from site S_2 (Fig. 3.2). Site S_1 was only used for preliminary reconnaissance sampling.

Field Analyses

P_{O_2}

P_{O_2} was measured using a "Delta Scientific 2010 Automatic Dissolved Oxygen Analyser" which has a probe containing a semi-permeable teflon membrane. The probe was lowered to the required depth, allowed to equilibriate with the solution, and the reading taken. Incorrect calibration of the probe means that the shape of the curves for individual profiles is correct but that the absolute values are not.

Temperature

Temperature was measured with a thermistor probe attached to the P_{O_2} probe.

pH

A pHM64 Research pH meter with glass and calomel electrodes was used. *In situ* pH measurements were unsuccessful because of problems with earthing so samples were returned to the campsite for analysis.

A problem in pH determinations was equilibration of CO_2 in solution with atmospheric CO_2. This was caused by lack of buffering and resulted in the pH changing rapidly thus limiting precision to about 0.1 of a pH unit. Attempts to seal the sample and electrodes from the atmosphere were unsuccessful. The technique employed was to allow the electrodes to equilibrate with the solution for 2 - 3 seconds, then take the reading before too much equilibration between solution and atmosphere occurred.

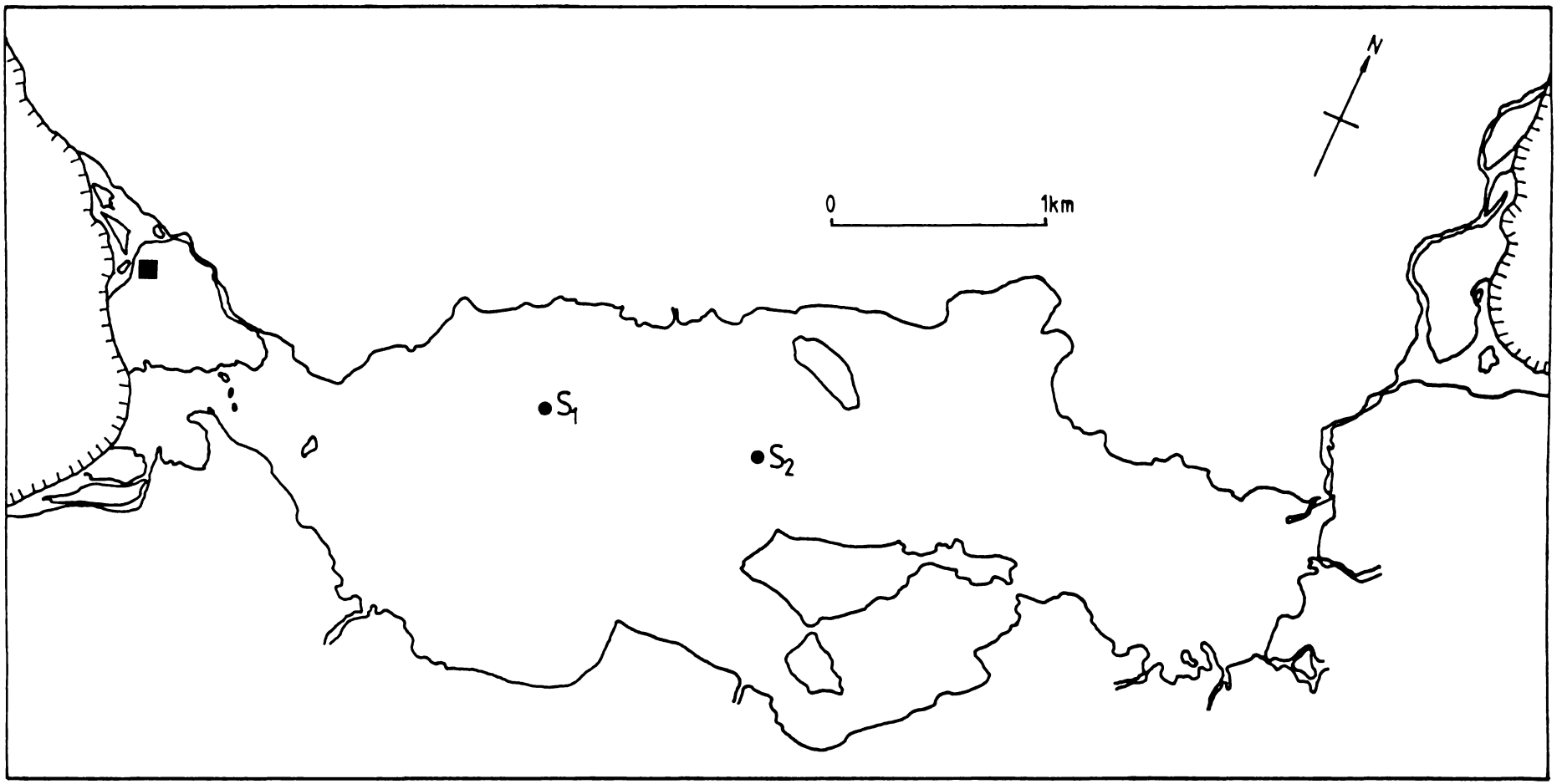

Figure 3.2 Map showing water sampling sites. The campsite is indicated by the black square.

P_{CO_2}

A CO_2 stripping line (Fig. 3.3a) was used to equilibrate N_2 with water from a 2.5ℓ water sample before the CO_2 was dried and admitted to a URAS 2T Infrared Gas Analyser (IRGA) (Fig. 3.4). The analysis required the use of two CO_2 standards: an upper 20,000 ppm CO_2 standard and a lower standard of 1080 ppm CO_2, both with N_2(g) as a carrier. The procedure modified from McCabe (1977) was:

(i) The CO_2 stripping line (Fig. 3.3a) was flushed with one of the standards and a positive pressure obtained.

(ii) A 2.5ℓ water sample bottle was attached to the line and CO_2 in the line was circulated through for 5 minutes to equilibrate CO_2 between the solution and gas phases.

(iii) After isolating the water sample bottle water vapour was frozen out with an ice/salt ($-20^{o}C$) cold trap.

(iv) Some of the purified CO_2 was isolated in the gas sample bottle, then placed on the IRGA line (Fig. 3.4).

(v) The IRGA and cycling line was flushed with the lowest standard and the reading noted.

(vi) The gas sample was then let in and the reading noted.

(vii) Finally the IRGA and cycling line were flushed with the upper standard and the reading noted.

(viii) P_{CO_2} concentration was then calculated (Appendix I).

Σ_{CO_2}

The standards used were the same as for P_{CO_2}. The procedure is modified from McCabe (1977):

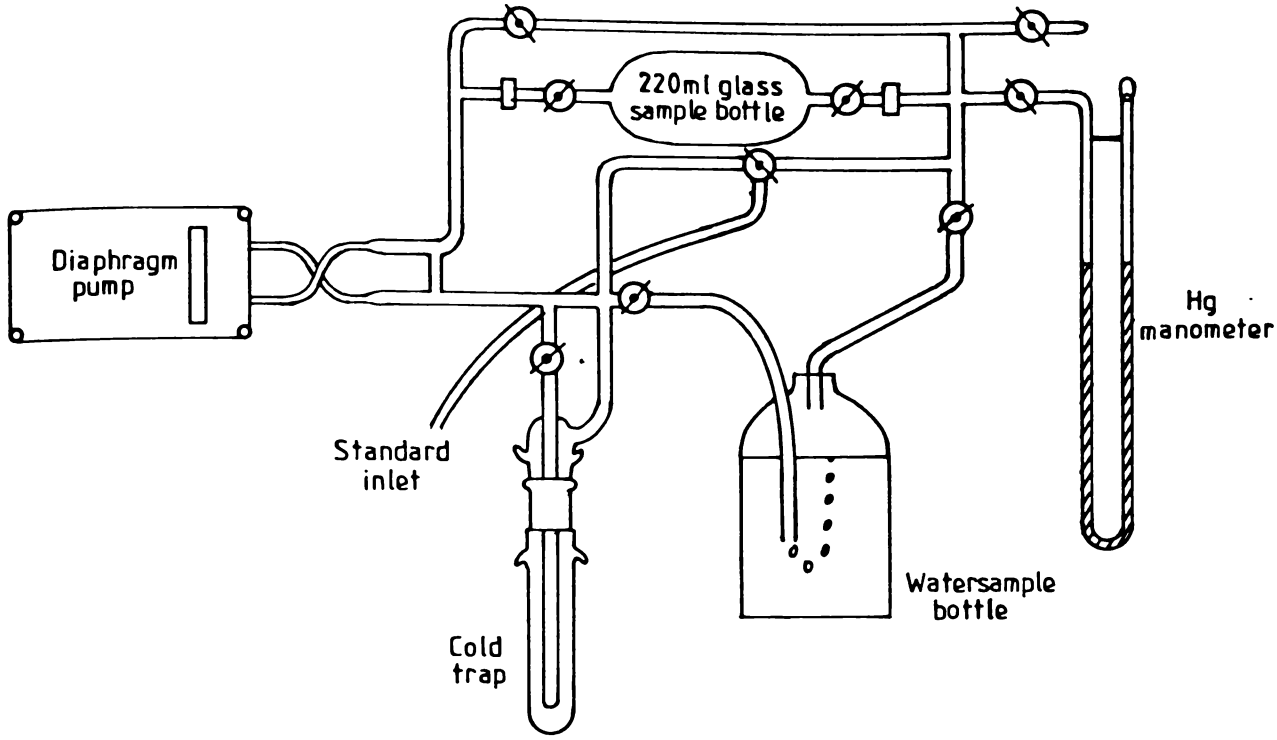

Figure 3.3a CO_2 stripping line for P_{CO_2} analyses.

(From McCabe, 1977)

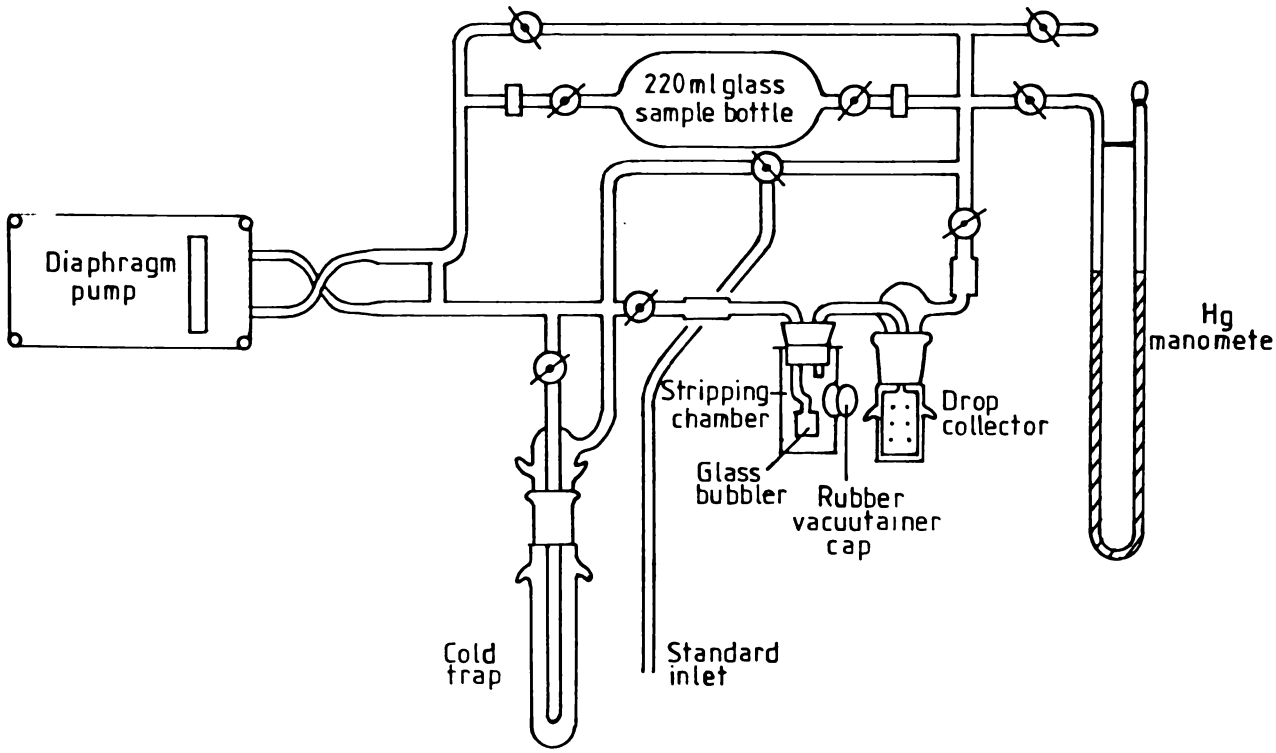

Figure 3.3b CO_2 stripping line for ΣCO_2 analyses.

(From McCabe, 1977)

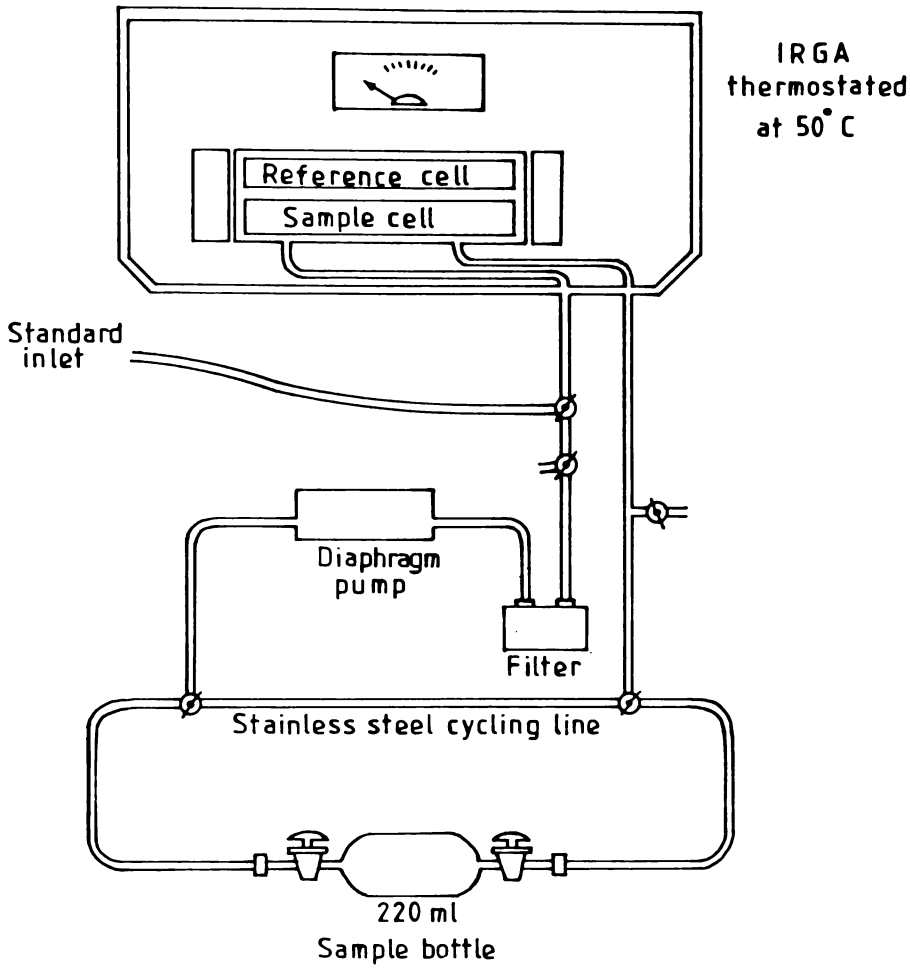

Figure 3.4 Infrared Gas Analyser (I.R.G.A.) with cycling line.
(From McCabe, 1977)

(i) The stripping line (Fig. 3.3b) was flushed with one of the standards and a positive pressure obtained.

(ii) A known volume of sample was injected by syringe into the stripping chamber. The volume of sample was determined by the expected concentration.

(iii) An excess of 0.1M HCl was then injected to react with the sample producing CO_2.

(iv) The CO_2 was then circulated through the line for 5 minutes to equilibrate between gas and solution.

(v) After the stripping chamber and drop collector had been isolated, water vapour was frozen down into the cold trap.

(vi) After some gas had been isolated in the gas sample bottle, it was placed on the IRGA line (Fig. 3.4). Thereafter the procedure is as for P_{CO_2}.

Turbidity

Water turbidity was analysed by Dr W. Vincent using a modified Turner III fluorometer, with a red excitation beam.

3.2.2 *LABORATORY ANALYSES*

Water samples returned to New Zealand were analysed for Ca^{2+}, Mg^{2+}, Na^{+} Sr^{2+}, Ba^{2+}, K^{+}, Fe^{2+}, Mn^{2+}, ZN^{2+}, Cl^{-} and $\delta^{13}C$ using the techniques set out in Table 3.1. The Atomic Absorption, (AA), and Atomic Emission (AE), analyses were performed using standards made up in solutions of similar matrix to Lake Fryxell water, using data from Torii *et al.*, (1975). Methods of analysis for AE and AA, flame photometry and Cl^{-} are standard techniques as listed in APHA (1975), (Table 3.1). $\delta^{13}C$ analyses are described in detail in section 4.3.

Table 3.1 Summary table of laboratory analytical methods.

ANALYTE	METHOD	INSTRUMENTATION
Mg, Ca, Fe, Mn, Zn	AA-air/acetylene flame (APHA 1975)	Instrument Laboratory AA/AE Spectrophotometer 357
K	AE-air/acetylene flame (APHA 1975)	"
Na	Flame photometry (APHA 1975)	Eel Flame Photometer
Sr, Ba	AE-Nitrons oxide/ acetylene flame (APHA 1975)	Varian Techtron model 1000 AAS
Cl	Argentometric titration (APHA 1975)	Wet Chemical Analysis
^{13}C	$BaCO_3$ precipitation from sample using $Ba(OH)_2$	Micromass 602c double inlet Mass spectrometer (Section 4.3)

3.3 RESULTS

3.3.1 *PHYSICAL CHARACTERISTICS*

Temperature

The temperature profile (Fig. 3.5) indicates Lake Fryxell to be mesothermic (Cole, 1979). The lowest temperature is $0^{o}C$ at 4 m; the maximum temperature is 3.4 - $3.8^{o}C$ at 9 - 10 m. The temperature variation of any given depth within the profile during the sampling season was no more than $0.4^{o}C$ and is possibly due to instrument deviation. A similar profile to that in Fig. 3.5 was obtained by the 1980/81 University of Waikato Expedition, to Lake Fryxell. Differences between these measurements and profiles by other workers may be due to differences in calibration.

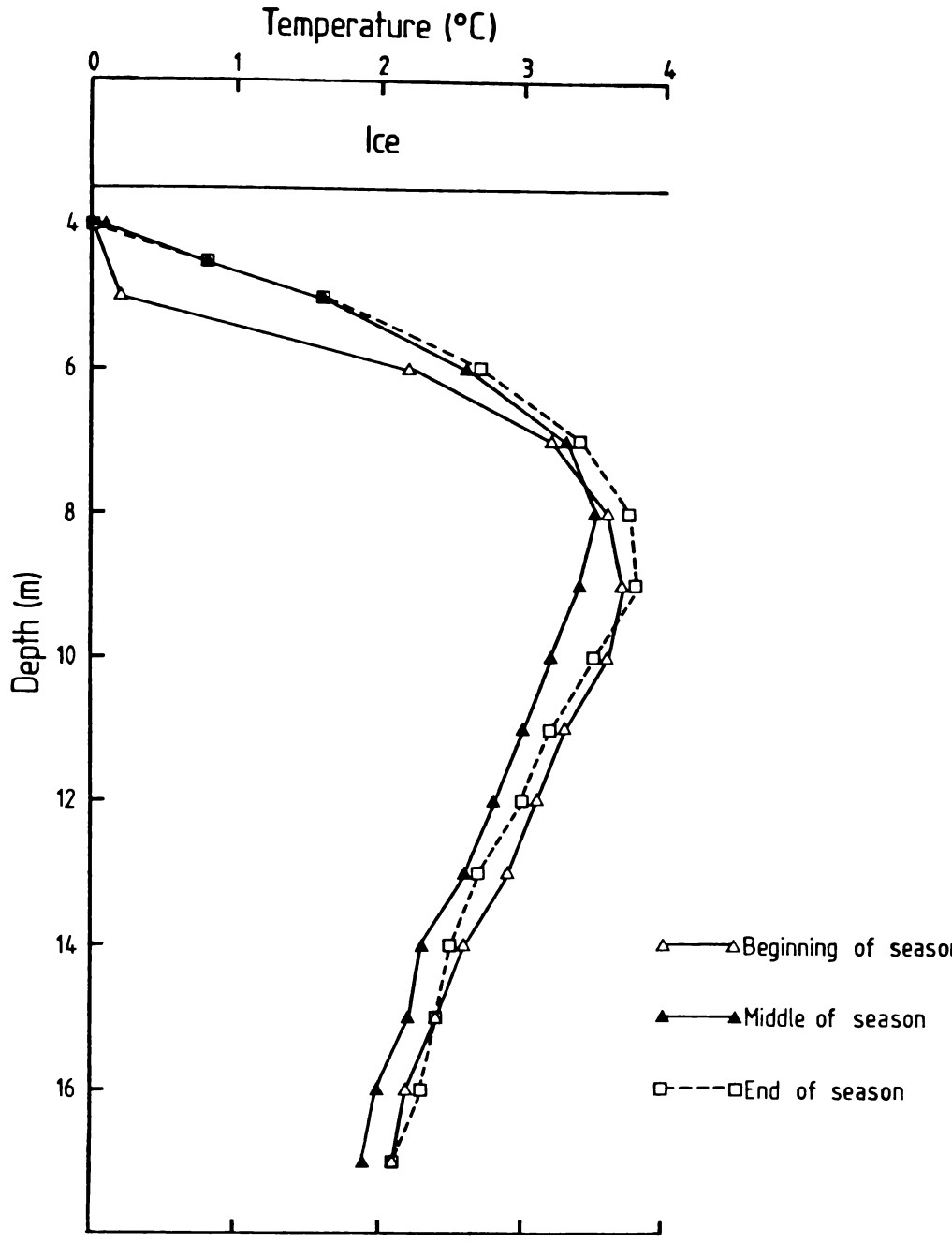

Figure 3.5 Lake Fryxell temperature profiles for beginning, middle and end of the summer season. The profiles indicate the lake to be mesothermal.

The profile has not changed significantly since detailed measurements were first made in 1963 (Hoare *et al.*, 1965). It therefore appears that temperature in the lake remains stable from year to year.

Wilson and Wellman (1962) first postulated the heat source for the temperature profile in Lake Vanda to be solar radiation. This mechanism was subsequently proven when Hoare *et al.* (1965) showed that the Lake Bonney temperature profile was caused by absorption of solar radiation by the lake water. Following a similar argument, a temperature profile for Lake Fryxell was calculated based on radiant energy (Hoare *et al.*, 1965). The calculated and observed profiles agree closely suggesting that as in the case of Lake Bonney, the Lake Fryxell temperature profile is controlled by solar heating.

There are a number of factors that may contribute to the generally low water temperatures in Lake Fryxell. One of these is the dispersive effect on incoming radiation by the lake ice cover (Hoare *et al.*, 1965; Vincent, 1980). Waters at the top of the water column are cooled by conductive cooling to the atmosphere as a result of freezing at the bottom of the ice cover, and ablation from the top. Inflowing meltwaters may create some form of convection in upper waters, aiding the preceding mechanism by bringing more water in contact with the overlying ice. The decrease in temperature towards the bottom of the lake may be due to either heat loss to lake bottom sediments or alteration of temperature gradients as a result of adding water to the lake. The latter effect means there is less heat absorbed per unit volume. The density distribution of organisms living in the water column may also change heating patterns.

Water temperatures up to 10^{o}C occurred in the moat around the lake margins. Such temperatures are similar to those in the meltwater stream flowing past the campsite. The flows in this stream (Figs. 2.6).

suggest that peak discharges of all the streams would add no more than 5 mm to the lake depth. Much of the heat in the water is lost through atmospheric contact and melting of any lake ice. Therefore inflowing stream waters have a significant effect on moat temperature, but a small effect on the lake as a whole

Turbidity

The turbidity profile appears complex (Fig. 3.6). The main features are the sharp rise in turbidity at 8.5 m and the turbidity maximum between 9 m and 15 m, and another peak at 17 m. Addition of dilute HCl to a sample decreased the turbidity, e.g. in a sample from 11 m depth this caused a 10% turbidity decrease and gave off a gas (possibly CO_2). Some of the samples below 9 m had a faint cloudy appearance and material filtered from solution was light grey. S.E.M. analysis showed some of the filtered material to be algal in origin. XRD patterns of these suspensions contained calcite peaks for samples taken below 7 m. The peaks were small and relatively broad indicating that the crystals were small (Griffin, 1971) or poorly ordered. Quartz and feldspar peaks also occurred but throughout the water column. As calcite only occurs below 7 m its origin is from within the water column, rather than detrital as with quartz and feldspar.

3.3.2 *CHEMICAL CHARACTERISTICS*

A full list of analytical results is contained in Appendix II, although a general summary follows.

Cations

The major cation present is Na^+ (Fig. 3.7), ranging from 200 ppm at 5 m depth to about 3000 ppm in bottom waters. K^+ has to some extent a similarly shaped profile (Fig. 3.7a) with a maximum concentration of

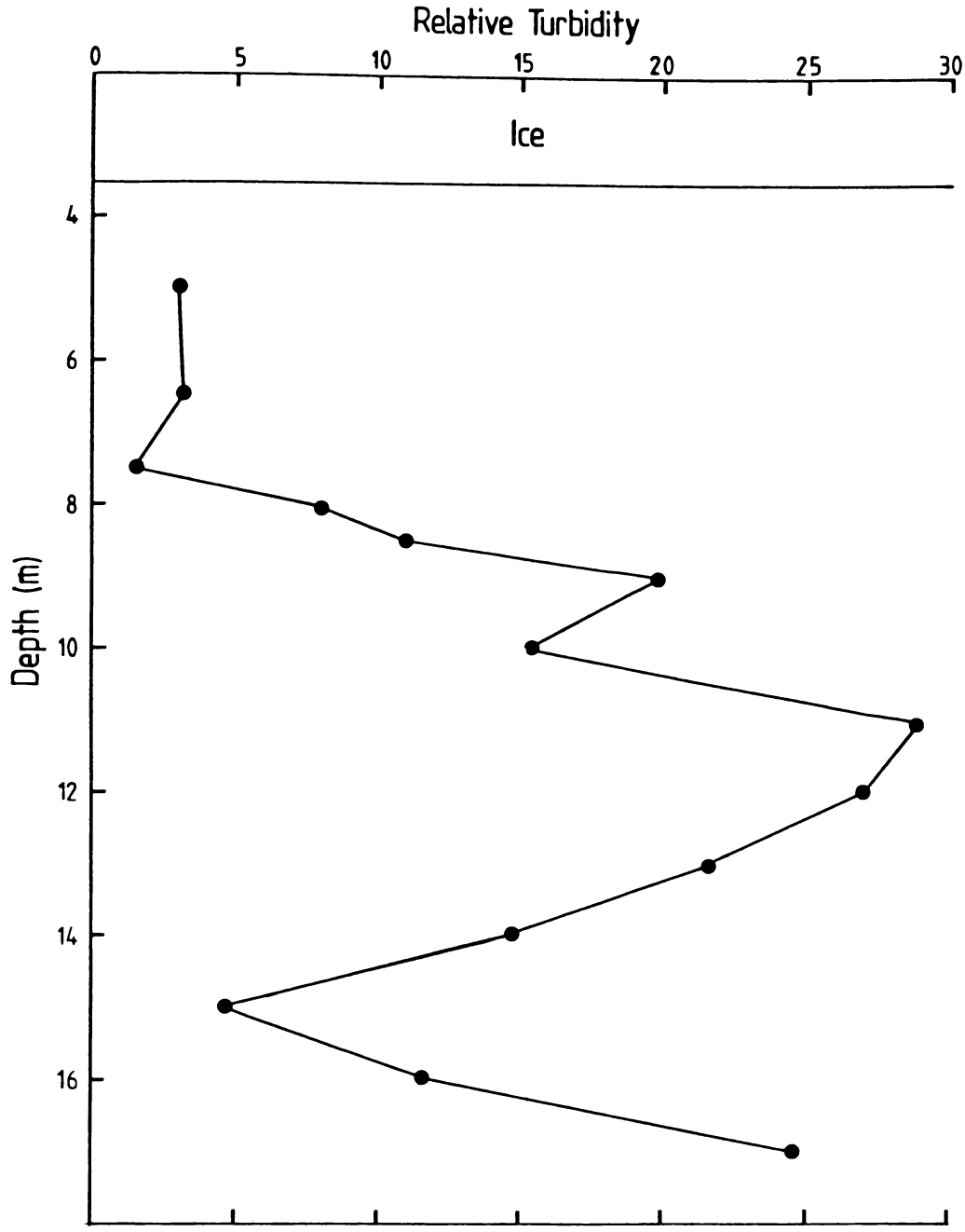

Figure 3.6 Lake Fryxell turbidity measured in arbitrary nephelometric units. Maximum turbidity occurs from 9 m to 14 m depth, and at 17 m depth.

Figure 3.7 Lake Fryxell cation profiles. Group 1 elements (3.7a), and Group II elements (3.7b and 3.7c) with the exception of Ca^{2+}, increase in concentration with depth. Ca^{2+} (3.7b) and the transition elements (3.7d) remain about the same.

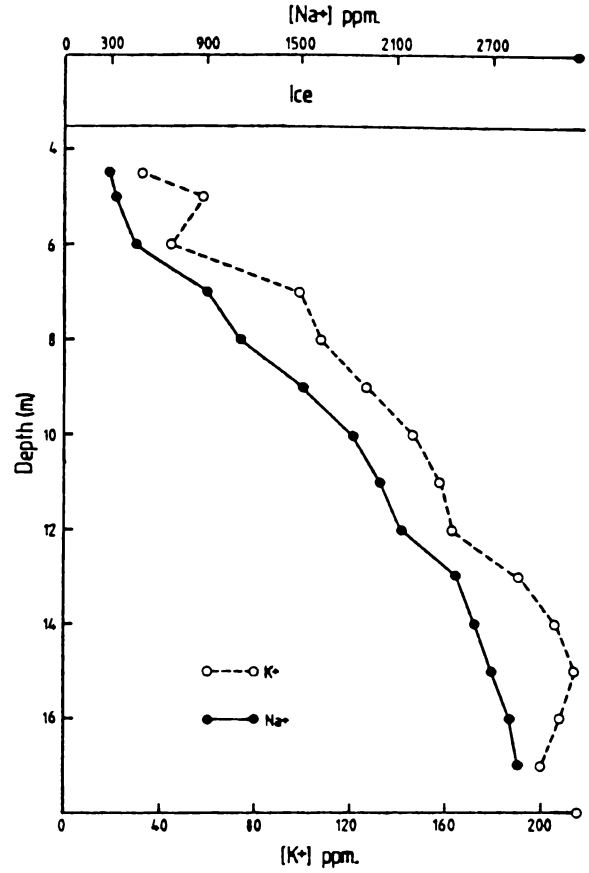

Fig. 3.7a

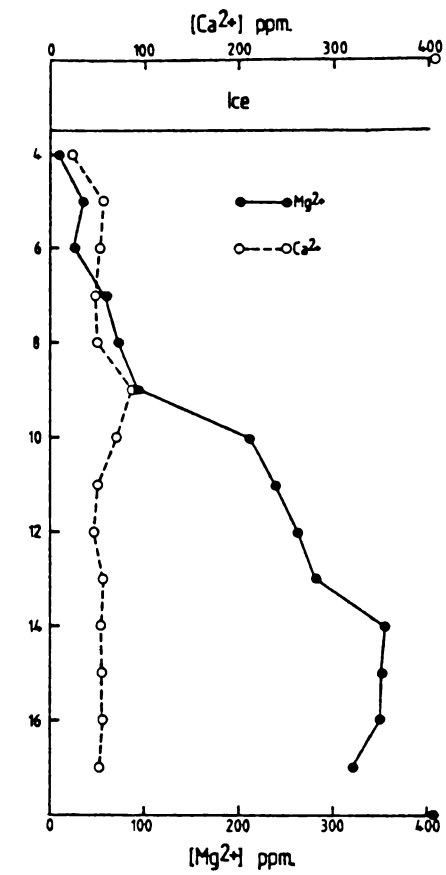

Fig. 3.7b

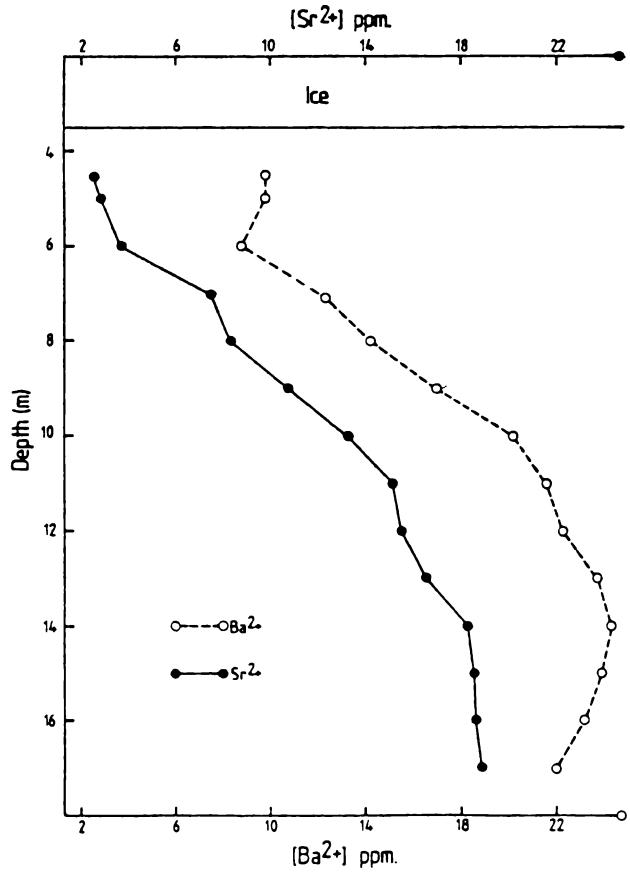

Fig. 3.7c

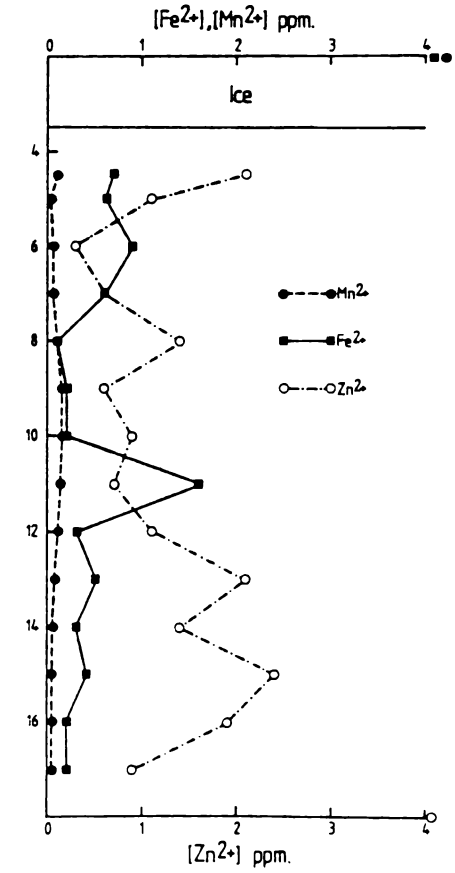

Fig. 3.7d

214 ppm at 15 m, though decreasing to 200 ppm of 17 m. Both profiles indicate a chemical stratification in the water column.

The major divalent cation in Mg^{2+} (Fig. 3.7b) with a maximum concentration of 350 ppm. Significantly, the Ca^{2+} profile (Fig. 3.7b) is similar to Mg^{2+} to a depth of 9 m only. Thereafter it displays marked deviation, remaining constant below this depth at about 50 ppm, suggesting some form of Ca^{2+} removal.

Ba^{2+} and Sr^{2+} (Fig. 3.7c) have similarly shaped profiles to Mg^{2+}, although of lower concentration. Like K^{+}, Ba^{2+} concentration decreases slightly below 15 m.

The transition elements analysed are all of low concentration. Fe^{2+} and Mn^{2+} are less than 1 ppm, and Zn^{2+} has a maximum value of 2.4 ppm and an erratic profile (Fig. 3.7d). It is, however, not possible to confirm whether Zn^{2+} profile is real or the variation due to sampling or analytical problems.

Anions

The major anions are Cl^{-}, SO_4^{2-} (Fig. 3.8) and HCO_3^{-} (discussed later). Cl^{-} reaches a concentration of 3700 ppm in bottom waters. Torii *et al.*, (1975) showed that SO_4^{2-} reaches a maximum concentration of 250 ppm. Torii *et al.* also reported maximum concentrations of HBO_2^{-} of less than 10 ppm. PO_4^{2-} and NO_3 concentrations were minimal, and NH_4, which is the predominant N-species, only appears in measurable quantities below 10 m depth.

pH

At any one level in the water column the pH remains comparatively stable throughout the summer season (Fig. 3.9). Maximum variations between profiles are of the order of 0.2 - 0.3 pH units for the reasons discussed in section 3.2.1.

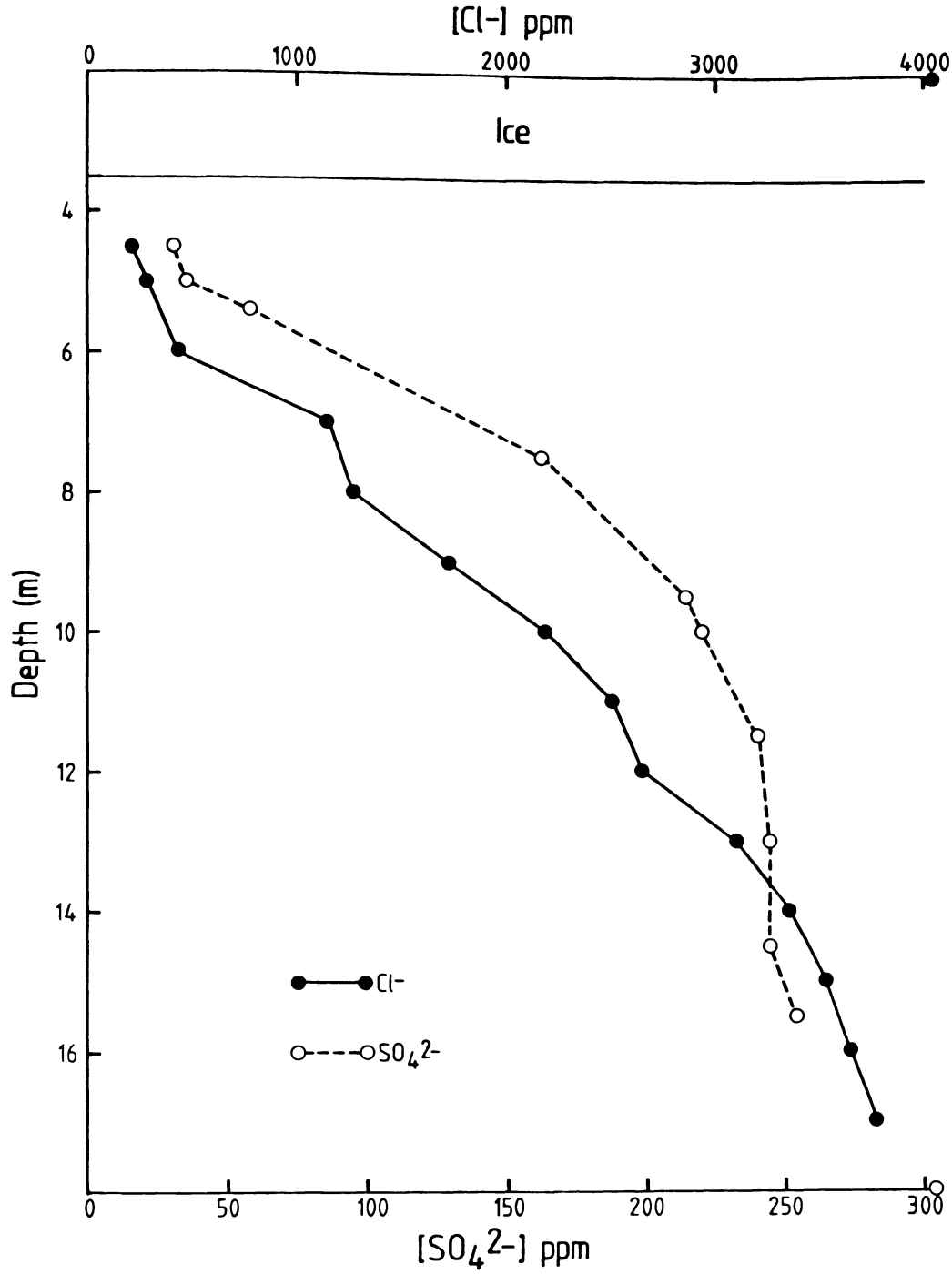

Figure 3.8 Cl^- and SO_4^{2-} profiles. The SO_4^{2-} data comes from Torii *et al.* (1975) with depths adjusted to measure from the water table.

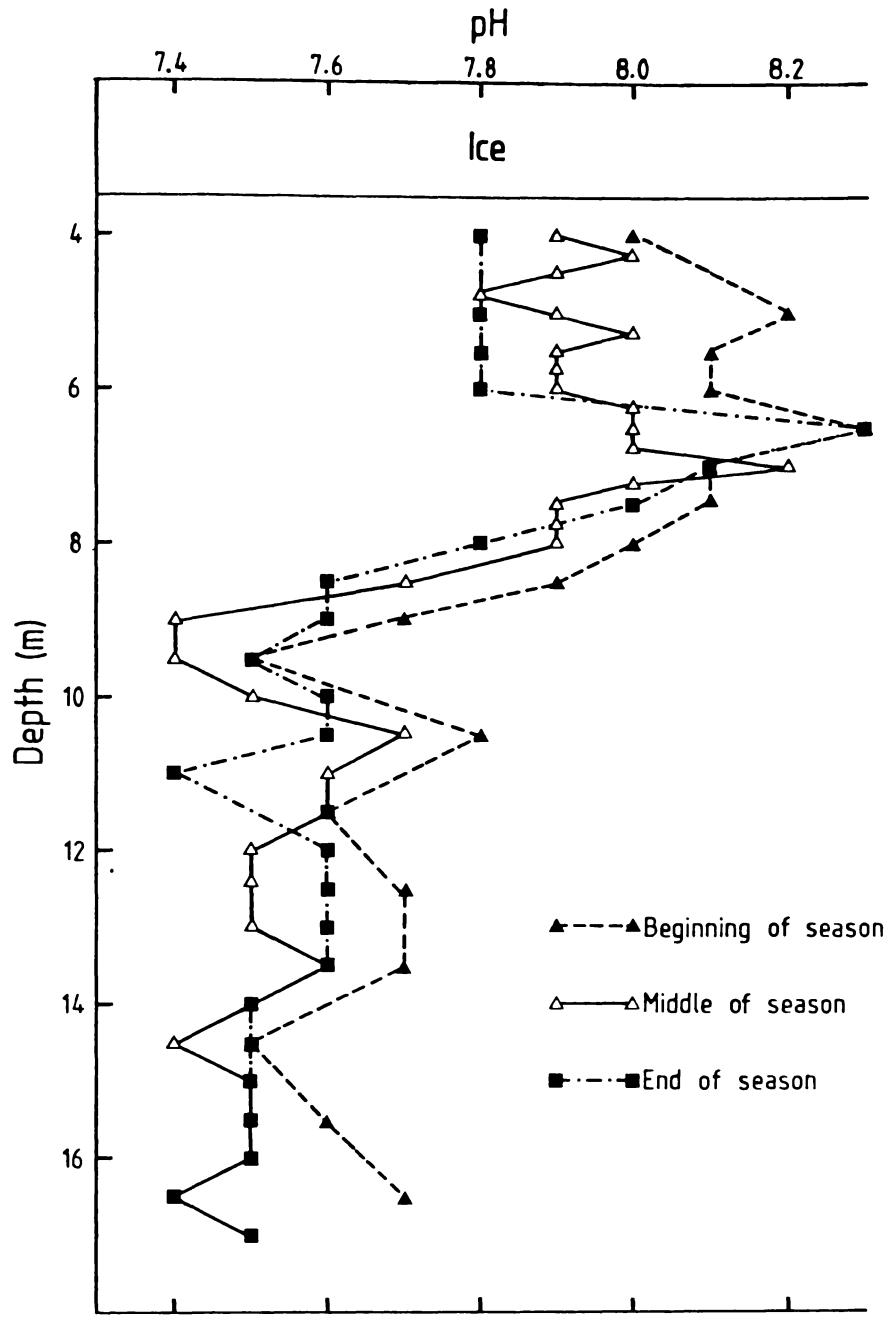

Figure 3.9 Lake Fryxell pH profiles for beginning, middle and end of the summer. The variability between profiles is probably caused by analytical problems.

The maximum pH occurs between 6 m and 7 m depth and ranges in value from 8.3 - 8.2. Below 7 m pH decreases to about 7.5 and remains constant at this value from about 9 m depth. The lower constant pH below 9 m depth indicates deeper waters to be better buffered than waters above 9 m. Poorer buffering of surface water may be due to mixing with incoming surface water or possibly some atmospheric diffusion through the lake ice cover.

Dissolved Gases

P_{O_2} was below the limits of detection (0.1 ppm) at depths below 9 m. Above 9 m the profile displayed marked seasonal fluctuation (Fig. 3.10a). Concentrations built up to a maximum in mid-summer, then decreased. The lower large peak remained at about 7 m depth throughout the summer season, although a secondary smaller peak further up the water column appears to have moved down as summer progressed (Fig. 3.10a). The large peak of 7 m matched trends displayed by cellular photochemical capacity assays (Vincent, 1981) and together defined the euphotic zone down to 10 m depth. Below 10 m waters are anaerobic (anoxic) (Fig. 3.10a).

The P_{CO_2} profiles (Fig. 3.10b) are similar in shape to the Na^+ profile. The beginning of season values tend to be the greatest in bottom waters, with mid and end of season values about the same. The amount of biologically produced O_2 should be equivalent to the amount of CO_2 fixed. As the P_{CO_2} is about 1000 times the maximum O_2 levels it is unlikely that the large differences between P_{CO_2} profiles (Fig. 3.10b) are caused by biological photosynthetic consumption and respiratory production processes. Therefore the differences are possibly due to problems with analysis in the field.

Figure 3.10 Dissolved gas profiles for Lake Fryxell.

Figure 3.10a The P_{O_2} profile shows 2 distinct peaks; a small upper peak 'a', which shifted down the water column as summer progressed, and a larger peak 'b' which reached a maximum in mid summer. The stipled area indicates the anaerobic (anoxic) waters.

Figure 3.10b P_{CO_2} profile. This is similar in shape to the Na^+ profile. The differences between samplings probably result from IRGA calibration problems.

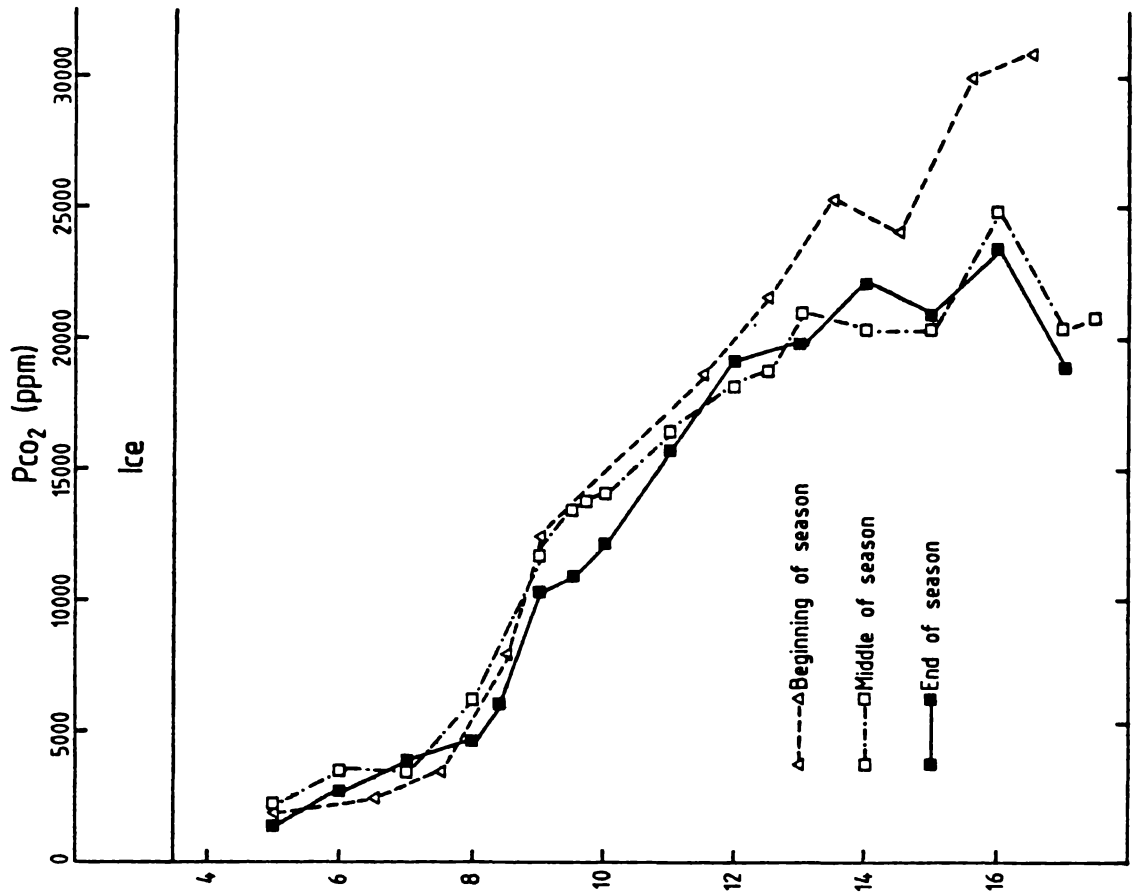

Fig. 3.10b

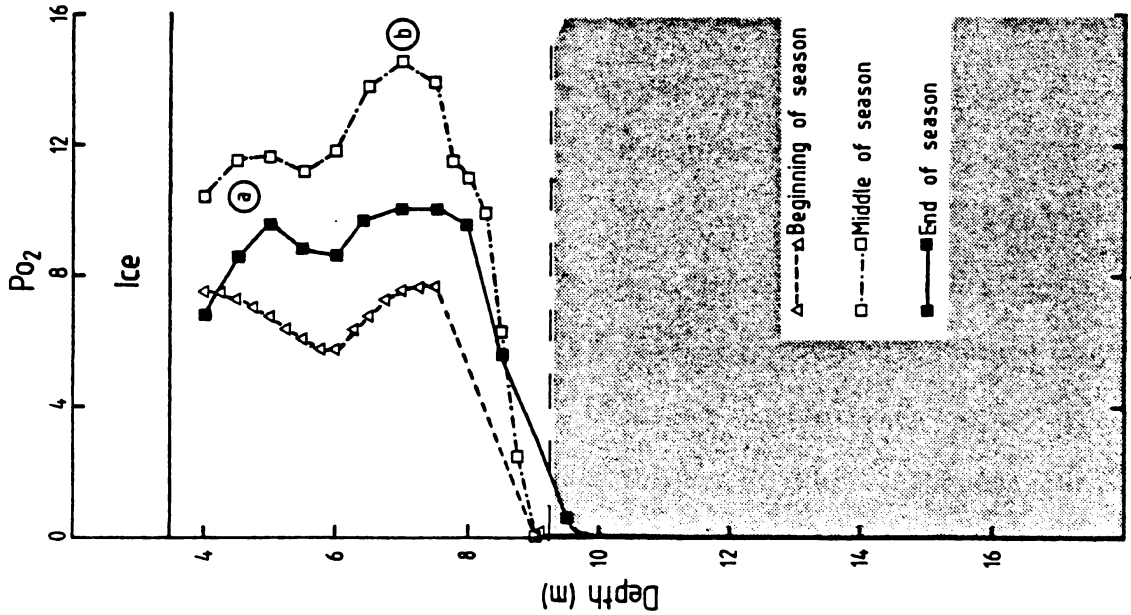

Fig. 3.10a

ΣCO_2

The ΣCO_2 profiles shown in Fig. 3.11 show an overall increase with depth. There is no end of season profile because one of the CO_2 standards was exhausted thus precluding analysis. As the lake is stratified it seems reasonable to assume that the end of season ΣCO_2 should not differ greatly from the profiles presented. ΣCO_2 values are 5 orders of magnitude greater than P_{CO_2}. As P_{CO_2} differences appear to be non-biological in origin, it is therefore unlikely that differences in ΣCO_2 profiles are biologically induced. The changes between the profiles cannot be easily explained except as a result of differences in calibration of the IRGA between analyses.

$\delta^{13}C$

Results are presented in Fig. 3.12. Photosynthesizers preferentially fix the ^{12}C of the CO_2, thus discriminating against ^{13}C. The peak of isotopic enrichment (Fig. 3.12) coincides with the bottom of the euphotic zone where maximum algal production occurs (Vincent, 1981). The salinity and density gradients in the lake waters (Fig. 3.7a,b,c,d) prevent disturbance of the water column except in the upper layers, thus the $\delta^{13}C$ values from 5 m to 6 m reflect the composition of incoming meltwaters. At depths below 7 m, addition of fresh meltwater is not possible under present conditions. As a result progressive removal of ^{12}C depleted photosynthates has caused the remaining C to become isotopically heavier. The effect is most marked at the zone of maximum PO_2 where algal photosynthetic production is greatest. Greatest productivity occurs at 9 m depth but ceases completely at 9.25 m (Vincent, 1981), although bacterial photosynthesis occurs at greater depths (Dr C.G. Harfoot, pers. comm. 1982). Oxidation of seston originating from the 7 m to 9 m zone, dissolution of the settling carbonate suspension, and evaporative concentration at an earlier stage of the lakes development will have influenced the $\delta^{13}C$ values of the dissolved inorganic carbon in bottom waters.

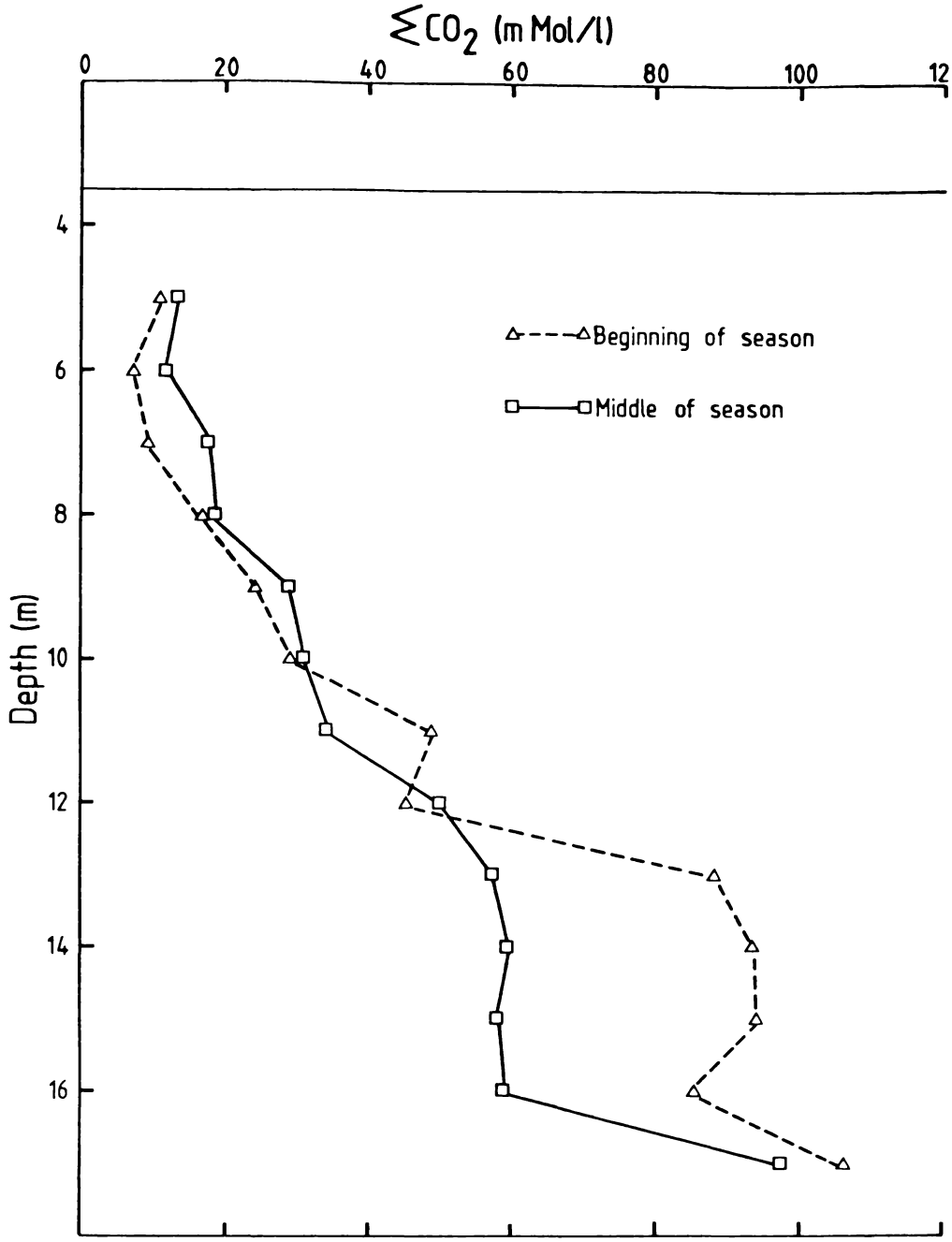

Figure 3.11 Lake Fryxell ΣCO_2 profiles. ΣCO_2 tends to increase with depth. The large differences between profiles possibly result from problems in IRGA calibration.

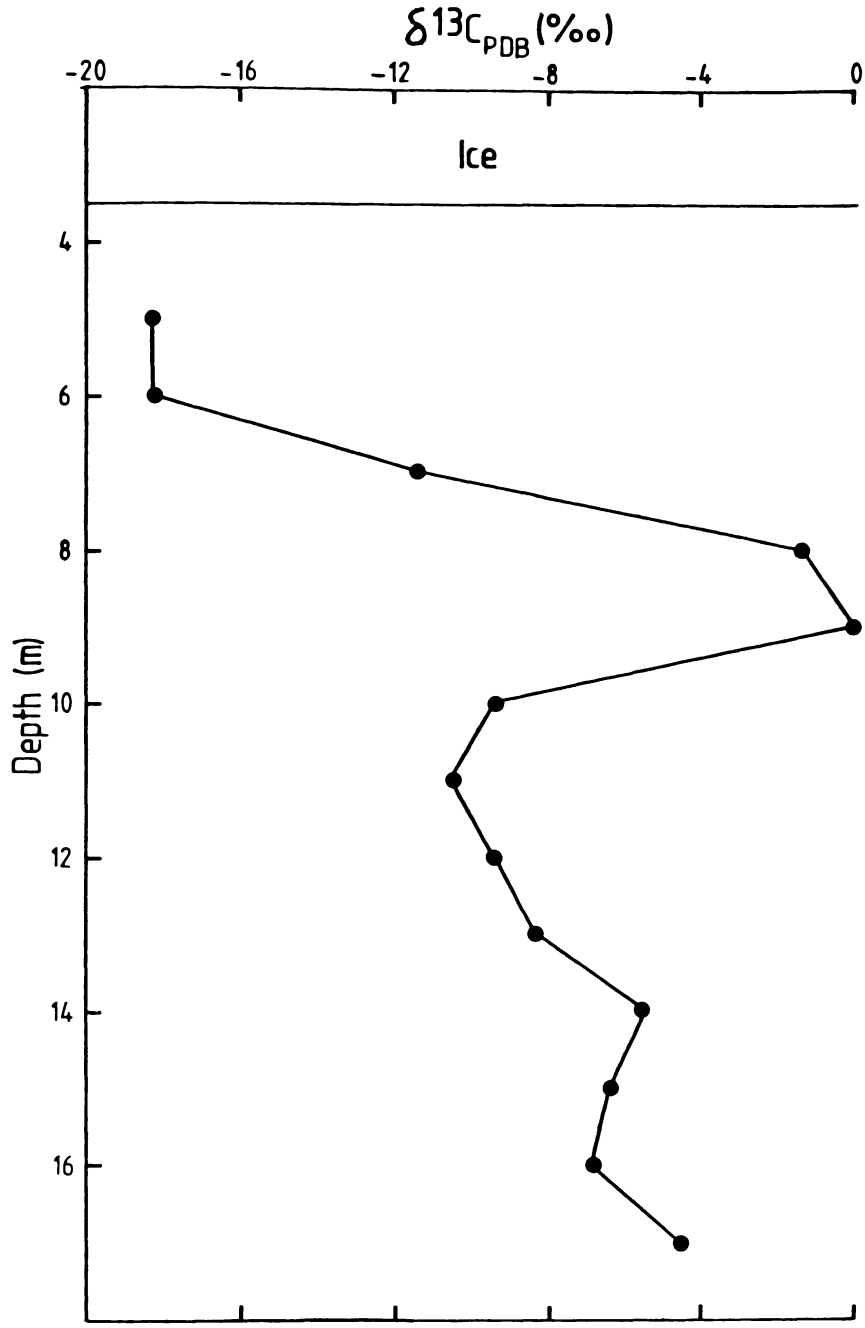

Figure 3.12 Lake Fryxell $\delta^{13}C$ profile. Maximum ^{12}C depletion has occurred in the zone of maximum algal photosynthetic production at 8 to 9 m depth. (Values are quoted with respect to PDB).

3.4 NON-CARBONATE CHEMISTRY

3.4.1 *ORIGIN AND EVOLUTION OF LAKE FRYXELL WATERS*

Lake Fryxell, along with other Dry Valley lakes is saline, i.e. it contains more than 5000 ppm total dissolved solids (Eugster and Hardie, 1978). It is further classified as a perennial saline lake (Hardie *et al.*, 1978) because it has persisted for a long period without drying up. To form and persist such lakes require (adapted from Eugster and Hardie, 1978):

(i) Restricted outflow. The divide at the seaward end of the Fryxell drainage basin (Fig. 1.1) prevents outflow. For outflow to occur a lake level rise of 80 m is required before waters overtop the ridge forming the divide.

(ii) Sufficient inflow to maintain a standing body of water. Monitoring lake levels since 1970 has shown that mean inflow has slightly exceeded mean ablation resulting in an overall rise in lake levels (Fig. 2.7). Despite considerable inflow variations, the evaporation rate is such that a complete inflow cessation for 60 years is required to completely evaporate the lake.

(iii) Evaporation must be greater than inflow. The occurrence of evaporites in the sediments of Lakes Vanda and Bonney, and the presence of saline to hypersaline waters in the bottom of most of the Dry Valley lakes indicate that evaporation has significantly exceeded inflow periodically in the past.

The Dry Valley lakes occur in ideal settings for saline lake formation; they are in "rain shadow" basins on arid valley floors between mountain ranges which act as precipitation (snowfall) traps (Eugster and Hardie, 1978).

The compositional history of closed basin waters consists of two phases: (1) the acquisition of solutes; (ii) brine evolution or concentration and subsequent precipitation of salts (Hardie and Eugster, 1970).

Solute Acquisition

In Dry Valley lakes the origin not only of the salts but of the water itself is important. Chemical data from Dry Valley lakes have been used previously in attempts to determine the origin of lake waters. Angino *et al.*, (1962b, 1964), Angino and Armitage (1963), and Nichols (1963) attempted to distinguish between marine and mineral spring origins but were unsuccessful (Hoare *et al.*, 1966). The technique applied was a comparison of various anion and cation ratios to those presented by White (1957). This is demonstrated by results from this study (Table 3.2). Such attempts at interpretation of the source fail because: (i) they used source waters which in most cases had little likelihood of being significant in the geological setting of Lake Fryxell; (ii) the effects of subsequent modifications to the waters by biological and physical processes (e.g. precipitation) are ignored.

Table 3.2 Ionic concentration ratios for Lake Fryxell, obtained in this study, compared to values determined for particular sources (White, 1957).

IONIC RATIO	TYPICAL SOURCE VALUES, WHITE (1957)				LAKE FRYXELL
	Volcanic H.S.	Oil Field Brines	Magmatic Waters	Oceans	Range
K/Na	0.03 - 0.3	-	-	-	0.1-0.7
$\frac{Ca + Mg}{Na + K}$	0.001 - 0.2	0.01 - 5	-	0.153	0.10-0.15
SO_4^{2-}/Cl^-	-	0 - 1	0.01 - 0.5	-	0.16-0.22

Wilson (1964) and Hoare *et al.* (1966) suggested that the waters presently in Antarctic lakes came from melting ice. This was tested by Hendy *et al.* (1977) on the west lobe of Lake Bonney. At some time in the past the lobe was thought to have evaporated to a negligible depth, so forming a brine. Meltwaters refilled the basin and the salts from the brine diffused back up the water column. Assuming a flat bottom and near vertical sides for the lake, the log of the concentration (C) plotted against h^2 (h = height above the lake bottom) should give a straight line (Hendy *et al.*, 1977). Applying this approach to the Lake Fryxell data it is found that the model fits well from 9 m depth to the bottom (Fig. 3.13).

The salts themselves have a number of different sources and pathways which are important in different areas, though salts of marine origin are regionally and quantitatively predominant (Keys and Williams, 1981). Salts of marine origins may come directly from sea spray (Hoare *et al.*, 1966), sea spray deposited on ice, which subsequently melts (Torii and Yamagata, 1981), or possibly relict seawater. Chemical weathering is a major source of Mg^{2+}, Ca^{2+}, and CO_3^{2-} ions (Keys and Williams, 1981) and Sr^{2+} (Jones and Faure, 1978). Despite the slowness of weathering reactions salts accumulate in Antarctic lake basins for long periods of time (Keys and Williams, 1981). In the case of Lake Fryxell accumulation probably continued throughout the Holocene. Salt accumulations in soils (Field, 1975) may also supply ions to lakes. Near the snowline where high relative humidities prevail, NaCl and $CaCl_2$ dissolve, soak into the soil, and travel downslope in ground or soil waters into drainage basins (Field, 1975; Wilson, 1981). Meltwater streams contain dissolved materials. Work by the Waikato University expedition during the summer of 1981/1982 showed considerable quantities of dissolved materials (Table 3.3) in the stream bypassing the Lake Fryxell campsite (Fig. 2.5).

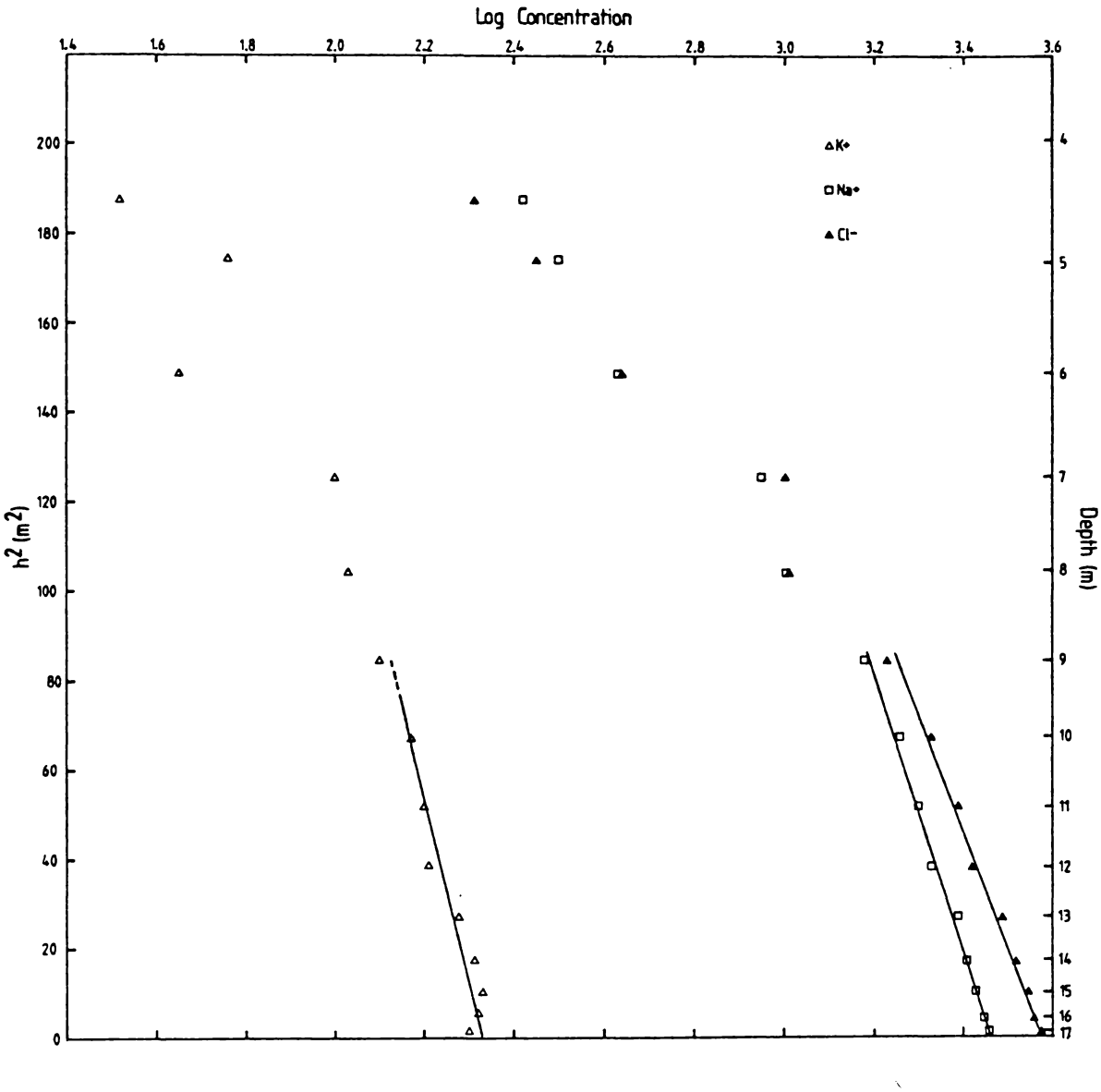

Figure 3.13 Plot of h^2 (where h = height above the bottom) against log concentration for K^+, Na^+ and Cl^-. These indicate diffusion control below 9 m depth.

Table 3.3 Mean values for dissolved materials analysed in stream samples taken at the weir (Fig. 2.5). The time period for sampling was 14 days commencing on 20.11.81. (K. Thompson, S. Green, pers. comm.).

SPECIES (ppm)	Alkalinity	Na	K	Ca	Mg	NO_3^{2-}	Cl^-	SO_4^{2-}	PO_4^{2-}	TOTAL
CONCENTRATION	15.2	2.9	0.8	6.1	0.9	1.9	5.3	6.4	26.3	279

Assuming an average continual discharge for a maximum of 60 days of 0.1 cumecs for each of the 10 inflow streams, and each with a total dissolved load of ∿280 ppm, implies about 200 x 10^3 kg of salt enters the lake each year.

Wind containing material from terrestrial salt efflorescences will also contribute to lake solutes (Field, 1975).

Brine Evolution

Saline lakes are compositionally controlled by relatively few solutes namely: SiO_2, Ca^{2+}, Mg^{2+}m K^+, HCO_3^-, CO_3^{2-}, SO_4^{2-} and Cl^- (Eugster and Hardie, 1978). On the basis of composition, saline waters may be described using Hardie and Eugster's (1970) ternary diagram (Fig. 3.14a) or in terms of the brine evolution system (Fig. 3.14b; Hardie and Eugster, 1970; Eugster and Hardie, 1978; Hardie *et al.*, 1978). The latter depends on evaporitic concentration. Torii and Yamagata (1981) indicate (Fig. 3.14a) that lake waters should approach the composition of seawater and then move to the right on figure 3.14a as a result of freeze concentration (Thompson and Nelson, 1956). This implies that later stages of precipitation and salt concentration should be the same irrespective of the original water composition (Torii and Yamagata, 1981). This sequence has been proposed as the origin for the Ca-enriched waters of Lake Vanda and Don Juan Pond (Yamagata *et al.*, 1967; cited Burton, 1981), and may suggest a similar origin for other Dry Valley lakes. The chemical precipitates found in lakes appear to correspond to pathways delineated in

Figure 3.14 Brine evolution diagrams.

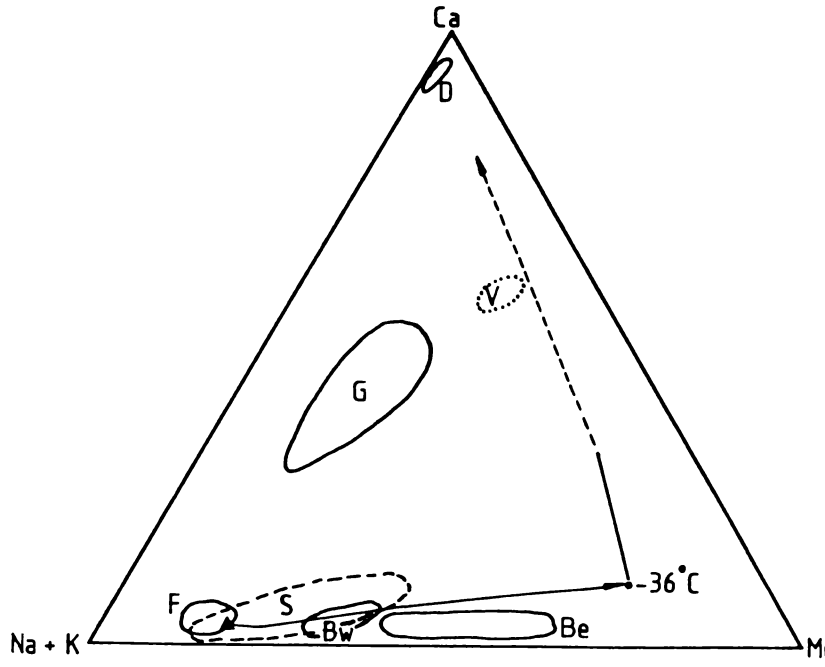

Figure 3.14a Ternary plot showing the relation of lake and seawater compositions. Arrow and dotted line indicate the compositional change of seawater under frigid conditions as described by the Thompson and Nelson (1956) Model (From Torii and Yamagata, 1981).

D = Don Juan Pond
F = Lake Fryxell
G = Glacial meltwater
S = Snow and ice
▲ = Seawater
Bw = West lobe, Lake Bonney
Be = East lobe, Lake Bonney
V = Lake Vanda

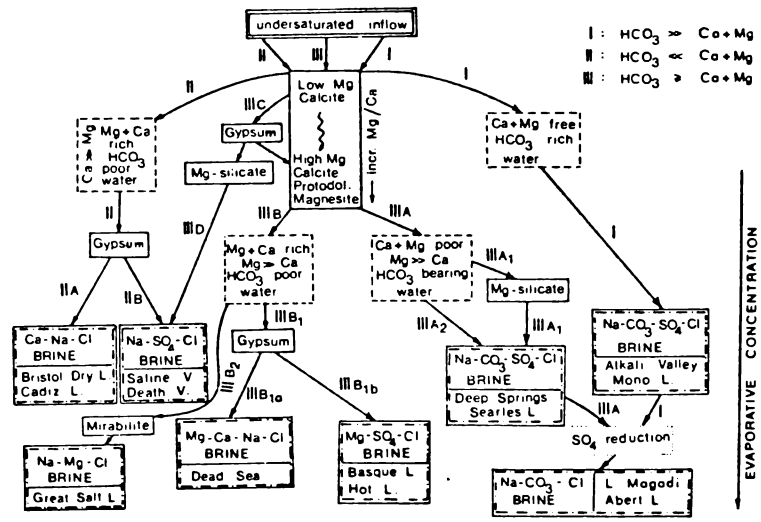

Figure 3.14b Flow diagram for brine evolution. Solid rectangles indicate critical precipitates and those with dashed borders are water compositions. (From Hardie and Eugster, 1978).

Fig. 3.14b (e.g. the gypsum-calcite layers of Lake Vanda recorded by Gumbley 1975, and the evaporite sequences in Lake Bonney (Gumbley, 1975; Wilson *et al.*, 1974). This suggests that evaporative concentration and freeze concentration may have similar effects and can possibly drive the evolution mechanism shown in Fig. 3.14b.

Summary of Lake Water Characteristics

Lake Fryxell shows a chemical stratification with most solutes reaching maximum concentration gradients between 8 and 14 m depth. This accords with the model presented above: evaporation or freeze concentration of the lake solutes at a previous stage in the lakes history. The lake basin was then flooded with low salinity meltwaters. Mixing processes, primarily chemical diffusion, have produced the chemical and density gradients which impart stability to the water column.

A number of solutes, however, show marked divergence from the diffusive mixing processes observed for the major ions. The P_{O_2} profile defines the euphotic (aerobic) zone between 9.25 m and the surface. Below this depth the lake is anaerobic and H_2S can be smelled in water samples. The low O_2 levels are attributed to either extreme activity by heterotrophs or very high rates of respiration by autotrophs (Vincent 1981). Ca^{2+} also shows marked deviation from the diffusion-controlled profile. This suggests that Ca^{2+} is or has been involved in precipitation reactions. Supporting evidence is carbonate layers in both modern and ancient Lake Fryxell sediments (Chapter 4). Low levels of Fe^{2+}, Mn^{2+}, and Zn^{2+} are due to the reducing environment below the euphotic zone. The presence of H_2S suggests their removal as sulphides, probably as pyrite. The Zn and Mn would be similarly removed or possibly "scavenged" as FeS_2 co-precipitates. As well as reducing Fe^{2+} and possibly Mn^{2+} and precipitating sulphides, the anaerobic waters will also reduce N species. This results in a build-up in concentration of NH_4^+ in bottom waters

(Torii *et al.*, 1975). The low concentrations of all N species in the euphotic waters presumably indicate rapid uptake of this nutrient by phytoplankton and algal mats.

3.4.2 *DIFFUSION AGE*

The chemical and density stratification resulting from the upward diffusion of salts prevents convective mixing of waters. The diffusion cell produced will persist until diffusion has reduced concentration gradients enough to allow convective mixing (Hendy *et al.*, 1977). For lakes such as Fryxell which evaporated to minimal volume and then re-filled, the following diffusion equation can be applied (Wilson, 1964):

$$C = \frac{M}{(\pi Dt)^{1/2}} \cdot \exp\left(\frac{-h^2}{4Dt}\right) \qquad (1)$$

where

C = concentration of the salt

D = diffusion coefficient

h = height above lake bottom

t = time elapsed

M = total mass of salt/unit area

Assuming the simple model of diffusion from a thin brine into an overlying thick body of freshwater, as outlined previously, the age of the diffusion cell can be solved (Wilson, 1964) by:

$$t = \frac{h_2^2 - h_1^2}{4D\,(\ln C_1 - \ln C_2)} \qquad (2)$$

Ages were calculated for the cell extending from 9 m depth to the bottom (Fig. 3.13), using Cl^-, K^+, and Na^+ concentrations. D values for the ions were obtained from Berner (1980) and are listed along with the calcalated ages in table 3.4.

Table 3.4 Diffusion ages calculated for individual ions using equation (2). D values are obtained from Berner (1980).

IONS	D VALUE (10^{-6} cm^2 sec^{-1})	AGE (years)
Cl^-	11.5	648
Na^+	8.0	1242
K^+	11.4	1240

The above ages are calculated on the diffusivity of sole ions. Usually ions diffuse as a salt i.e. NaCl and KCl. Therefore the diffusion age of the lake is somewhere between the anion and cation ages, i.e. about 1000 years.

3.5 CARBONATE CHEMISTRY

3.5.1 *GENERAL PRINCIPLES*

In dissolved carbonate equilibria six solute components are involved, CO_2, H_2CO_3, HCO_3^-, CO_3^{2-}, H^+, OH^- (Stumm and Morgan, 1981). Their inter-relationships are shown in Fig. 3.15.

Fig. 3.15 The inter-relationships for the system CO_2 - H_2O - $CaCO_3$ in the solid, liquid and gas phases. (From Roques, 1969)

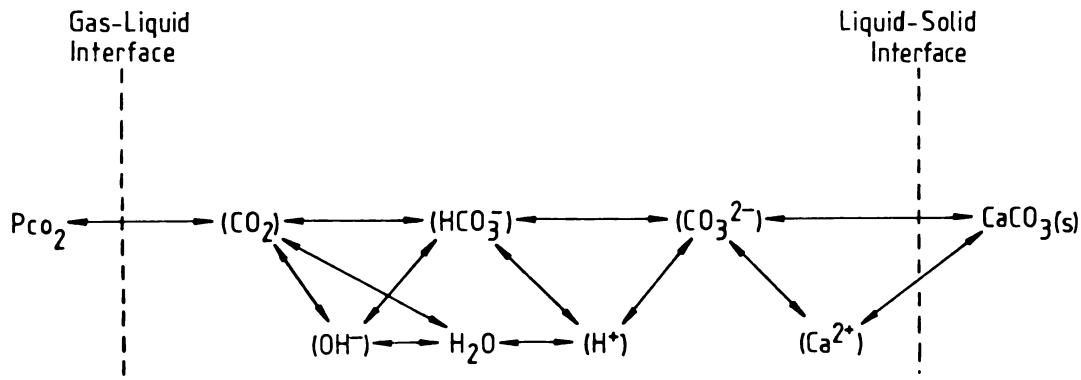

The system is defined by five equilibria (Garrels and Christ, 1965):

$$\frac{[Ca^{2+}]\ [CO_3^{2-}]}{[CaCO_3]} = K_{CaCO_3} = K_{sp} \qquad (3)$$

$$\frac{[H^+]\ [HCO_3^-]}{[H_2CO_3]} = K_{H_2CO_3} \qquad (4)$$

$$\frac{[H^+]\ [CO_3^{2-}]}{[HCO_3^-]} = K_{HCO_3^-} = K_2 \qquad (5)$$

$$\frac{[H_2CO_3]}{P_{CO_2(g)}} = K_{CO_2} \qquad (6)$$

$$\frac{[H^+]\ [OH^-]}{[H_2O]} = K_w \qquad (7)$$

In determining the distribution of species two equilibrium models are used: (i) A system closed to the atmosphere, and (ii) a system open to the atmosphere.

In open systems the equilibrium between the gas and solution phases has to be considered. In such systems P_{CO_2} and $CO_{2(g)}$ are interrelated by Henry's Law*, such that, when the aqueous system is in equilibrium

---

* $CO_{2(g)} \quad CO_{2(aq)}$

Assuming ideal behaviour:

$$K_H = [CO_{2(aq)}] \ / \ [CO_{2(g)}] \ / \ RT = \text{Henry's Law constant}$$

and

$$[CO_{2(g)}] = P_{CO_2} \ / \ RT$$

$$[CO_{2(aq)}] = \frac{[CO_{2(aq)}] \ / \ [CO_{2(g)}]}{RT} \cdot P_{CO_2} = K_H \cdot P_{CO_2}$$

with the gas phase then the P_{CO_2} of the gas in solution is equal to the P_{CO_2} in the gas phase. Simple models for the system are outlined in Garrels and Christ (1965), and Stumm and Morgan (1981).

Open systems predominate in nature. The most frequently studied systems are in caves (e.g., Ingle-Smith (1962), Roques (1969), McCabe (1977)) and ocean waters (e.g., Li *et al.*, (1969), Pytkowicz (1963, 1965, 1973, 1975), Edmond and Gieskes (1970), Morse and Berner (1979), Berner (1976), Berner and Wilde (1972), Berner and Morse (1974)). Usually solubility saturation determinations involve the use of ion activities and equilibrium ion activity products. For seawater a separate procedure for calculating carbonate species has been established (Berner, 1980). This is a semi-empirical approach (Morse and Berner, 1979) where instead of using thermodynamically derived activity equilibrium constants, published values of directly measured concentration equilibrium constants for a given temperature, pressure and salinity are used (Berner, 1980). Constants are in terms of total molalities because of problems in the determination of activity coefficients for Ca^{2+} and CO_3^{2-} ions and, concommitant effects of pressure and temperature. Much of the problem stems from the breakdown of the Debye-Hückel theory at high concentrations. However, there are other problems such as the differences in the definition of the constants between different workers. The variations arise from differences in techniques used to measure the constants (Edmond and Gieskes, 1970).

It seems therefore that to calculate parameters of a carbonate system one must select a scheme which best suits the environmental conditions and the raw data. Edmond and Gieskes (1970) used the constants of Leyman (1957; cited in Edmond and Geiskes, 1970) on Σ_{CO_2}, P_{CO_2} and chlorinity data at known temperature and pressure. These were used to calculate pH and saturation Ca^{2+} concentration as well as the ionization fractions. In their calculations Morse and Berner (1979) differentiate

between measured pH and *in situ* pH.

Closed systems are not as common in nature. Such systems include laboratory acid-base titrations, some ground waters and, to a lesser extent very deep ocean waters. As such systems are closed to the atmosphere H_2CO_3 is treated as a non-volatile acid (Stumm and Morgan, 1981), where

$$[H_2CO_3^*] = [CO_{2(aq)}] + [H_2CO_3] \text{ (Stumm and Morgan, 1981)} \quad (8)$$

This $CO_{2(aq)}$ is not in equilibrium with atmospheric CO_2, therefore Henry's Law relating CO_2 to P_{CO_2} of the atmosphere cannot be applied. For this situation Stumm and Morgan (1981) define:

$$\frac{[CO_{2aq}]}{[H_2CO_3]} = K \quad (9)$$

$$\frac{[H^+]\ [HCO_3^-]}{[H_2CO_3^*]} = K_1 \quad (10)$$

which when used in comination with equations (4), (5), and (7) describe the equilibrium in a closed system. The concentration of $CO_{2(aq)}$ is nearly identical to the measured concentration of $H_2CO_3^*$ (Stumm and Morgan, 1981).

3.5.2 *CALCULATION OF LAKE FRYXELL CARBONATE DATA*

As the lake's permanent ice cover and chemical stratification would reduce exchange with the atmosphere considerably the lake is treated as in a closed system. Hence the equilibria defined by equations (4), (5), (7), (8), (9) and (10) are used. Numerical values for K_1 and K_2 at various temperatures are listed in Stumm and Morgan (1981), from which K_1 and K_2 values for the water column are graphically interpolated. Having thus corrected for temperature the values are also adjusted for

ionic strength and total pressure.

Ionic strength (I) is obtained from:

$$I = \tfrac{1}{2} \Sigma C_i . Z_i^2 \qquad (11)$$

where:

C_i = measured concentration of species i

Z_i = ionic charge of species i

In this determination Fe^{2+}, Mn^{2+}, NO_3^{2-}, and PO_4^{2-} make negligible contributions. SO_4^{2-}, NO_3^{2-} and PO_4^{2} concentrations were obtained from Torii *et al.* (1975). Since HCO_3^- comprises the bulk of the ΣCO_2, the ΣCO_2 values were averaged over the three samplings to estimate the HCO_3^- concentration. The calculation yields values for the ionic strength (I) ranging from 0.03 at 5 m to 0.20 at 17 m depth.

K_1 and K_2 values at each depth were corrected for salinity using the equations of Larsen and Buswell (1942), viz:

$$pK_1^1 = pK_1 - \frac{0.5\sqrt{I}}{(1 + 1.4\sqrt{I})} \qquad (12)$$

and

$$pK_2^1 = pK_2 - \frac{2\sqrt{I}}{(1 + 1.4\sqrt{I})} \qquad (13)$$

In a body of water there is approximately one atmosphere increase in pressure for every 10 m depth. This can have a significant effect on the equilibrium of the system. Total pressures are calculated from:

$$p = \rho.g.h \text{ (Pascals)} \qquad (14)$$

where

$\rho = 1 \times 10^{-3}$ g. kg^{-1}

$g = 9.8$ m.sec^{-2}

h = height of the water colume. (This was measured from the top of the ice; ρ for the ice was assumed $\approx 1 \times 10^3 g.kg^{-1}$).

The effects of these pressures on the equilibrium constants were evaluated using a Van't Hoff equation (Stumm and Morgan, 1981):

$$\ln \frac{K_1}{K_1^1} = \frac{\Delta V^o}{RT} \cdot (P_2 - P_1) \qquad (15)$$

where:

K_1^1 = K with I and T adjustments only

K_1 = final pressure adjusted K

ΔV^o = partial molas volume change for the reaction

for K_1, $\Delta V^o = -19\ cm^3.mol^{-1}$

for K_2, $\Delta V^o = -10.7\ cm^3.mol^{-1}$

} Li *et al.* (1975)

R = gas constant = 8.314 $mol^{-1}.K^{-1}$

P_1 = atmospheric pressure, Pascals

P_2 = pressure at the depth of interest, Pascals.

The above treatment provided the K_1 and K_2 values used in determining the ionization fractions. The equations for the ionization fractions come from Stumm and Morgan (1981):

$$[H_2CO_3^*] = \Sigma CO_2.\alpha_o \qquad (16)$$

$$[HCO_3^-] = \Sigma CO_2.\alpha_1 \qquad (17)$$

$$[CO_3^{2-}] = \Sigma CO_2.\alpha_2 \qquad (18)$$

where:

$$\alpha_o = (1 + (K_1 / [H^+]) + K_1.K_2 / [H^+]^2)^{-1} \qquad (19)$$

$$\alpha_1 = (1 + ([H^+] / K_1) + K_2 / [H^+])^{-1} \qquad (20)$$

$$\alpha_2 = ([H^+]^2 / K_1.K_2 + ([H^+] / K_2) + 1)^{-1} \quad (21)$$

The concentration condition required is:

$$\Sigma CO_2 = [H_2CO_3^*] + [HCO_3^-] + [CO_2] \quad (22)$$

$[H^+]$ is determined from pH by:

$$[H^+] = \gamma_{H^+} \; 10^{-pH} \quad (23)$$

Solubility calculations are in terms of activities as this gives a more accurate description of the system than using absolute concentrations. Activities are related to concentrations by:

$$\{i\} = [i].\gamma_i \quad (24)$$

where:

γ_i = the activity coefficient of component i

γ's are calculated using the Güntelberg approximation:

$$\log \gamma = \frac{-Az^2 \sqrt{I}}{1 + \sqrt{I}} \quad (25)$$

where:

A = 0.5

I = ionic strength

z = charge of the ion

This provides the mean activity coefficients ($\gamma\pm$) for both Ca^{2+} and CO_3^{2-}. The technique, however, becomes progressively more inaccurate as I > 0.1. More complicated treatments for greater ionic strengths are available, but these have not been used since values obtained by the above treatment for I = 0.2 compare well with those of Whitfield (1975). Whitfield calculated single-ion activity coefficients for sea water mixtures of particular ionic strengths using the Bronsted-Guggenheim

hypothesis of specific ion interaction, and the ionic interaction equations of Pitzer. K_{sp} values (equation (3)) were adjusted for temperature and pressure in the same manner as K_1 and K_2*. These values, which were for both calcite and aragonite were converted to equilibrium ion activity (solubility) products (Berner, 1980) by multiplying by $\gamma\pm^2$

3.5.3 *SOLUBILITY INTERPRETATIONS*

Ionization fractions for the 3 sampling periods have been calculated using equations (16), (17) and (18) and are plotted in Fig. 3.16. The end of season profile was obtained by averaging ΣCO_2 from initial and mid season profiles. Important points are summarized as follows:

(i) $[HCO_3^-]$ and $[H_2CO_3^*]$ values are of similar magnitude, and $[CO_3^{2-}]$ concentrations are low. The $[CO_3^{2-}]$ has the most erratic profile with the major profile differences in bottom waters.

(ii) Discrepancies between samplings are large and difficult to explain by fluxes of C into or out of the lake. The lake ice cover and the stability imparted to the water column by the chemical stratification would prevent significant diffusion of C through the water colume. P_{O_2} levels indicate that differences are not of biological origin. Therefore it is more likely that the differences in C reflect difficulties in standardization.

(iii) Comparison of IAP and equilibrium activity products (solubility product) (Fig. 3.17) indicates the thermodynamic feasibility of calcite precipitation to be mainly in the euphotic zone. The water column is undersaturated with respect to aragonite. This finding is supported by the presence of calcite flakes (section 4.2.3) on the lake bed.

---

* Original K_{sp} value = $10^{-8.35}$ (Krauskopf, 1979)
Temperature factor evaluated from $\ln K_2/K_1 = \Delta H^o/R\ (1/T_1 - 1/T_2)$
where $\Delta H^o = -12530\ J.mol^{-1}$, calculated from data in Stumm and Morgan (1981).
Pressure correction, $\Delta V^o = -58.3\ cm^3\ mol^{-1}$ Owen and Brinkley (1941).

Figure 3.16 Carbonate ionization fractions calculated from equations (16), (17), (18). H_2CO_3* (3.16a) and HCO_3^- (3.16b) increase with depth, whereas CO_3^{2-}(c) has an erratic profile.

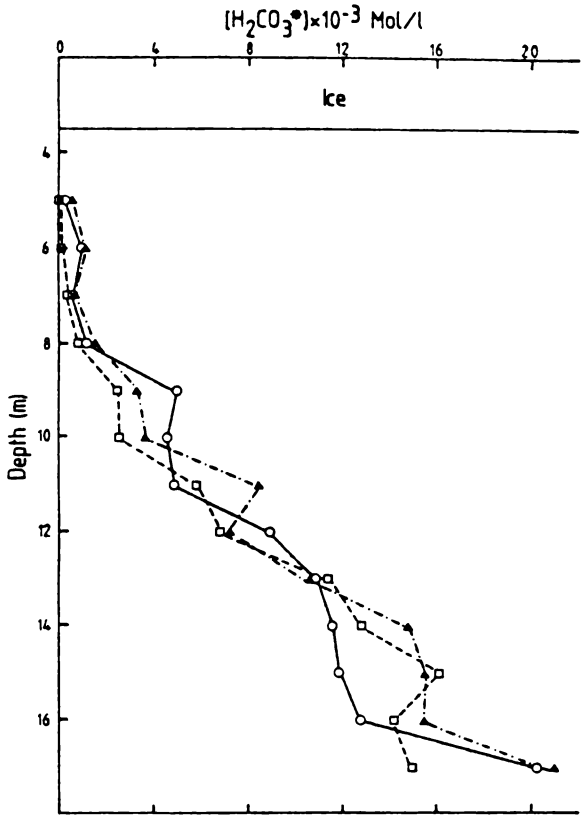

Fig 3.16a

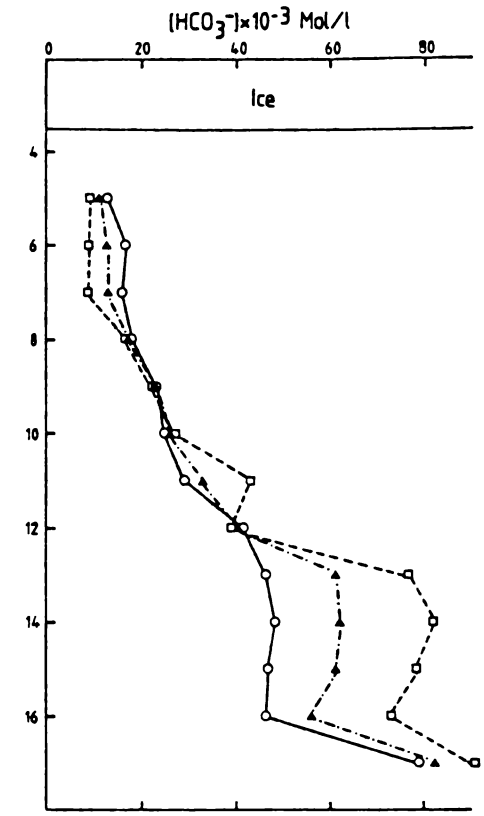

Fig 3.16b

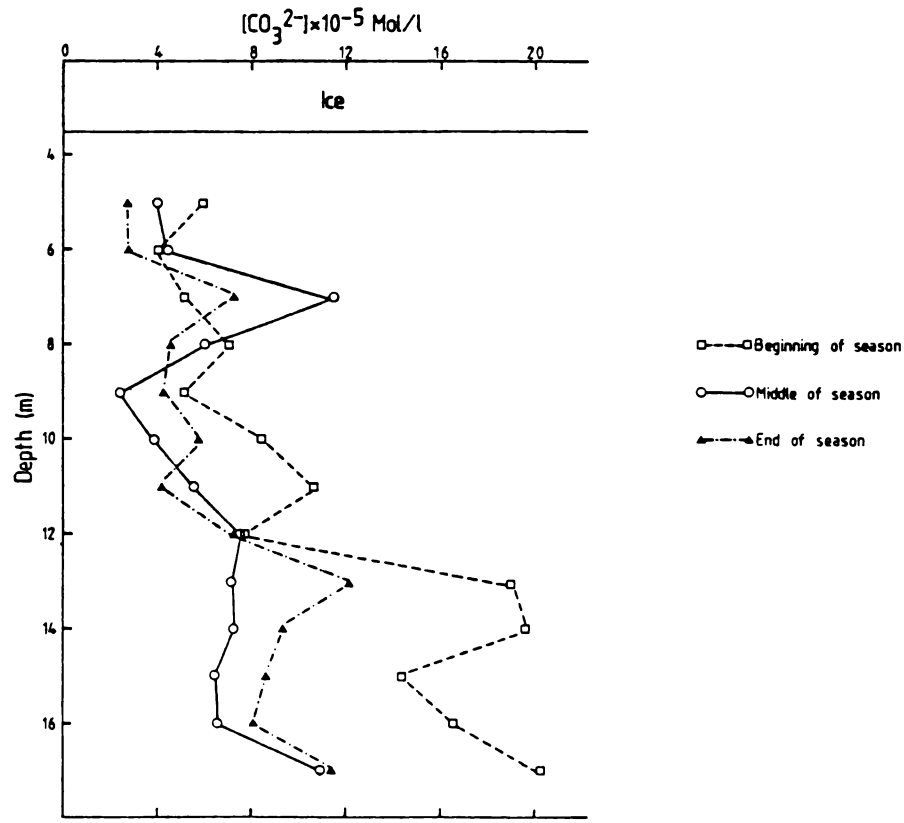

Fig. 3.16c

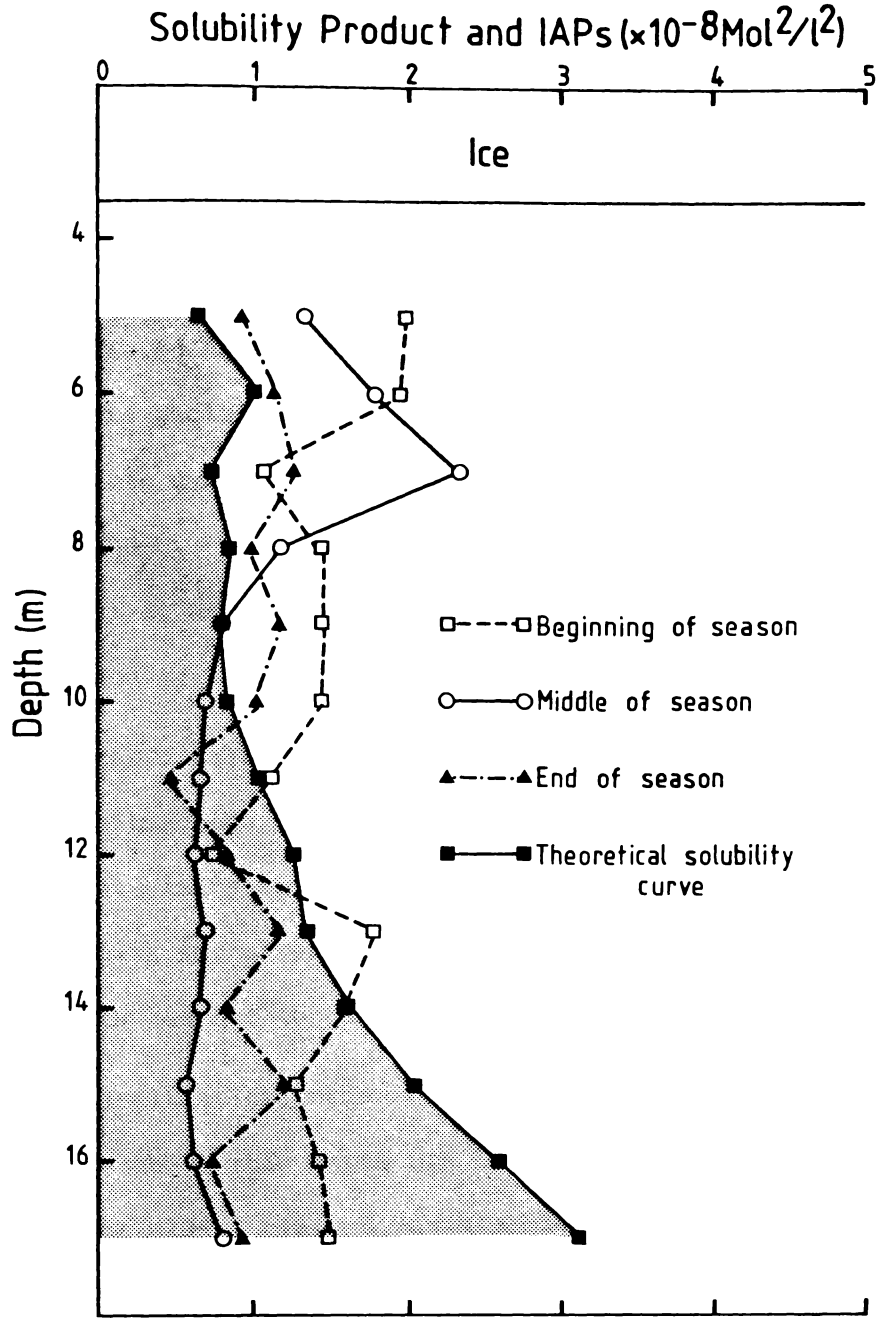

Fig. 3.17 Calcite solubility profile for Lake Fryxell. The stippled area indicates undersaturation. The calcite precipitation reaction is thermodynamically feasible mainly in the euphotic zone.

3.6 DISCUSSION

Lake Fryxell can be considered as a stratified amictic lake with an upper euphotic zone and a lower anaerobic zone. The dissolved materials in the lake water are derived from a number of sources with marine origins predominating (Keys and Williams, 1981).

The calculated diffusion cell age indicates that the present system in the waters is geologically very recent, therefore implying that the present carbonate system is younger still. Considering this together with the age and quantity of calcium carbonate sediments in lake cores (Section 4.2.3) it appears that the major depletion of Ca^{2+} is a much older phenomenon.

The carbonate data indicate saturation with respect to calcite down to 10 m for initial and end of season sampling and to 7.5 m for mid-season samples. lAP's show a drop at 6 m but then peak at 7 m. The size of this peak increases with the progression of summer. There is no saturation with respect to aragonite.

As a generalization, organisms below about 10 m depth are CO_2 evolvers and those above this depth are CO_2 fixers (H. Morgan, pers. comm., 1982). Vincent (1981) claimed maximum biomass accumlation occurred in early summer, prior to sampling. During the course of the season the biomass between 8 and 10 m depth declined. The mid euphotic zone (6-7 m) remained a zone of nett production. The increasing predominance of CO_2 fixation in the mid euphotic zone explains the upward movement of the $[CO_3^{2-}]$ peak.

There are differences between concentrations of salts in the streams (Table 3.3) and surface waters of the lake (Appendix II). There are two possible explanations for this: the first is that diffusive mixing, in fact, extends to surface waters. As the sides of the lake flatten out at shallow depths solution of the diffusion equation becomes complex.

This possibility remains unverified. The other possibility is that evaporation and/or freeze concentration of upper lake waters has occurred. Therefore evaporation increases the alkalinity [A], which is defined as the excess of positive changes over the anions of strong acids (Stumm and Morgan, 1981):

$$[A] = [Na^+] + [K^+] + 2\ [Ca^{2+}] + 2\ [Mg^{2+}] + \ldots - [Cl^-] - 2\ [SO_4^{2-}] - [NO_3^-] \ldots \quad (26)$$

Assuming the latter process the effect of evaporative concentration on the carbonate system can be assessed. The CO_2 concentration of the waters depends on the pH, (Ingle-Smith, 1962) and ΣCO_2 (Broecker, 1974), but its removal will not affect A (Stumm and Morgan, 1981). pH is dependent upon the alkalinity (equation 27).

$$10^{-pH} = P_{CO_2} . K_1 \ / \ A \quad \text{(Broecker and Oversby, 1971)} \quad (27)$$

Therefore combining (27) and the following equation (Broecker, 1974)

$$P_{CO_2} = \frac{1}{\alpha K} \frac{(2\ \Sigma CO_2 - A)^2}{A - \Sigma CO_2} \quad (28)$$

where:

α = CO_2 solubility

$K = \frac{K_1}{K_2}$

and K_1 = equation 5

K_2 = equation 10

we get

$$10^{-pH} = \frac{K_2}{A\alpha} \cdot \frac{(2\Sigma CO_2 - A)^2}{(A - \Sigma CO_2)} \quad (29)$$

Evaporation of the lake water would increase A, and ΣCO_2 so if evaporative concentration without precipitation occurs the pH remains

the same because the solution is still buffered. Should the evaporation cause precipitation, then $CaCO_3$ will be removed, which will decrease both A and ΣCO_2. The factors by which both A and ΣCO_2 decrease will be the same. If, for the sake of argument, A and ΣCO_2 decrease by a factor of 2, then from equation (29) we get:

$$10^{-pH} = \frac{K_2}{2A} \cdot \frac{(2 \times 2\Sigma CO_2 - 2A)^2}{(2A - 2\Sigma CO_2)} \qquad (30)$$

This indicates that the pH must rise since the $2\Sigma CO_2$ will decrease twice as fast as A. P_{CO_2} will also drop. These above considerations apply to the lake with an ice cover.

The argument can be advanced one stage further to a situation where evaporation has concentrated the lake water solutes enough to preclude ice formation. In this case the water will be in direct contact with the atmosphere and CO_2 will be rapidly lost. This will increase the pH and increase the precipitation of $CaCO_3$.

Thermodynamic arguments thus indicate the feasibility of calcite precipitation in the euphotic zone. X-ray diffractograms of suspended sediments indicate the presence of calcite in the water column below 8 m depth. The $\delta^{13}C$ values of lake bed carbonate flakes at the top of sediment cores (Section 4.2.3) are close to $\delta^{13}C$ values for waters between 8 and 9 m. Combining these lines of evidence, and assuming the carbonates form in isotopic equilibrium with the waters, then the calcite is precipitated within the 8 to 9 m depth interval.

Other carbonate reactions were also investigated, namely:

$Ba^{2+} + CO_3^{2-}$ $BaCO_3$ (witherite)

$Mg^{2+} + CO_3^{2-}$ $MgCO_3$ (magnesite)

$Sr^{2+} + CO_3^{2-}$ $SrCO_3$ (strontianite).

Witherite initially appeared the most likely precipitate because, plots

of Ba/Cl against depth in the water column have a different slope from element ratios for ions less likely to participate in reactions (e.g. Na/Cl. C.H. Hendy, pers. comm., 1982). The Ba/Ca ratio in the water column is at most 1.5 times the Sr/Ca ratio, compared to an average 4 times the Sr/Ca ratio in the surface calcite flakes in the sediments. The preference for Ba over Sr is contrary to the expected distribution coefficient for inclusion in the calcite lattice. Therefore this suggests either co-precipitation or a competing precipitation reaction. Applying the same thermodynamic treatment to the above reactions, as for calcite, it is found that none of them are thermodynamically feasible. This is supported by the absence of these carbonates in X-ray diffractograms of either suspended or lake bottom sediments.

A kinetic treatment of the system has also been attempted. The rate of change of concentration of carbonate species with time (dC/dt) can be expressed as a balance between the precipitation and dissolution reactions. Thus (modified from Lerman, 1979).

$$dc/dt = -k_4 (C_s - C)^4 + k_2 (C_s - C)^2 \quad (31)$$

where:

C_s = the Ca^{2+} concentration to which the solution tends with time (i.e. concentration below 9 m depth)

C = the Ca^{2+} concentration of the solution (at 9 m)

k_2 = rate constant for the dissolution reaction

k_4 = rate constant for the precipitation reaction

Precipitation is a 4th order process and dissolution is 2nd order. To determine k_2 a value for the activation energy for dissolution is obtained from equation (32) (Frost and Pearson, 1961):

$$k_{act} = A.\exp. \frac{-E^*}{RT} \quad (32)$$

where:

A = collision frequency factor for a bimolecular reaction

$= 10^{15}$ $cm^3.mol^{-1}.sec^{-1}$

k_{act} = 0.031 $cm.sec^{-1}$ at 25°C (Plummer and Wrigley, 1976)

R = gas constant = 8.314 $J.mol^{-1}$ K^{-1}

T = 298°K

E^* = activation energy

This yielded $E^* = 9.4229 \times 10^4$ J. When resubstituted into equation (32), using the temperature in the lake, this E^* value gave $k_2 = 0.001602$. k_4 is evaluated from equation (33):

$$K_{sp} = \frac{k_4}{k_2} \qquad (33)$$

$$k_4 = 1.055 \times 10^{-11}$$

The treatment shows that the dissolution process clearly predominates, irrespective of the concentrations used. This may be in part due to the magnitude of the constants used (equations (32) and (33)). S.E. Micrographs of calcites (Fig. 3.18) support the conclusion that calcites in bottom waters are dissolving. The crystals appear broken and rounded. Obviously a purely inorganic treatment does not provide a complete picture because rate constants are affected by biological interaction.

Algae, mainly cyanobacteria (blue-green algae) (Wharton *et al.*, 1982) and possibly photosynthetic bacteria (C.G. Harfoot, pers. comm.) are the most likely possible sources of any such interaction. In the case of cyanobacteria there are 3 types of metabolism: (i) oxygenic photosynthesis, (ii) anoxygenic photosynthesis and (iii) heterotrophy.

(i) Oxygenic photosynthesis involves the fixation of CO_2 to cellular organic carbon (CH_2O). Both photosystem I and photosystem II are required to generate the reductant (NADPH) and the energy (ATP),

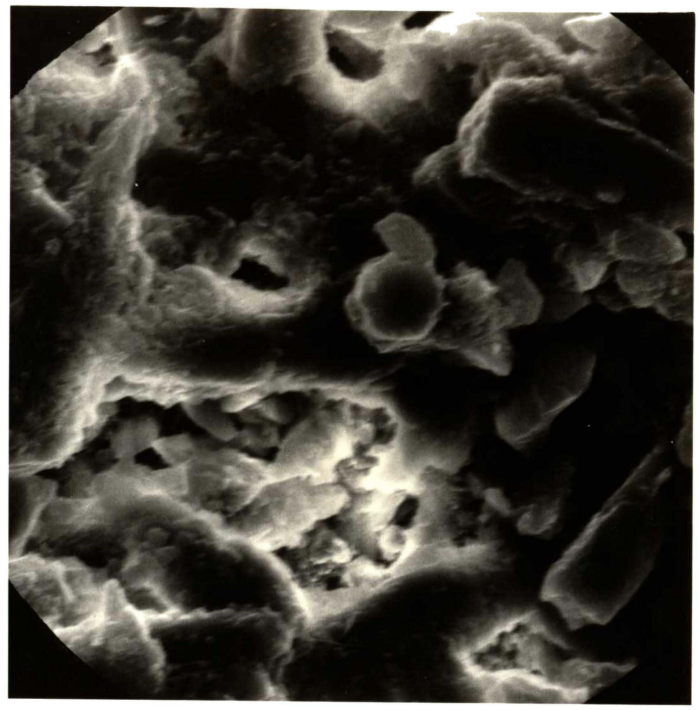

Figure 3.18 Scanning electron micrograph of the surface of a precipitated calcite flake. The expected rhombic structures show rounding indicative of dissolution.

by way of non-cyclic photophosphorylation. Electrons for this process are ultimately derived from water. The reaction is summarized as follows:

$$2H_2O \rightarrow 4H^+ + 4\bar{e} + O_2 \quad \text{- (Photosystem II)}$$

$$CO_2 + 4H^+ + 4\bar{e} \rightarrow CH_2O + H_2O \quad \text{- (Photosystem I)}$$

Under dim light conditions (or light >700 nm wavelength) only photosystem I operates. Under such conditions only ATP is generated, and no NADPH (reducing power).

(ii) Anoxygenic photosynthesis utilizes photosystem I only to fix CO_2. ATP is generated from cyclic photophosphorylation and reducing power is generated from electrons from S^{2-}, i.e.

$$2S^{2-} \rightarrow 2S^{o} + 4\bar{e}$$

$$CO_2 + 4\bar{e} + 4H^+ \rightarrow CH_2O + H_2O$$

Cyanobacteria are capable of both oxygenic and anoxygenic photosynthesis.

(iii) Heterotrophic metabolism involves the synthesis of cellular material from pre-formed organic compounds derived from their metabolism by other micro-organisms. Energy is obtained by respiration in the presence of O_2 or fermentation in its absence. The latter process results in the production of organic acids and other small organic molecules. Of the 3 metabolic processes heterotrophy is the only one which can occur throughout the water column.

The photosynthetic bacteria are not capable of oxygenic photosynthesis, but 2 groups (the *Chromatiaceae* and the *Chlorobiaceae*) use S^{2-} of S^{o} in conjunction with photosystem I. A third group (the *Rhodospirillaceae*) use either reduced organic compounds in conjunction with

photosystem I, or direct photo-assimilation of organic compounds.

The importance of biological activity in Lake Fryxell, carbonate precipitation has been demonstrated. The extent of the influence the above processes have is difficult to assess. However, evidence presented in this study indicates that precipitation occurs in the euphotic zone, with resultant precipitates falling through the water column. These carbonate precipitates arise as a result of oxygenic algal metabolism and are not skeletal. The morphology of calcite in sediments below the euphotic zone shows forms typical of inorganic precipitates and does not show intercalated algal material.

In shallow waters, where the euphotic zone intersects the lake bed, a slightly different picture emerges. From work on Lakes Hoare and Fryxell, Parker and Simmons (1981), Parker *et al.*, (1981) and Wharton *et al.*, (1982) claim that stromatolites are forming. Stromatolites are defined by Walter (1976, p.1).

> "Stromatolites are organosedimentary structures produced by sediment trapping, binding, and/or precipitation as a result of the growth and metabolic activity of micro-organisms, principally cyanophytes (blue-green algae)".

Parker *et al.*, (1981) and Wharton *et al.*, (1982) describe "columnar-stratiform algal mats" in Lakes Hoare and Fryxell consisting primarily of *Phormidium frigidum* . The columnar morphology is a shallow water phenomenon and is caused by the trapping of photosynthetically produced O_2 which can also cause the algae to become buoyant and lift off the lake bed (Parker *et al.*, 1982). Those authors found calcite attached to the bottom surface of buoyed algal mats. Like Wharton *et al.* (1982) this study found some nodular or "vertical" calcite structures in shallow (euphotic zone) cores in Lake Fryxell but none in deep (anarobic) water cores.

Cyanobacterial mats with stratiform morphology are found in deep anaerobic waters (Parker and Simmons, 1981, Wharton *et al.*, 1982, Wharton pers. comm., 1982). They are claimed to be photoautotrophic i.e. presently photosynthesizing (Parker and Simmons, 1981) which means either using anoxygenic photosynthesis S^{2-} as an electron donor for cyclic photophosphorylation, or heterotrophic metabolism. Wharton *et al.* (1982) show there to be 0% transmission of 400 - 700 nm wavelength light below 14 m depth suggesting anoxygenic photosynthesis to be unlikely. Anoxygenic photosynthesis removes CO_2 which increases pH and may cause $CaCO_3$ precipitation, as does oxygenic photosynthesis (which is unlikely here as there is no O_2 present in deep waters). Therefore stromatolite formation as a result of photosynthesis in depths greater than 14 m is unlikely. Heterotrophic metabolism in cyanobacteria has been demonstrated *in vitro*, but its significance *in vivo* is uncertain particularly in anaerobic conditions where energy generation is inefficient. There would also be extensive competition for organic substrates with heterotrophic bacteria, including those that respire such substrates using SO_4^{2-} as an electron acceptor. Even if the cyanobacteria could heterotrophically metabolise successfully their role in *in situ* carbonate precipitation would be debatable as such metabolism does not raise the pH by CO_2 removal.

Alternatively, metabolizing cells in deep water algal mats may be non-photosynthetic ones, with photosynthetic cells dormant. If cultured in a lab the dormant cells may recommence metabolsing and hence give an inaccurate picture of the *in situ* mats (K. Thompson, pers. comm., 1982).

Anaerobic sulphate-reducing bacteria such as *Desulfouibrio desulfuricans*, are capable of precipitating $CaCO_3$ by the following reactions (Cole, 1979):

$$CaSO_4 + 2C \rightarrow CaS + 2CO_2$$

and

$$CaS + CO_2 + H_2O \rightarrow CaCO_3 + H_2S$$

Whether such reactions have significant effects on the Lake Fryxell bottom water carbonate system is unknown.

Members of the 3 bacterial groups (*Chromatiaceae, Chlorobiaceae* and *Rhodospirillaecea*) have been demonstrated to occur in the anaerobic zone of water column and the sediments of Lake Fryxell (C.G. Harfoot, pers. comm.). In the anaerobic illuminated zone it is possible that anoxygenic photosynthesis by these 3 groups would make a larger contribution than cyanobacteria to any possible carbonate precipitation. Any heterotrophic metabolism if fermentative may counter these effects by the production of organic acids which would tend to dissolve carbonate. A band of bacteriochlorophyll has been demonstrated at 8.85 m depth in the upper anaerobic zone of Lake Fryxell (Rawley, 1982) which may also contribute to cyanobacterial effects on carbonate precipitation.

Therefore carbonate precipitation at Lake Fryxell is primarily a euphotic zone phenomenon resulting in pelagic sedimentation of precipitated calcite in deeper waters and stromatolite formation in shallow waters. Some *in situ* deep water precipitation may occur but cannot be proven further through lack of evidence. The major problem is that little chlorophyl breakdown occurs in the bottom sediments, making it difficult to determine the nature of algal mats in deep waters (K. Thompson, pers. comm., 1982). The possible biological effects are summarized in Fig. 3.19.

3.7 CONCLUSIONS

(1) Lake Fryxell is a chemically stratified amictic lake with a mesothermal temperature profile. Solar radiation is the source of heat.

COLUMN	LIGHT INTENSITY	PROCESS	EFFECT ON PRECIPITATION	ORGANISMS
ICE				
EUPHOTIC ZONE	↓	OXYGENIC PHOTOSYNTHESIS	Promotes precipitation	CYANOBACTERIA
	↓	PHOTOSYSTEMS I and II		"Bacteriochlorophylls."
	↓	Heterotrophy	Probably insignificant	?
UPPER ANAEROBIC ZONE	↓	ANOXYGENIC PHOTOSYNTHESIS	May cause some	Cyanobacteria
	↓	Photosystem I	precipitation	Bacteria (*Rhodoc.*, *Chromat.*, *Chloro.* species)
LOWER ANAEROBIC ZONE		HETEROTROPHY	May cause dissolution	?
		Anoxygenic photosynthesis	Probably none	-
		Heterotrophy	?	cyanobacteria ?
SEDIMENTS		SO_4^{2-} Reduction	?	*Desulfovibrio*

Figure 3.19 A summary diagram of the possible biological effects on the carbonate system in Lake Fryxell. The euphotic zone is taken to mean the zone in which nett photosynthesis occurs, re CO_2 fixation by photosynthesis is equal or greater than CO_2 loss by respiration. In this sense (which is the one used by ecologists who study algal productivity i.e. photosynthesis involving photosystems I and II) the fact that some bacterial photosynthesis occurs anaerobically is ignored.

(2) Lake waters originate from ice meltwaters and their contained salts have a mixed, though predominantly marine origin (Keys and Williams, 1981). Chemical stratification arises from molecular diffusion of a brine and redissolved lake bottom salts up into overlying lake meltwaters. The diffusion age of about 1000 years indicates this to be a geologically recent phenomenon.

(3) $CaCO_3$ in sediment cores (4.2.3), and the Ca^{2+} depletion in the water column (Fig. 3.16), indicates Ca removal by $CaCO_3$ precipitation prior to the establishment of the present chemical stratification.

(4) Precipitation of $CaCO_3$ presently occurs in upper lake waters. Thermodynamic arguments indicate the feasibility of the calcite precipitation reaction above 11 m depth during summer. This is supported by the occurrence of calcite in X-ray diffractograms of suspended sediments. Below 11 m depth chemical precipitation is not thermodynamically feasible and the present kinetic considerations show the predominance of dissolution processes.

(5) The coincidence of algal populations, O_2 peaks, CO_3^{2-} peaks and the $\delta^{13}C$ peak shows the precipitation of calcite to be a biologically induced process. The precipitation is probably restricted to the euphotic zone. The sedimentary expression of this however, is a function of depth of the water column. In shallow waters, where the lake bed lies within the euphotic zone, stromatolites occur, which may form nodular carbonate morphologies. Elsewhere, calcite precipitated within the euphotic zone, over deeper areas, falls from suspension and forms flat layered flakes on the lake bed (4.2.3). Dissolution occurs as the calcite crystals fall through the water column. Aspects of dissolution and possible reprecipitation from deposited carbonates are discussed in greater detail in the following chapter. The *in situ* precipitation of carbonate flakes in deep water is unproven.

CHAPTER FOUR

LAKE FRYXELL SEDIMENTS

4.1 AIMS AND OBJECTIVES

The previous chapter discussed the geochemistry of the lake waters and the present $CaCO_3$ precipitation regime. This chapter describes the lake sediments with the following aims:

1) To interpret the stratigraphic significance of Lake Fryxell deposits. Prior to this study, stratigraphic investigation within the Lake Fryxell basin have concentrated only on the basement rocks and glacial deposits (Haskell *et al.*, 1965, Denton *et al.*, 1971, Stuiver *et al.*, 1981 and others). Kellog *et al.* (1980) have, however, worked on diatoms from perched deltas in the area.

2) To determine the mineralogical and chemical characteristics of any $CaCO_3$ material in cores to assist in interpretations of depositional environment and if possible post-depositional changes. A differentiation between carbonate deposits on a chemical as well as stratigraphic basis is attempted.

The field and laboratory techniques are also outlined.

4.2 STRATIGRAPHY AND SEDIMENTOLOGY

4.2.1 *FIELDWORK*

Fieldwork consisted of the collection of cores of lake sediments. Lake ice cores were also kept to analyse any sediments therein. Core disposal and location are summarized in Table 4.1 and Figure 4.1 respectively.

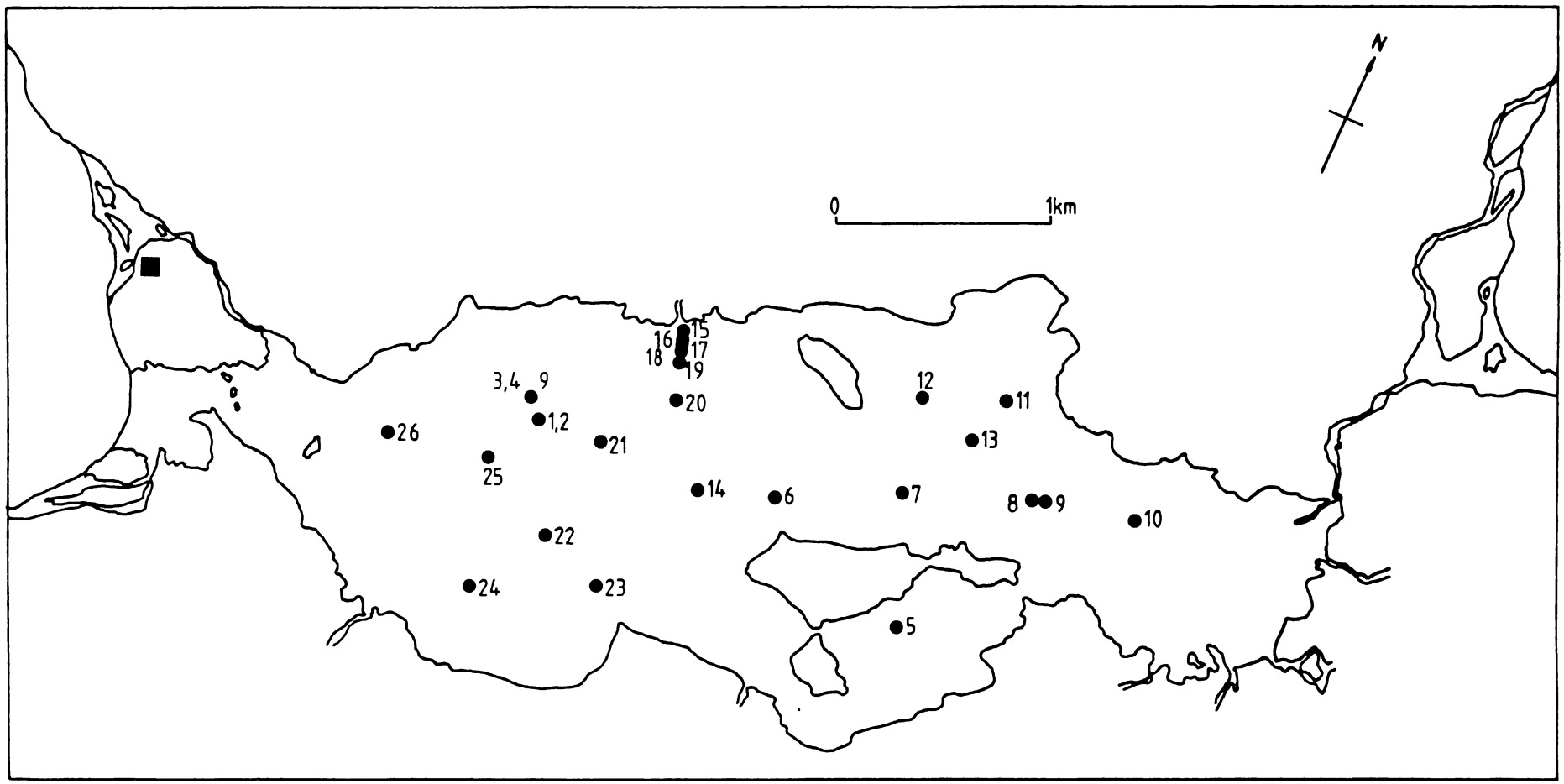

Figure 4.1 Location map of Lake Fryxell coring sites. Cores obtained were numbered according to site. The black square is the campsite.

Table 4.1 Core disposal summary

Holes drilled	Cores lost or not obtained	Cores returned to New Zealand	Cores to other Investigators
26	6	C1,C4,C5,C7,C9,C10, C11,C12,C13,C14, C17,C18,C19,C21, C22,C23,C24,C25, C26	C3-Dr Komura J.A.R.E.

Coring equipment is shown in Figure 4.2. It consists of a 2 m long steel pipe with a sharpened bit. The pipe contains a 4 cm diameter P.V.C. liner. A non return valve at the top of the core liner prevented re-entry of water while the core was being raised, and generally resulted in core retention. The corer is pounded into the sediments using a lead sleeve. A tripod frame is used for raising and lowering the corer. A full description of the corer and its operating procedure is given in the University of Waikato Antarctic Research Report 4.

4.2.2 *LABORATORY WORK*

The laboratory work consisted of:

1) Core description
2) Textural and mineralogical analyses of non-carbonate components
3) Sampling carbonate horizons for mineralogical and geochemical analysis.

1) Core descriptions included: colour using the Standard Soil colour charts (1970); grain size, sorting and rounding estimates using a visual comparator (Appendix III); recognition of any sedimentary structures; and unit differentiation. Units were distinguished mainly on the basis of grain size and structural associations, e.g. alternating coarse and fine laminations in the upper unit; the presence/absence of precipitates; and also colour.

Figure 4.2 Coring gear. Cores were hauled up using the tripod. Under the tripod is the core casing, plastic core liners are in the sledge in the foreground.

2) Grain size analyses follows procedures outlined in Carver (1971, Ingram R.L., Chp. 3, Galehous J.S., Chp. 4). As the same general sequence occurs in all cases, 2 samples of each unit from different cores were analysed. The mineralogy of the non-carbonate and fraction was determined optically from thin-sections. Splits of the bulk sand samples from textural analyses were tipped into moulds containing epoxy resin, stirred to ensure even grain distribtuion, and allowed to settle before the resin set hard. This artificial "rock" was then thin-sectioned for petrographic microscope examination. From these slides the minerals were identified and abundance estimates made. Clay mineral determinations were made on the <4ϕ size fraction by X.R.D. analysis. Aliquots of 2-4 mls of <4ϕ suspension were prepared using the dropper-on-glass-slides technique (Hume, 1978). Initially poor results prompted further attempts using differing methods of particle disagregation and slide preparation: i) Wet sieve and disperse in water only

ii) Wet sieve acidify carbonate with either CH_3COOH or 10% HCl and disperse in water only

iii) (ii) plus removal of organic matter with H_2O_2

iv) Smear-on-glass slide (Hume, 1978) and dropper-on-glass-slide air-dried were also tried.

In all the above cases the samples were washed in water a number of times before final dispersion.

3) Where possible, carbonate units were sampled at top, middle and bottom. Sample positions are listed with core logs in Appendix III. X-ray diffraction was used to estimate the percentage by weight of aragonite and calcite in carbonate horizons, following construction of calibration curves relating peak height to the proportion of each polymorph (cf. Nelson and Cochrane, 1970). Powdered aragonite and calcite admixtures in known proportions were used (Fig. 4.3). The instrument

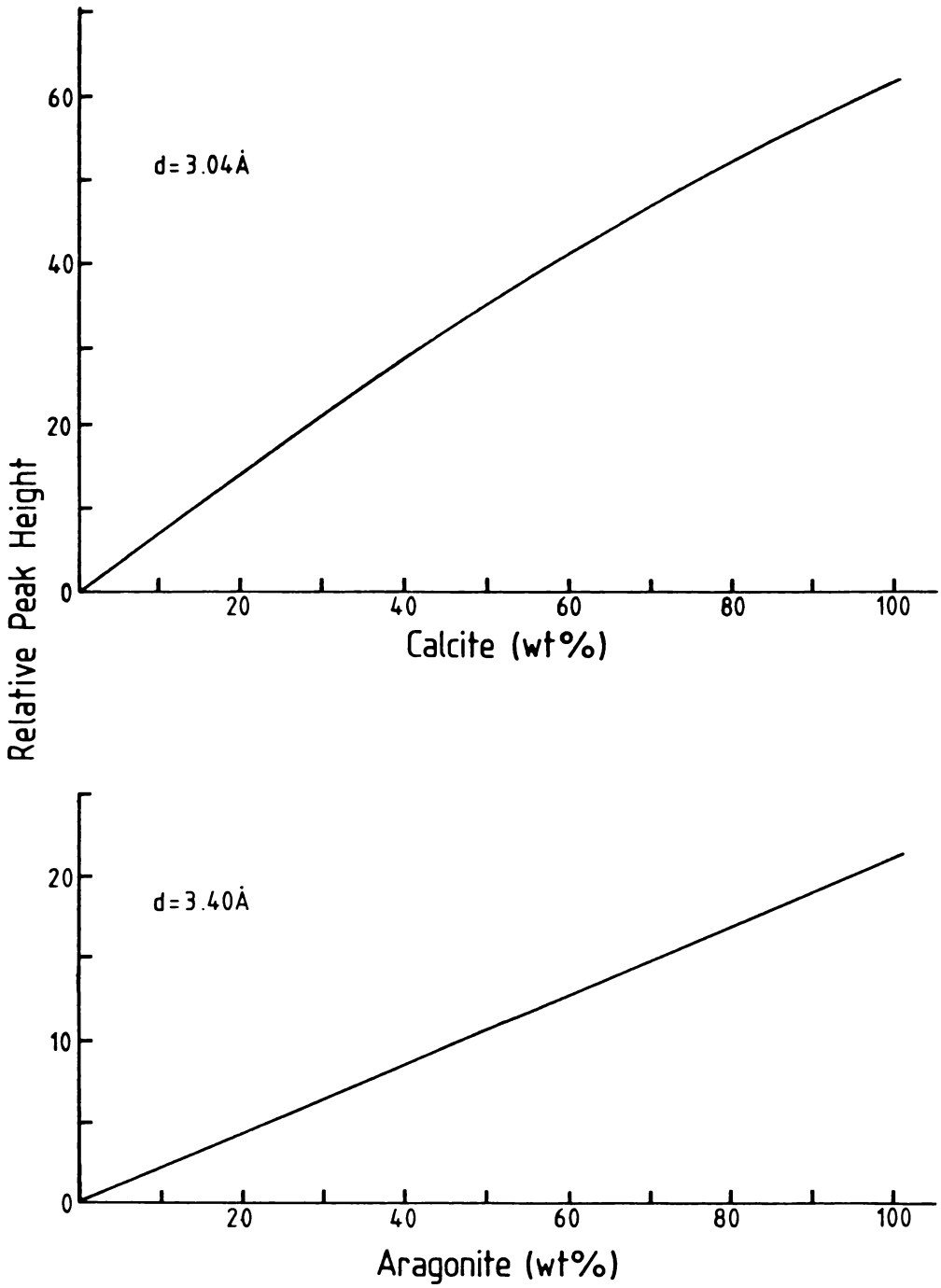

Figure 4.3 XRD calibration curves relating peak height to wt% calcite or aragonite. Peak heights are measured minus background height. KV = 36 mA = 16.

used was a Phillips PW 1130/00 X-Ray Generator. Instrument settings were standardized usually at about 30-36 KV and 16 mA, using a standard of powdered quartz (<4.5ϕ) set in epoxy resin (Hume, 1978). For any sample or standard, peak heights varied by up to 15-20% so at least 3 separate mounts for each sample or standard were used, and the peak heights averaged.

Scanning electron microscopy (S.E.M.) was used to examine the crystal morphology of the carbonates. Samples were attached to brass studs using double-sided cellotape. The whole sample was then coated with 500Å gold/paladium using a Polaron E5000 Diode Sputter Coater. Examination of samples was done using a JEOL-JSM 35 Scanning electron microscope (Dr C. Beltz, pers. comm.).

4.2.3 *STRATIGRAPHY*

The stratigraphy of Lake Fryxell sediment cores consists of 5 distinct units, designated A to E, in the same sequence in all cores. Figure 4.4 shows the lake sediment stratigraphy for a typical core (C12). In 3 cores only an additional unit (unit B_b) occurs and appears to be redeposited material (Refer Appendix III - C4, C7, C13?).

Unit E

The non-carbonate fraction consists of alternating sand-rich and mud-rich layers of variable thickness (Fig. 4.5). Overall, the bulk texture ranges from slightly gravelly mud to slightly gravelly muddy sand (Fig. 4.14). The texture of individual sand layers appears moderately sorted (visual comparator) and grains are subangular to subrounded. Occasional small pebbles occur. Organic matter is associated with mud layers and is derived from water column biota. Sediment colour is generally olive green, grey or black. Upper portions of this unit were disturbed by coring owing to the unconsolidated nature of the sediments. Variations in water depth from probing indicates high water

Figure 4.4 Stratigraphic log of core 12.

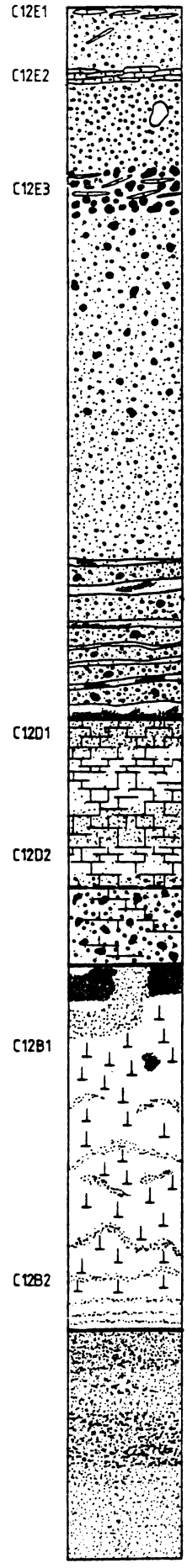

Unit	
	Calcite (79 wt%) flakes, colour 7.5Y 4/3 dark olive.
E	Moderately sorted medium, predominantly quartz sand; with organic material giving a dark olive colour (7.5Y 4/3).
	Calcareous layer (aragonite 40% wt and calcite 51 wt%).
	Medium to coarse grained sand containing 1 medium sized granite pebble.
	Very coarse moderately sorted sand containing organically stained dark olive (7.5Y 4/3) calcite flakes (95 wt%).
	Coarse to muddy calcareous sand, poorly sorted, colour 2.6GY 3/1 dark olive grey.
	Medium to coarse, poorly to moderately sorted sand, 5GY 3/1 dark olive grey.
	Alternating laminations of mud/organic material (10Y 3/2 olive black) with poorly sorted medium to coarse sands.
D	Sharp contact, mud/organic layer 10Y 3/2 olive black.
	Laminated calcite (59 wt%) with high fine sand content, 5GY 3/1 dark olive grey. Fine sand content varies down the unit. Low sand content, N 7/0 greyish white.
	5GY 3/1 dark olive grey.
	100 wt% aragonite.
C	Gradational boundary.
	Very poorly sorted muddy to coarse sand containing fragmentary aragonitic layers.
B	Sharp contact. Organic layer, 10Y 3/2 olive black in a dark olive grey (5GY 4/1) calcareous mud. Fine sand layers become more evident down the unit.
	4 wt% calcite.
	5 GY 4/1 dark olive grey.
	8 wt% calcite, 5GY 4/1 dark olive grey.
A	Reasonably sharp boundary.
	Well sorted fine sand, 10Y 2/1 black.
	5Y 2/2 olive black.
	10Y 2/1 black.

Figure 4.5 Alternating mud-rich and sand-rich layers of the uppermost unit, unit E. Overall bulk sample textures range from slightly gravelly mud to slightly gravelly muddy sand. Individual sand layers appear moderately sorted. Organic matter is associated with the mud layers.

Scale = 1 cm.

Figure 4.6 Scanning electron micrograph of the surface of a calcite flake. The individual crystals occur as randomly oriented irregular laths.

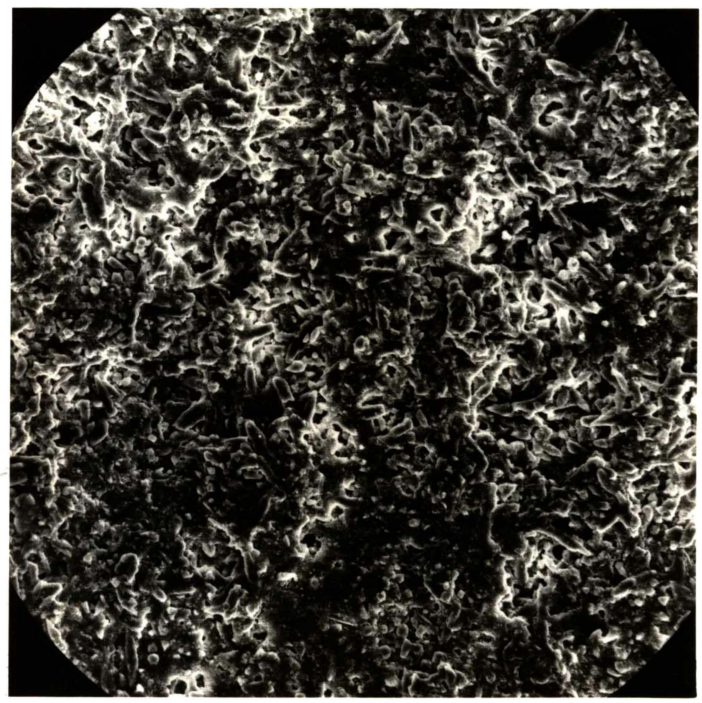

contents in these upper sediments. Non-carbonate mineralogy is summarized in Table 4.2. The rock fragments are predominantly diorites.

Table 4.2 Estimated abundance of non-carbonate minerals in unit E.

Mineral	Estimated Abundance %
Quartz	25
Feldspar (Mainly Plagioclase)	25
Pyroxenes (Augite > Hypersthene)	20
Hornblende	10
Rock Fragments	10
Opaques, Biotite, Volcanic Glass, Chlorite	10

with minor basalt. Both mineralogy and grain size are similar to that for materials obtained from lake ice cores.

Irregularly shaped calcite flakes occur at or near the sediment surface. This is best shown in C21 where the flakes overlie a mud layer, apparently the preserved lake bed. In one shallow water core, nodular calcite morphology occurred suggesting a stromatolitic origin (Wharton *et al.*, 1982). The flakes vary in size from the diameter of the core to only a few millimetres. More than one layer can occur within each flake with the thickness of each layer <1 mm. Flakes are seldom more than 5 mm in total thickness. S.E.M. examination shows that the flakes consist of aggregates of irregular laths about 10 µm diameter (Fig. 4.6). Occasional carbonate layers occur lower in unit E (Fig. 4.4) but are difficult to correlate between cores. Some of the flakes have dark grey to black coatings, possibly sulphides.

Unit D

This is a varve-like, grey to greenish grey carbonate unit with a composite ^{14}C age of 10,410 ± 120 yrs B.P. (Appendix III). The boundary between units E and D is usually sharp and consists of an organic layer

Figure 4.7 The contact between unit E above and D below. The darker grey colour (circled) in the carbonate indicates a muddier carbonate texture than light grey colours.

immediately above the carbonate (Fig. 4.7). The carbonate is primarily aragonite (Table 4.6) with acicular crystal habit (Fig. 4.8). The average length for crystals is about 15 μm. Unit D isopachs thicken away from the centre of the lake (Fig. 4.9).

The varve-like sequences arise from alternations of detrital-rich and detrital-poor sand layers within the carbonate (Fig. 4.10). The sands have similar rounding and mineralogy to sands in unit E. Here rock fragments have metamorphic as well as igneous origins. Some of the volcanic glasses are brown to brown-green.

Unit C

Unit C consists of alternating sands and muds with increasing carbonate at the top as it grades up into unit D (Fig. 4.11). The content of sand diminishes progressively downwards and in some cases where unit C is thin the sand content is minimal. Textures are slightly gravelly muddy sand to sandy mud (Fig. 4.14). Sand mineralogy (Table 4.3) appears to show differences in the relative proportions of minerals to the overlying units. The overall abundance of $CaCO_3$ is not great (<5 wt%) and olive green to black organic material is present.

Table 4.3 Summary of the estimated non-carbonate mineral abundances in unit C

Mineral	Relative Abundance (%)
Quartz	40
Feldspars (mainly plagioclase)	30
Pyroxene (Augite > hypersthene)	25
Volcanic glass, rock fragments	5
Muscovite	Traces

This unit appears to be a transitional unit between the carbonate dominated units D and B.

Figure 4.8 Scanning electron micrograph of acicular argonite from unit D. The average length of crystals is about 15 µm. Photo. - C. Beltz.

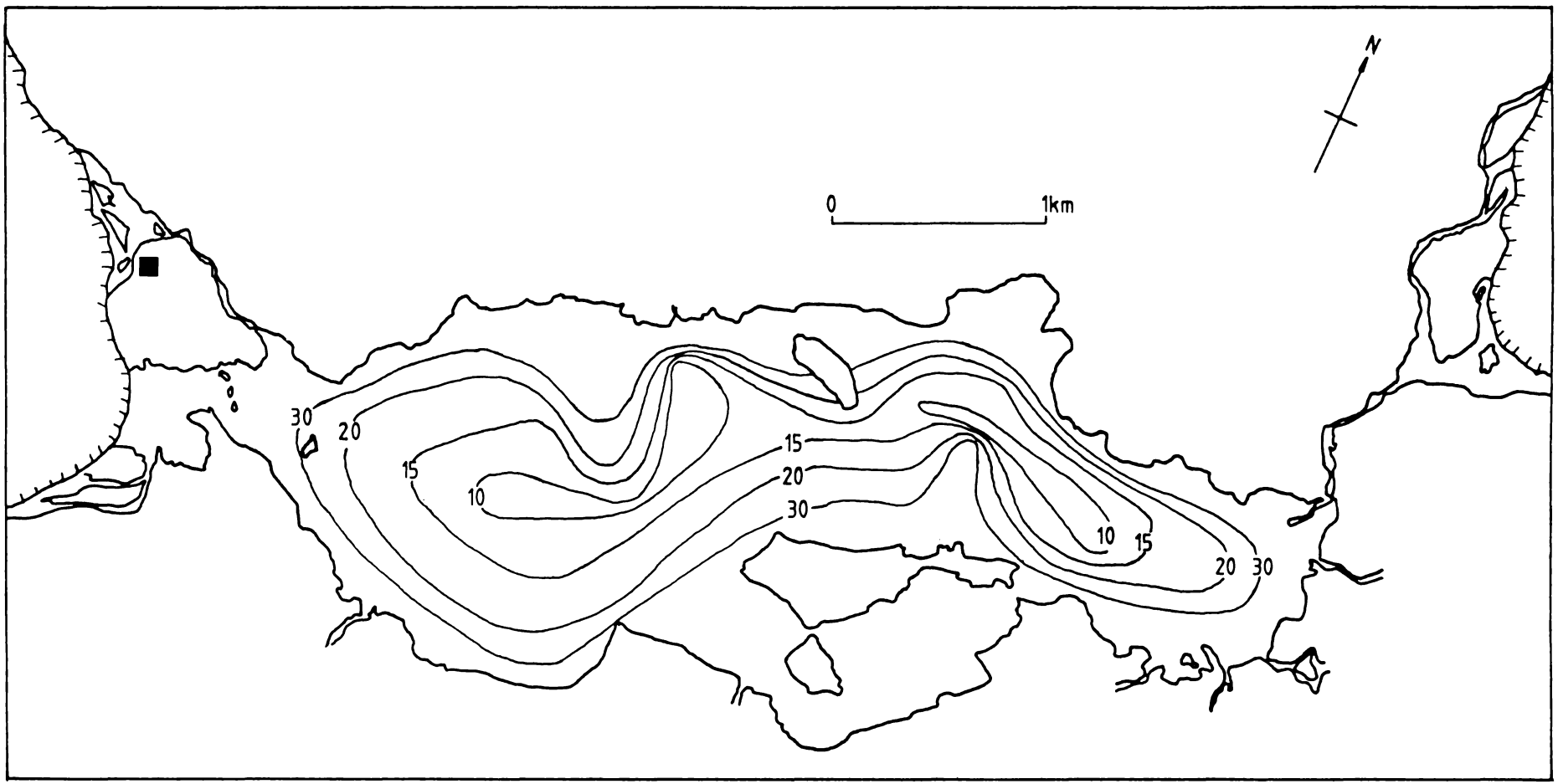

Figure 4.9 Isopach map for calcareous unit D showing thickening shorewards. Contours are in centimetres.

Figure 4.10 Close-up of the varve-like alternations of detrital rich and detrital poor carbonate in unit D. The thickness of individual layers is variable.

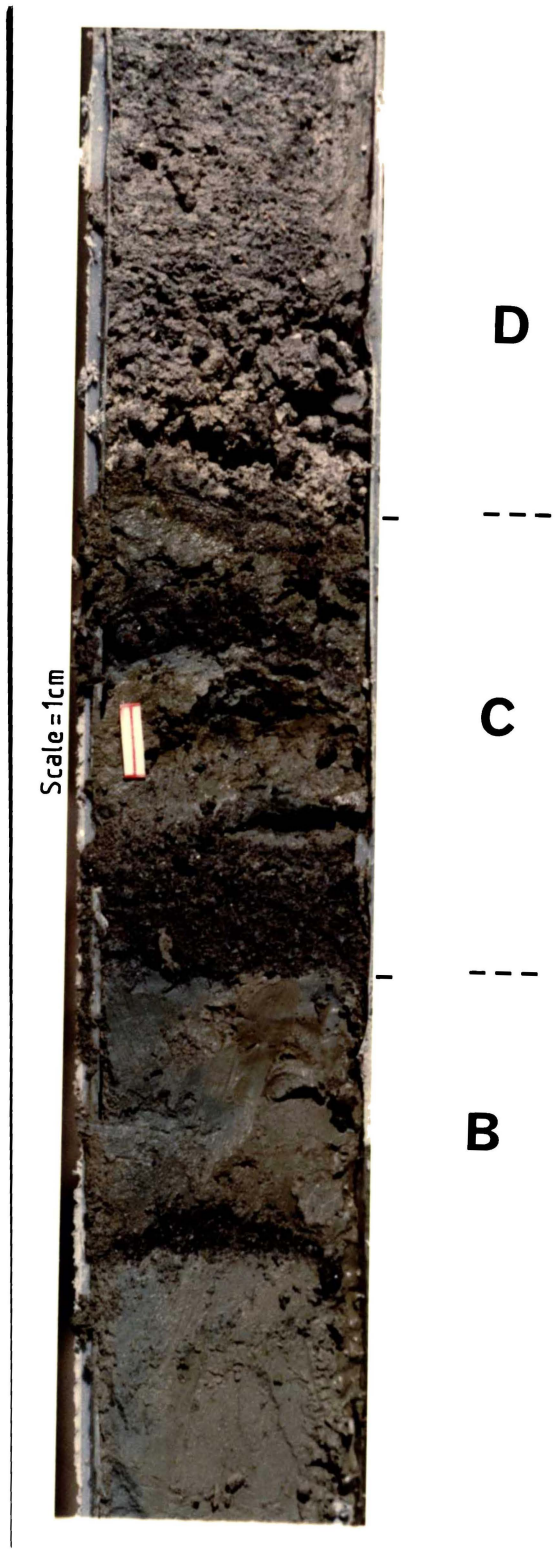

Figure 4.11 Unit C with unit D above and the upper part of unit B below. Olive green-grey organic material is evident in both units C and B.

Unit B

Unit B is a calcareous olive green to grey mud, containing up to 20% by weight $CaCO_3$, with aragonite predominantly over calcite (Table 4.6). The upper boundary is usually marked by a sand layer (Fig. 4.11). Fine sand layers become more abundant with depth and olive green to black organic material occurs in the upper portions of the unit. Non-carbonate mineralogy is markedly different to the overlying units, with a predominance of micas (Table 4.4).

Table 4.4 Summary of relative abundances of non-carbonate minerals in unit B

Mineral	Relative abundance (%)
Micas (mainly brown-green pleochroic biotite)	40
Quartz	15
Feldspar (mainly plagioclase)	15
Rock fragments	15
Augite	15
Volcanic glass	5

Many of the grains have a "dirty" or mottled appearance suggesting some form of weathering.

Isopachs of this unit show thickening towards the centre of the lake (Fig. 4.12), the reverse of that for unit D (Fig. 4.9).

A composite ^{14}C age on the $CaCO_3$ from the bottom half of unit B collected from several cores is 21,000 ± 300 years (Appendix III).

Unit A

This unit is a black muddy sand to slightly gravelly muddy sand (Fig. 4.14) with sub-angular to subrounded grains, and occasional pebbles. The unit is homogeneous but in some cases, particularly if oxidation has occurred during core storage, faint laminations are discernable. The contact between unit A and B is usually sharp. Non-

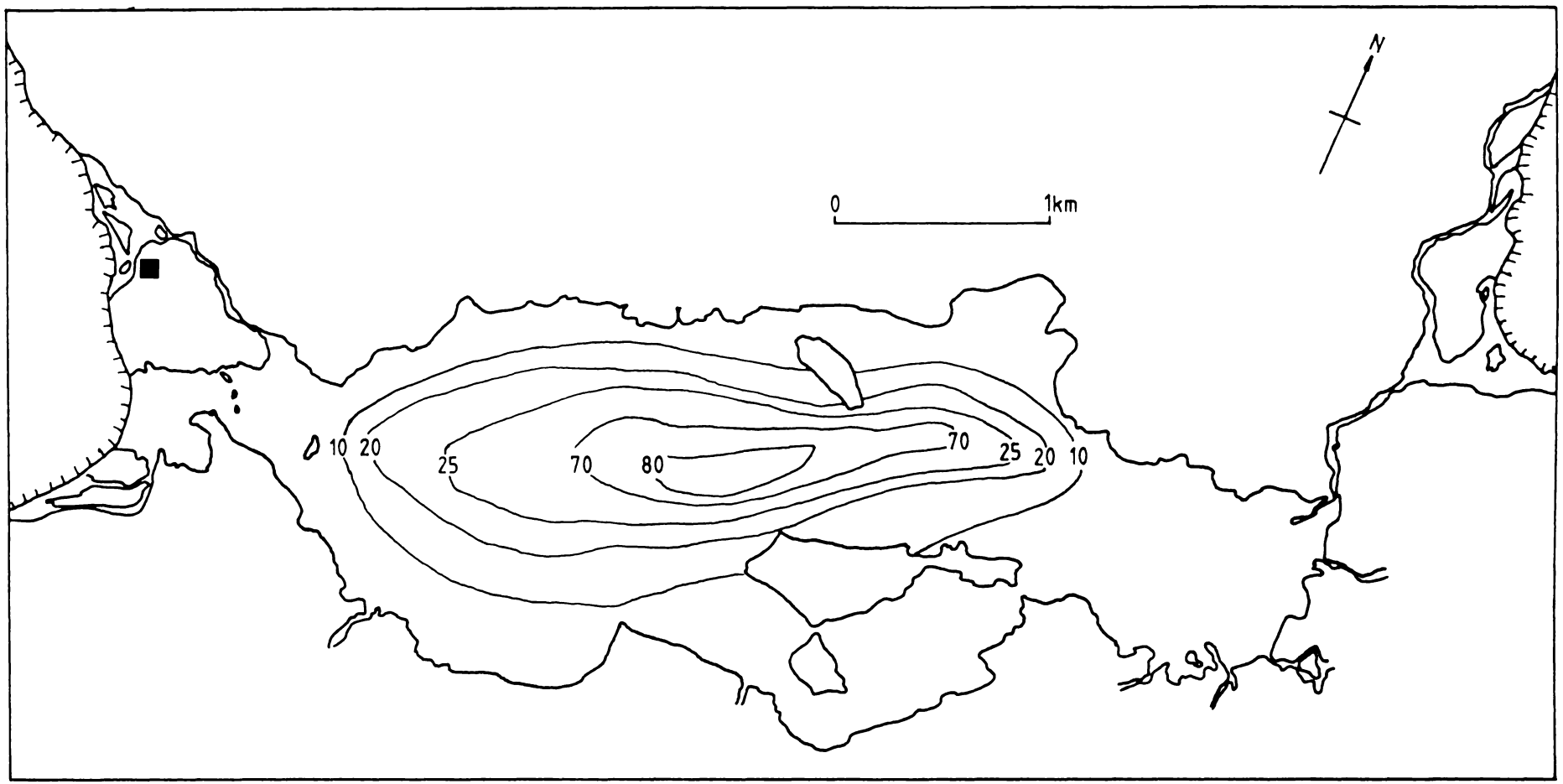

Figure 4.12 Isopach map of calcareous unit B showing thickening offshore. Contours are in centimetres.

carbonate mineralogy is listed in Table 4.5

Table 4.5 Summary of relative non-carbonate mineral abundances for unit A

Mineral	Relative Abundance (%)
Quartz	20
Feldspar (mainly plagioclase)	20
Pyroxenes (Augite > Hypersthene)	20
Hornblende (green-brown pleochroic)	15
Volcanic glass	10
Opaques	10
Rock fragments (mainly basaltic)	5

Other Units

Two other units occur in Lake Fryxell cores. The first is a poorly sorted, chaotic unit consisting of chunks of $CaCO_3$, fine to coarse sands and muds (Fig. 4.13). The dark coloured muds give the unit a mottled appearance. Upper contacts are sharp. The unit occurs in the eastern end of the lake (cores 7 and possibly 13), and in the western end on a small topographic high (C4) (Fig. 2.5). The chaotic nature and discontinuous distribution of the unit suggest it has been redeposited. The presence of carbonate chunks indicates the possible existence of older carbonate beds below those found in these cores. The unit is designated Bb.

Only one core penetrates below the sequence of sediments shown in Fig. 4.4. This is core 1 from a topographic high at the western end of the lake. In this case unit A grades into a poorly sorted deposit of sands, silts and pebbles. Texturally it is a gravelly muddy sand and it is possibly a till.

Textural and Mineralogical Summary

The complete list of analytical results is given in Appendix III.

Non-carbonate textural data are summarized in Figure 4.14, as well

Figure 4.13 Redeposited unit Bb, which occurs within unit B. Bb has a sharp upper boundary, marked by a layer of carbonate (not shown) and contains a chaotic mixture of sands, muds, and chunks of $CaCO_3$. Colours range from blacks to olive greys.

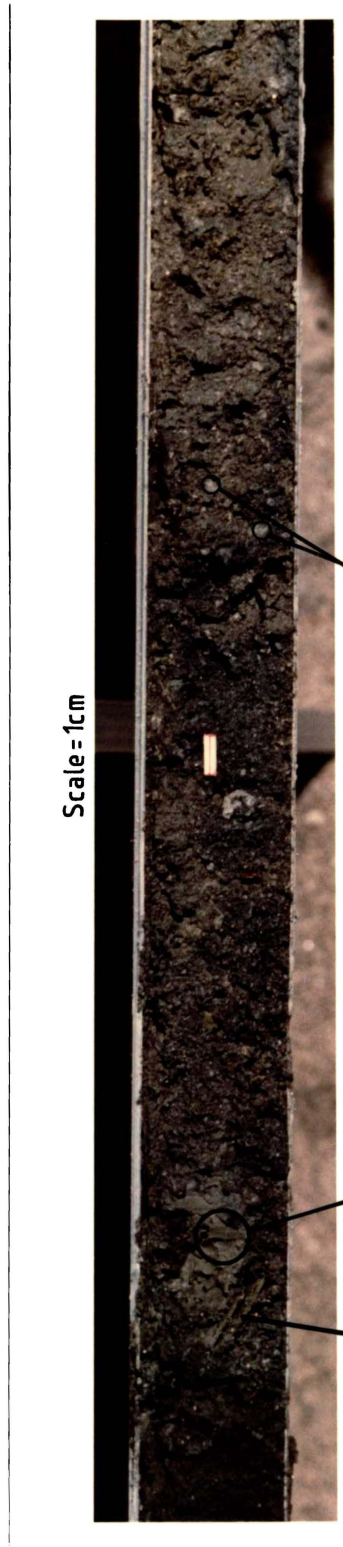

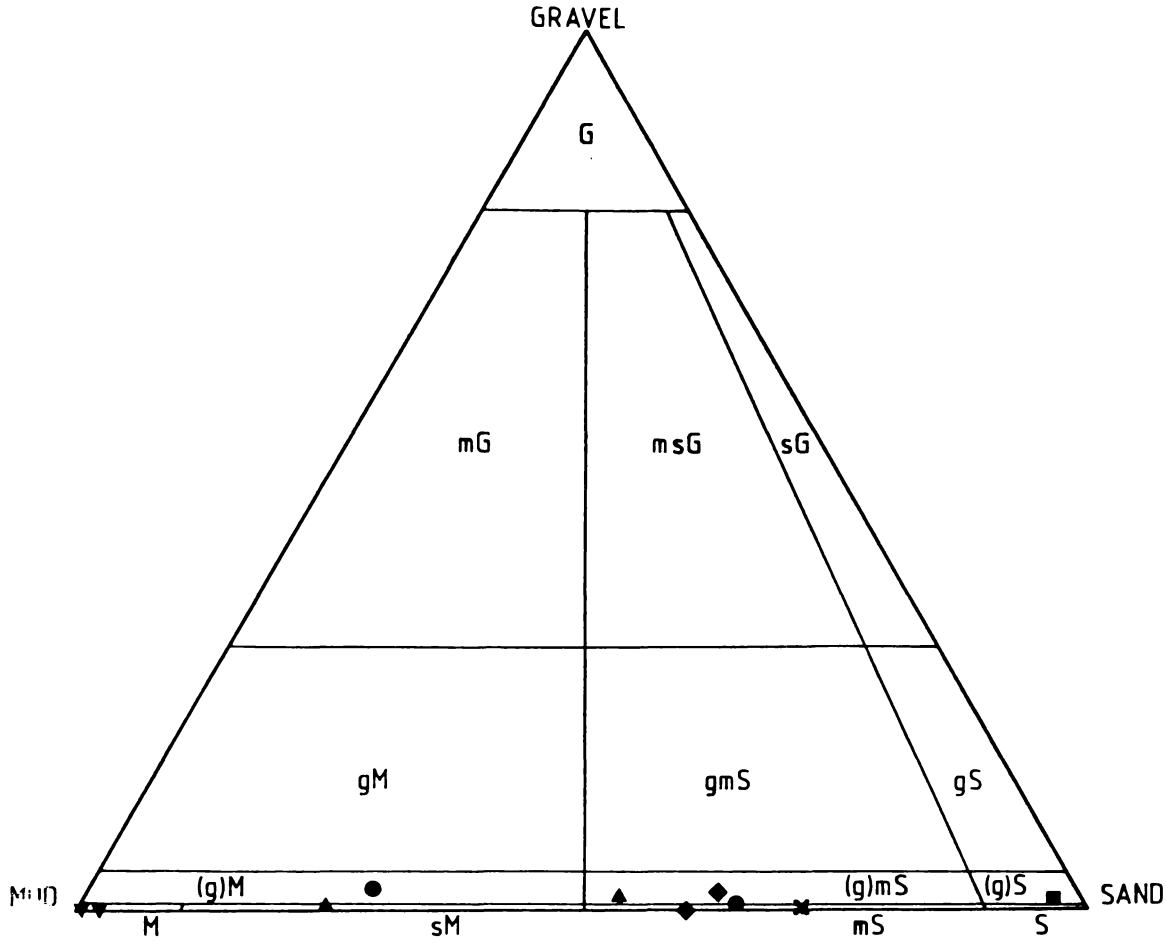

● Unit E

■ Unit D

▲ Unit C

▼ Unit B

◆ Unit A

✖ Sediment from ice cores

G=gravel

g=gravelly

(g)=slightly gravelly

S=sand

s=sandy

M=mud

m=muddy

Figure 4.14 Textural plot (Folk, 1968) of the non-carbonate fractions from units A to E, Lake Fryxell sediments.

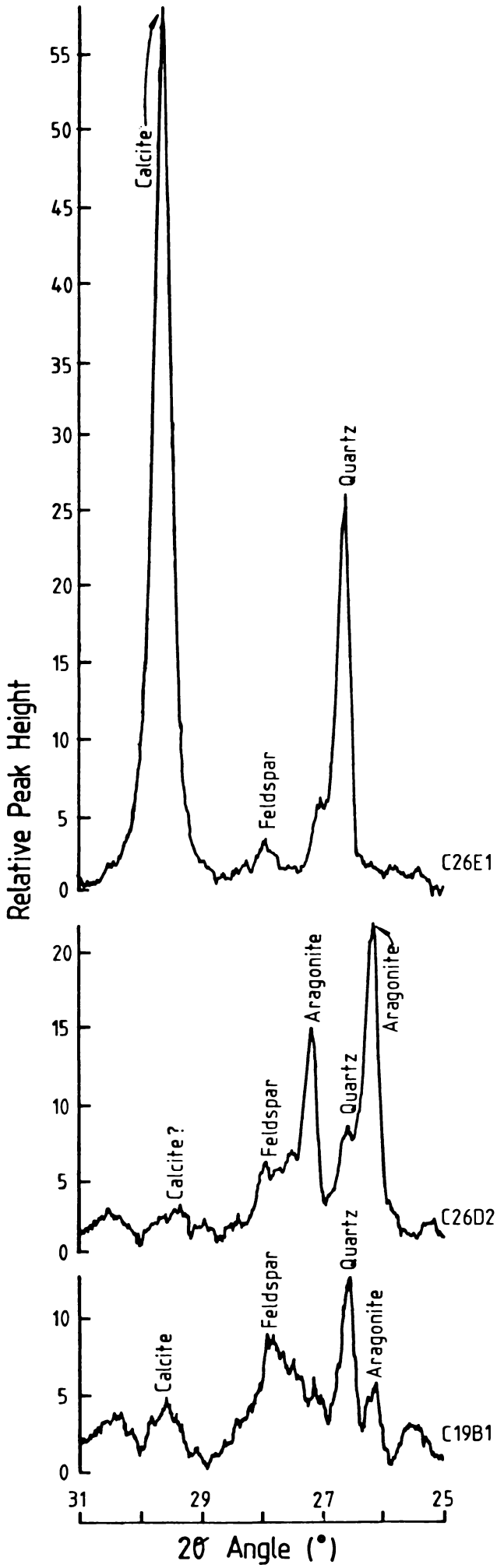

Figure 4.15 Sample X-ray diffractograms from units E, D and B. Note that unit E in this case has no aragonite, indicating it to be a surface carbonate. For semi-quantitative abundance estimates the background is subtracted from the total peak height to obtain the true peak height for the mineral investigated.

as the preceding text. The clay mineralogy of the units consists of micas which produce poor X-ray diffraction peaks corresponding to d = 10.4 - 9.9 Å.

The average weight % composition of carbonates is given in Table 4.6.

Table 4.6 Summary of carbonate mineralogy from XRD analysis. Unit E though averaging 10% aragonite, in many cases has none at all. Most of the aragonites in unit E come from carbonate layers below the sediment surface.

Unit	Calcite (Wt%)	Aragonite (Wt%)
E	64	10
D	4	67
B	5	13

A complete list of the results is in Appendix IV. Examples of XRD spectra from each calcareous unit are shown in Figure 4.15.

4.3 CARBONATE CHEMISTRY: ANALYSIS AND INTERPRETATIONS

4.3.1 INTRODUCTION

The lake bed stratigraphy indicates the presence of 3 carbonate-containing units. Chemical investigation of these units has been made in an attempt to establish the regime prevailing at their respective times of deposition e.g. both Sr^{2+} and Mg^{2+} inclusion in carbonates can have a temperature dependence (Wolf *et al.*, 1967, Bathurst, 1975). In addition, post-depositional effects may be indicated by changes in isotopic ratios and concentrations of trace elements. Chilingar *et al.* (1979) states that the expulsion of elements such as Mg, Sr, Mn, and Ba is commonly associated with inversion, recrystallization and possibly grain growth. Combined with the sedimentologic aspects of the carbonates the chemical analyses should complete the picture of carbonate depositional history in Lake Fryxell.

4.3.2 *LABORATORY TECHNIQUES*

(1) Carbonate sediments from cores C7, C9, C12, C14, C23, and C26 were analysed for Mg, Ca, Sr, Ba, Fe, Mn and Zn. These cores were selected to give as broad a coverage of the lake as possible and because they contained the best carbonate record. After air drying, the samples were powdered in a ring mill for 3 - 4 seconds. Known weights of each powder were dissolved in ∿10% (v/v) analytical grade HCl. Once all visible reaction had ceased the solutions were filtered through pre-weighed Type Ha 0.45 μm Millipore filter papers, and made up to known volume. The amount of non-carbonate residue was calculated after drying and weighing; and the percentage $CaCO_3$ calculated by weight difference. Solutions were analysed by AA/AE methods as for the water column samples (Table 3.1).

Originally the carbonate from all cores was to be analysed. Firstly, selected cores, as above, were to be analysed by AA/AE for accurate results. Secondly, the rest of the cores were to be analysed using quantitative X.R.F. techniques to check if the observed AA trends occurred throughout all the lake carbonate sediments. The latter technique, although less accurate, is considerably quicker. Unfortunately, however, the X.R.F. analysis proved more difficult than originally conceived and would have required more time than warranted to have worked satisfactorily. Consequently only the AA/AE analyses were used, and these have been assumed to be representative of the entire lake.

(2) Stable isotope analyses were performed using the technique of Burns (1980). A diagram of the line for analysis is shown in Figure 4.16. The procedure was:

(i) A known weight (10-20 mgm) of powdered sample was placed in the bottom of the reaction vessel; a few ml of 100% H_3PO_4 was pipetted into the side arm.

Figure 4.16 Vacuum line for the evolution and purification of CO_2 from carbonate samples analysed for $\delta^{18}O$ and $\delta^{13}C$ by mass spectrometry.

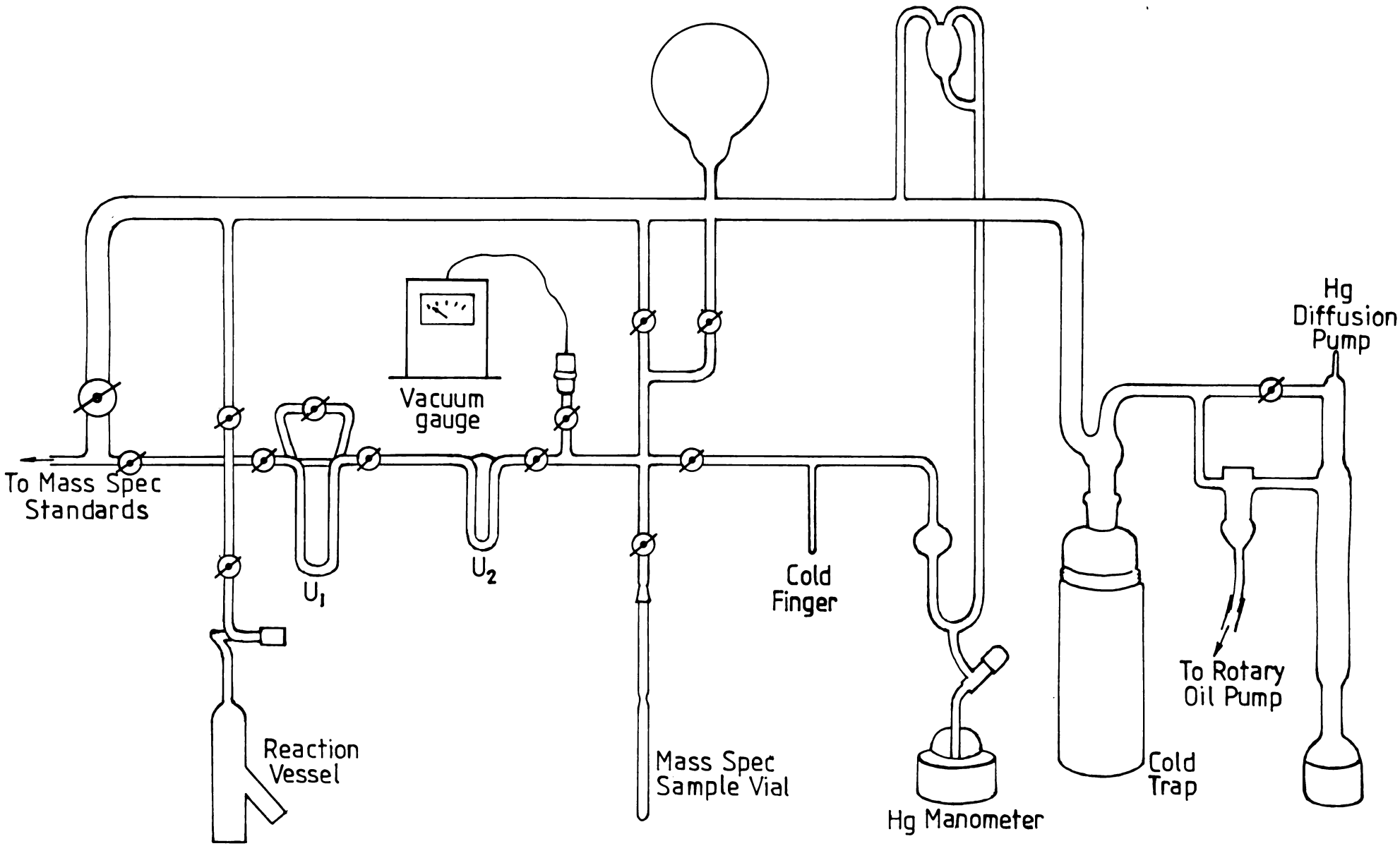
To Mass Spec
Standards
Vacuum
gauge
U_1
U_2
Reaction
Vessel
Mass Spec
Sample Vial
Cold
Finger
Hg Manometer
Cold
Trap
To Rotary
Oil Pump
Hg
Diffusion
Pump

(ii) The vessels were outgassed, with the aid of heating, for 30 minutes and then placed in a 25°C constant temperature water-bath to thermally equilibrate.

(iii) The acid was then tipped onto the carbonate and left to react overnight.

(iv) Following reaction, the vessels were put back on the line and the system was evacuated. The pumps were then isolated.

(v) CO_2 from the sample was frozen into "U_1", using liquid N_2. The sample vessel isolated, an ethanol slush bath replaces the liquid N_2, and the N_2 placed on "U_2".

(vi) "U_1" was isolated and non-condensible gases were pumped off the CO_2 in "U_2".

(vii) The slush bath replaced the liquid N_2 on U_2 whilst the CO_2 sample was frozen into the cold finger of the Hg-manometer. The pressure of the CO_2 was then measured.

(viii) The CO_2 was then frozen into the sample vial which was flamed off ready for mass spectrometry.

Both the $\delta^{13}C$ and $\delta^{18}O$ analysis were obtained from the one gas sample using a Micromass 602 C Double inlet mass spectrometer.

4.3.3 *RESULTS*

Results of chemical analyses are summarized in Table 4.7. A complete list of results appears in Appendix IV.

Table 4.7 Chemical analyses summary. Elemental concentrations are in ppm.

	CALCITE (from unit E)		ARAGONITE (unit D)		MUD (unit B)	
	Mean	Range	Mean	Range	Mean	Range
Ca	340000 ppm	297666 - 381781 ppm	320900	210986 - 363199	135381	36849 - 243168
Mg	13816 "	5441 - 26820 "	10065	2054 - 42789	26418	12687 - 47078
Sr	1542 "	954 - 3992 "	2008	831 - 4865	1886	1081 - 3490
Ba	5494 "	683 - 7290 "	5868	2614 - 7503	4234	2407 - 6892
Fe	551 "	158 - 1271 "	889	197 - 2326	2382	742 - 4630
Mn	702 "	328 - 1500 "	644	212 - 2162	2134	1419 - 2535
Zn	218 "	23 - 403 "	131	51 - 281	452	117 - 1321
$\delta^{13}C_{PDB}$	+0.54 ^{o}/ooPDB	-1.59 - 3.35 ^{o}/ooPDB	-1.577	+0.06 - 3.73	-2.9007	-1.27 - -4.07
$\delta^{18}O_{PDB}$	-26.912 %PDB	-20.74 - 28.67 %PDB	-28.545	-26.594 - -29.838	-20.859	-17.627 - -29.562

4.3.4 *STABLE ISOTOPES*

Theoretical Considerations

The stable isotopes considered here are ^{13}C and ^{18}O. Their relative abundances are given in Table 4.8

Table 4.8 Isotope abundances of oxygen and carbon (Hoeffs, 1973)

Carbon	Oxygen
^{12}C = 98.89%	^{16}O = 99.763%
^{13}C = 1.11%	^{17}O = 0.0375%
	^{18}O = 0.1995%

Analytical results are expressed relative to an arbitrary standard (Craig, 1957, Hoefs, 1973). The difference between the isotopic ratios of the sample and the standard (δ) is given in per mille ($^{o}/_{oo}$), and is defined by:

$$\delta \text{ in } {}^{o}/_{oo} = \frac{R_{(sample)} - R_{(standard)}}{R_{(standard)}} \times 1000 \qquad (34)$$

where:

R = isotope ratio. (Craig, 1957, Hoeffs, 1973)

Carbon isotopes in the biosphere and carbonates are most commonly separated from each other by two fractionation mechanisms:

(i) a kinetic effect during photosynthesis, which concentrates ^{12}C in synthesized compounds.

(ii) A chemical exchange effect in the CO_2 - HCO_3 - $CaCO_3$ system which enriches ^{13}C in bicarbonate. Brownlow (1979) points out that these fractionations are not always equilibrium processes.

The reactions which distribute ^{13}C and ^{18}O into carbonates are (Milliman, 1974):

$$H_2{}^{18}O_{(l)} + 1/3\ CaC^{16}O_{3(s)} \rightleftharpoons H_2{}^{16}O_{(l)} + 1/3\ CaC^{18}O_{3(s)}$$

$$^{13}C\ O_3{}^{2-}{}_{(aq)} + {}^{12}CO_{3(s)} \rightleftharpoons {}^{12}CO_3{}^{2-}{}_{(aq)} + {}^{13}CO_{3(s)}$$

For both oxygen and carbon isotopes the carbonate mineralogy is important in the fractionation. The ^{18}O content of aragonite at 25°C is 0.6°/oo higher than co-precipitated calcite, and increases by 0.06°/oo for each mol% of $MgCO_3$ (Tarutani *et al.*, 1969). Calcite is enriched in ^{13}C relative to HCO_3^- in water by 0.9°/oo, and aragonite is enriched by 1.8°/oo relative to calcite (Robinson and Clayton, 1969; cited in Milliman, 1974).

The working standard used for analyses was "Waikato Pinus Radiata - (WPR)" (Grinsted, 1977), where:

$$\delta^{13}C_{PDB} = 1.0408\ \delta^{45}{}_{WPR}^{1} - 0.0336\ \delta^{46}{}_{WPR}^{1} - 25.95 \qquad (35)$$

and

$$\delta^{18}O_{PDB} = 0.9865\ \delta^{46}{}_{WPR}^{1} + 0.0094\ \delta^{45}{}_{WPR}^{1} - 15.54 \qquad (36)$$

$\delta^{13}C$

The $\delta^{13}C$ values of the carbonates in Lake Fryxell tend to become more negative with increasing age. Generally calcite flakes (unit E) are approximately 0°/oo w.r.t. PDB. $\delta^{13}C$ for the unit D aragonite decreases from top to bottom whereas the reverse is the case for unit B (refer to Appendix IV for specific examples). $\delta^{13}C$ appears to increase with increasing Ca (Fig. 4.17a) and Ba concentration and decreasing Mg (Fig. 4.17b) and Sr concentration.

The photosynthetic products of most plants are enriched in ^{12}C with respect to the original CO_2 starting material. For Lake Fryxell most photosynthesis occurs within a physically stable euphotic zone.

Fig. 4.17a.

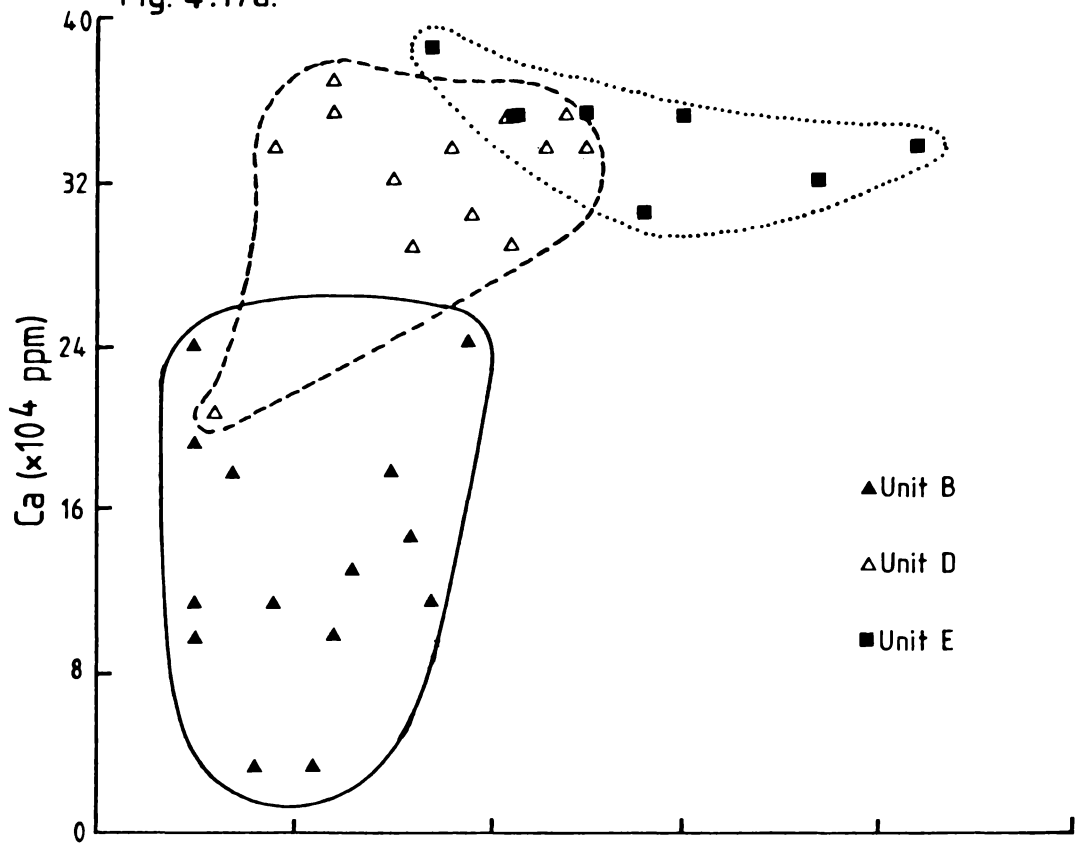

Fig. 4.17b

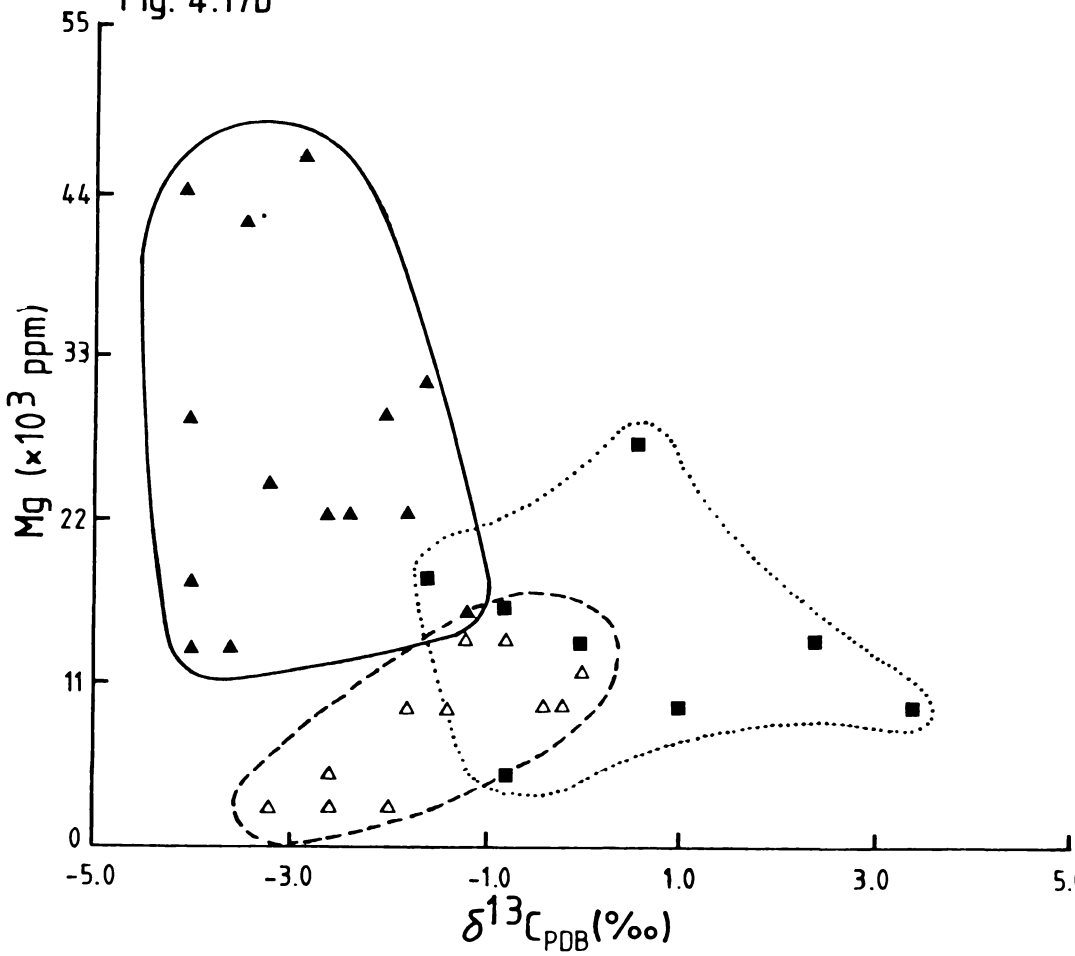

Figure 4.17a Plot of Ca vs $\delta^{13}C$ showing increasing $\delta^{13}C$ with Ca concentration.

Figure 4.17b This plot of Mg vs $\delta^{13}C$ shows a decreasing $\delta^{13}C$ with decreasing Mg concentration.

Therefore, photosynthesis followed by settling of seston to underlying anoxic waters results in a relatively greater loss of ^{12}C than ^{13}C from the euphotic zone. However, calcium carbonate precipitated under equilibrium conditions will contain relatively more ^{13}C than ^{12}C compared to the aqueous CO_2. The mass budget for the simultaneous removal of seston and calcium carbonate is:

$$\Delta\ \delta^{13}C = \frac{17\ Mp - 9\ Mc}{\Sigma CO_2} \tag{37}$$

where

$\Delta\ \delta^{13}C$ = $\delta^{13}C$ change of any species

Mp = number of moles/l of photosynthates removed from the euphotic zone

Mc = number of moles/l of calcium carbonate precipitated

ΣCO_2 = $[CO_2] + [H_2CO_3] + [CO_3^{2-}]$

It may be expected that until saturation of calcite is achieved that $M_c = 0$, so equation (37) reduces to:

$$\Delta\ \delta^{13}C = \frac{17\ Mp}{\Sigma CO_2} \tag{38}$$

However once precipitation of calcite is initiated, it would be expected that Mp $\approx$ Mc so that equation (38) reduces to:

$$\Delta\ \delta^{13}C = \frac{8\ Mp}{\Sigma CO_2} \tag{39}$$

Thus, continued removal of seston and calcium carbonate will result in steadily increasing $\delta^{13}C$ values for all species, provided that the CO_2 pool in the euphotic zone is not being replenished from without.

Thus the increasingly positive $\delta^{13}C$ profile up the sedimentary column indicates progressive removal of C from the euphotic zone.

The reverse trend in unit B is more difficult to explain. The $\delta^{13}C$ values for present Lake Fryxell waters at 4 m and 5 m are surprisingly negative and are probably representative of stream inflows. It is possible that $\delta^{13}C$ values as low as these may result from respiration of mosses and algae that grow profusely in the stream flushes. Therefore $\delta^{13}C$ for unit B is possibly explained by carbonate deposition occurring as the lake was filling up and/or during fluctuations in lake level. Thus the values are a mixture of $\delta^{13}C$ of the lake waters themselves and inflowing meltwater.

$\delta^{18}O$

$\delta^{18}O$ values lie within the range $-30^{o}/oo$ to $-16^{o}/oo$ w.r.t. PDB. Unit D and E carbonates have similar values, usually from about $-25^{o}/oo$ to $-30^{o}/oo$ w.r.t. PDB, but mud values are more positive (Table 4.7, fig. 4.18). These changes are too great to be the result of temperature changes ($-0.24^{o}/oo$ /^{o}C) and hence suggest either drastic changes in the composition of the waters occupying the Fryxell Basin, or the presence of "imported" detrital carbonate of radically higher $\delta^{18}O$ values.

Evaporation of an open water body leads to an enrichment in $\delta^{18}O$ (Sofer and Gat, 1975; Gat, 1980), which continues until a steady state is achieved. Thus the $\delta^{18}O$ value finally achieved is a function of the salinity, the temperature and relative humidity. However if the lake has an ice cover little evaporative enrichment is possible since the isotopic fractionation between $H_2O_{(l)}$ and $H_2O_{(s)}$ is very small.

At present the $\delta^{18}O$ values of the meltwaters feeding Lake Fryxell are about $-32^{o}/oo$ w.r.t. SMOW, (Canada Glacier values are in the range -28 to $-34^{o}/oo$ w.r.t. SMOW, Hendy *et al.*, 1979), and thus carbonates precipitated from these waters at $\approx 3^{o}C$ should have $\delta^{18}O$ values at about $-28^{o}/oo$ w.r.t. PDB. There is no obvious source of water with a more positive $\delta^{18}O$ value, except seawater. Thus an explanation for the high

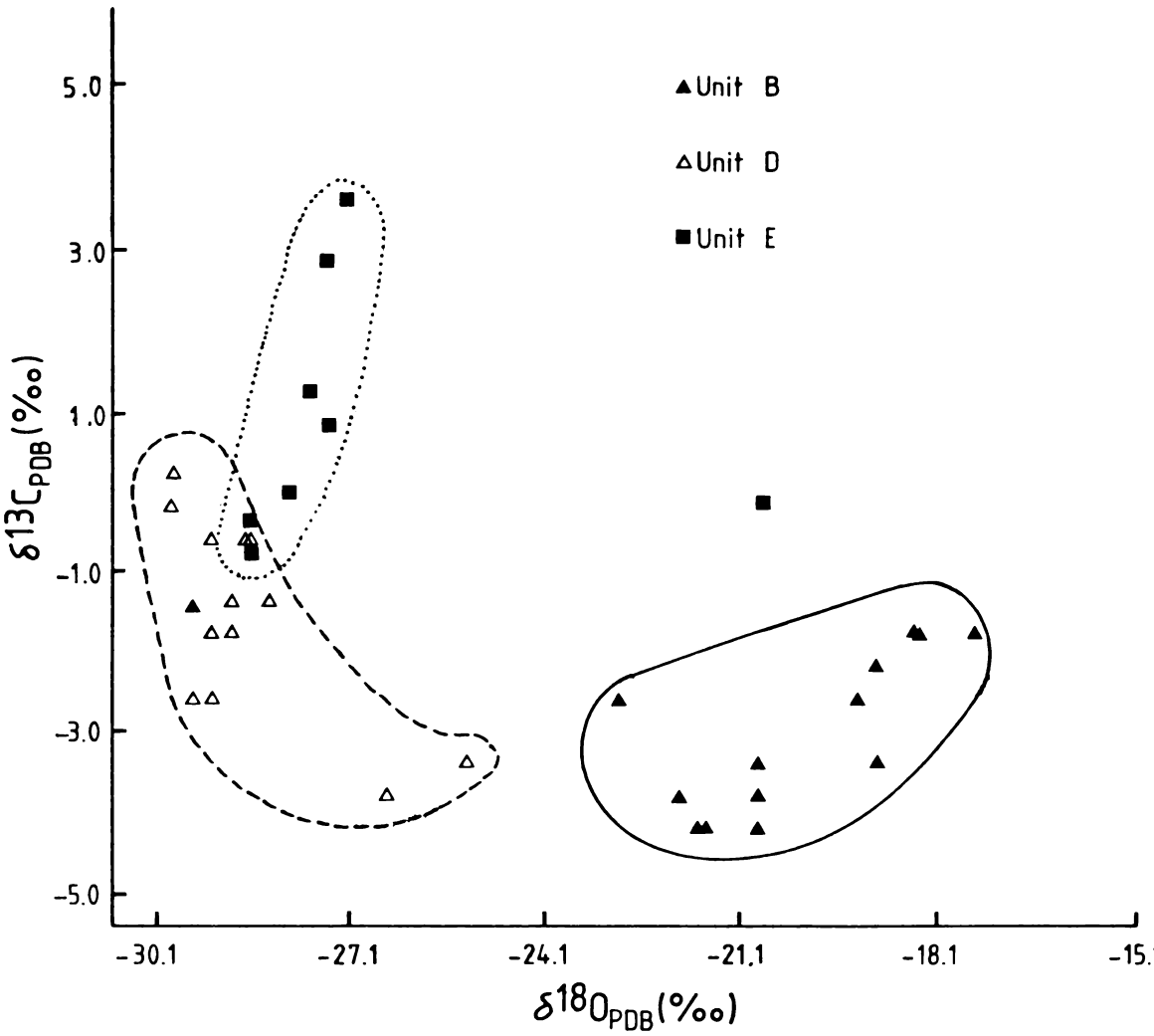

Figure 4.18 Plot showing the relationship of $\delta^{13}C$ to $\delta^{18}O$ for Lake Fryxell carbonates. Each unit has a reasonably well defined field with unit B mud having the more positive $\delta^{18}O$ values.

$\delta^{18}O$ values found in unit B is that there was a contribution from seawater and/or carbonate of seawater origin to waters occupying the Fryxell Basin. Since the ^{14}C age of this unit is about 21,000 yrs B.P. it is considered the water body would have been part of Glacial Lake Washburn.

The suggestion of imported carbonate to waters in which unit B was deposited implies the ^{14}C date of that unit may be a slight over estimate. As the unit is fine grained implying slower deposition rates it is expected that the age would be nearer the maximum stand of the lake ($\sim$19 - 20,000 yrs) rather than soon after lake formation.

Unit D aragonite samples appear to become progressively isotopically heavier up the profile. This indicates that evaporative deposition and increasing salinity may have occurred possibly to the point that an ice cover was no longer in existance. Unit B values tend to show a reverse trend implying contamination with incoming meltwater, hence supporting the $\delta^{13}C$ implication of lake infilling.

4.3.5 *ELEMENTAL ANALYSES*

Theoretical Considerations

Trace elements will substitute, to varying degrees, for Ca^{2+} in the $CaCO_3$ lattice. The substitution occurs in a number of forms: (1) diadochic (2) interstitial (3) adsorption for unsatisfied charges, and (4) filling of unoccupied lattice positions in lattice structural defects (Brand and Veizer, 1980). The occurrence and abundance of trace elements in minerals is generally controlled by their availability at the time of mineral formation, by ionic size and charge, and by the nature of the host mineral structure (Brownlow, 1979; Volfinger and Robert, 1980). From ionic radii considerations alone aragonite structures (orthohombic - 9 fold co-ordination) show preferential substitution with larger cations e.g. Ba, Sr; whereas calcite structures (rhombo-

hedral - 6 fold co-ordination) favour smaller ions, e.g. Mg, Fe, Mn, Zn (Milliman, 1974).

If crystallizing in equilibrium, trace components will partition between the two phases in a characteristic manner, described by the partition or distribution coefficient (McIntire, 1963). The partition coefficient (K_D) is defined as:

$$(Tr/Cr)_s \; / \; (Tr/Cr)_{aq} \; = \; K_D \qquad (40)$$

where

Tr = concentration of the trace component (moles)

Cr = concentration of the carrier component (moles). In this case Ca and subscript 's' = solid

aq = solution

Correcting for deviations from ideality using activities, equation (40) becomes:

$$(Tr.f_{Cr} \; / \; Cr.f_{Cr})_s \; / \; (Tr.\gamma_{Tr} \; / \; Cr.\gamma_{Cr})_{aq} \; = \; K_D \qquad (41)$$

where

f = activity coefficient for ions in the solid phase

γ = activity coefficient for ions in the aqueous phase

When $K_D > 1$ the crystals growing from solution are enriched in the trace component with respect to the solution. If $K_D < 1$ the crystals are impoverished in the trace component compared to the solution (McIntire, 1963). The greater the deviation from unity the stronger the depletion or enrichment in the trace element (Brand and Veizer, 1980). The outlined element partitioning applies to both inorganic and biogenic carbonates (Brand and Veizer, 1980). A biological fractionation can occur when the biological partition coefficient does not equal the inorganic coefficient. As yet this biological fractionation is not fully understood (Milliman, 1974).

Calcium

Ca concentrations in the carbonate are high in the calcite (unit E) and the aragonite (unit D), but are reduced markedly in the calcareous mud (unit B) (Table 4.7). Extreme aragonite and calcite samples with low Ca concentrations and high in trace components in the solid phase all tend to be muddier than their counterparts. Therefore it appears that substitution for Ca is more prevalent in muddy samples.

Magnesium

The average Mg concentrations decrease from calcareous mud (unit B) to calcite (unit E) to aragonite (unit D). However, there is some overlap between each unit, although when plotted against Ca concentration the individual fields separate well (Fig. 4.19). This confirms the separations drawn on a stratigraphic basis and from the XRD data (Figs 4.4, 4.15). Much of the chemical separation is due to differences in Ca concentrations.

The Mg content, particularly of calcites, is sedimentologically and chemically significant. Mg in the precipitating solution governs the resultant polymorph (Müller *et al.*, 1972; Bathurst, 1975; Folk, 1974 and others). Bischoff and Fyfe (1968) showed that Mg^{2+} (and SO_4^{2-}) ions inhibit the growth of calcite crystals from solution. Folk (1974) proposed that Mg^{2+} and SO_4^{2-} ions promote growth primarily parallel to the c-crystallographic axis by selectively poisoning growth at side faces (Figure 4.20). A calcite lattice consists of alternating Ca^{2+} and CO_3^{2-} "sheets". If, as in Case A (Fig. 4.20), a Mg^{2+} ion is incorporated near the middle of a calcite sheet, other Ca^{2+} ions will attach alongside and be covered over by the next CO_3^{2-} sheet without much difficulty. Case B shows what happens if Mg^{2+} ion attaches to the edge of a sheet. The smaller size of the Mg^{2+} will cause the over- and underlying CO_3^{2-} sheets to be drawn together. The associated contraction will not allow further

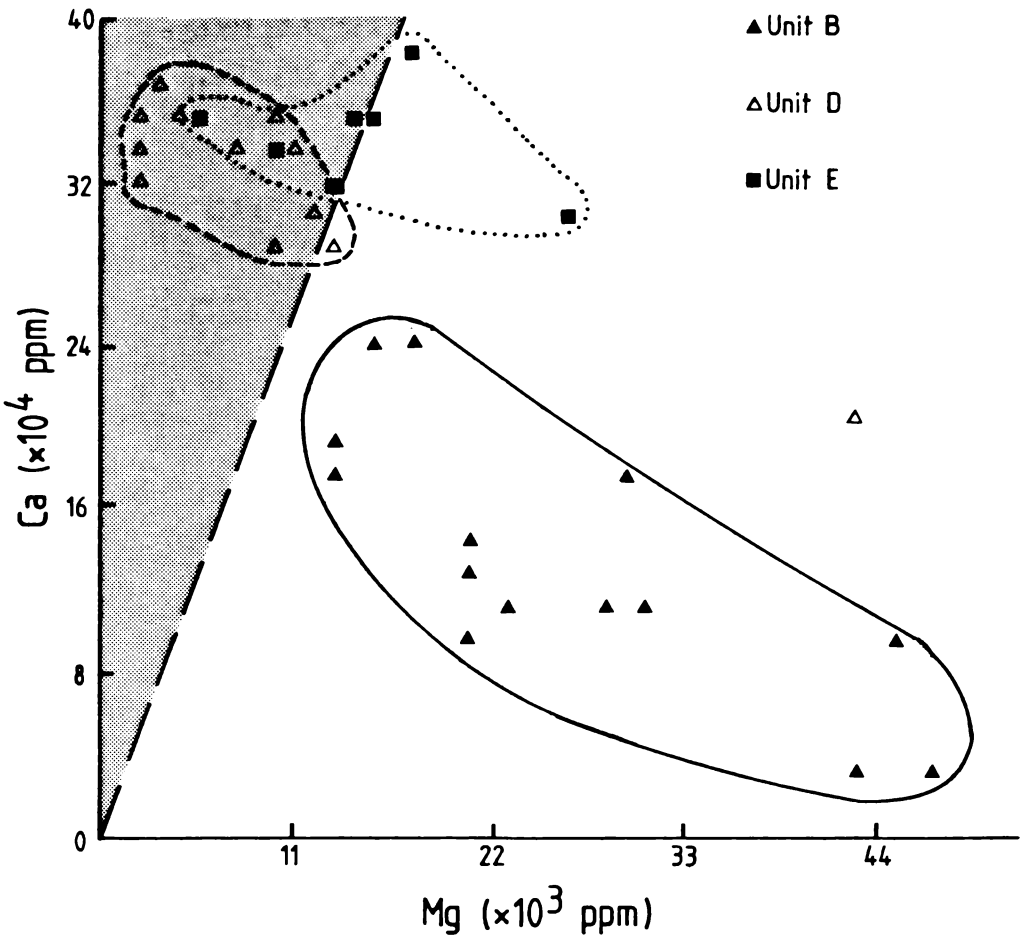

Figure 4.19 Plot of Ca vs Mg concentrations in carbonates from units E, D and B showing the separation of the units. The stippled area denotes the low Mg-calcite field.

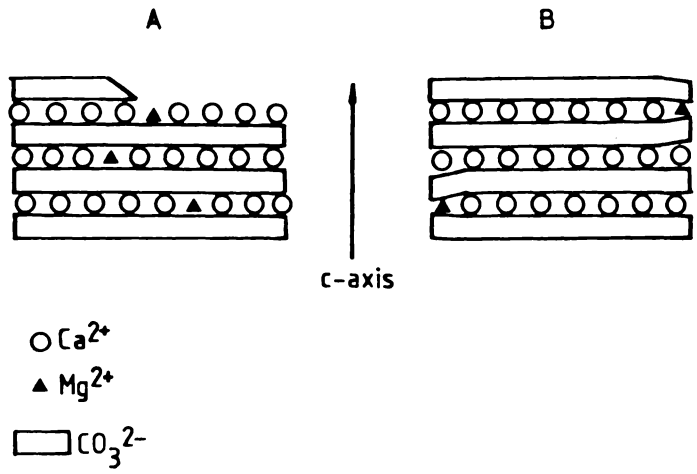

Figure 4.20 Diagrammatical representation of the effect of Mg^{2+} on $CaCO_3$ crystal growth (from Folk, 1974). Case A shows calcite growth and B is the aragonite case.

incorporation of Ca^{2+}. Thus low Mg^{2+} in solution implies more sideways growth and the formation of low Mg-calcites, whereas high Mg^{2+} favours elongation along the c-axis forming high Mg-calcites and aragonites.

The effect of Mg^{2+} on carbonate mineralogy has been quantitatively estimated in terms of Mg/Ca ratios of the precipitating solutions (Table 4.9, Müller *et al.*, 1972).

Table 4.9 Tabulated reslationship between Mg/Ca ratios in solution and resultant precipitate (Müller *et al.*, 1972).

Mg/Ca ratios of the precipitating solution	Mineralogy of precipitates
<2	low Mg-calcite
2-12	high Mg-calcite
>12	aragonite
very high values	hydrous Mg-carbonates

The present Mg/Ca ratios of Lake Fryxell in the euphotic zone range from 1 - 3. Below, in the anaerobic waters, ratios are about 6. Surface calcites (unit E) average about 4 mol% $MgCO_3$ (with the exception of one sample which is 9 mol% $MgCO_3$) classifying them as low Mg-calcites (Chave, 1952), suggesting that they precipitate from within the euphotic zone. The calcareous mud has a mean concentration of 17 mol% $MgCO_3$ (this excludes 2 values which were 56 and 60 mol% $MgCO_3$) indicating on average high Mg-calcites (Fig. 4.19). (Some of this Mg may be associated with the aragonite however). There are several possible causes for the dual mineralogy. (i) Co-precipitation of both aragonite and calcite, as is presently observed in Tüz Golon (Müller *et al.*, 1972). (ii) Post-depositional aragonite/calcite transformation. (iii) A detrital component derived from marine sediments. The first suggestion is a possibility although (ii) is probably more likely. (iii) has already been indicated by stable isotope analyses and may subsequently be effected by (ii). Pingitore (1978) suggests that an increase in Mg content, such as in unit

B, is due to the aragonite-calcite transformation. This suggests that the primary mineral was possibly aragonite, subsequently altering to calcite, thus partially explaining the aragonite predominance.

Using the model of Müller *et al.* (1972) an estimate of the minimum palaeosalinity can be made. To do this the present maximum concentration of Ca at 9 m depth in the water column (i.e. 80 ppm) is assumed to be the minimum for waters when unit D was deposited. This is because Ca from below was removed to form the aragonite. From Muller *et al.* (1972) for aragonite to precipitate Mg/Ca = 12, if Ca = 80 ppm then the Mg concentration of the water equals 960 ppm. Next, assuming the ratio of Mg to other elements in the water column was the same as it is at present then their concentration can be calculated. This appears a reasonable assumption as the present water column profile does not show significant Mg removal. Supportive evidence comes from calculated K_D values for Mg which are all less than unity, implying that more Mg remained in solution than was removed. The result gives an estimated minimum salinity for the water column of about 32 ppt when the unit D aragonite was deposited (Table 4.10). Assuming the primary precipitate in unit B was aragonite then a similar minimum salinity is likely. If the primary mineralogy was either high Mg-calcite or both Mg-calcite and aragonite then a lower salinity would be expected.

Chillingar (1962; cited in Wolf *et al.*, 1967) suggested from comparison of chemical precipitates with invertebrates that Ca/Mg ratios of these organisms are controlled by the effect of temperature and solubility product. Chave, 1954 (a, b) stated the Mg/Ca ratio reflects environmental temperature combined with mineralogy and phylum. The relationship is a direct one, the greater the wt% $MgCO_3$, the higher the temperature of precipitation for both aragonite and calcite skeletal materials. For Lake Fryxell carbonates (Fig. 4.21), it appears that the relationship is not straightforward. The $\delta^{18}O$ record suggests a combination of

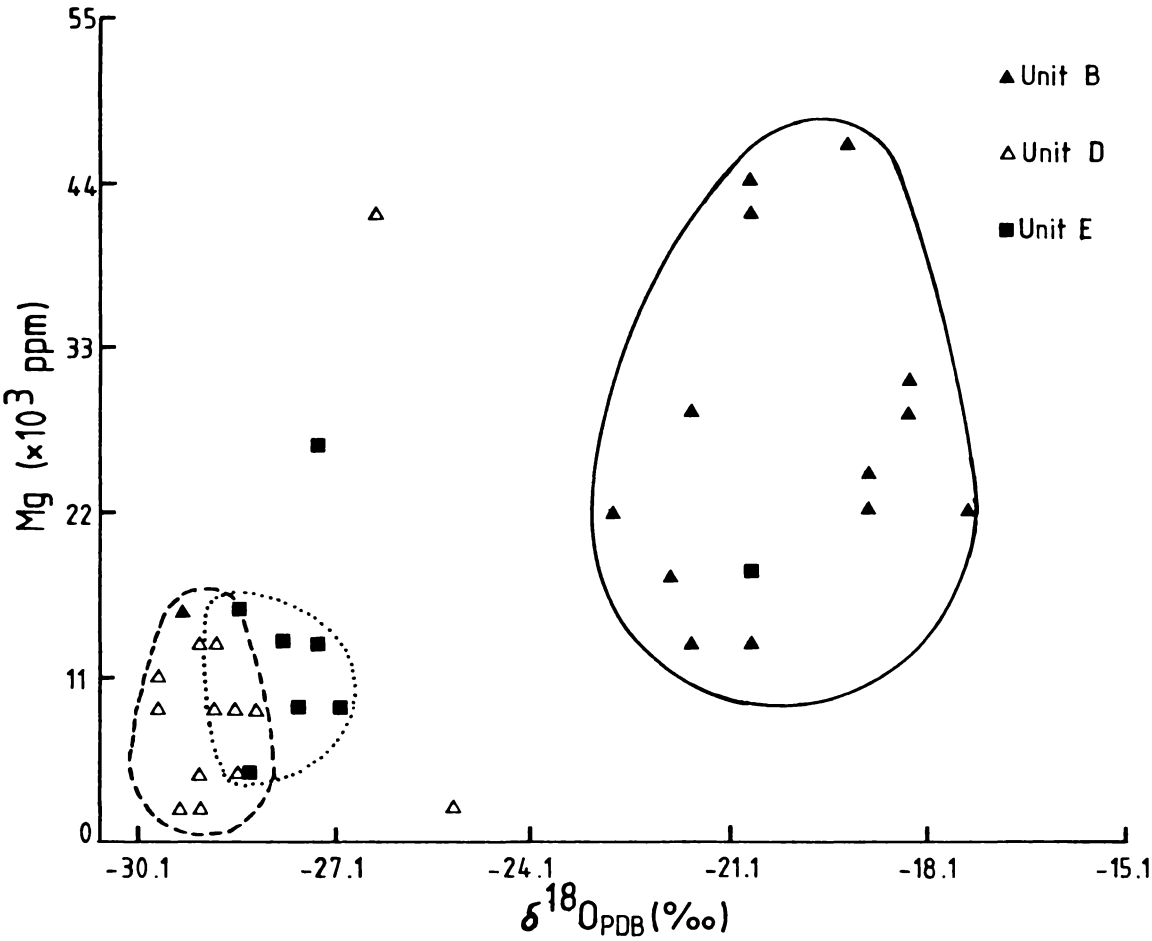

Figure 4.21 Plot of Mg vs $\delta^{18}O$. This shows no definite relationship suggesting that Mg incorporation in Lake Fryxell carbonates is not purely temperature dependent.

Table 4.10 Tabulated salinity calculation assuming a constant species/Mg ratio

PALAEOSALINITY CALCULATION

Species	Mg Ratio	Calculated Concentration of species (ppm)
Na^+	9.2	8832
K^+	0.64	614
Mg^{2+}	1.0	960
Ca^{2+}	0.95	912
Sr^{2+}	0.057	55
Ba^{2+}	0.078	75
Cl^-	10.4	9984
SO_4^{2-}	0.78	748
HCO_3^-	10.07	9667
	Total salinity	31847

salinity changes and detrital sedimentation in unit B, with unit D being controlled by increasing salinity. The latter is supported by the up-column increase in the Mg/Ca ratio of the carbonates. Temperature effects on the $\delta^{18}O$ record are probably masked by the above salinity effects.

Strontium

Like Mg, Sr is an important trace component in carbonates (Kinsman, 1969; Milliman, 1974). Sr concentrations in all three carbonate-bearing units are comparable, although the mean concentration in the aragonite unit is marginally higher (Table 4.7). This is probably due to lattice structural control on Sr substitution.

Separation of calcareous units on the basis of Sr analyses is poor, when plotted against Ca, separation is primarily due to Ca variation (Fig. 4.22).

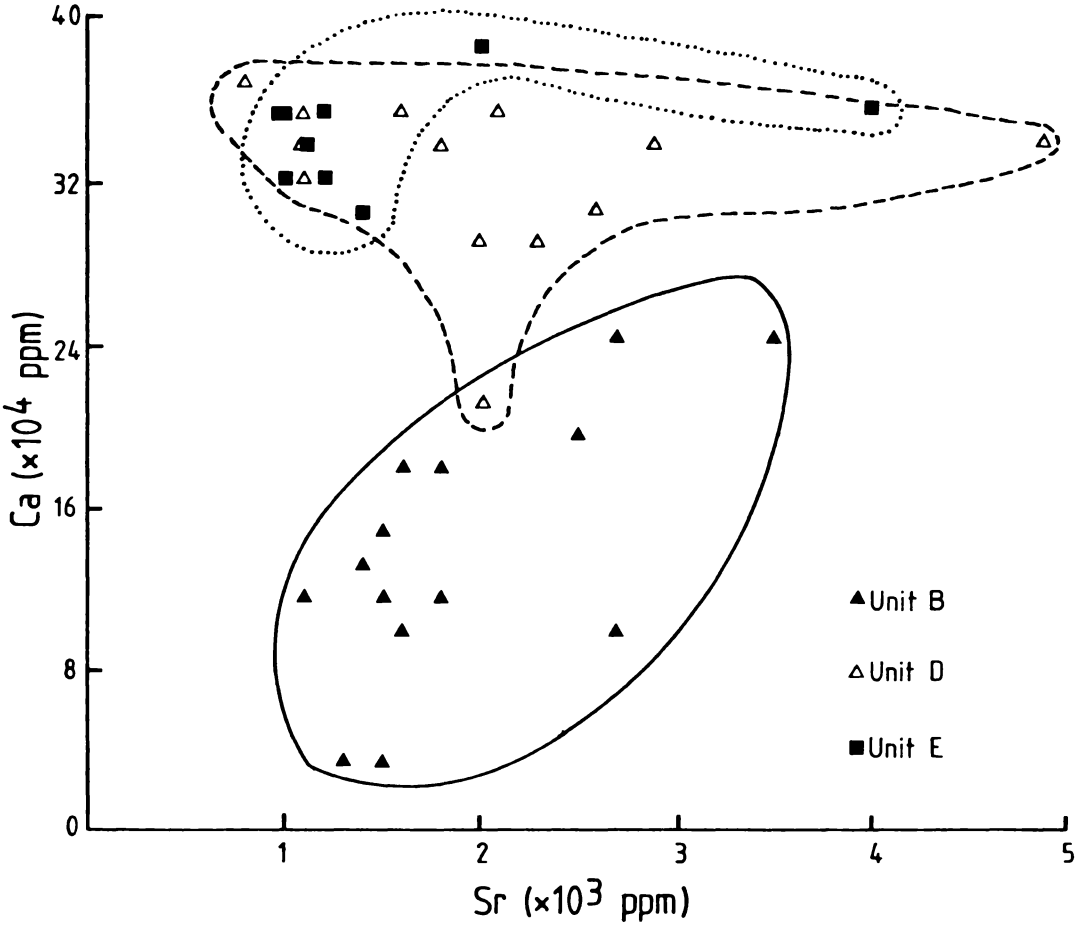

Figure 4.22 Plot of Ca vs Sr concentrations in carbonates from units E, D and B. There is considerable overlap of Sr concentrations between units. Separation of units B from E and D is primarily by Ca concentration.

Sr/Ca ratios for Lake Fryxell carbonates (0.0045 - 0.017), increase down profile and are similar to those for limestones generally (0.00027 - 0.0004, Veizer and Demovic, 1974) and recent skeletons (0.021 - 0.008). Wolf *et al.* (1967) claim that the Sr/Ca ratio should be higher in low salinity waters, partially supporting the salinity calculation in the previous section.

Only the calcareous mud (unit B) shows correlations between Sr and Mg (-0.546) and Sr and Ca (0.654)*. These correlations probably reflect competition for lattice positions. K_D values increase down profile: unit E $K_{D_{Sr}} = 0.029$, unit D $K_{D_{Sr}} = 0.042$ and unit B $K_{D_{Sr}} = 0.112$ (calculated from equation 41). Combined with the negative correlation of Sr to Mg they can be explained in the manner described by Ichikuni (1973) who stated, "the partition coefficient of Sr is increased by the presence of smaller cation is small excess of Sr". (These being divalent cations smaller in size than Ca^{2+}; e.g. Mg^{2+}).

Diagenetic equilibration tends to decrease Sr contents, hence depressing Sr/Ca ratios (Kinsman, 1969; Brand and Veizer, 1980). The Sr/Ca ratios in Lake Fryxell carbonates change little between units E and D, however are significantly higher in unit B. This increased Sr/Ca ratio matches the abundance of aragonite within the unit. It would appear that diagenesis resulting in dissolution of the primary aragonite and precipitation of calcite cement results in a loss of Sr from the sedimentation. This implies that the sediment is to some extent open to solution and solute migration. The Sr/Ca ratios indicate that significant diagenesis of this sort is limited to unit B.

---

* The correlation coefficients, in brackets, are calculated as the Pearson Product moment = $\Sigma \frac{(x - \bar{x})\ (y - \bar{y})}{((N - 1)\ (S_1)\ (S_2)}$

where: $\bar{x}$ and S_1 = mean and standard deviation of sample 1

and $\bar{y}$ and S_2 = mean and standard deviation of sample 2.

As with Mg the incorporation of Sr may also be temperature dependent, however the Mg case indicates difficulties with this argument in Lake Fryxell.

Barium

Separation of carbonate units on the basis of Ba analyses is poor because concentration ranges are similar irrespective of unit (Fig. 4.23). Unit B average concentrations are only slightly lower than units D and E (Table 4.2).

The only significant feature of Ba concentrations is that they are greater than Sr concentrations in each sample, (refer Appendix IV), in some cases by a factor of 2. This suggests, that $BaCO_3$ may have formed a discrete co-precipitate. Attempts to isolate $BaCO_3$ failed, therefore Ba concentrations are taken to be of trace components supporting the thermodynamic evidence for the non-feasibility of $BaCO_3$ precipitation (Section 3.6). Compared to skeletal carbonates (Milliman, 1974) Lake Fryxell carbonates have high Ba concentrations. Overall Ba/Ca ratios and K_D values increase down profile paralleling similar overall trends in Sr and Mg. In general, however, Ba is not a useful salinity predictor (Landergren and Manheim, 1963; cited Wolf *et al.*, 1967).

Iron, Manganese, and Zinc

Average Fe concentrations tend to increase from the calcite (unit E) to the mud (unit B). Mn and Zn concentrations show the reverse trend with the mud (unit B) > the calcite (unit E) > aragonite (unit D) (Table 4.7). These latter trends (Zn and Mn) can be partly explained by the variability between samples and probably to some extent thermodynamically, i.e. calcite minerals energetically favour the substitution of smaller cations. Fe, which is in greater concentration in the aragonite (unit D) than in the calcite from unit E, does not follow the thermodynamic

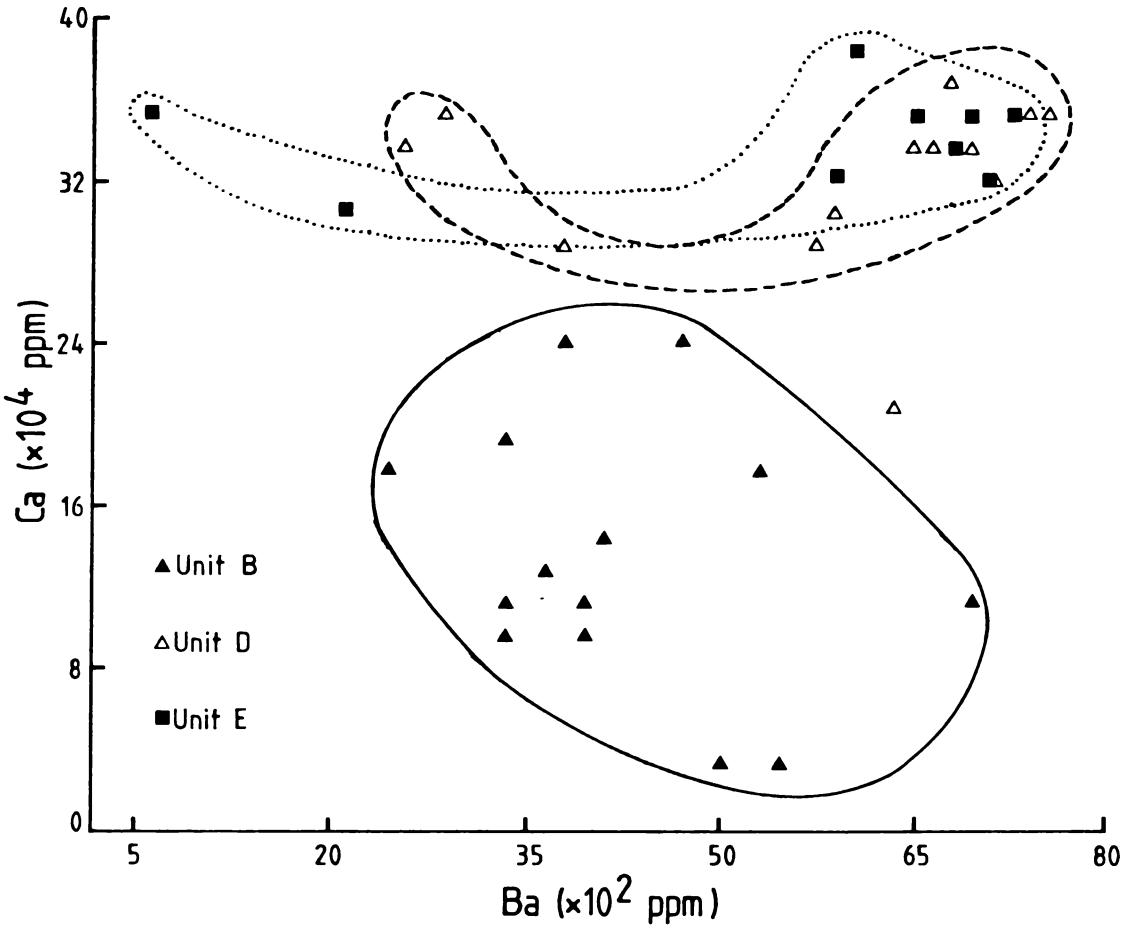

Figure 4.23 Plot of Ca vs Ba. As with Sr there is overlap of Ba concentrations between units. Combined with the spread of values unit differentiation is poor on the basis of Ba analyses.

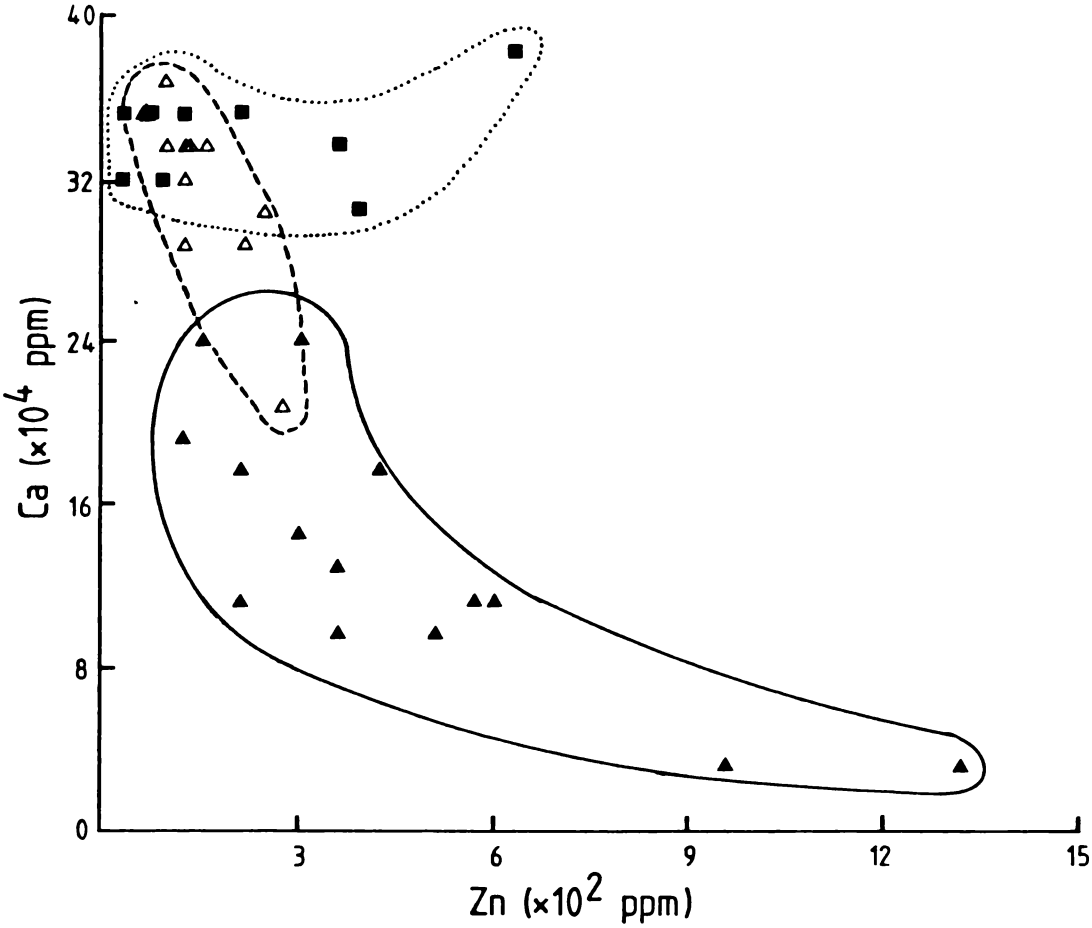

Figure 4.24 Plot of Ca vs Zn in Lake Fryxell carbonates. Note the overlap in Zn concentrations despite the relatively small spread (with 2 notable exceptions) of values within each unit.

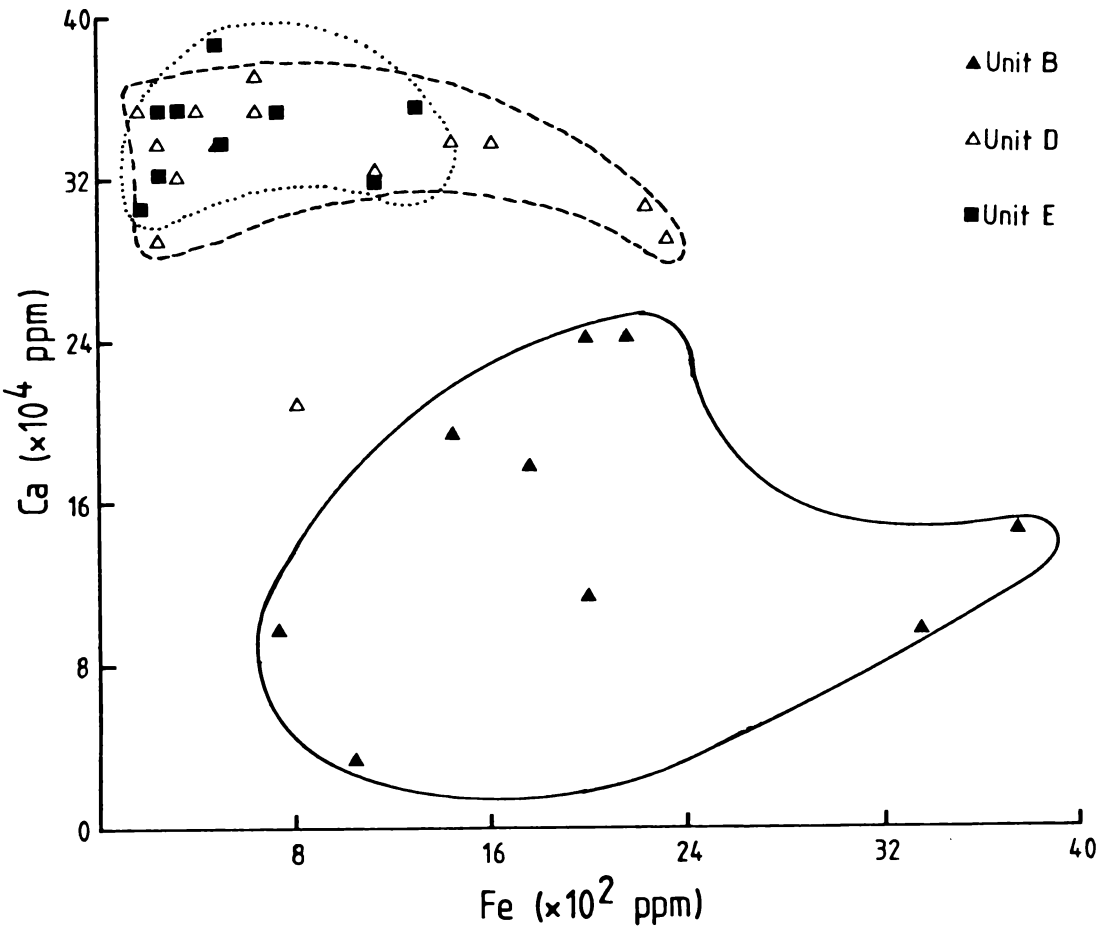

Figure 4.25 Plot of Ca vs Fe concentrations. Units E and D are similar and unit B shows considerable spread.

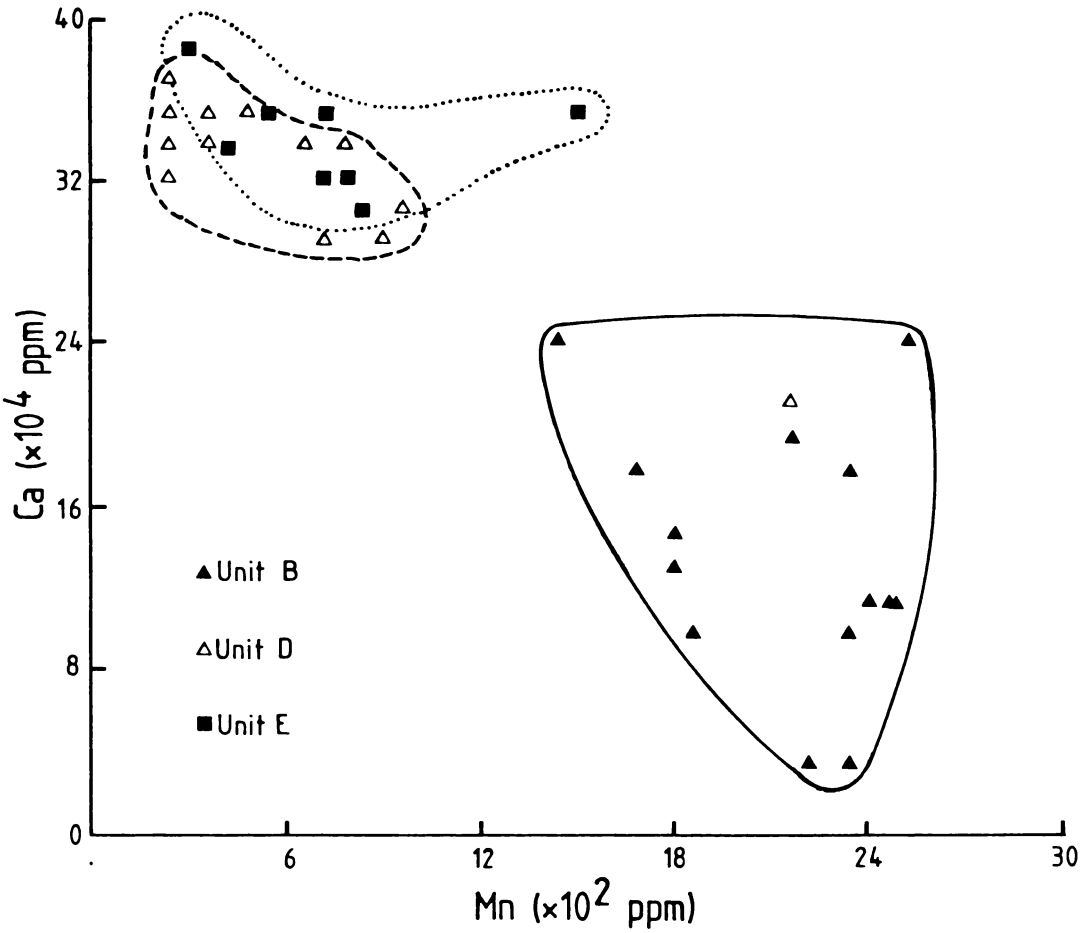

Figure 4.26 Ca vs Mn plot for Lake Fryxell carbonates. The unit D and E fields are similar though small and fairly distinct. Unit B Mn values are more spread out but noticeably higher.

pattern and may possibly be explained by surface adsorption, or by changes in the oxidation state of the lake waters. The larger percentage of fine grain sizes in the mud may be responsible for a large amount of surface adsorption, and hence may explain some of the considerable concentration increases observed in these samples. No systematic trends within the units for these elements occur.

Zn analyses do not differentiate the carbonate units particularly well as the ranges for respective units overlap (Fig. 4.24). However for Fe the Unit E (calcite) field lies within that of unit D whilst unit B show considerable variability (Fig. 4.25). Thus Fe analyses are marginally better than Zn for carbonate unit differentiation.

Mn analyses appear more useful than the above two; while units D and E overlap, unit B shows a noticable increase in Mn concentration (Fig. 4.26).

The earlier discussion on Sr content indicates the possibility of some diagenetic alteration. Pingitore (1978) reported Sr and Mg depletion, and Zn and Mn enrichment occurred in the calcite/calcite recrystalization during limestone evolution. For an aragonite/calcite transformation Sr depletion occurred, Zn remained the same, Mn and Mg^{2+} increased. When the Mn/Ca ratio is plotted against aragonite percentage for unit B an inverse relationship is obtained (Fig. 4.27). A similar though less pronounced relationship is observed in unit D. Thus it appears that aragonite, is transforming to calcite, particularly in unit B and also in unit D.

4.3.6 *STATISTICAL ANALYSIS*

One of the aims of this work is to develop a model of carbonate deposition in Lake Fryxell. As part of this overall aim a statistical analysis was performed in the hope of picking out relationships between carbonate sediment characteristics that are not readily obvious, and

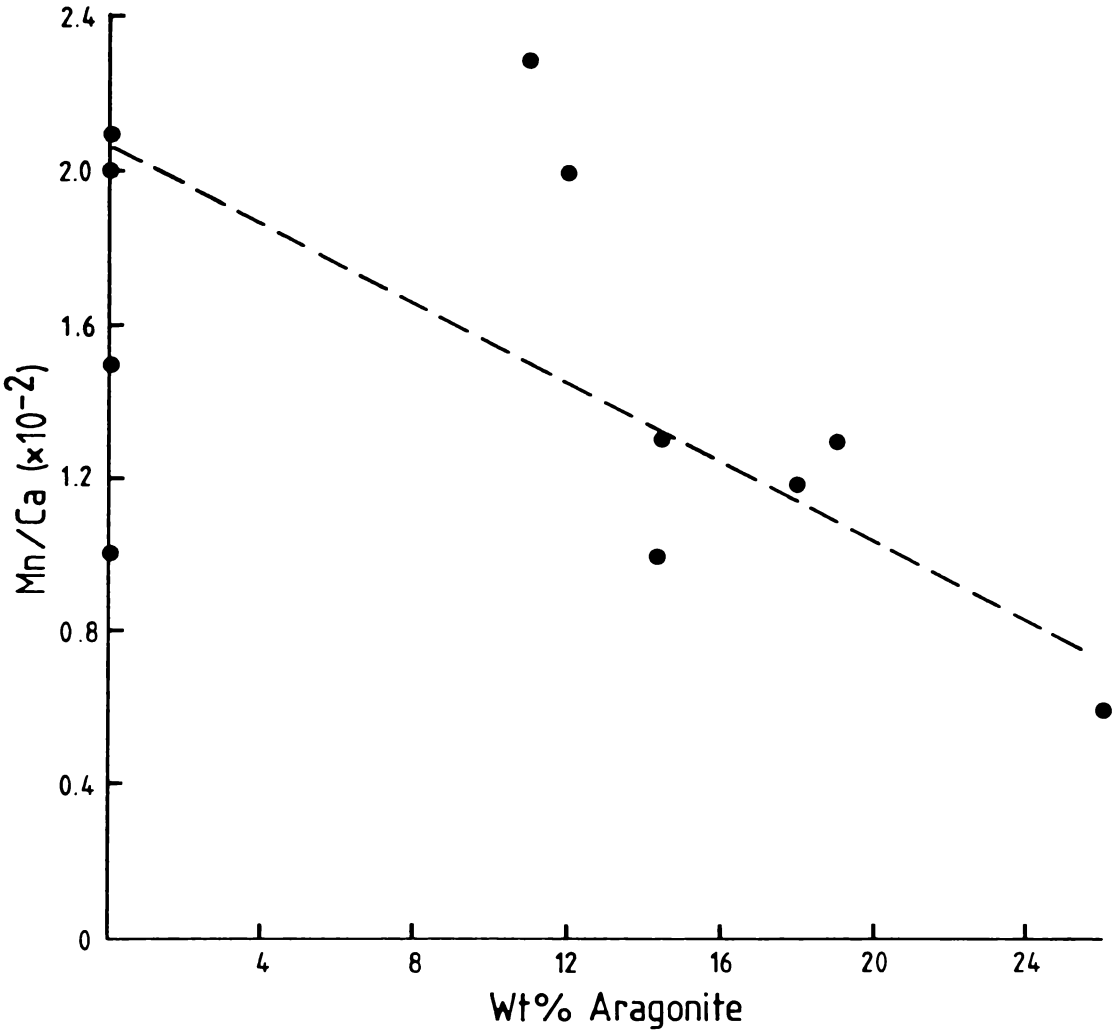

Figure 4.27 Plot of Mn/Ca us wt% aragonite for unit B. This shows a general decreasing Mn/Ca ratio with increasing wt% aragonite, suggesting the transformation of aragonite to calcite.

to try and obtain statistical relationships that describe the data.

Discriminant analysis was employed. This has been defined by Koch and Link (1971, Vol. II, p.102) as "a set of methods for classifying multivariate observations into 2 or more groups through developing one or more linear combinations that comprise the observations". The analysis was performed using the BMDP7M - Stepwise Discriminant Analysis programme (Jennrich and Sampson, 1981).

The carbonate units have previously been shown to be differentiated on the basis of mineralogy, $\delta^{18}O$ and Ca concentration. The statistical analysis verified this but provided no additional conclusions.

4.4 DISCUSSION

4.4.1 *NON-CARBONATE SEDIMENTATION*

The non-carbonate mineralogy reflects the surrounding bedrock geology and glacial sediments. The quartz and feldspars are probably derived from the Irizar Granite, Larson Granodiarite and associated schists described by Haskel *et al.* (1965). Biotites come from both the above igneous sources, with hornblendes from the Irizar Granite. The source of pyroxenes is the dyke complexes (Gumbley, 1975) and basaltic erratics within till sheets (Stuiver *et al.*, 1981) which also supply some of the rock fragments.

In deep lakes deposition is almost entirely from suspension. Flow into a standing water body deposit deltas at stream mouths which fine offshore (Collinson, 1979). Where underflow occurs delta formation is inhibited. Wind may also be important as a transport mechanism (Collinson, 1979). The present thermal and chemical characteristics of the lake and meltwaters, plus presently observed delta formation at stream mouths indicates inflow onto the top of the water column in Lake Fryxell. Lateral deflection of inflowing water by the ice cover is also possible.

Numerous ancient deltas line streams up valley walls marking old lake levels (e.g. Kellog *et al.*, 1980; Stuiver *et al.*, 1981) indicating similar inflow conditions in the past. It appears that deposition of fluvially transported material in Lake Fryxell and its ancient counterparts is from suspension with the coarse fractions remaining at or near river mouths or lake margins.

Wind action constitutes an additional sediment input. Material of up to sand size deposited on the lake ice was observed melting its way through, thus adding significant quantities of sand sized sediment to the lake. Apparently sand sizes are the largest material capable of conducting enough heat to facilitate such melting.

Most of the non-carbonate sedimentation occurs during summer when the ice melts. Varve-like laminations in the aragonite (unit D) and the alternating coarse/fine laminations of unit E are probably formed by summer pulses of detrital sediment. Unit E laminations consisting of a couplet of a coarse and fine layers probably represent a single year's deposition. How often they occur depends on the efficiency of ice melting and subsequent stream runoff.

Fine grained sediments tend to accumulate in the central and deeper parts of a lake (Collinson, 1979). Lake Fryxell occupies the deepest portion of the drainage basin covering much of the area where ancient lacustrine mud (unit B) deposition occurred. This explains the increase in thickness of unit B offshore (Fig. 4.12).

Redeposition of lake sediments is exemplified by unit Bb. The material has slumped from oversteepened depositional surfaces (Collinson, 1979). Significantly unit Bb indicates the presence of older carbonate deposits than are encountered in the described stratigraphy.

Unit A is possibly a fluvial deposit resulting from the advance of the Ross Sea Ice (Stuiver *et al.*, 1981).

Lake bottom waters are anaerobic, as are the sediments as indicated by unoxidized organic matter. The latter quickly oxidized after cores were opened. Groundwater movement would be limited because of permafrost, thus diminishing any likely oxidation from this source. Dark coatings on some carbonate flakes suggest sulphide precipitation. Although not sought, such sulphides may also be present in the non-carbonate phases.

4.4.2 *CARBONATE SEDIMENTATION*

The three carbonate-bearing units are each distinguished by their distinctive carbonate mineralogy. Statistical treatment indicates that the three carbonate units are differentiated best on the basis of wt% calcite and Ca concentration, as well as oxygen isotope data. Element plots in a number of cases show separation primarily on the basis of the Ca concentration alone, thus supporting the statistical evidence. Ba, Fe, and Zn appear to be the least useful distinguishing elements, with Sr being marginally useful, although this may be partly explained by the small sample size from each carbonate. A larger sample size may better define the fields and hence be more indicative of trends. Much of the data presented have skewed distributions, particularly Sr and Fe, and to some extent Mg.

The statistical analysis did not, for some reason, pick up the fact that Mg is an important means of separating the units containing calcites. Unit B contains high Mg-calcites and unit E tends to have lower Mg-calcites (Fig. 4.19) implying different depositional and/or post-depositional history. The Mg data confirm the differentiation of the carbonates from XRD analysis.

Calcites at the top of the sediment column (unit E) are deposited as outlined in Chapter 3, i.e. from biologically governed reactions.

Unit B (calcareous mud) is a probable deep water deposit as suggested by its fine grain size. ^{14}C dates from this unit slightly predate the ages obtained by Stuiver *et al.* (1981) on algae from perched deltas. From these dates Stuiver *et al.* (1981) showed that about 20,000 years ago the Ross Sea Ice Sheet had dammed the lower end of the Taylor Valley. A large lake, Glacial Lake Washburn, formed as a result of the increased supply of meltwaters from the expanded ice sheet (Stuiver *et al.*, 1981). The large volume of water suggests that carbonate precipitation in unit B was not due to evaporitic concentration but was probably analogous to precipitation of the present calcites in unit E. The organic matter content and low weight percent of total carbonate argue for this latter mechanism. If the solubility profile of this ancient lake was similar to that presently observed then increased dissolution would have occurred because precipitated grains had further to fall through the water column, giving the low $CaCO_3$ percentage. This may also account for some of the poor crystallinity indicated by XRD peaks (Fig. 4.15).

$\delta^{13}C$ analyses of unit B show waters become isotopically lighter as deposition proceeded. Stream inflows are also isotopically light (section 3.3.2, Fig. 3.12). Therefore it is concluded that the $\delta^{13}C$ measurements reflect a mixing of lake and inflowing meltwaters in the euphotic zone. The large ice sheet would maximize meltwater supplies (Stuiver *et al.*, 1981) possibly masking the effect of biological activity. Thus instead of an increasing $\delta^{13}C$ trend up the unit, the reverse is the case because the organisms could not precipitate carbon as fast as it was being supplied from the meltwaters.

From the evidence presented it appears that the primary $CaCO_3$ mineral deposited in unit B was aragonite, implying a greater salinity than that presently found in Lake Fryxell, according to the Müller *et al.* (1972) model. Biogenic involvement in the precipitation is suggested by

the presence of organic material in the mud, but cannot be definitely proven.

The aragonite of unit D was deposited under conditions of greater salinity. Section 3.4.1 showed that in the past the lake had been substantially reduced in volume. Stuiver *et al.* (1981) indicated a rapid drop in lake levels from about 17,000 years to 12,000 years B.P. (Fig. 2.3) as a result of the retreat of the Ross Sea Ice. The retreat of the ice which had formerly dammed the seaward end of the valley meant lake waters then occupied areas once under glacial ice (Stuiver *et al.*, 1981). The result was an increased ablation surface combined with a diminution of meltwaters from a diminished glacial source. Thus evaporation exceeded input, causing concentration of salts possibly to the extent that the ice cover no longer existed, and subsequent carbonate precipitation. Thus unit D is an evaporite with precipitation occuring where evaporation was greatest. During the initial stages of precipitation some dissolution of grains falling through the water column (Hardie *et al.*, 1978) would have occurred. Consequently precipitates near the lake margins were subject to less dissolution because of a smaller water column through which to fall. This combined with the greater evaporation occuring in the shallower lake margins resulting in the thickening of unit D shorewards. Gradually dissolution in progressively deeper waters diminished due to continued brine concentration.

Other than the single organic layer at the top of unit D there is little direct evidence of biogenic activity associated with deposition of the aragonite. The carbonate becomes isotopically heavier in $\delta^{13}C$ up the unit indicating biological CO_2 fixation. While still affecting the CO_2 budget, biological reactions were probably overshadowed by evaporitic processes.

^{14}C Dates (yrs BP) This study	^{14}C Dates (yrs BP) Stuiver *et al* 1981	UNIT	THICKNESS OF UNIT (cm) Mean	Max.	Min.	SEDIMENTATION RATES (cm/yr) Mean	Max.	Min.
		E	28.3	79.5	7.5	0.003	0.009	0.001
	9200							
10,700		D	18.7	32.5	9.5	0.007	0.012	0.003
	12000							
	14000							
21,000		B	25.9	86.5	11.0	0.004	0.012	0.002
	21200							

Figure 4.28 Sedimentation rates for calcareous units E, D and B. As shown sedimentation rates are extremely low.

4.4.3 *SEDIMENTATION RATES*

Sedimentation rates calculated from ^{14}C ages and unit thicknesses, are summarized in figure 4.28. Sediment thickness was measured immediately upon opening the cores which probably reduces any dewatering effects. Compaction effects were difficult to assess because of the fluid nature of the sediment/water interface and because of possible settling out of the material as a result of core transport.

The sediment rates obtained, however, are very low probably reflecting a slow low energy depositional mechanism, possibly settling of grains from suspension. Depositional rates would depend upon meltwater runoff and wind for the transport of detrital grains, biological activity, and in cases such as unit D, evaporation plus the rates of precipitation and dissolution. Dissolution may possibly have removed some of the top of unit D implying that the unit D/E boundary may be an unconformity.

4.4.4 *CARBONATE POST-DEPOSITIONAL CHANGES*

Any physical diagenetic processes, if occurring, appear to be at an early stage. The unconsolidated nature of the sediments indicates minimal pore reduction, and the aragonite of unit D is reasonably friable. Skrinkage of unit B occurred upon drying, indicating significant porosity. Problems arise with respect to unit B as there is some debate in the literature as to whether compaction in calcareous muds occurs in the same manner as it does in other muds (Pettijohn, 1975). It is suggested that there is little physical pore reduction because of early cementation.

Sr results indicate change within individual carbonate units whereas the Zn and Mn concentrations show changes between units. The problem is determining whether Mn and Zn concentrations are primary or post-depositional features although the latter is more probable.

Calcites at the top of unit E are unstable with respect to modern lake bottom waters. The same situation may have applied to the other calcareous units suggesting dissolution and possible reprecipitation. Evidence of reprecipitation of calcite as a cement in the aragonite unit (D) is shown in Fig. 4.29. Small rhombs surround aragonite needles and probably accounts for the minor calcite indicated in XRD traces (Table 4.6, Fig. 4.15).

The Sr content of a precipitated cement is controlled by the Sr content of the original aragonite and its dissolving solution (Kinsman, 1971). The Sr concentrations of the primary mineral and cement will differ. If the system were open then the cement may be precipitated elsewhere thus leaving a Sr-depleted carbonate. In the Lake Fryxell carbonates enough water movement appears to have taken place causing the Sr originally precipitated in aragonite in unit B to be lost on re-crystallization to calcite.

The inverse relationship between Mn/Ca ratios and aragonite abundance in unit B (Fig. 4.27) and D is consistant with the preferential substitution of the smaller Mn^{2+} ion the calcite lattice compared to the aragonite lattice. The source of the Mn is not clear. It may result from autoenrichment (Pingitore, 1978), or it may come from the weathering of non-carbonate minerals during diagenesis, or possibly both. The calcite/calcite recrystallization in the evolution of limestones also leads to autoenrichment in Mn (Pingitore, 1978).

Bathurst (1975) states that if the rate of precipitation of calcite exceeds the rate of dissolution of aragonite then the rate controlling process in the aragonite/calcite transformation in aragonite dissolution: and *vice versa*. From the Lake Fryxell carbonate data it is not possible to determine which is the rate determining step.

Lake Fryxell, being essentially a closed, though natural system,

Figure 4.29 Scanning electron micrograph of unit D showing acicular aragonite crystals surrounded by what appear to be rhombic calcite. Rhombic calcites are circled. Photo - C. Beltz.

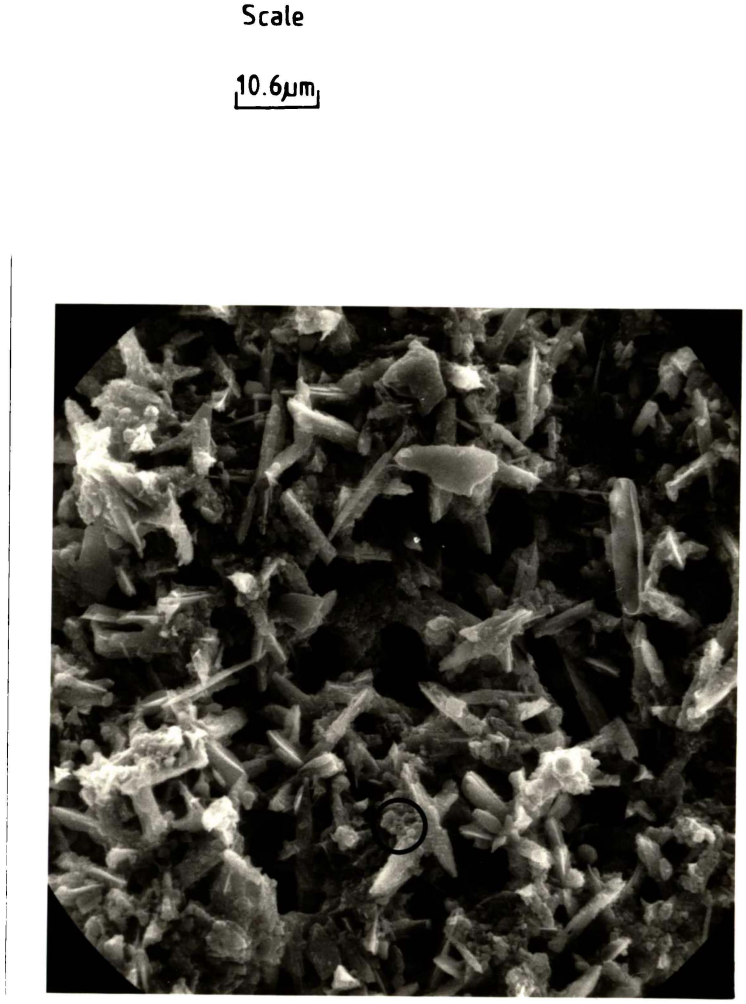

is an interesting site for the investigation of early diagenetic effects on carbonate chemistry.

4.5 CONCLUSIONS

1) Five distinct lithologic units are recognized in Lake Fryxell sub-bottom sediments. Three of them, units E, D and B contain $CaCO_3$ deposits.

2) The carbonate-bearing units can be distinguished on the basis of their mineralogy, Ca and Mg concentrations, and to some extent on $\delta^{13}C$ and $\delta^{18}O$ analyses. Ba and Fe analyses are the lease useful for this purpose. Sr, Mn, and to some extent Mg, are indicative of post-depositional change, with Mg also being an important depositional paleoenvironmental indicator.

3) $\delta^{13}C$ analyses indicate biogenic control of the $CaCO_3$ precipitation process, particularly in the surface calcites of unit E (Chapter 3). The effect is not as clear for unit B, although precipitation mechanisms were probably similar to those now present. Evaporatic processes during deposition of unit D (aragonite) dominated precipitation mechanisms, although biological CO_2 fixation continued to occur. Salinities based on $\delta^{18}O$ and Mg were greater for units B and D than at present.

4) The primary mineralogy of units B and D is aragonite to which post-depositional alteration is indicated by geochemical and mineralogical analyses.

CHAPTER FIVE

CONCLUSIONS : A CARBONATE DEPOSITIONAL MODEL FOR LAKE FRYXELL

5.1 INTRODUCTION

Deposition of carbonates in Lake Fryxell both past and present have been outlined. This chapter outlines generalized depositional models for each of the calcareous units in Lake Fryxell sediments.

5.2 DEPOSITIONAL MODELS

5.2.1 *UNIT B*

The environmental setting and processes operating the deposition of Unit B are shown schematically in Fig. 5.1. The unit corresponds in time to a period of high lake levels in proglacial Lake Washburn during the last Ross Sea Ice advance.

Carbonate precipitation and deposition is taken to have occurred as it does today, the main difference being that aragonite was precipitated. Precipitation was possibly concentrated in a euphotic zone, the position of which was governed by light and nutrient availability. The solubility profile was possibly similar to that presently in Lake Fryxell. Thus precipitated grains settling out of suspension dissolved as they fell through the water column. This dissolution may have caused the diminished grain size and crystallinity, giving poor X.R.D. peaks (Fig. 4.15). The dissolution may also account for the relatively low total weight percent $CaCO_3$ in unit B, although this may also be due to a large fine sediment input from increased meltwater flows.

Non-carbonate sedimentation consisted of the deposition of material by meltwaters, and redeposition of lake sediment by slumping from oversteepened depositional surfaces within the enlarged lake. Coarse sedi-

Figure 5.1 Diagrammatic representation of unit B depositional environment.

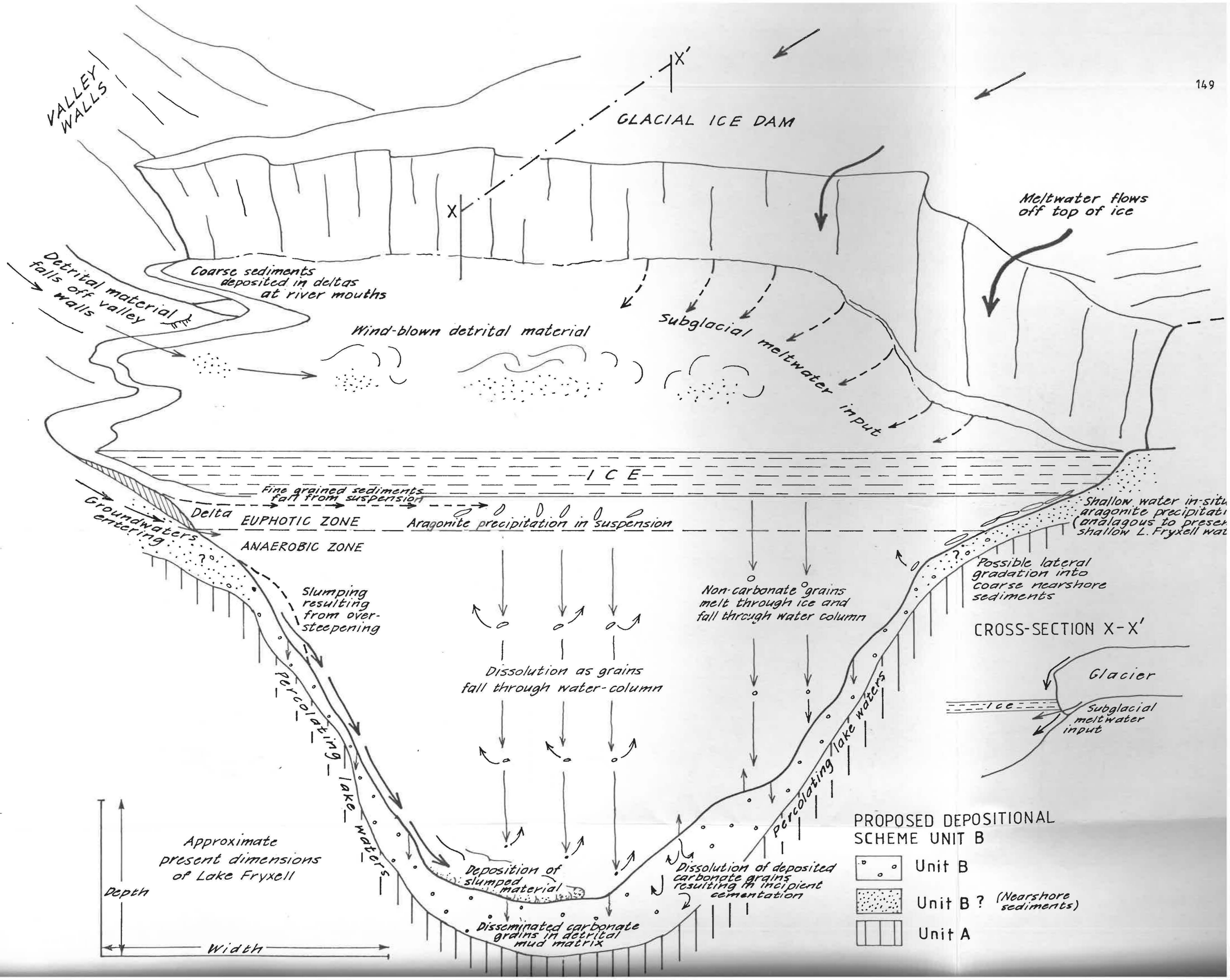
VALLEY WALLS
X
X'
GLACIAL ICE DAM
Meltwater flows off top of ice
Detrital material falls off valley walls
Coarse sediments deposited in deltas at river mouths
Wind-blown detrital material
Subglacial meltwater input
ICE
Fine grained sediments fall from suspension
Delta
EUPHOTIC ZONE
Aragonite precipitation in suspension
Groundwaters entering
ANAEROBIC ZONE
Shallow water in-situ aragonite precipitati (analagous to preser shallow L. Fryxell wat
Slumping resulting from over-steepening
Non-carbonate grains melt through ice and fall through water column
Possible lateral gradation into coarse nearshore sediments
CROSS-SECTION X-X'
Glacier
Ice
Subglacial meltwater input
Percolating lake waters
Dissolution as grains fall through water-column
Approximate present dimensions of Lake Fryxell
Depth
Width
Deposition of slumped material
Disseminated carbonate grains in detrital mud matrix
Dissolution of deposited carbonate grains resulting in incipient cementation
PROPOSED DEPOSITIONAL SCHEME UNIT B
Unit B
Unit B ? (Nearshore sediments)
Unit A

ment fractions entrained in meltwaters were deposited in deltas and/or near lake margins. These probably graded laterally into the unit B mud deposited from suspension in deeper parts of the lake. Aeolean sands melting through the ice cover would also have contributed to the sediment however,as much of the valley was covered by ice the amount of sand blown onto the lake ice would have been less than at present.

$\delta^{13}C$ measurements suggest that precipitation occurred as the lake filled. Inflowing meltwaters diluted the lake "solution" and masked the effect of biological activity on $\delta^{13}C$. The influx of meltwaters came from a greatly expanded ice sheet which dammed the lower end of the valley (Stuiver *et al.*, 1981). The precipitation of aragonite suggests that the salinity of this lake was similar to that of seawater. The $\delta^{18}O$ analyses suggest that seawater may have contributed to the lake. Diatom fossils found in perched deltas however, indicate that the water in glacial Lake Washburn was non-marine (Kellog *et al.*, 1980). This however, does not preclude relict seawater supplemented with glacial meltwater, or the possibility that the character of glacial Lake Washburn altered during the course of its ∿10,000 year history.

5.2.2 *UNIT D* (Fig. 5.2)

Retreat of the Ross Sea Ice caused a reduction in lake volume because of a reduced meltwater supply and removal of ice from the lake basin. As a result, the lake had to physically occupy areas that were once under ice. Consequently there was an increased ablation surface area (Stuiver *et al.*, 1981) which instigated an evaporative concentration of lake waters. This evaporative concentration was the main driving force for carbonate precipitation. $\delta^{13}C$ values indicated continued biological activity which enhanced the evaporative mechanism.

Unit D carbonates are thicker in shallow water than deep waters. This may reflect undersaturated deep waters such, that in the initial

Figure 5.2 Diagrammatic representation of unit D depositional environment.

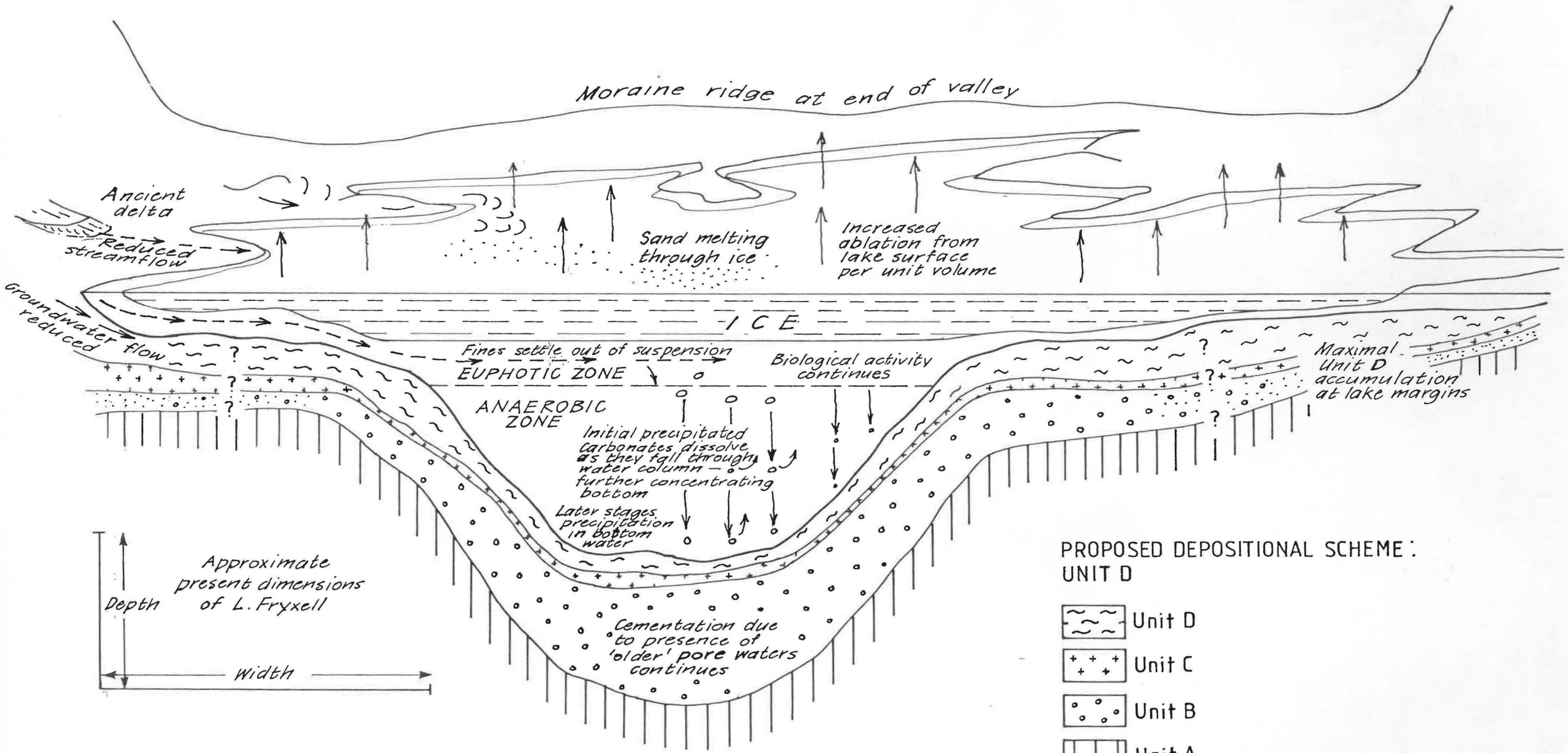
Moraine ridge at end of valley
Ancient delta
Reduced streamflow
Groundwater flow reduced
Sand melting through ice
Increased ablation from lake surface per unit volume
ICE
Fines settle out of suspension
EUPHOTIC ZONE
Biological activity continues
ANAEROBIC ZONE
Initial precipitated carbonates dissolve as they fall through water column — further concentrating bottom
Later stages precipitation in bottom water
Maximal Unit D accumulation at lake margins
Approximate present dimensions of L. Fryxell
Depth
Width
Cementation due to presence of 'older' pore waters continues
PROPOSED DEPOSITIONAL SCHEME: UNIT D
Unit D
Unit C
Unit B
Unit A

stages of the evaporative cycle, much of the precipitated aragonite rain was dissolved as it fell through the deeper waters. In addition it may also be possible that biological productivity may have been greater in the shallow waters where more efficient nutrient recycling would have been possible.

The varve-like nature of the carbonate probably results mainly from a discontinuous input of non-carbonate sediment of aeolian or fluvial origin. Each detrital-rich layer may also be associated with a hiatus in carbonate deposition as the inflow which transported the detritus might have reduced carbonate precipitation.

The overall thickness and high total weight percent of the carbonate suggest a greater water salinity than when unit B was deposited. The abundance of trace elements in unit D (and E) carbonates generally differ from those of unit B, suggesting a change in water composition between the two lakes, with $\delta^{18}O$ and Mg/Ca ratios decreasing to the present composition.

5.2.3 *UNIT E*

Unlike units B and D in which properties of the waters are inferred from analyses of the sediment, the waters from which unit E was deposited have been analysed and the carbonate system is more readily understood.

The lake waters are divided into an upper euphotic (aerobic) zone, and a lower anaerobic zone. Saturation with respect to calcite occurs in the euphotic zone, while waters are undersaturated with respect to calcite in the anaerobic zone. Carbonate precipitation results from CO_2 fixation in the euphotic zone by organism, predominantly cyanophytes (blue-green algae). In areas where the water is deep, precipitated grains fall from the euphotic zone down through the water column and undergo some dissolution. Grains reaching the bottom form the observed calcite flakes. Importantly, calcite does not occur throughout unit E signifying the precipit-

Figure 5.3 Depositional environment presently prevailing in Lake Fryxell.

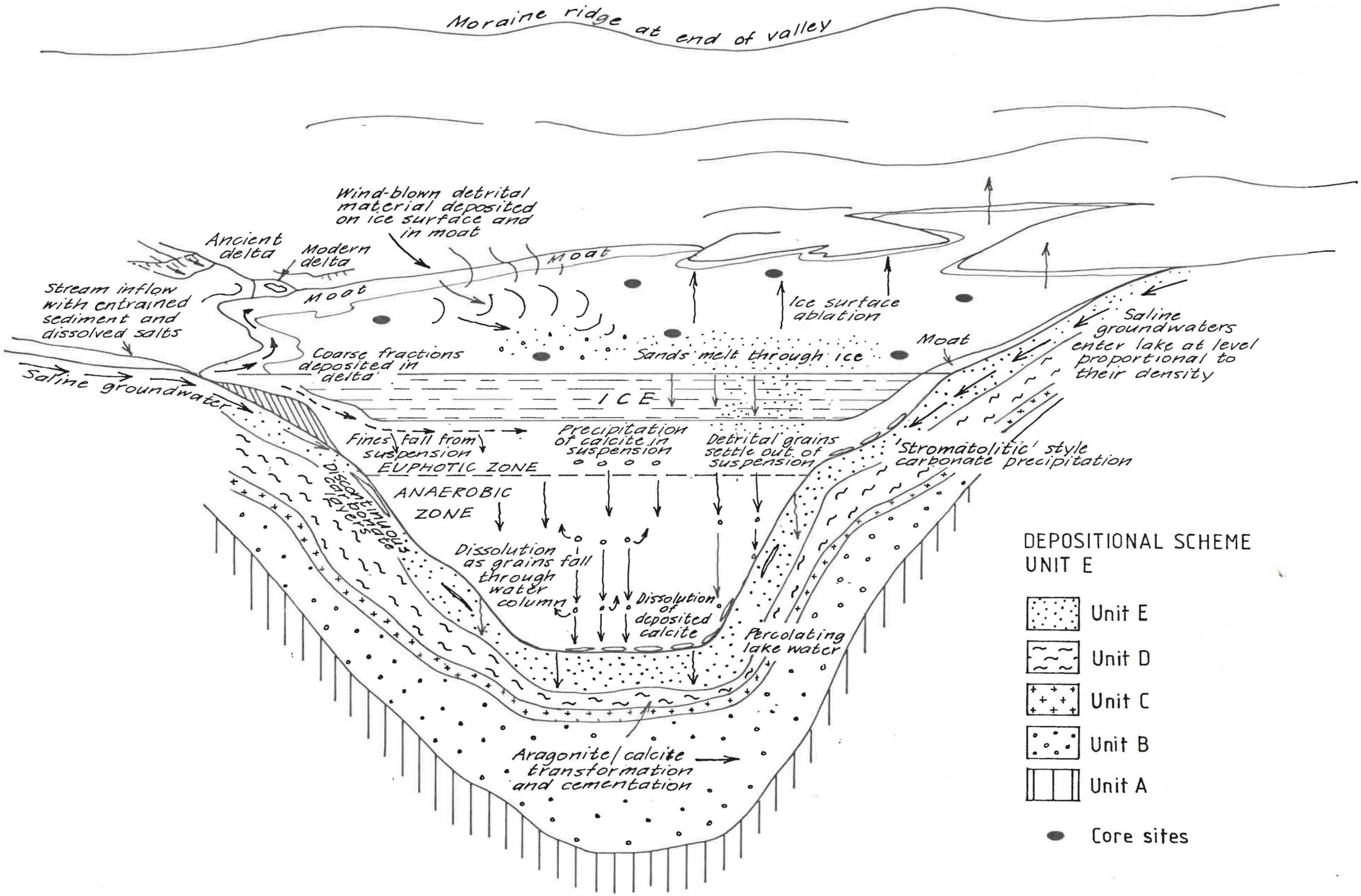
Moraine ridge at end of valley
Wind-blown detrital material deposited on ice surface and in moat
Ancient delta
Modern delta
Moat
Moat
Stream inflow with entrained sediment and dissolved salts
Ice surface ablation
Saline groundwaters enter lake at level proportional to their density
Moat
Coarse fractions deposited in delta
Sands melt through ice
Saline groundwater
ICE
Fines fall from suspension
Precipitation of calcite in suspension
Detrital grains settle out of suspension
'Stromatolitic' style carbonate precipitation
EUPHOTIC ZONE
ANAEROBIC ZONE
Discontinuous carbonate layers
Dissolution as grains fall through water column
Dissolution of deposited calcite
Percolating lake water
Aragonite/calcite transformation and cementation
DEPOSITIONAL SCHEME UNIT E
Unit E
Unit D
Unit C
Unit B
Unit A
Core sites

ates instability with respect to lake bottom waters and sediment pore waters. Occasional carbonate layers below the sediment surface indicate an interelated-set of processes (Fig. 5.4).

Where the lakebed is within the euphotic zone carbonate settling from free floating algae is augmented by carbonates precipitated *in situ* by the algal mat. The formation of stromatolites is unlikely in deep waters because of the constraints on algal productivity in that environment.

Non-carbonate inputs are the same as for units B and D. Coarse fractions settle out first followed by muds with associated organic detritus, thus giving rise to alternating coarse/fine laminations. The variable spacing between these laminations suggests that they may not be varves as they may not represent seasonal sedimentation.

5.2.4 *POST-DEPOSITIONAL CHANGES*

Precipitated calcites in unit E are unstable with respect to Lake Fryxell bottom waters. The calcites appear to show dissolution effects (Fig. 3.18). Both mineralogical and geochemical evidence indicates that aragonite dissolution and calcite re-precipitation is occurring in calcareous units B and D. This has caused cementation resulting in the partially indurated, though still somewhat friable nature of unit D. The cementation may also have reduced somewhat the compaction in unit B in the manner suggested by Pettijohn (1975).

5.2.5 *ORIGIN AND EVOLUTION OF LAKE WATER*

Present Lake Fryxell waters are derived from glacial meltwaters. These meltwaters come from present alpine glaciers which are now at their maximum positions since the Ross Sea Ice retreat (Stuiver *et al.*, 1981). The salts in the waters are derived from: the original brine and/or redissolved salts from the bottom of the lake basin, glacial meltwater,

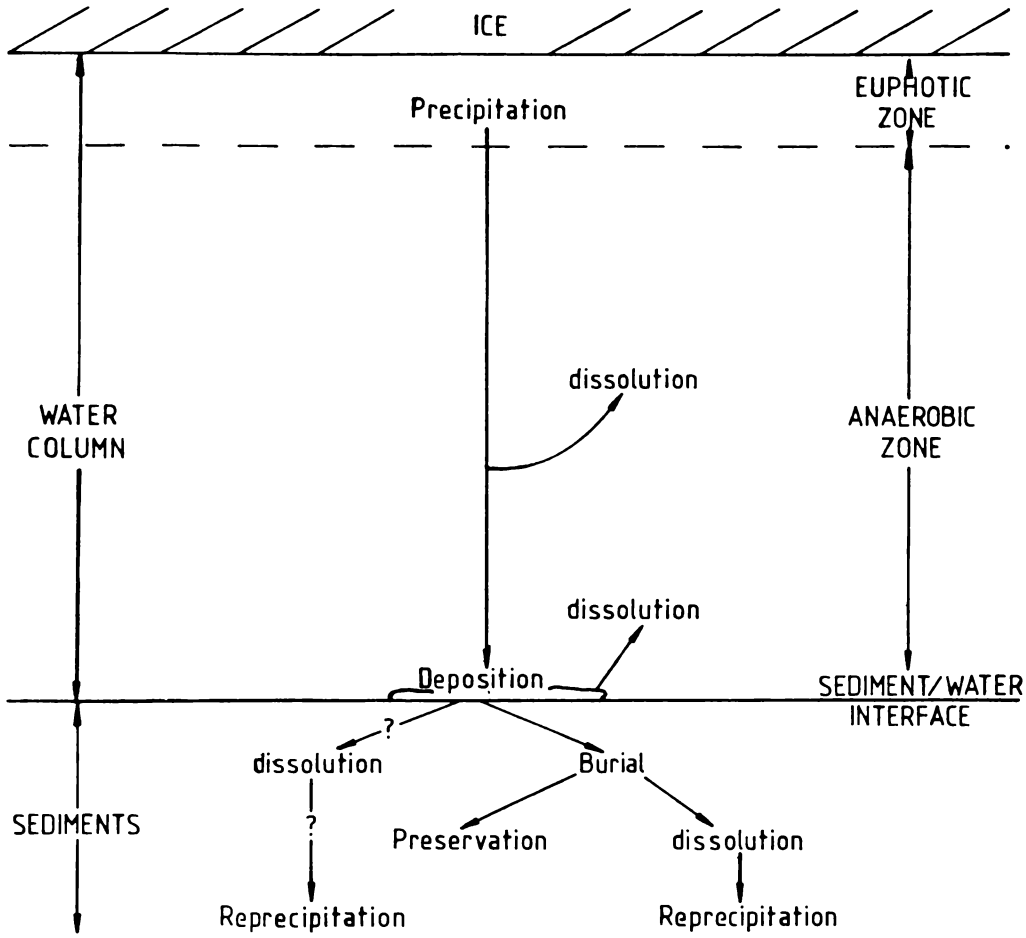

Figure 5.4 Schematic illustration of the interrelated processes in carbonate deposition indicating the possible fate of precipitated grains.

salt effloresences and saline ground waters, and seawater. The original salts from the lake bottom have diffused back up the water column creating a diffusion cell below 9 m depth.

Early carbonate precipitation has important effects on the evolution of saline waters by governing the subsequent water composition and resultant precipitates (Fig. 3.14b; Hardie *et al.*, 1978). Already mentioned is the possibility that freeze concentration may drive the brine evolution system (Fig. 3.14b). However, in Lake Fryxell, the evidence suggests that in the initial stages of brine evolution biological activity can cause carbonate precipitation. This provides an organically derived kinetic control on the lake chemistry. Therefore to suit the present Lake Fryxell situation, the model of brine evolution (Fig. 3.14b) requires consideration of the combined effects of organic and inorganic processes. Consequently any estimates of the future evolution of Lake Fryxell waters must be generalized and speculative. The possibilities are:

(i) Status quo situation, where water inputs are greater than or equal to outputs.

(ii) Outputs exceed inputs causing the lake value to diminish resulting in increased carbonate and possibly gypsum precipitation.

In the past (e.g. unit D deposition), the evaporative evolution model (Fig. 3.14b) of Eugster and Hardie (1978) has been more applicable.

Although the origin of the lake water prior to and during deposition of units B and D is less evident than for the present waters, it seems reasonable to assume that the waters and dissolved salts had similar origins to those at present. Kellog *et al* (1980) suggested that the unit B waters were non-marine as no marine diatoms were found in the sediments. However, the presence of marine salts and higher than expected $\delta^{18}O$

values suggests that a subglacial marine input occurred. The carbonate deposition in unit D was responsible for the present Ca-depletion in Lake Fryxell waters.

5.3 SUMMARY

The precipitation and dissolution regime in Lake Fryxell is not adequately explained by thermodynamic arguments alone. It is proposed that carbonate deposition in units E and B was primarily controlled by biogenic processes. Biogenic processes during unit D deposition are evident but were probably subordinate to inorganic solute concentrative mechanisms. Subsequent dissolution of carbonates, irrespective of precipitation mechanism, was affected by the composition, pressure and temperature of the water column through which the carbonate particles fell and by the same factors in pore waters after deposition and burial. The kinetic effects resulting from a particular regime are controlled and modified by changes in the precipitation/dissolution regime. These changes in depositional regime are caused by larger scale phenomena such as climate changes (e.g. if Ross Sea advances or retreats) and/or smaller and possibly more local seasonal changes which appear as "overprints". The well defined units A, B, C, D and E reflect control by large scale phenomenon whilst varve-like sequences attest to local overprinting.

CHAPTER SIX

APPLICATION OF THE LAKE FRYXELL MODEL TO THE MARSHALL VALLEY

6.1 INTRODUCTION

From the knowledge gained by the study of carbonate sedimentation in the modern Lake Fryxell and its precursors it is desirable to be able to interpret other Antarctic carbonate deposits. Of these the Marshall Valley carbonates are particularly interesting because they are unusually well exposed and because of the multiplicity of carbonate sequences.

6.2 LOCATION

The Marshall Valley (78° 04'S, 164° 00'E) is situated between the Garwood Valley to the north and the Miers Valley to the south (Fig. 6.1). It arises near an arm of the Blue Glacier and opens out to a shelf extention of the Koettlitz Glacier. The valley is about 10 km long and contains a small alpine cirque glacier (Rivard Glacier) at its head.

6.3 STRATIGRAPHY AND SAMPLE LOCATION

There are no lakes or ponds at present in the Marshall Valley, but a meltwater stream flowing from the Rivard Glacier has cut down into unconsolidated lacustrine, glacial and fluvial sediments. The deposits include carbonate and gypsum precipitates, with interbedded lacustrine silts, sands and some gravels. The presence of gypsum associated with most of the carbonates strongly suggests that the carbonates precipitated as a result of evaporative concentration rather than from biogenic precipitation.

The stratigraphy (Figs. 6.2, 6.3, 6.4) was supplied by Denton and

Figure 6.1 Location map of the Marshall Valley.

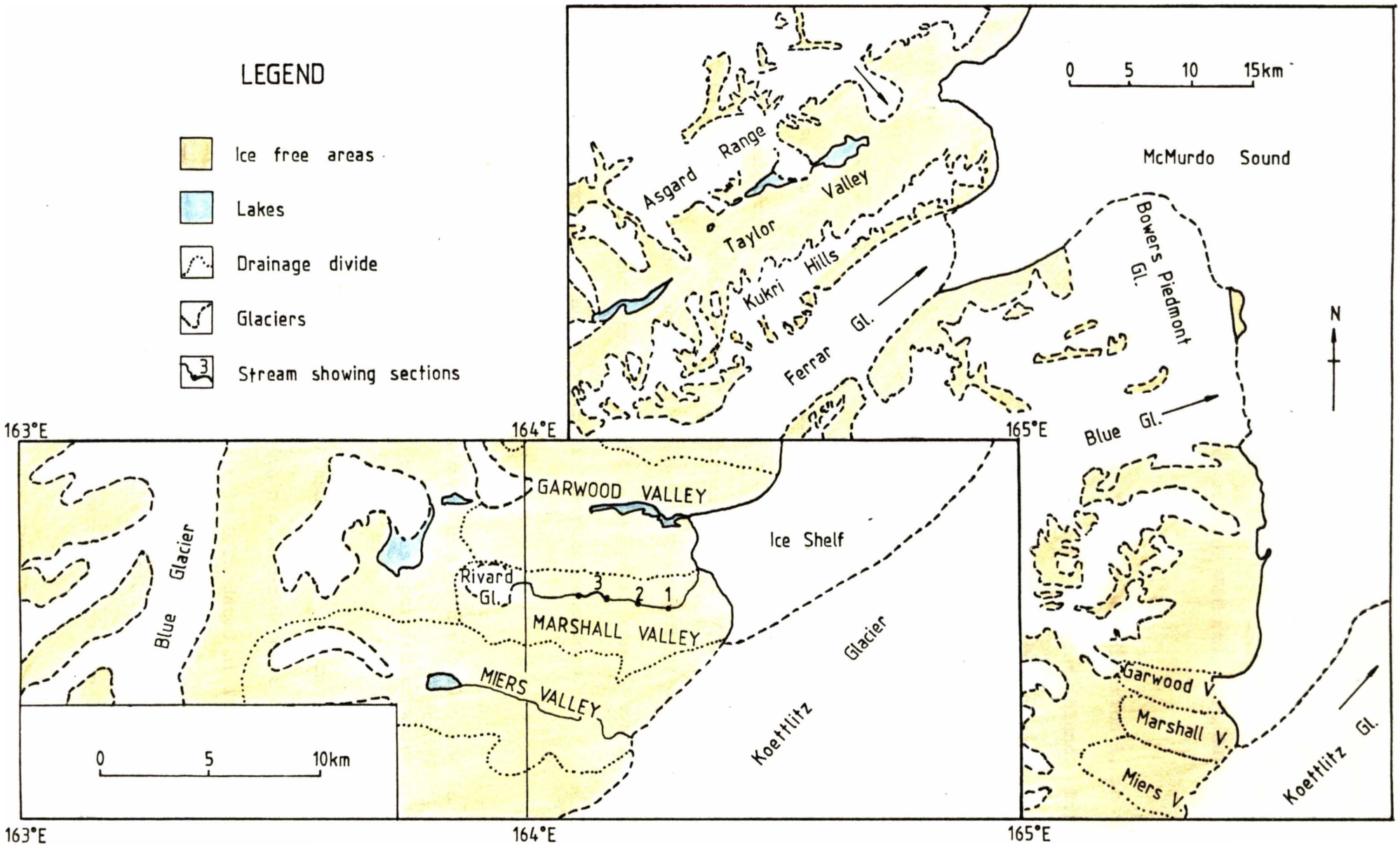
LEGEND
Ice free areas
Lakes
Drainage divide
Glaciers
3
Stream showing sections
0 5 10 15km
McMurdo Sound
Asgard Range
Taylor Valley
Kukri Hills
Ferrar Gl.
Bowers Piedmont Gl.
Blue Gl.
N
163°E
164°E
165°E
GARWOOD VALLEY
Ice Shelf
Blue Glacier
Rivard Gl.
3 2 1
MARSHALL VALLEY
MIERS VALLEY
Koettlitz Glacier
0 5 10km
Garwood V.
Marshall V.
Miers V.
Koettlitz Gl.

Dragel pers. comm. (1982) but without detailed descriptions. Samples were obtained from precipitate layers by Dr C.H. Hendy and analysed at the University of Waikato using the same methods as outlined in Chapter 4.2. U/Th dates were done at the University of Waikato, U/Th dating laboratory.

The sections are spread along 5 km of stream with section 1, in the east, nearest the sea and section 3 to the west, furthest inland. For the purposes of this discussion precipitate or evaporite horizons are referred to as units and are labelled from the base of the sections, upwards.

6.3.1 *SECTIONS AND SAMPLE LOCATION*

The sections consist of precipitate or evaporite units interlayered between diamictons, sands, silts, and gravels. The evaporite units are old lake bed deposits. With confirmation from U/Th dates some units can be traced from one section to the next. Descriptions of non-precipitate materials are those of Denton and Dargel pers. comm. Evaporite unit sample numbers are shown on the illustrated sections.

Section 1

Section 1 (Fig. 6.2) is at the seaward end of the valley and is approximately 42 m long and 8 m high, the lowest portion of which stands at an altitude of about 150 m.

There are two evaporite units, 1A and 1B. The lowermost unit, 1A (Fig. 6.2) is aragonitic and occurs within a mixed deposit of sand, gravel, cobbles, and boulders. The unit is U/Th dated at 180,000 ± 10,000 years B.P. and is continuous throughout the section. Immediately overlying unit 1A at the eastern end of the section are what appear to be deltaic foreset beds indicating these materials to have been deposited in a standing body of water.

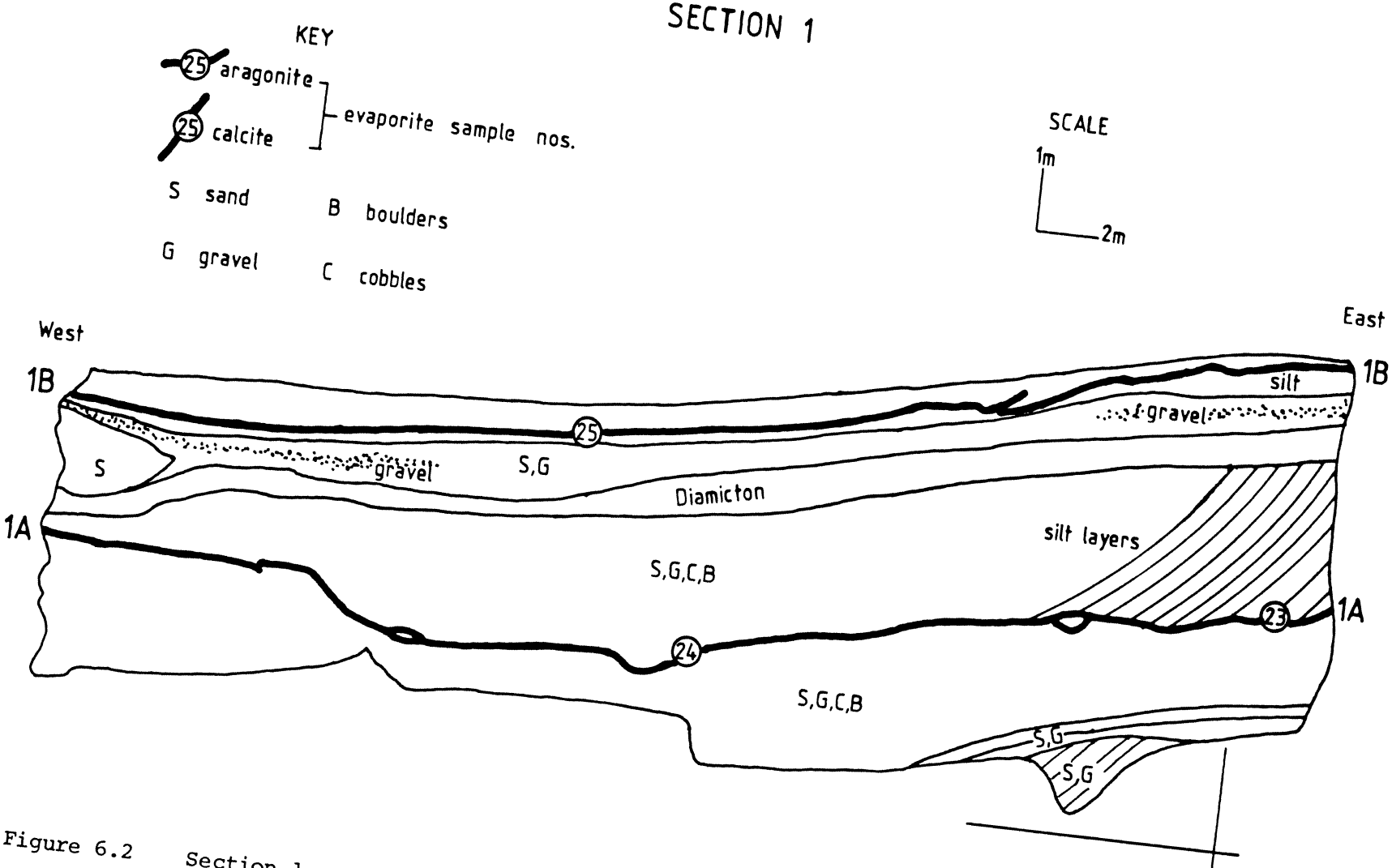

Figure 6.2 Section 1.

Overlying the mixed deposit and the foreset beds is a thin diamicton, which is in turn overlain by a deposit of sand and gravel layers. Algae within one of the gravel layers has been dated at 13,300 ± 5000 years B.P. Overlying the sand/gravel layers is a silt covered by evaporite unit 1B. This evaporite is U/Th dated about 8000 years B.P., is gypsum and like 1A is continuous throughout the section.

Section 2

This is a larger and more complicated section (Fig. 6.3) than section 1. It is approximately 82 m long and about 9 m high, and the lowest portion of which stands at an altitude of about 200 m. In this section 5 evaporite units are identified. The bottom unit, 2A, overlies a coarse sand/gravel layer. The evaporite is primarily calcite, is discontinuous, and has been U/Th dated at 190,000 to 210,000 years B.P.

Overlying unit 2A is a sand, with another discontinuous calcareous unit, 2B. on top. Unit 2B can be traced to the western end of the section (Fig. 6.3) but has poor exposure to the east. Two samples in the unit are primarily calcite, but one is a mixed calcite aragonite precipitate.

Between unit 2B and a continuous unit, 2D, is a mixture of sediments consisting of 2 diamictons, a and b, plus fragmentary calcareous layers. These fragmentary calcareous layers have been grouped together as unit 2C. They appear to be a mixture of aragonites and calcites of U/Th age ranging from 164,000 - 145,000 years B.P. From the available stratigraphic evidence alone it is difficult to tell if they constitue a separate unit or are fragments of other units.

The deposits described above appear to be overlain unconformably by evaporite unit 2D. This unit is primarily aragonite but contains one gypsum sample at the eastern end of the section. No dates on this unit are presently available for this section but would appear to be in the order of 130,000 years B.P. The unit is continuous to about half

Figure 6.3 Section 2.

SECTION 2

KEY

7 cement sample nos.

19 aragonite
10 calcite — evaporite sample nos.
22 gypsum

S sand B boulders

G gravel C cobbles

SCALE
1m
2m

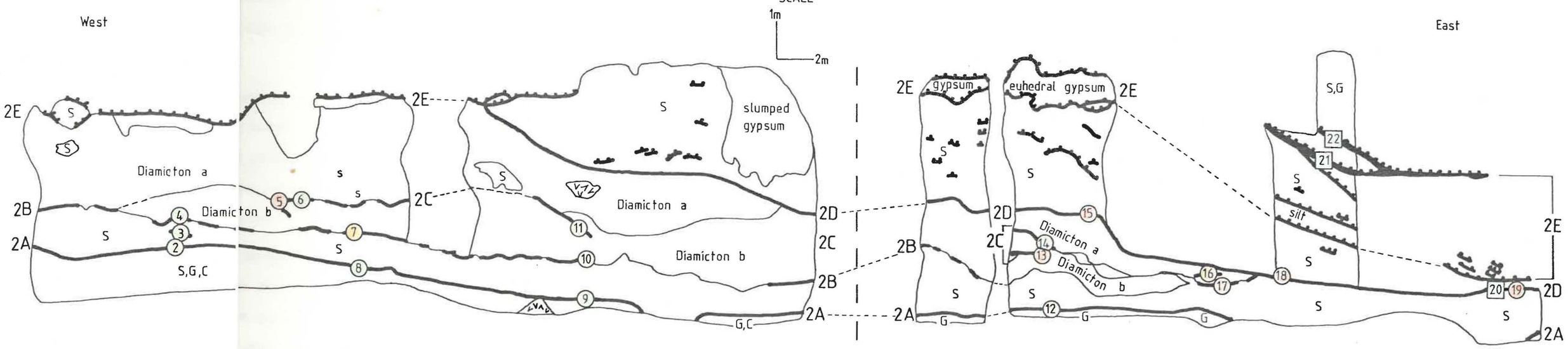

way through the western end of the section. Some of the samples from 2D appear to be oxidized, fragmented and have probably been subjected to subareal weathering.

Overlying unit 2D is a sand containing variously fragmented gypsum evaporite deposits, grouped together as unit 2E. A surface outcrop of these materials truncates unit 2D at an angular unconformity in the western end of the section. One sample of unit 2E, from the eastern end of the section, gives an age of 11,000 years B.P.

Section 3

Though discontinuous, section 3 (Fig. 6.4) is the longest of the 3 sections, being about 500 m long of which about 130 m have been mapped in detail. The section is up to 10 m high and at an altitude of about 250 m. In the middle of the section is a rip up clast consisting of a piece of folded lake bed. The character of the 4 evaporite units is different from previous sections owing to the association of carbonate and gypsum.

Overlying a coarse cemented sand in the western end of the section is unit 3A. The unit has two U/Th dates, 170,000 ± 6000 and 240,000 ± 16,000 years B.P., and consists of calcite, gypsum (selenite) and a gypsum cemented detrital layer. The unit is untraceable eastwards beyond the folded segment in the middle of the section.

The diamicton overlying unit 3A incorporates unit 3B. Unit 3B is similar to Unit 2C (in the previous section) as both are fragmentary units. U/Th dates on unit 3B which consists of gypsum, calcite and aragonite, range from 182,000 ± 14,000 years B.P., at the eastern end of the section, to 205,000 ± 16,000 years B.P. at the western end. The unit cannot be confidently traced from one end of the section to the other. Like unit 2C, 3B may be either fragments of other units or a separate unit. Differences in U/Th ages do not enable a correlation between 2C and 3B.

Figure 6.4 Section 3.

SECTION 3

KEY

- Cement sample nos.
- aragonite
- calcite
- gypsum
- evaporite sample nos.
- S sand
- G gravel
- B boulders
- C cobbles

SCALE

1m

2m

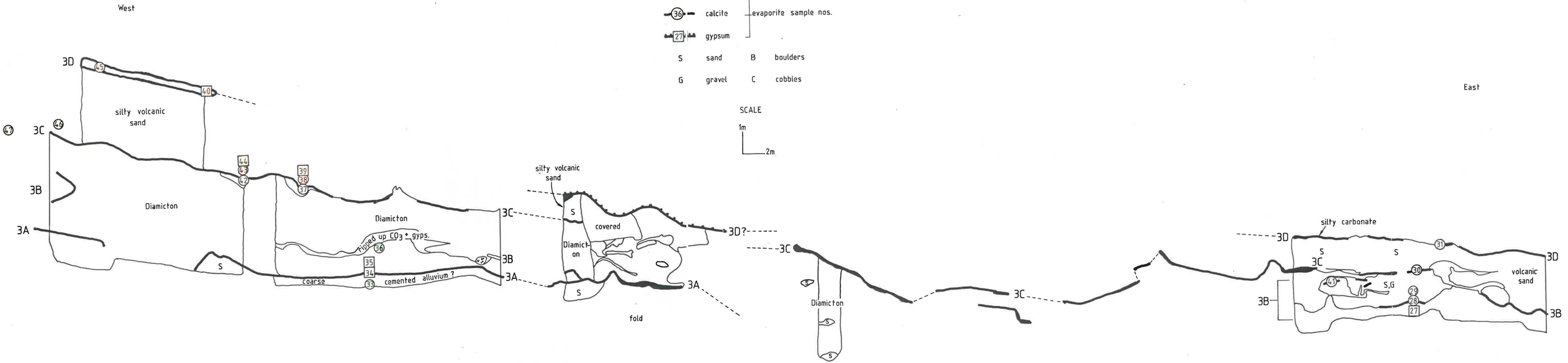

The diamicton is overlain by a discontinuous unit, 3C, which appears traceable throughout the section. U/Th dates on unit 3C range from 180,000 ± 12,000 years B.P. to 172,000 ± 20,000 years B.P. It has the same 3 layered morphology as unit 3B, in this case calcite, overlain by aragonite, overlain by gypsum.

Overlying unit 3C is a silty volcanic sand (Denton and Dargel, pers. comm.) capped by unit 3D. Unit 3D consists primarily of aragonite with some gypsum. Overlying the silty volcanic sand in the centre of the section is gypsiferous material which may be part of unit 3D. No samples were obtained from this material so no definite conclusion can be made.

6.3.2 *UNIT CORRELATION*

An attempt has been made to correlate units between sections. This is summarized in Table 6.1. For comparison the Lake Fryxell units are included.

Table 6.1 Correlation of units and events for Marshall Valley sections in relation to Lake Fryxell units. Dashed lines indicate suggested correlations.

Age (10^3 Yrs B.P.)	Event	Marshall Valley Sections 1	2	3	Lake Fryxell
Present					E
∿10			2E		D
∿20	Ross Sea I	IB			B
			2D?----3D		
∿150					
	Ross Sea II		2C		
∿180		1A		3B — 3C	
				3A	
∿200	Ross Sea III ?		2A		

6.4 CHEMISTRY AND MINERALOGY OF MARSHALL VALLEY PRECIPITATES

Two important differences exist between Lake Fryxell precipiates and the Marshall Valley sediments; (i) the presence of identifiable "cemented" detrital layers within the Marshall Valley precipitate units, and; (ii) the occurrence of gypsum. These indicate a differing chemical environment from that presently prevailing in Lake Fryxell.

6.4.1 *MINERALOGY*

Most of the samples contain more than one precipitate phase, though one phase usually predominates. The uppermost units in sections 1 and 2 are gypsum. In section 2 units 2B and 2C become more aragonitic seawards, which from the Lake Fryxell model implies a salinity gradient in this direction. No such trend occurs in unit 2A, or 1A where too few samples are available.

The occurrence of calcite, aragonite and gypsum in section 3 indicate what appears to be a progressive salinity increase resulting from the evaporation of a brine (Holser, 1979). In some cases carbonate casts appear around crystals which were subsequently dissolved. Upper carbonate layers are primarily aragonitic. Most of the gypsum is of the selenite variety.

Cemented detrital layers are frequently associated with the units. The cement mineralogy is primarily aragonite but some gypsum cements also occur. These cements can be either above or below the originally precipitated layers in the units.

6.4.2 *ELEMENTAL ANALYSES*

Marshall Valley samples have been analysed for Ca, Mg and Sr only, and results are listed in Appendix V. Carbonates only have been chemically analysed.

Calcium

Ca concentrations in these samples are generally greater than 300,000 ppm with a maximum of about 386,000 ppm. The lowest values are in aragonite-dominated samples from units 1A, 2D and 3C, and these are oxidized (sample from unit 2D) or reprecipitated cements (3C samples). The 2D samples have high detrital contents and may have been precipitated.

Magnesium

When Ca is plotted against Mg (Fig. 6.5) the calcite-dominated samples lie in or near the field defined by unit D aragonite from Lake Fryxell. The Marshall Valley calcites are low Mg-calcites, samples which plot below the unit D field are all aragonite dominated. Units cannot be differentiated on the basis of Mg analyses as differences between units are small.

Strontium

Sr is plotted as a function of Ca in Fig. 6.6 and compared to the fields for Lake Fryxell units. Generally Sr values are higher than those found in Lake Fryxell and they have a much greater range. Aragonite-dominated samples have the highest Sr concentrations, cemented samples lie below all the other Marshall Valley units because of their lower Ca concentrations.

Differentiation of units on the basis of Sr content is not possible because of the spread of values within individual units. Only altered or reprecipitated cement samples show differences and this is primarily due to Ca content.

6.4.3 *STABLE ISOTOPES*

$\delta^{13}C$

The $\delta^{13}C$ values are all about $0^{o}/oo$ (Fig. 6.7) cement samples have values which are only slightly higher than the other carbonates. These

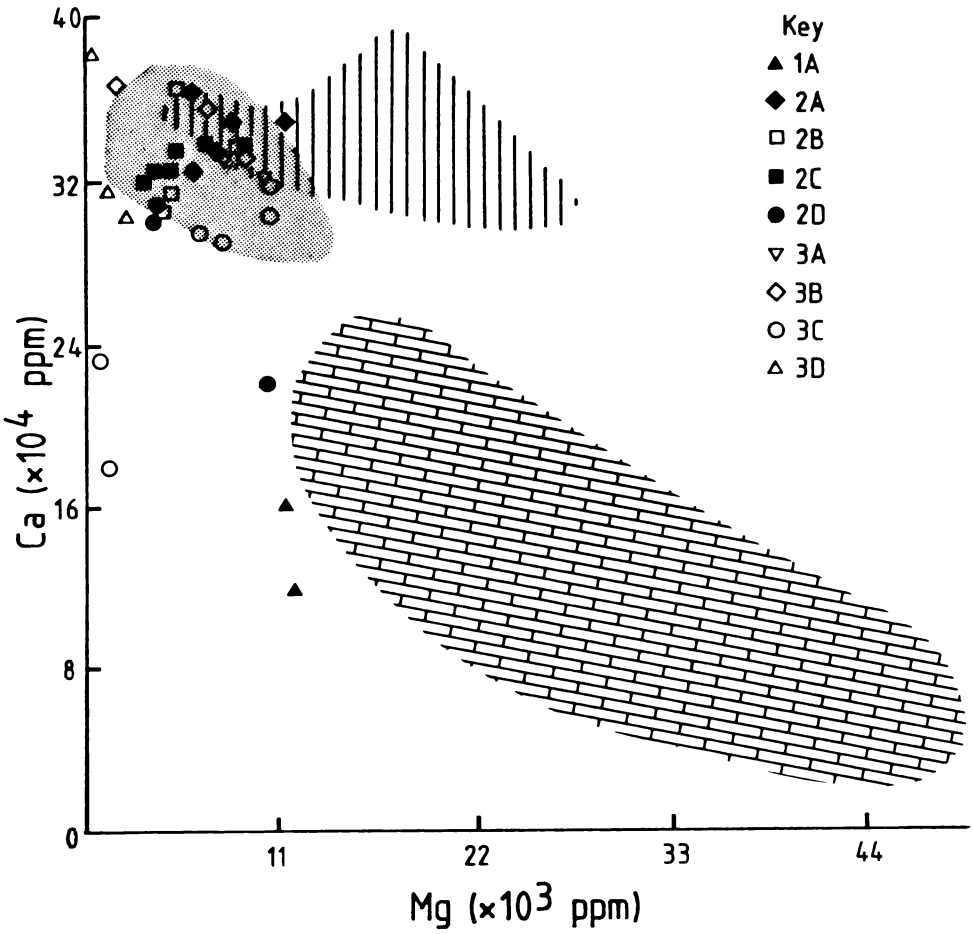

Figure 6.5 Plot of Ca vs Mg concentrations in Marshall Valley carbonates. For comparison the Lake Fryxell fields are also plotted: Unit D = stippled, unit E = vertical lines, unit B = rectangles. Most of the Marshall Valley samples plot near the Lake Fryxell unit D field, and all samples have Mg concentrations of about the same range as unit D. The 5 samples which plot below 24 x 10^4 ppm Ca are predominantly aragonite.

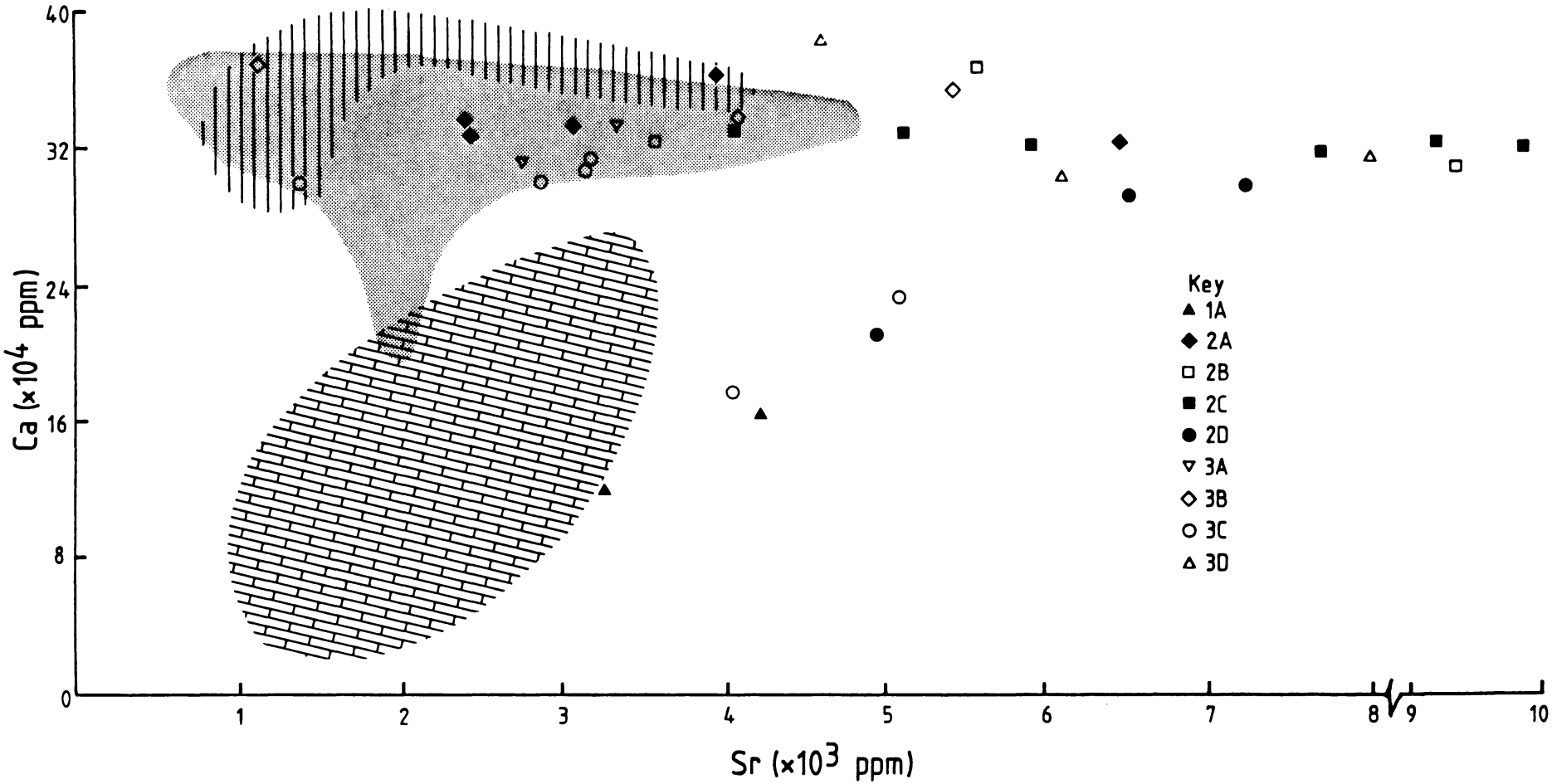

Figure 6.6 Ca vs Sr plot for Marshall Valley carbonates with Lake Fryxell units for comparison (same symbols as figure 6.5). Sr concentrations in Marshall Valley carbonates are in general greater and show more spread than Lake Fryxell samples. (One sample from unit 2B with a Sr concentration of 12880 ppm is omitted).

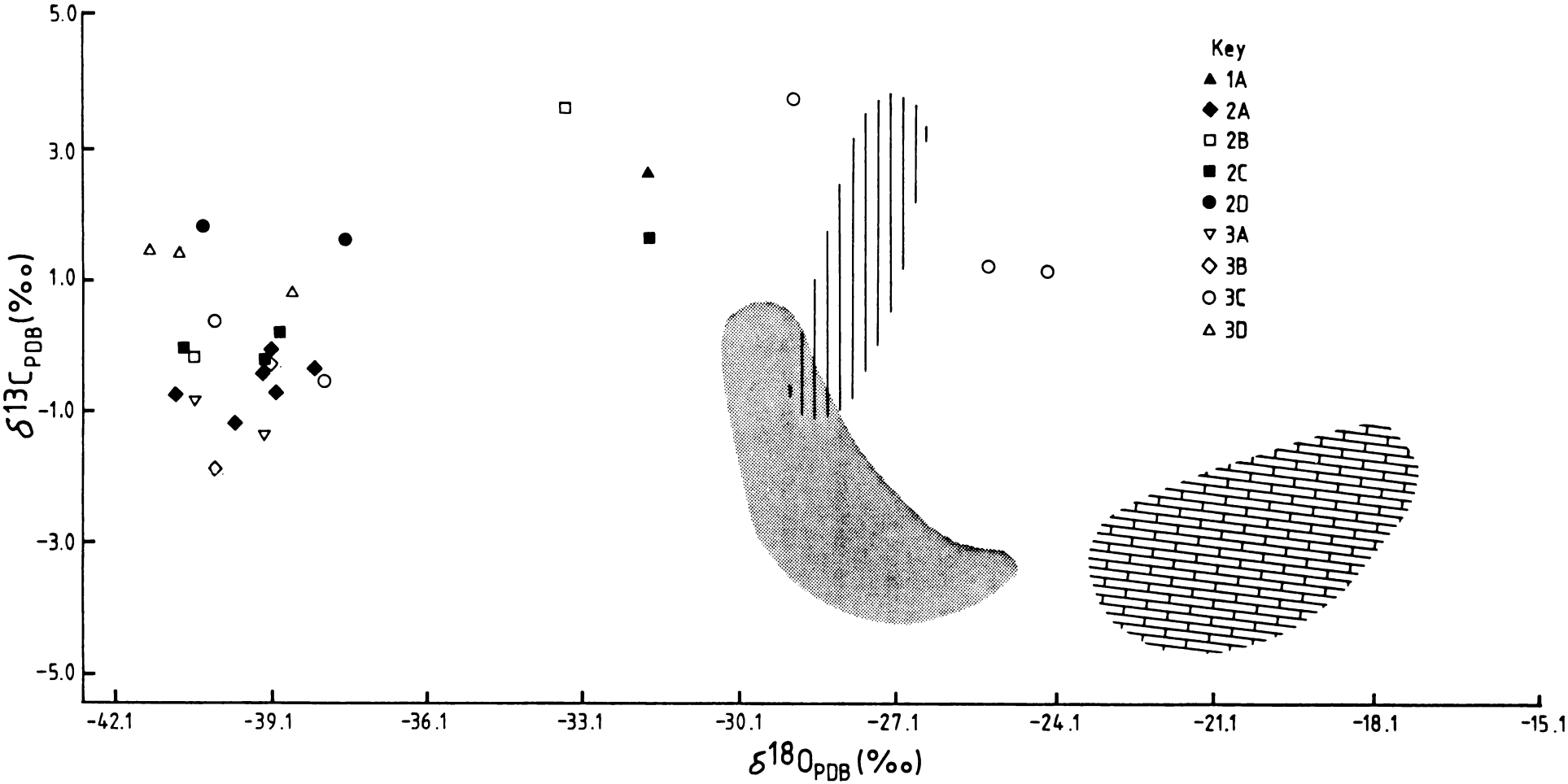

Figure 6.7 Stable isotope plot for Marshall valley carbonates in relation to Lake Fryxell carbonates. (Same symbols as Figures 6.5 and 6.6). Most of the Marshall Valley samples plot about $0^{o}/oo$ PDB for $\delta^{13}C$ but are generally isotopically lighter in $\delta^{18}O$ than Lake Fryxell carbonates. The six samples which plot nearest to Lake Fryxell fields are all carbonate cements.

values indicate ^{12}C depletion in the precipitating waters to a similar extent to that presently in Lake Fryxell.

$\delta^{18}O$

Fig. 6.7 shows the relationship of Marshall Valley units to Lake Fryxell units. The $\delta^{18}O$ values fall within 2 groups, those about $-40^{o}/oo$ and those about $-30^{o}/oo$. The latter group consists of those materials which appear to be cements. All the other carbonates are in the $\sim 40^{o}/oo$ group.

$\delta^{18}O$ values for the East Antarctic Ice Sheet are about -40 to -42‰ w.r.t. SMOW (Hendy *et al.*, 1979), which give carbonates with a $\delta^{18}O$ value of $\sim 40^{o}/oo$ w.r.t. PDB at a temperature of $0^{o}C$. Therefore the non-carbonate units were precipitated from waters of continental ice origin with minimal ^{18}O enrichment. The cements however are enriched in ^{18}O by $\sim 10^{o}/oo$ suggesting either a different source for the water or possibly evaporitic enrichment.

6.5 DISCUSSION

The evaporite units in the Marshall Valley span at least 2 and possibly 3 major glacial advances. The youngest of these can be correlated directly with the Ross Sea I drift as mapped by Stuiver *et al.* (1981). The older advances are probably Ross Sea II and Ross Sea III respectively but direct correlation to type locality has not yet been achieved. As these evaporites are generally greater in age than the carbonate deposits in Lake Fryxell, and as they have been repeatedly flooded and drained, post-depositional changes have affected the Marshall Valley carbonates to a greater degree. The result is the development of 2 distinct and recogniseable sub-units within each precipitate horizon; i) the evaporites themselves, and ii) cemented detrital zones.

6.5.1 *EVAPORITES*

Concentrations of Ca and Mg and the $\delta^{13}C$ values are all similar to those for units D and E in Lake Fryxell. Sr values tend to be greater than the Lake Fryxell units and show a greater range. $\delta^{18}O$ values are similar to each other for Marshall Valley samples but as a group they have about $\sim 20^{o}/oo$ less ^{16}O depleted than Lake Fryxell unit B, and $\sim 10^{o}/oo$ less than Lake Fryxell units D and E. Differentiation of Marshall Valley units on the basis of these analyses is not possible because most of the analyses are similar to each other, or in the case of Sr are too scattered.

Unlike the Lake Fryxell units, Marshall Valley units contain more than one of the primary minerals, aragonite, calcite or gypsum. These may be either laterally associated, as in units 2B and 2C; or vertically associated as in unit 3C. These indicate salinity gradients, both seawards and vertically. With the exception of unit 2E, gypsum becomes more prevalent inland, which is the reverse expected from the increasing salinity gradient seawards inferred from association of calcite and aragonite. This suggests that gypsum may have been dissolved by water influxes after deposition of the lake beds, giving rise to crystal casts within the carbonate cements. However, the absence of either gypsum or crystal casts in the lower parts of many beds also suggests that gypsum accumulation may have been restricted to shallower waters.

The carbonate casts are more prevalent west of section 3 (C.H. Hendy, pers. comm.). The possible minerals around which the casts formed were either ice crystals, halite, thermadite, minabalite or gypsum. The cast cavities tend to be tabular and would have required the original crystals to have remained for some time before dissolving. This precludes all the above suggested minerals except the selenite variety of gypsum. This supports the premise of gypsum dissolution suggested above.

In outcrop the precipitated carbonates have the same varve-like nature as unit D in Lake Fryxell. With the exception of $\delta^{18}O$ and possibly Sr analyses, the chemistry of the Marshall Valley carbonates appears consistant with deposition in the same manner as unit D of Lake Fryxell. The $\delta^{13}C$ suggest that deposition may have been similar to that presently prevailing in Lake Fryxell. However, an evaporitic regime with some biological CO_2 fixation is preferred because the thickness of the carbonate in the units and the presence of gypsum. To deposit the quantity of these carbonates in a similar manner to the present Lake Fryxell would probably require considerable biological activity to counter any dissolution effects in the water column.

The biological activity is incapable of precipitating gypsum. Biologically induced precipitation may have occurred during the initial stages of formation of the lake.

Greater Sr concentration than in Fryxell carbonates are probably a function of greater Sr availability in the water column. The reason for the variation in $\delta^{18}O$ between Lake Fryxell and Marshall Valley samples is uncertain. It is probably a function of the source of the water, i.e. the modern Lake Fryxell waters are alpine in origin (-28 to $34^{o}/oo$ SMOW, Hendy *et al.*, 1979), whereas Marshall Valley carbonates were precipitated in waters derived from the Ross Sea Ice Sheets, in turn derived from the East and West Antarctic Ice Sheets. These ice sheets currently have $\delta^{18}O$ values ranging from $-40^{o}/oo$ to $-50^{o}/oo$ (Dansgaard, 1964) and $-30^{o}/oo$ to $-40^{o}/oo$ (Johnsen *et al.*, 1972) w.r.t. SMOW respectively. The higher $\delta^{18}O$ values for unit B, Lake Fryxell, are not easily explained, but as mentioned previously, could reflect a mixture of glacial meltwater and seawater.

Synthesis

Precipitation in the Marshall Valley can be broadly summarized as follows:

i) Advance of a tongue of the Ross Sea Ice sheet into the mouth of the valley. This dammed the valley and allowed a meltwater lake to build up. Isotope studies of sulphates in Koettlitz tributary valleys indicated that they are marine in origin. Thus it can be assumed that much of the Marshall Valley salts were also marine in origin and transported into the valley by the Ross Sea Ice Sheet.

ii) Evaporation from the ice dammed lake resulted in precipitation of carbonates throughout the lake, and accumulation of gypsum in shallower waters.

iii) Subsequent advances of the ice tongue resulted in burial of the evaporites by fluvial and glacial sediments. In some cases erosion and reworking also occurred.

iv) Retreat of the ice tongue from the valley resulted in drainage of the lake, subareal weathering of the surficial beds, and possible cementation of deeper beds.

v) Resumption of down-valley drainage of meltwaters from the Rivard Glacier and local snowfall resulted in dissolution of some of the gypsum beds.

vi) Repeat the entire sequence.

The above is a generalized synthesis. While the details change from unit to unit, e.g. unit 2E where only gypsum occurs, it appears that the Lake Fryxell model is applicable to other environments.

6.5.2 *CEMENTS*

Marshall Valley cements show 2 major differences from associated evaporites, i) they are enriched by $\sim 10^{o}/oo$ in $\delta^{18}O$, and ii) they generally have lower Ca concentrations. Their mineralogy is predominantly aragonite, though gypsum can also occur.

In cases where sediments are lithified by aragonite, the aragonites are sometimes isotopically heavier in both C and O than the original sediments, though the reasons are not clear (Hudson, 1977). A possible explanation in the Marshall Valley is that the cement is in inorganic equilibrium with the water, but with the sediments out of equilibrium (Hudson, 1977). This implies that the cements are either formed in waters derived from different sources to those of the original precipitates, or, the waters were evaporitically enriched in ^{18}O. Therefore cementation is probably post-depositional.

Lake Fryxell cements tend towards the more stable polymorph, i.e. aragonite transforms to calcite. Marshall Valley carbonates display the reverse trend. Milliman (1974) suggests that aragonite cementation is a shallow water phenomenon, in waters of approximately equivalent salinity to seawater (Blatt *et al.*, 1972), thus implying cementation in the Marshall Valley to be at least a shallow water phenomenon.

The Marshall Valley cements appear to have formed after the original dessication of the lake. Pore waters within the sediment were either derived from the lake or subsequent meltwater flow percolating into the sediment. Cement precipitation probably occurred either close to the ground surface or at depth. Near-surface evaporation could have concentrated pore waters, enabling the precipitation of aragonite and, in some cases, gypsum. In cases where the cement is above the original evaporite bed, evaporation drew the pore waters upwards. For cements below the evaporites downward percolation of waters, as suggested for Lake Fryxell carbonates, occurred. Freezing by permafrost may also cause the precipitation of cement if the evaporite lies deeper in the sediment column. The freezing may occur both from the sediment surface downwards or the bottom upwards and result in concentration of pore waters and cement precipitation. Both the freezing or evaporation mechanisms could

give rise to the salinity required and the ^{18}O enrichment that occurs in the Marshall Valley cements.

A speculative extension of the upward evaporative movement of pore waters in near surface cementation is the possible precipitation of gypsum. Clear or nearly clear selenite crystals are known to grow displacively in subaerially exposed sediments from the evaporation of pore waters under arid conditions (Murray, 1964). Whether such a process is likely in the Marshall Valley is uncertain.

In both Lake Fryxell and Marshall Valley carbonate units cementation has been demonstrated to occur. The greater age of the Marshall Valley sediment and differing environmental conditions have led to different modes of cementation.

6.6 CONCLUSIONS

The deposits in the Marshall Valley have been briefly outlined and their origin described in terms of the Lake Fryxell model. From the discussion of the Marshall Valley sediments it is apparent that evaporite deposition and cementation of units reaches stages beyond that observed in Lake Fryxell sediments. It appears that carbonate minerals were deposited in a similar manner to unit D of Lake Fryxell. Both the Marshall Valley and Lake Fryxell carbonates show similar biological overprints in the form of $\delta^{13}C$ values. $\delta^{18}O$ and Sr contents differ however, but this is probably due to differences in the local environmental conditions. Cementation in Marshall Valley carbonates was able to continue to a greater extent probably because of the complete disappearance of the Marshall Valley lake.

From the foregoing discussion it appears that 2 conclusions can be reached:

1) The Lake Fryxell model is an adequate depositional mechanism for the Marshall Valley carbonates, and by implication can be used to

explain other Dry Valley evaporite sediments.

2) The Lake Fryxell model can be extended so that the unit D style of deposition can advance further through the evaporite depositional cycle culminating in gypsum and possibly even halite deposition.

APPENDICES

APPENDIX I

CALCULATION OF ΣCO_2 AND P_{CO_2} FROM INFRARED GAS ANALYSIS

1) Calibration of IRGA

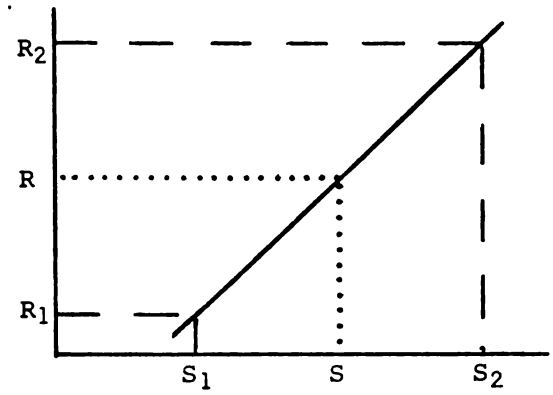

Calibration curve is linear,

where

R_1 = reading for Standard S_1

R_2 = reading for Standard S_2

R = reading for sample S

so

$$S = K R + B$$

where: B = constant

$$S_1 = KR_1 + B \qquad (1)$$

and

$$S_2 = KR_2 + B \qquad (2)$$

2) To solve for K subtrace (2) from (1)

$$S_1 - S_2 = K (R_1 - R_2)$$

$$K = \frac{S_1 - S_2}{R_1 - R_2} = \frac{S_2 - S_1}{R_2 - R_1}$$

solve for B

$$S_2 = \frac{(S_1 - S_2)}{(R_1 - R_2)} R_2 + B$$

$$B = S_2 - \frac{(S_1 - S_2)}{R_1 - R_2} R_2$$

$$= \frac{R_1 S_2 - R_2 S_1}{R_1 - R_2}$$

$$P_{CO_2} \text{ in IRGA} = \frac{(S_1 - S_2)}{R_1 - R_2} R + \frac{R_1 S_2 - R_2 S_1}{R_1 - R_2}$$

$$= C_s$$

From P_{CO_2} in the IRGA to P_{CO_2} in the stripping line:

where

V_B = volume of the sample bottle

C_B = concentration in the equilibration line

V_{GA} = volume of IRGA

C_{GA} = concentration in IRGA before mixing with sample

The total quantity of $CO_2 = V_B C_B + V_{GA} C_{GA}$

$$= (V_B + V_{GA}) C_s$$

$$C_B = \frac{(V_B + V_{GA}) \cdot \left[\frac{(S_1 - S_2)}{R_1 - R_2} R + R_1 S_2 - R_2 S_1\right] - V_{GA} C_{GA}}{U_B}$$

= P_{CO_2} in equilibration line

= P_{CO_2} of the solution if equilibrated at the same temperature

3) ΣCO_2

$$P_{CO_2} \text{ in stripping line} = \frac{(V_B + V_{GA})\ C_s - V_{GA}\ C_{GA}}{V_B}$$

The total quantity of CO_2 in the stripping line

$$= (V_B + V_L) \quad \frac{(V_B + V_{GA})\ C_s - V_{GA}\ C_{GA}}{V_B}$$

$$= (V_L + V_B)\ C_{FG} + CO_2 \text{ from sample}$$

where

V_L = volume of the stripping line

C_{FG} = concentration of the gas mixed with the sample in the line (i.e. a standard)

and

$$CO_2 \text{ from sample} = V_S\ M_S \times 22.414$$

where

V_S = volume of solution used (litres)

M_S = number of m/mol of CO_2 = ΣCO_2

$$\Sigma CO_2 = \frac{1}{V_S \times 22.414 \times 10^6} \left[\frac{(V_B + V_L)}{V_B} \quad (V_B + V_{GA})\ C_s - V_{GA}\ C_{GA} \right.$$

$$\left. - (V_L + V_B)\ C_{FG} \right]$$

DEPTH (m)	pH Beg	pH Mid	pH End	pCO2 (ppm) Beg	pCO2 (ppm) Mid	pCO2 (ppm) End	CO2 (mMol/l) Beg	CO2 (mMol/l) Mid
4.00	8.0	7.9	7.8					
4.25	8.1	8.0						
4.50	8.1	7.9						
4.75	8.1	7.8						
5.00	8.2	7.9	7.8	2032	2380	1712	10.1	13.6
5.25	8.2	8.0						
5.50	8.1	7.9	7.8					
5.75	8.1	7.9						
6.00	8.1	7.9	7.8		3198	2284	7.5	12.0
6.25	8.2	8.0						
6.50	8.3	8.0	8.3		2494			
6.75	8.3	8.0						
7.00	8.1	8.2	8.1		3158	3488	9.9	17.6
7.25	8.2	8.0						
7.50	8.1	7.9	8.0	2711				
7.75		8.0						
8.00	8.0	7.9	7.8		6423	4503	17.3	18.3
8.25		7.8						
8.50	7.9	7.7	7.6	7604		5978		
8.75	7.9	7.6						
9.00	7.7	7.4	7.6	12498	11618	10282	24.9	28.2
9.25	7.7	7.5						
9.50	7.5	7.4	7.5		13844	11024		
9.75					13992			
10.00		7.5	7.6		14143	12063	29.6	30.2
10.50	7.8	7.7	7.5					
11.00		7.6	7.4		16395	15922	49.0	34.1
11.50	7.6	7.6	7.6	18420				
12.00		7.5	7.6		18197	18594	45.9	50.0
12.50	7.7	7.5	7.6	21074	18497			
13.00		7.5	7.6		21205	19917	89.2	57.4
13.50	7.7	7.6	7.6	25132				
14.00		7.5	7.5		20793	22348	94.9	59.8
14.50	7.5	7.4	7.5	24344				
15.00		7.5	7.5		20640	20525	95.0	58.3
15.50	7.6	7.5	7.5	30050				
16.00		7.5	7.5		24613	23563	86.0	58.9
16.50	7.7	7.4	7.4	30780				
17.00		7.5	7.5		20334	18094	107.0	99.5
17.25		7.4						
17.50	7.7	7.4	7.5		20702			
17.75		7.4	7.5					

DEPTH (m)	pO2 (uncalib.) Beg	pO2 (uncalib.) Mid	pO2 (uncalib.) End	TEMPERATURE (C) Beg	TEMPERATURE (C) Mid	TEMPERATURE (C) End	RELATIVE TURBIDITY
4.00	9.5	10.4	6.8		0.1	0.0	
4.25	8.3						
4.50	7.7	11.5	8.5	0.0	0.8	0.8	
4.75	7.5						
5.00	7.3	11.6	9.6	0.2	1.6	1.6	3.1
5.25	7.1						
5.50	6.8	11.2	8.8	1.6	2.1	2.2	
5.75	6.4						
6.00	6.1	11.8	8.6	2.2	2.6	2.7	
6.25	5.9						
6.50	5.9	13.8	9.7	2.7	3.0	3.1	3.4
6.75	6.4						
7.00	6.8	14.5	10.0	3.2	3.3	3.4	6.0
7.25	7.3						
7.50	7.6	13.9	10.0	3.4	3.4	3.6	1.5
7.75	7.7	11.5			3.4		
8.00	7.7	11.0	9.5	3.6	3.5	3.7	8.0
8.25		9.9					
8.50		6.3	5.5	3.8	3.5	3.8	11.0
8.75		2.5			3.4		
9.00		0.2	3.2	3.7	3.4	3.8	20.0
9.10	0.9						
9.20	0.7						
9.30	0.4						
9.40	0.4						
9.50	0.2		0.6	3.7	3.4	3.6	
9.60	0.2						
10.00				3.6	3.2	3.5	15.3
10.50				3.5	3.1		
11.00				3.3	3.0	3.2	28.8
11.50				3.2			
12.00				3.1	2.8	3.0	27.0
12.50				2.9			
13.00				2.9	2.6	2.7	21.6
13.50				2.8			
14.00				2.6	2.3	2.5	14.8
14.50				2.5			
15.00				2.4	2.2	2.4	4.5
15.50				2.3			
16.00				2.2	2.0	2.2	11.7
16.50				2.1			
17.00				2.1	1.9	2.1	24.7
17.50				2.0			
18.00				1.9			7.7

ELEMENTAL AND C-13 ANALYSES OF LAKE FRYXELL WATERS

DEPTH (m)	Ca (ppm)	Mg (ppm)	Sr (ppm)	Ba (ppm)	Fe (ppm)	Mn (ppm)	Zn (ppm)	K (ppm)	Na (ppm)	Cl (ppm)	C-13 ‰,PDB
4.0	22.5	5.8								61	
4.5			2.5	9.8	0.7	0.08	2.1	33	263	204	
5.0	55.0	35.0	2.8	9.8	0.6	0.03	1.1	58	313	281	-18.25
6.0	51.5	25.0	3.6	8.8	0.9	0.05	0.3	45	426	440	-18.32
7.0	47.5	57.5	7.5	12.3	0.6	0.04	0.6	99	900	1103	-11.52
8.0	49.5	72.5	8.3	14.2	0.1	0.05	1.4	108	1119	1191	-1.41
9.0	87.0	92.5	10.8	17.0	0.2	0.26	0.6	127	1500	1694	-0.05
10.0	70.5	212.5	13.2	20.2	0.2	0.15	0.9	147	1813	2160	-9.40
11.0	49.5	237.5	15.1	21.6	1.6	0.14	0.7	158	1991	2470	-10.56
12.0	47.5	262.5	15.5	22.3	0.3	0.10	1.1	163	2126	2634	-9.45
13.0	57.5	280.0	16.5	23.7	0.5	0.06	2.1	191	2478	3099	-8.40
14.0	55.0	355.0	18.3	24.3	0.3	0.04	1.4	206	2579	3332	-5.47
15.0	56.0	350.0	18.5	23.9	0.4	0.05	2.4	214	2690	3520	-6.56
16.0	56.5	350.0	18.6	23.2	0.2	0.04	1.8	208	2800	3672	-6.85
17.0	51.5	320.0	18.9	22.0	0.2	0.04	0.8	200	2861	3768	-4.56
18.0	40.5	370.0								4007	-4.96

APPENDIX III CORE LOGS

All cores except C1 were examined once returned to N.Z. C1 was examined in the field. Examination of cores took place immediately after they were opened. Colour was obtained using the Standard Soil Colour Charts. Grain size, sorting and rounding were obtained using the following visual comparators:

Rounding

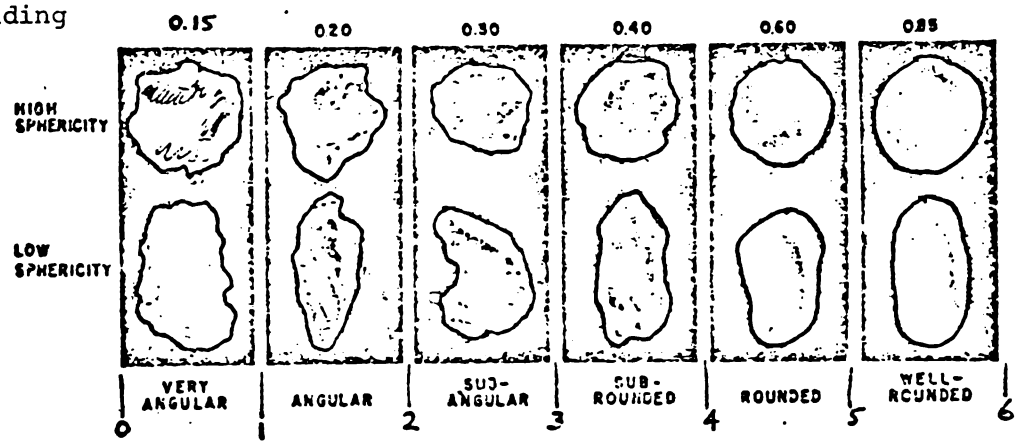

Sorting

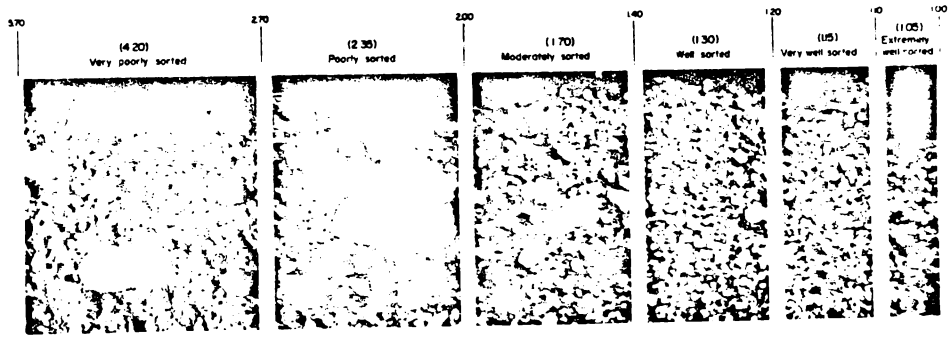

Grain Size

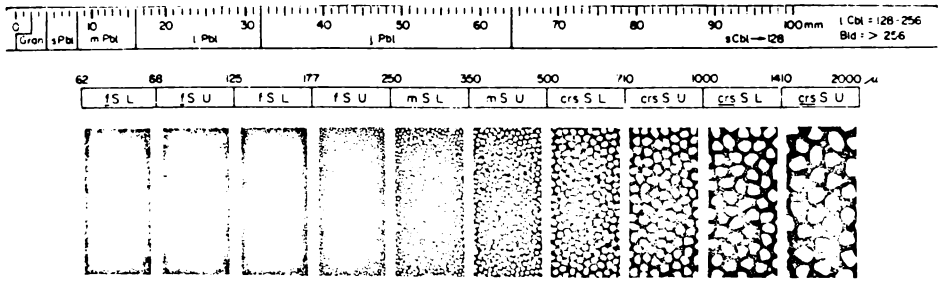

Carbonate mineralogical analyses come from XRD analysis and are also listed in Appendix IV.

LEGEND

Sharp boundary

Diffuse/gradational boundary

Disturbance of sediment


Mud/calcareous mud


Fine sand


Medium sand


Coarse sand


Pebble


Carbonate


Carbonate flakes


Organic matter

d = dark

blk = black

A,D Unit

LAKE FRYXELL STRATIGRAPHIC COLUMN C1

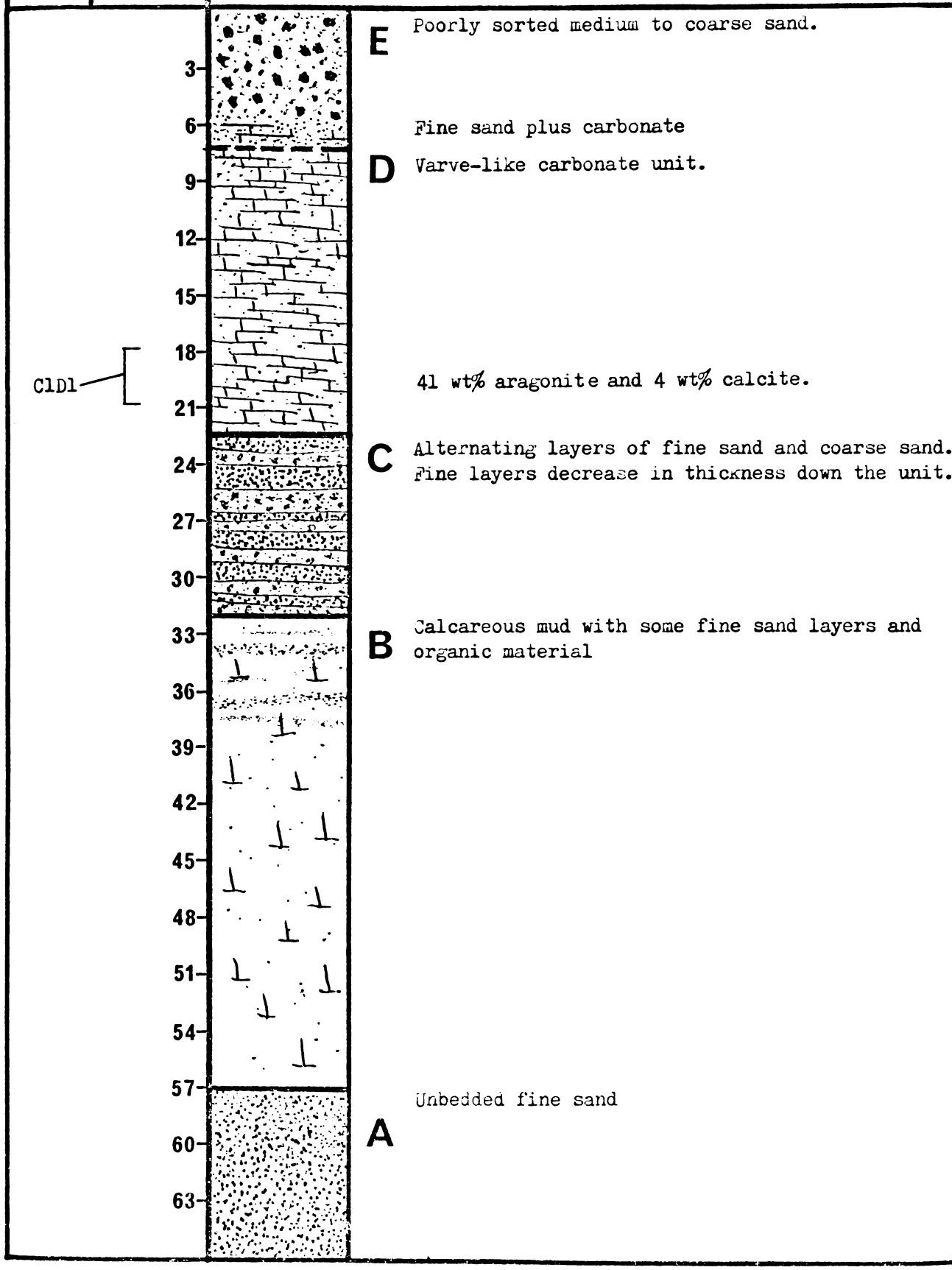

LAKE FRYXELL STRATIGRAPHIC COLUMN C1

Depth (cm) and Sample No.	Lithology
69	Poorly sorted unit cantaining muds, sands and gravels. The unit shows a crude grading from fi at the top to coarse at the bottom of the unit.
72	
75	
78	
81	
84	
87	
90	
93	
96	Quartz pebble, 20mm long by 15mm wide.
99	
102	
105	
108	
111	
114	
117	
120	
123	
126	Dolerite pebble, 46mm long by about 20mm wide
129	

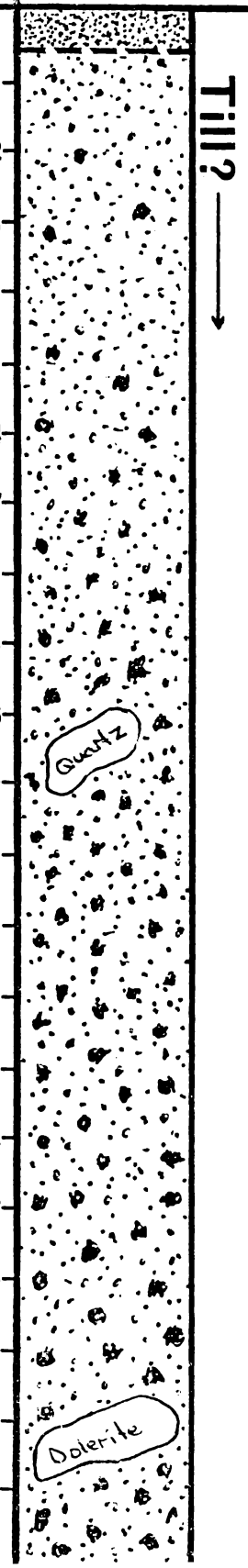

LAKE FRYXELL STRATIGRAPHIC COLUMN C1

Depth (cm) and Sample No.	Lithology
135	
138	Dolerite pebble, 32mm long by 27mm wide.
141	
144	
147	Dolerite pebble, 35mm long by 28mm wide.
150	
153	
156	
159	A? Unbedded fine sand
162	Dolerite pebble, 20mm long by 14mm wide.
165	
168	
171	
174	
177	
180	
183	

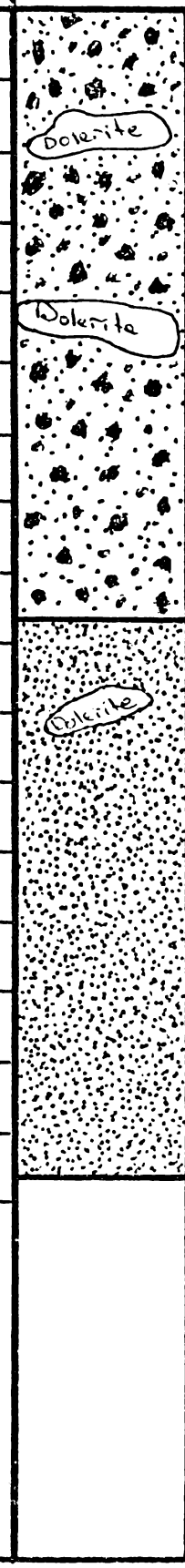

LAKE FRYXELL STRATIGRAPHIC COLUMN C4

Depth (cm) and Sample No.	Lithology
C4E1, E2 E3	E — Severely disturbed mixture of muds to coarse sand 10Y 2/1 blk, carbonate flakes 10Y 4/2 olive grey and organic material.
3	D — Laminated carbonate, disturbed by coring. Containing fine sands giving the material the colour 5GY 3/1 d. olive grey where sand is abundant.
6	Low sand content, N 7/0 greyish white.
9	
12	Sand rich layers.
15	
18 C4D1	75 wt% aragonite and 2 wt% calcite. N 7/0 greyish white.
21	
24	C — Alternating layers of fine and medium sized sand, with some mud associated with the fine sands. The layers vary from a few grains to 30mm thick. Over all colour is 7.5Y 2/1 blk to 2.5Y 3/1 d. olive grey. Mud content in unit increases with depth and contains organic material with colour 10Y 3/2.
27	
30	
33	10Y 3/2 olive blk. organic material in a calcareous mud.
36	
39	Organic material in calcareous mud.
42 C4B1	B — Fine sand layer, 7.5R 3/2 brownish blk. Organic layer 10Y 3/2 olive blk. Calcareous mud, 7.5GY 4/1 d. greenish grey, 18 wt% aragonite and 5 wt% calcite. Some fine sand.
45	
48	
51	
54	
57 C4B2	34 wt% aragonite and 5 wt% calcite. Fine sand content begins to increase.
60	
63	High fine sand content; 2.5GY 2/1 blk.
C4X1	Bb — Carbonate layer, 59 wt% calcite, 10Y 4/2 olive-

LAKE FRYXELL STRATIGRAPHIC COLUMN C4

Depth (cm) and Sample No.	Lithology
	grey. Poorly sorted mud to coarse sand material containing larger lumps of mud and organic matter. The material has a mottled appearance from the N 1.5/0 blk to 10Y 3/2 olive blk. coloured muds.
69	
72	
75	
78	
81	Flake - like and larger chunks of carbonate material in a poorly sorted mud to coarse sand matrix. Chunks are up to granule size.
84	
C4X2 — 87	Carbonate chunks are 51 wt% aragonite and 4 wt% calcite.
90	
93	
96	Carbonate flakes, possibly dragged down from top of core by the corer. 96 wt% calcite.
C4X3 — 99	Calcareous mud, 7.5GY 4/1 d. greenish grey.
102	A
105	
108	Well sorted fine sand, 2.5GY 2/1 blk.
111	
114	
117	
120	
123	
C4X4 — 126	Mud with large percentage of fine sand, no carbonate.
129	Alternating layers of fine and coarse sands, the layers being of variable thickness but no greater than a few mm.

LAKE FRYXELL STRATIGRAPHIC COLUMN C5

Depth (cm) and Sample No.	Lithology
3	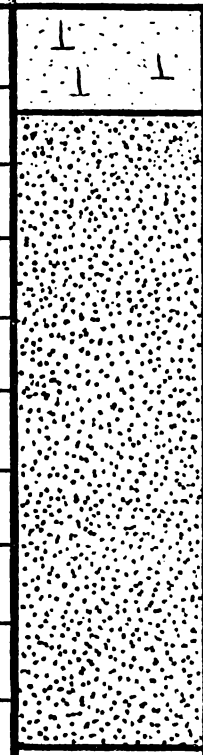
6	
9	
12	
15	
18	
21	
24	
27	
30	

E Organic rich calcareous mud with some fine sand, colour 5Y 4/2 greyish olive.

A Well sorted fine sand, N 1.5/0 blk.

LAKE FRYXELL STRATIGRAPHIC COLUMN C7

Depth (cm) and Sample No.	Lithology

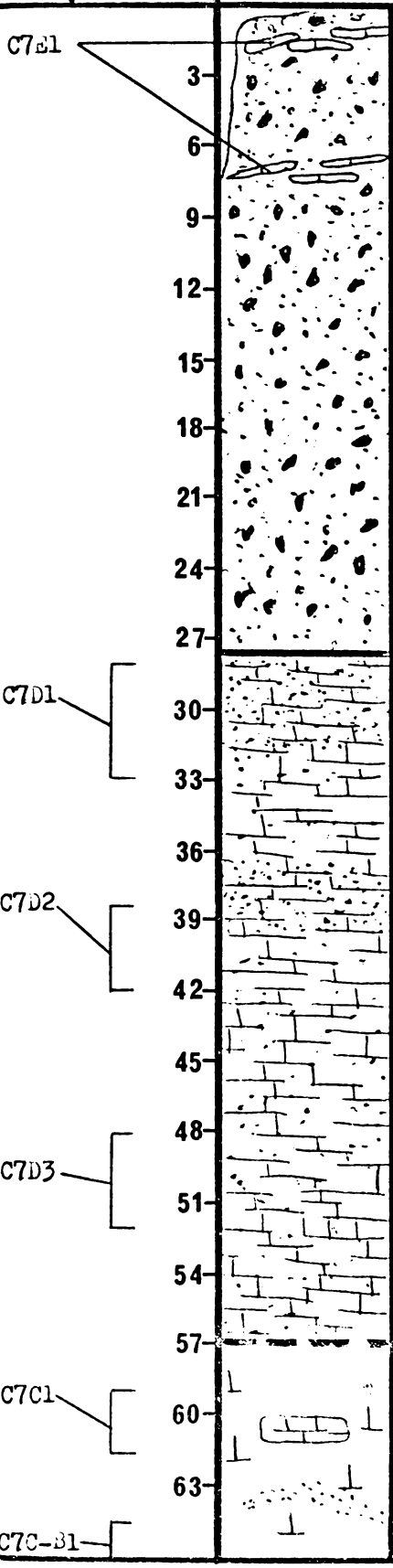

E Carbonate flakes, 68 wt% calcite, 2.5GY 4/1 d. olive grey.
Poorly sorted mud to sand size material, 7.5GY 2/1 greenish blk.
Fragmentary calcite (68 wt%) layer.

Poorly sorted mud/coarse sand, 2.5GY 3/1 d. olive grey. Large grains have rounding 0.4.

D Laminated carbonate unit (74 wt% aragonite and 1 wt% calcite.), colour 5G 3/1 d. greenish grey, includes medium to coarse sands.

62 wt% aragonite and 7 wt% calcite, muddier than upper parts of the unit, 10GY 4/1 d. greenish grey

83 wt% aragonite and 3 wt% calcite, non-carbonate content low, colour 5GY 6/1 olive grey.

10GY 4/1 d. greenish grey.

C? Calcareous mud, 2.5GY 3/1 d. olive grey with organic material, 10Y 3/2 olive blk. Contains some fine sand and a single lump of aragonite-like material. Overall 18 wt% aragonite and 4 wt% calcite.

↓ **B**

LAKE FRYXELL STRATIGRAPHIC COLUMN C7

Depth (cm) and Sample No.	Lithology
69	10Y 4/2 olive grey.
72	
75	**Bb** Poorly sorted mud to coarse sand material, 10Y 2/1 blk; the mud is calcareous and also included are chunks of carbonate resembling material from unit D. Rounding of sand is 0.3-0.4.
78	
81	**B** Calcareous mud, 10Y 4/2 olive grey, plus organic material, 10Y 3/2 oliv blk. 24 wt% aragonite and 4 wt% calcite.
C7B1 84	

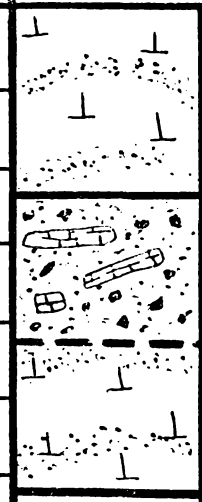

LAKE FRYXELL STRATIGRAPHIC COLUMN C9

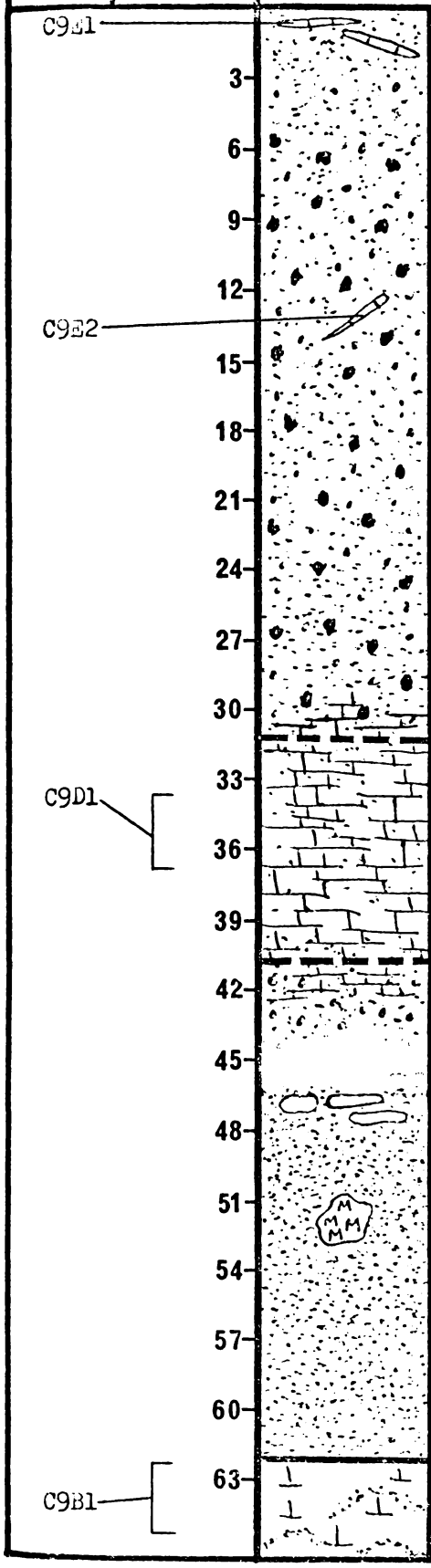

Lithology

E

Calcite flakes-66wt%. 7.5Y 6/3 olive yellow.
Poorly sorted mud to coarse sand, 7.5Y 4/3 d. olive.
Organic material present.

2.5GY 3/1 d. olive grey.

Calcite flakes - 87wt% calcite.

?

D

Laminated aragonite unit, upper portions severely disturbed and muddy. 10GY 4/1 d. greenish grey.

34 wt% aragonite.

C

Moderately sorted medium to coarse sand, colour 7.5GY 5/1 d. greenish grey, with some aragonitic material in upper portions.
Organic material, 10Y 5/2 olive blk.
Lumps of calcareous mud surrounded by fine to medium sand.

Moderate to well sorted fine to medium sand, rounding 0.3-0.4, with the occasional pebble.
Overall colour 2.5GY 2/1 blk.

B

Calcareous mud, 10Y 4/2 olive grey, with fine sand layers. 11 wt% aragonite and 5 wt% calcite

LAKE FRYXELL STRATIGRAPHIC COLUMN C9

Depth (cm) and Sample No.	Lithology
69	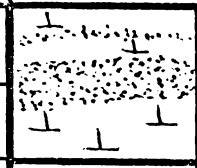
72	

LAKE FRYXELL STRATIGRAPHIC COLUMN C10

Depth (cm) and Sample No.	Lithology
3	E Upper portions of the core have been severely disturbed by coring. Mixture of muds and fine sands, 7.5YR 4/2 greyish olive. Carbonate flakes throughout upper 6cm.
6	Medium to coarse sands evident, poorly sorted, 7.5GY 3/1 d. greenish grey.
9	
12	Faint laminations evident.
15	
18	Alternating mud/organic layers with fine to medium sands. Thickness of layers is variable
21	Large mud layer, 5GY 4/1 olive grey. Organic layer,
24	D Laminated carbonate containing medium to coarse sands; similar to the above unit. 10GY 3/1 d. greenish grey.
27	Decreased sand content 7.5GY 6/1 grey.
30	High fine sand content in carbonate.
33	C? Fine sand, N 1.5/0 blk.
36	Mud layer, 5GY 4/1 d. olive grey.
39	Fine sand , N 1.5/0 blk.
42	
45	
48	

LAKE FRYXELL STRATIGRAPHIC COLUMN C11

Depth (cm) and Sample No.	Lithology
	E Moderately sorted medium grained sands. Grains rounded 0.3-0.4. Evidence of organic material. Colour 5GY 2/1 greenish black.
3	
6	
9	
C11E1 — 12	Carbonate layer, muddy, 14% wt aragonite and 6% wt calcite, varved. Colour 10Y 3/2 olive blk. Jet black sulphide ? between layers.
15	Alternating mud layers and medium to coarse sand. Muds 10Y 3/2 olive blk-some N 1.5/0 black. Some traces of carbonate. Sand layers are poorly sorted, grain rounding 0.3-0.4.
18	
21	
24	
C11E2 — 27	Muddy carbonate layer 10Y 3/2 olive blk colour, 3 mm thick. 7% wt calcite, no aragonite.
30	
33	
36	
C11D1 — 39	**D** Aragonite unit with organic layer at upper boundary. 36% wt aragonite and 3% wt calcite. Colour 7.5GY 4/1 d.greenish grey. Laminations evident. High fine sand content in upper portions
42	
45	
C11D2 — 48	98% wt aragonite Lower fine sand content, Colour N 7/0 greyish white
51	
C11C1 — 54	**C** Poorly sorted carbonate containing, very coarse sand. Grain rounding 0.2-0.4. Colour 5GY 3/1 d.olive grey.
57	**B** Calcareous mud 10GY 4/1 d.greenish grey with organic matter 10Y 3/2 olive blk.
60	Irregularly spaced fine sand layers
63	
C11B1	13% wt aragonite and 7% wt calcite

LAKE FRYXELL STRATIGRAPHIC COLUMN C11

Depth (cm) and Sample No.	Lithology
69 72 75 78 81	**A** Well sorted fine sand unit with faint evidence of layering. Very minimal carbonate.

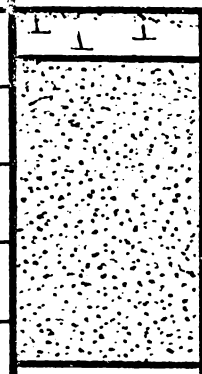

LAKE FRYXELL STRATIGRAPHIC COLUMN C13

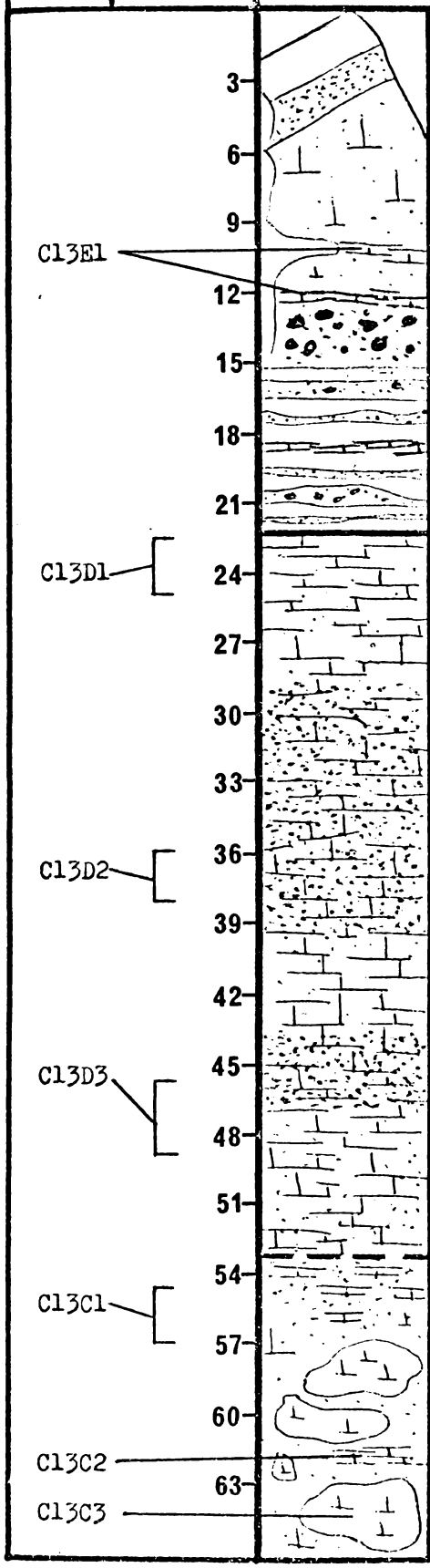

Lithology

E Fine sand, 2.5GY 2/1 blk., and mud 7.5Y 4/3 d.olive
Moderately sorted fine sand, 2.5GY 2/1 blk.

Calcareous mud with some fine sand.

65 wt% calcite 7.5Y 5/2 greyish olive.
Mud
Carbonate, 7.5Y 5/2 greyish olive.
Coarse sand, moderately sorted, rounding 0.3–0.4.
Alternating layers of coarse sand only a few grains thick, with mud/organic layers.
Thin carbonate layer

Organic layer.

D 25 wt% aragonite and 4 wt% calcite, 10Y 7/1 light grey, with some fine sand.

Increased fine sand content, 10GY 4/1 d.greenish grey.

36 wt% aragonite and 5 wt% calcite.

Lower fine sand content, 10Y 7/1 light grey.

Increased fine sand content, 10GY 4/1 d. greenish grey. 80 wt% aragonite and 3 wt% calcite.

Sand content diminished, 10Y 7/1 light grey.

C Calcareous mud with some aragonite from the above unit, and some fine sand. 29 wt% aragonite and 4 wt% calcite.

Carbonate chunk, 62 wt% aragonite and 5 wt% calcite.
22 wt% aragonite and 6 wt% calcite.

LAKE FRYXELL STRATIGRAPHIC COLUMN C13

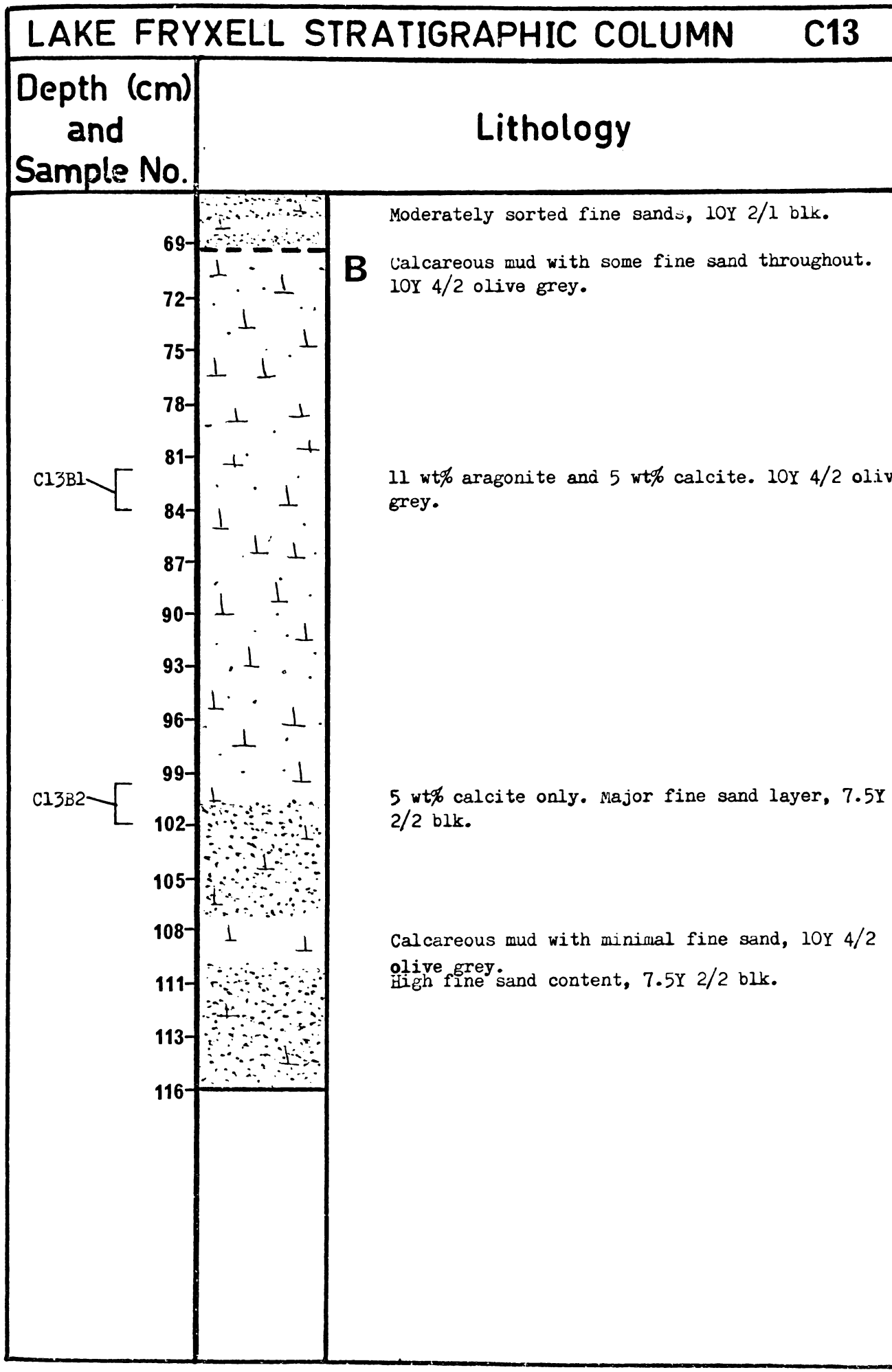

LAKE FRYXELL STRATIGRAPHIC COLUMN C14

Depth (cm) and Sample No.	Lithology
C14E1	E Carbonate flakes near top of unit, primarilly calcite, colour 5Y 5/3 greyish olive.
3	Alternating medium to coarse sand layers, 1-2cm thick, 7.5GY 3/1 d. greenish grey, and muddy to sand layers, 10Y 4/2 olive grey. Dark olive (10Y 3/2) coloured organic material associated with fine grained layers.
6	
9	
12	
15	
18	Number of fine layers increases and thickness of coarse grained layers decreases.
21	
24	
27	
30	
C14D1	D Varve-like carbonate unit, 50 wt% aragonite and 8 wt% calcite, 5BG 4/1 d. bluish grey. Non-carbonate fraction consists of medium to fine sand.
33	
36	
39	
42	Sand concentration increases. 100 wt% aragonite
C14D2	
45	C Medium sand, well sorted, with carbonate material from the above unit. Colour is 10BG 3/1 d. bluish grey.
48	
51	Coarse sand, moderately well sorted, grains rounded 0.3 - 0.4.
54	
57	Medium sand as a top of unit but with minimal carbonate.
60	
C14B1	B Calcareous mud with some fine sand, colour 2.5 GY 3/1 d. olive grey, 4 wt% calcite.
63	

LAKE FRYXELL STRATIGRAPHIC COLUMN C14

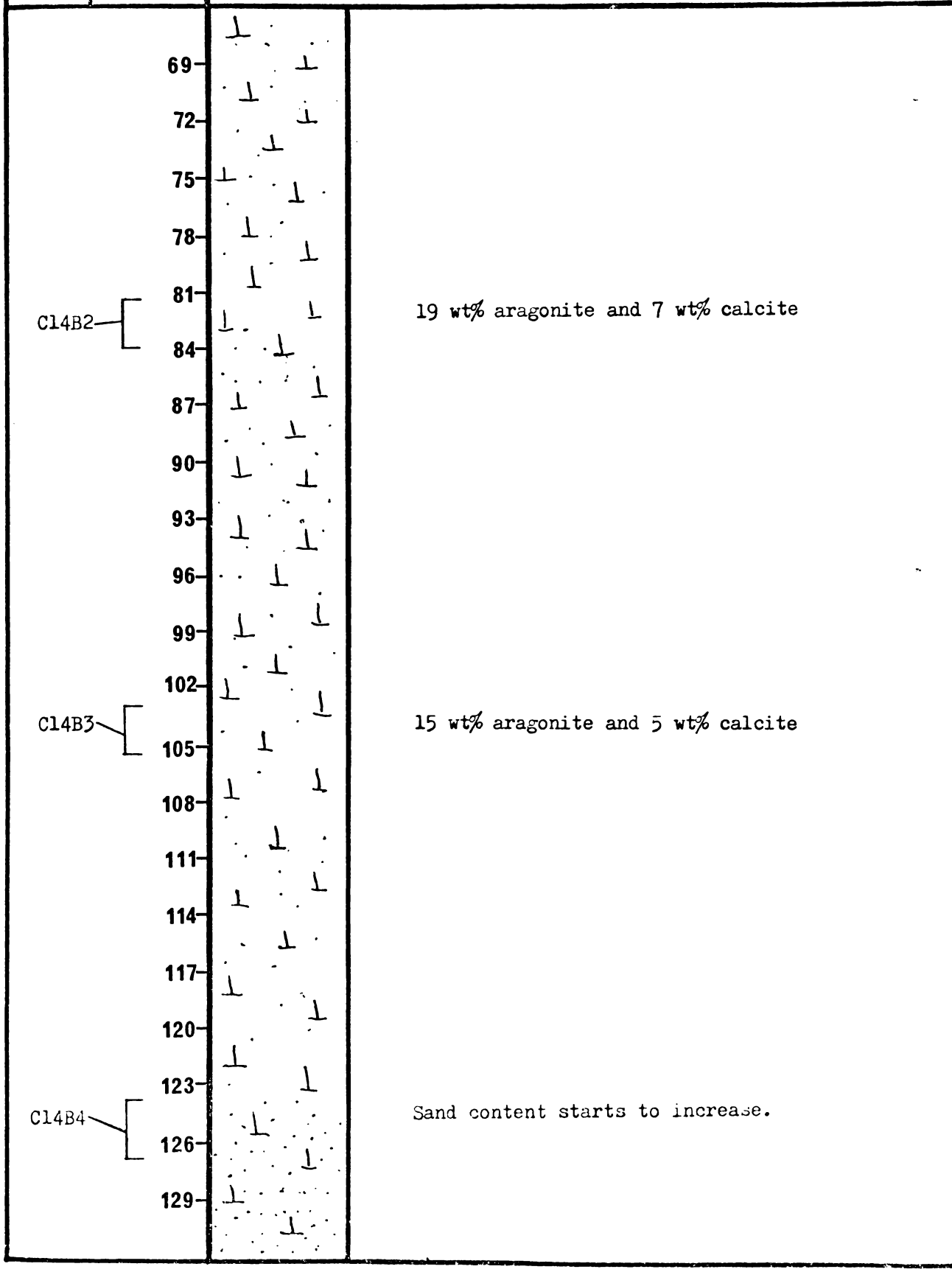

LAKE FRYXELL STRATIGRAPHIC COLUMN C14

Depth (cm) and Sample No.	Lithology
135	
138	
141	
144	
C14B5	12 wt% aragonite and 6 wt% calcite
147	
150	A Well sorted fine sand, colour 7.5Y 2/1 blk. No laminations evident.
153	
156	
159	
162	
165	
168	
171	
174	
177	
180	
183	
186	
189	

LAKE FRYXELL STRATIGRAPHIC COLUMN C17

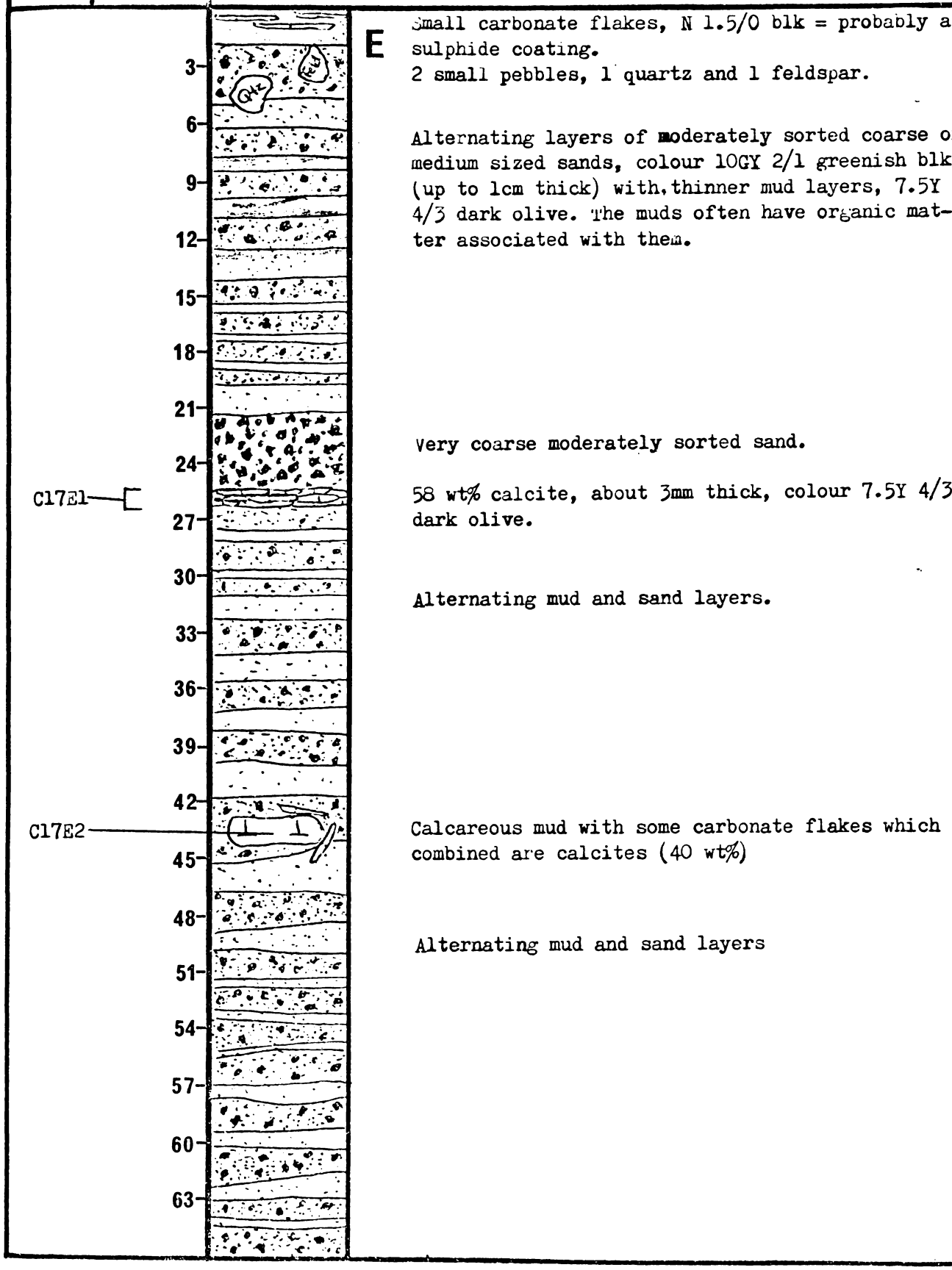

LAKE FRYXELL STRATIGRAPHIC COLUMN C17

Depth (cm) and Sample No.	Lithology
69	
72	
75	
78	
C17D1 81	D 86 wt% aragonite and 7 wt% calcite, colour 7.5GY 5/1 greenish grey. From 83cm the detrital content is greatest giving the carbonate a dark greenish grey colour(7.5GY 4/1). The detritals are fine sands.
84	
87	
C17D2 90	83 wt% aragonite and 6 wt% calcite.
93	
96	
99	
102	
C17D3 105	54 wt% aragonite and 5 wt% calcite
108	In the bottom 2cm of the unit the detrital sands are coarser than above.
C17C1 111	C Mud/organic layer, colour 10Y 3/2 olive blk. Fine sand
114	Calcareous mud, 3 wt% calcite Medium sand, well sorted. Mud with organic material
117	Fine sand
C17B1 120	B Calcareous mud with some fine sand throughout.
123	17 wt% aragonite and 3 wt% calcite. 10GY 4/1 d. greenish grey.
126	
129	A Moderately sorted coarse,with some fine sand. Grain rounding 0.2-0.3, colour 10GY 4/1 d. greenish grey.

LAKE FRYXELL STRATIGRAPHIC COLUMN C18

Depth (cm) and Sample No.	Lithology

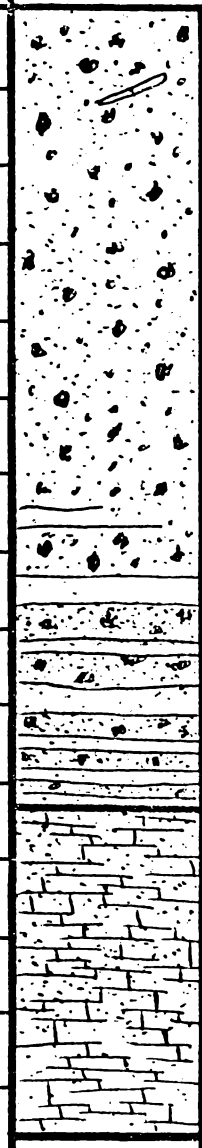

C18E1 = varcarbonate flakes from throughout unit.

C18D1

E Severely disturbed mixture of muds to coarse sands ranging in colour from 7.5GY 3/1 d. greenish grey to 10Y 4/2 olive grey. Organic rich material is 10Y 3/2 d. olive.

Some alternating sand/mud layers evident, becommore distinct towards the bottom of the unit.

D Organic layer.
Calcareous unit, 2.5GY 3/1 d. olive grey.

10GY 6/1 greenish grey

LAKE FRYXELL STRATIGRAPHIC COLUMN C19

Depth (cm) and Sample No.	Lithology
C19E1	
3	E Poorly sorted chaotic mixture of mud to sand sizes, colour 5GY 2/1 olive blk. Where organic rich the colour is olive black (10Y 3/2). Some calcite flakes evident.
6	
9	
12	
15	Alternating sand and mud layers.
C19E2 18	Fragmental calcite (42 wt%) layer
21	
24 C19D1	Organic layer. D Varve-like aragonite (42 wt% with 4 wt% calcite), muddy, 10GY 3/1 d. greenish grey
27	
30	Muddiness decreases and carbonate is harder. The detrital rich layers are more apparent.
33 C19D2	100 wt% aragonite, 7.5GY 6/1 grey.
36	
39	C Calcareous mud overlying a fine sand layer.
42 C19B1	Calcareous mud with organic matter (10Y 3/2)overlying a fine sand. B Large organic layer, 10Y 3/2 olive blk.
45	Calcareous mud, 18 wt% aragonite and 4 wt% calcite, 5G 4/1 d. greenish grey.
48	Fine sand or silt layers increasing towards the bottom of the unit.
51	
54 C19B1	4 wt% calcite, 2.5GY 2/1 blk.
57	A Poorly sorted medium to coarse sand with some very coarse sand, 5GY 2/1 olive blk.
60	Well sorted fine sand, 2.5GY olive blk., which a diorite and a sandstone pebble.
63	

LAKE FRYXELL STRATIGRAPHIC COLUMN C21

Depth (cm) and Sample No.	Lithology
C21E1	E Carbonate flakes, 50 wt% calcite, 5Y 5/4 olive overlying calcareous mud, 10Y 3/2 olive blk. Moderately sorted medium to coarse sand, rounding 0.3-0.4, colour 2.5GY 2/1 blk.
3	
6	
9	
12	Alternating medium to coarse sand layers of variable thickness with mud layers of about 2-4mm thick. Organic matter frequently associated with the muds.
15	
18	
21	
24	
27	Alternations become indistinct. Material is more poorly sorted.
30	
C21D1 33	D Aragonitic unit, 36 wt% aragonite, 10GY 3/1 d. greenish grey, with varve-like laminations. Variable amounts of fine sand.
36	
39	
42	
C21D2 45	62 wt% aragonite and 8 wt% calcite. 7.5GY 5/1 greenish grey.
48	
51	
C21D3 54	66 wt% aragonite and 1 wt% calcite. 10GY 3/1 d. greenish grey.
57	
C21C1	C Chunks of aragonitic material in a medium to coarse sand matrix.
60	
63	Large lumps of mud/organic material in a matrix

LAKE FRYXELL STRATIGRAPHIC COLUMN C21

Depth (cm) and Sample No.	Lithology
C21E1	E Carbonate flakes, 30 wt% calcite, 5Y 5/4 olive overlying calcareous mud, 10Y 3/2 olive blk. Moderately sorted medium to coarse sand, rounding 0.3-0.4, colour 2.5GY 2/1 blk.
3	
6	
9	
12	Alternating medium to coarse sand layers of variable thickness with mud layers of about 2-4mm thick. Organic matter frequently associated with the muds.
15	
18	
21	
24	
27	Alternations become indistinct. Material is more poorly sorted.
30	
C21D1 33	D Aragonitic unit, 36 wt% aragonite, 10GY 3/1 d. greenish grey, with varve-like laminations. Variable amounts of fine sand.
36	
39	
42	
C21D2 45	62 wt% aragonite and 8 wt% calcite. 7.5GY 5/1 greenish grey.
48	
51	
C21D3 54	66 wt% aragonite and 1 wt% calcite. 10GY 3/1 d. greenish grey.
57	
C21C1	C Chunks of aragonitic material in a medium to coarse sand matrix.
60	
63	Large lumps of mud/organic material in a matrix

LAKE FRYXELL STRATIGRAPHIC COLUMN C21

Depth (cm) and Sample No.	Lithology
	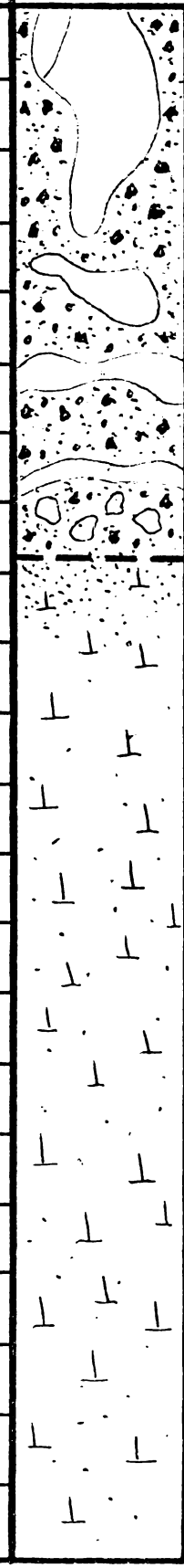
	of medium to coarse moderately sorted sand. Mud colour 10GY 4/1 d. greenish grey; where organic material present 10Y 3/2 olive blk.
69	
72	
75	
78	
C21C2 81	11.6 wt% aragonite and 6 wt% calcite. Size of mud/organic lumps decreases and some discrete layers become evident.
84	
87	
90	B Calcareous mud with fine sand.
93	
C21B1 96	19 wt% aragonite and 5 wt% calcite. Colour 10GY 4/1 d. greenish grey.
99	
102	
105	
108	
111	
114	
117	
120	
C21B2 123	15 wt% aragonite and 5 wt% calcite. 5G 4/1 d. greenish grey.
126	
129	

LAKE FRYXELL STRATIGRAPHIC COLUMN C21

Depth (cm) and Sample No.	Lithology
135	2.5GY d. olive green.
138	Organic material becomes more prevalent. Colour 10Y 3/2 oliv blk.
141	
144	
147	
150	
153	12 wt% aragonite and 4 wt% calcite.
C21B3	
156	
159	
162	

LAKE FRYXELL STRATIGRAPHIC COLUMN C22

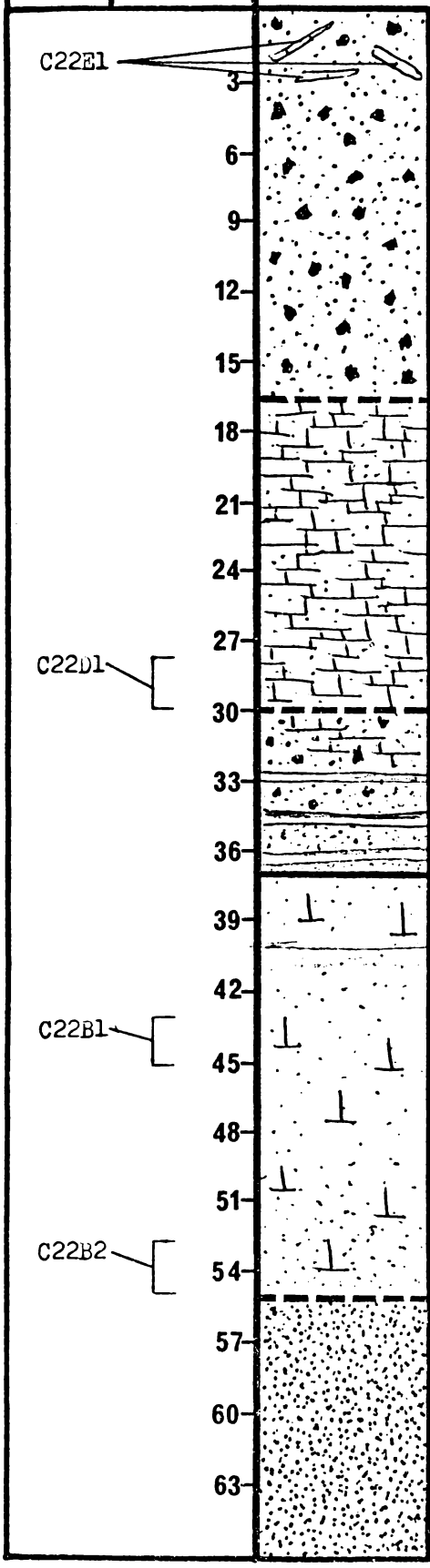

Lithology

E Calcite flakes (64 wt%), 2.5GY 4/1 d. olive grey.

Very poorly sorted medium to coarse muddy sand. No sedimentary structure probably because of dist-urbance during coring. Colour ranges from 7.5Y 5/2 greyish olive to 7.5Y 4/3 d. olive.

D Laminated muddy aragonite, colour 2.5GY 6/1 olive grey. Upper portions of the unit are mixed with the overlying unit.

Muddiness decreases and the aragonite becomes harder.

100 wt% aragonite, colour 7.5GY 4/1 d. greenish grey.

C Moderately sorted medium to coarse sand, 5Y 2/2 olive blk., alternating with mud/organic layers, 10Y 3/2 olive blk. to 5G 4/1 d. greenish grey. Thickness of the mud layers increases down the unit.

B Calcareous mud with some fine sand.

Organic rich layer, colour 10Y 3/2 oliv blk.

17 wt% aragonite and 5 wt% calcite, colour 10GY 4/1 d. greenish grey. The fine sand content starts to increase with depth.

14 wt% aragonite and 5 wt% calcite, 10GY 4/1 d. greenish grey.

A Well sorted fine sand, minimal structure, colour N 1.5/0 blk.

LAKE FRYXELL STRATIGRAPHIC COLUMN C23

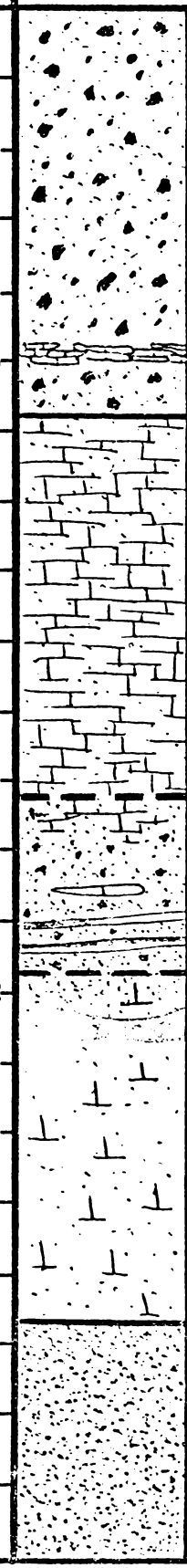

LAKE FRYXELL STRATIGRAPHIC COLUMN C23

Depth (cm) and Sample No.	Lithology
69	
72	
74	

LAKE FRYXELL STRATIGRAPHIC COLUMN C24

Depth (cm) and Sample No.	Lithology
C24E1	E Carbonate flakes, 66 wt% calcite } Disseminated
C24E2 — 3	Carbonate flakes, 68 wt% calcite
6	Severely disturbed unit consisting of a mixture of mud to coarse grain sizes plus organic matter.
9	Overall colour is 10Y 3/2 olive blk.
12	
15	
18	
C24D1	D Laminated carbonate with high fine sand content, 42 wt% aragonite and 5 wt% calcite. Colour is 10GY 4/1 d. greenish grey.
21	
24	Decreased sand content.
27	7.5GY 6/1 greenish grey
30	
C24D2	84 wt% aragonite and 3 wt% calcite
33	
36	C Moderately sorted medium to coarse sand, 5GY 2/1 olive blk., with some aragonitic material.
39	Alternating mud/organic layers, 10Y 3/2 olive blk and medium to coarse sands. Mud layers increase in number with depth in the unit, but are only a few mm thick.
42	
45	B Organic material, 10Y 3/2 olive blk.
48	Calcareous mud with included fine sand. Colour is 5G 4/1 d. greenish grey.
51	
C24B1	18 wt% aragonite and 5 wt% calcite.
54	
57	A Well sorted fine sand, rounding 0.2-0.3, 2.5Y 2/1 blk., massive.
60	
63	

LAKE FRYXELL STRATIGRAPHIC COLUMN C24

Depth (cm) and Sample No.	Lithology
69	

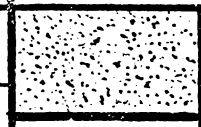

LAKE FRYXELL STRATIGRAPHIC COLUMN C25

Depth (cm) and Sample No.	Lithology
C25E1	E Calcite flakes (62 wt%), 10Y 4/2 olive grey and some are N 1.5/0 blk, possibly sulphide coating. Medium to coarse sands alternating with mud layers. Sands are moderately sorted, 7.5Y 2/1 blk. Some organic matter associated with mud layers, olive blk, (7.5Y 3/2 - 10Y 3/2).
3	
6	
9	
12	
15	
18	
21	
24	Organic layer. Varve-like carbonate with fine sand throughout.
27 C25D1	D 52 wt% aragonite and 5 wt% calcite, 5GY 5/1 olive grey.
30	
33	
36 C25D2	83 wt% aragonite and 4 wt% calcite.
39	

LAKE FRYXELL STRATIGRAPHIC COLUMN C26

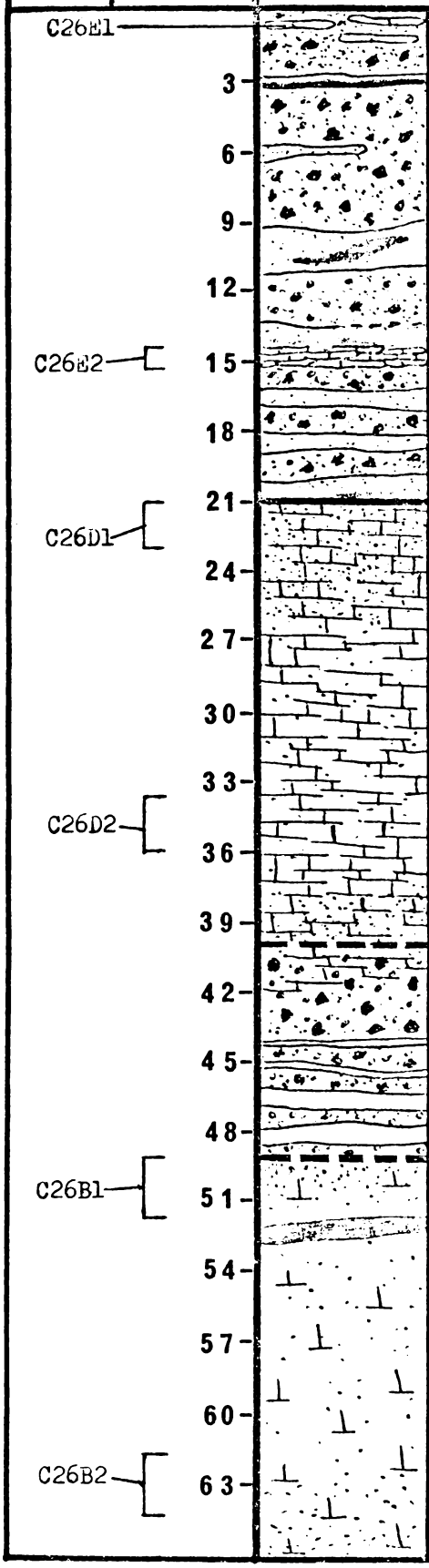

Lithology

E

Carbonate flakes 82% wt calcite. Colour 5Y 4/2 greyish olive.

Poorly defined alternations of fine sand, 10Y 3/2 olive black, and coarse sand 10Y 2/1 blk. Both moderately sorted, rounding 0.3-0.4. Organic material associated with fine sands.

5mm thick carbonate, 50% wt calcite and 19% wt aragonite. 5 distinct layers. Colour 7.5GY 5/2 greyish olive.

Alternating fine/coarse layers, as above but layering more distinct.

D

Mud/organic layer at top of unit B boundary. Laminated carbonate, 38% wt aragonite and 6% wt calcite. High fine sand content at top, decreases down profile. Colour 10GY 4/1 d.greenish grey.

Fine sand content diminished.

90% wt aragonite, no calcite. Colour 7.5GY 6/1 greenish grey.

C

Small increase in sand content owing to gradational boundary.

Moderately sorted coarse sands, rounding 0.3-0.4, alternating with thin carbonate muds. Organic material in muds gives olive blk. (10Y 3/2) colour. Mud layers thicken towards bottom of unit.

B

Calcareous mud, 10GY 4/1 d.greenish grey, 26% wt aragonite and 6% wt calcite. Organic layer 10Y 3/2 olive blk.

Fine sand content starts to increase with depth.

6% wt calcite and 15% wt aragonite.

2.5GY 3/1 d.olive grey

LAKE FRYXELL STRATIGRAPHIC COLUMN C26

Depth (cm) and Sample No.	Lithology
69	Maximum fine sand concentration.
72 – A	Well sorted fine sand, grain rounding 0.3–0.4, no bedding structure.
75	

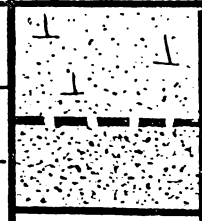

UNIVERSITY OF WAIKATO RADIOCARBON DATING LABORATORY

Dr. A.G. Hogg,
Radiocarbon Dating Laboratory,
School of Science,
University of Waikato,
Hamilton,
NEW ZEALAND.

Your sample (your reference no. C549) has had its Radiocarbon Age determined (10,410 σ = ± 120).
The details and significance are as you supplied them. Please amend if necessary and return this form to the University of Waikato Radiocarbon Dating Laboratory.

COLLECTOR	Lat. & Long. or NZMS 1 Sheet Grid Ref.	Sample No.	Locality
DR C.H. HENDY	163°32'E; 77° 37's	WK222	LAKE FRYXELL
MR M. LAWRENCE			TAYLOR VALLEY, VICTORIA LAND
			ANTARCTICA

Libby Age based on a mean life of 8033 years (used for all C-14 dates) (years before 1950)	True Age based on a mean life of 8300 years (years before 1950)
10,410 σ = ± 120	10,750 σ = ± 120

DETAILS & SIGNIFICANCE as you wish it to appear in *Radiocarbon:*

Lake Fryxell contains modern carbonate sediments similar to exposed lake beds elsewhere in Taylor Valley, which have been dated ~100,000 years by U/Th. Age required to determine sedimentation rate and when last major carbonate sedimentation occurred.

COMMENTS : The "True Age" has <u>not</u> been adjusted for any marine correction.

UNIVERSITY OF WAIKATO RADIOCARBON DATING LABORATORY

Dr. A.G. Hogg,
Radiocarbon Dating Laboratory,
School of Science,
University of Waikato,
Hamilton,
NEW ZEALAND.

Your sample (your reference no. UNIT 8) has had its Radiocarbon Age determined (21,000 σ=±300).
The details and significance are as you supplied them. Please amend if necessary and return this form to the University of Waikato Radiocarbon Dating Laboratory.

COLLECTOR	Lat. & Long. or NZMS 1 Sheet Grid Ref.	Sample No.	Locality
Mr M. Lawrence		Wk-390	Lake Fryxell, Taylor Valley, Antactica

Libby Age based on a mean life of 8033 years (used for all C-14 dates) (years before 1950)	True Age based on a mean life of 8300 years (years before 1950)
21,000 σ=±300	21,700 σ=±300

DETAILS & SIGNIFICANCE as you wish it to appear in *Radiocarbon:*

Date for Lake Fryxell carbonate mud. The date will assist in the correlation of the lake's stratigraphy with materials of similar origin in other valleys, determination of sedimentation rates, and provide a maximum age for commencement of deposition of the material.

COMMENTS :

NO reservoir correction applied to "True-Age".

LIST OF UNIVERSITY OF WAIKATO THESIS SAMPLE NUMBERS

FIELD NO.	UNIVERSITY THESIS NO.
C1	18151
C4	18152
C5	18153
C7	18154
C9	18155
C10	Held Dr C.G. Harfoot. Biol. Sci. Dept.
C11	18156
C12	18157
C13	18158
C14	18159
C17	18160
C18	18161
C19	18162
C21	18163
C22	18164
C23	18165
C24	18166
C25	18167
C26	18168

APPENDIX IV

SEDIMENT DATA

MINERALOGICAL AND STABLE ISOTOPE ANALYSES FOR LAKE FRYXELL CARBONATES

SAMPLE Nos.	ARAG wt%	CALC wt%	C-13 ‰PDB	O-18 ‰PDB	SAMPLE Nos.	ARAG wt%	CALC wt%	C-13 ‰PDB	O-18 ‰PDB
C1D1	40.5	4.2			C14B3	14.5	5.0	-1.96	-18.26
C4E1	-	81.8			C14B4			-1.81	-17.63
C4E2	-	96.5			C14B5	12.0	6.0	-1.67	-18.53
C4E3	-	88.0			C17E1	-	58.0	-0.16	
C4D1	75.0	1.5	-2.70	-29.36	C17E2	-	39.5		
C4B1	17.8	5.0	-3.81		C17D1	85.5	6.5	-1.29	
C4B2	33.7	4.5			C17D2	83.0	5.5	-1.96	
C4X1	-	58.5	0.40	-27.16	C17D3	54.0	4.5	-3.61	-30.20
C4X2	50.5	4.2	-1.88	-29.05	C17C1	-	3.0		
C4X3	-	95.8	0.30	-27.52	C17B1	17.0	2.8		
C4X4	?	?			C18E1	15.0	65.9	-0.91	-27.98
C7E1	-	67.5	0.66	-27.32	C18D1	58.8	4.5	-1.79	-28.23
C7D1	74.0	1.3	-0.12	-29.91	C19E1			0.20	-27.43
			-0.14	-29.77	C19E2				
C7D2	61.8	6.5	-0.77	-29.13	C19D1	41.5	3.5	-2.47	-29.37
C7D3	82.6	2.8	0.06	-29.71	C19D2	100	-	-3.25	-30.68
C7B4	17.5	4.0	-3.73	-26.59	C19B1	17.9	4.0		
C7B1	15.0	5.4	-3.36	-20.92	C19B2	-	4.5		
C7B2	23.5	3.9	-2.77	-19.34	C21E1	-	30.0	0.03	-29.17
C9E1	8.0	66.0	-0.72	-28.67	C21D1	36.0	8.0	-2.57	-29.31
C9E2	-	86.5	-0.02	-27.86	C21D2	62.0	4.0	-2.35	-28.87
C9D1	33.5	3.5	-0.47	-29.57	C21D3	66.4	1.2	-2.40	-29.25
C9B1	11.0	4.5	-4.01	-20.78	C21C1	50.5	3.8		
C11E1	14.4	5.5	0.55	-24.57	C21C2	11.6	5.6		
C11E2	-	6.5			C21B1	18.7	4.5	-1.62	-21.02
C11D1	36.0	3.0	-2.54	-28.69	C21B2	15.0	5.0	-2.83	-19.12
C11D2	98.5	3.0	-3.35	-29.57	C21B3	11.7	4.2	-1.97	-18.88
C11C1	45.5	11.0	-6.46	-18.88	C22E1	-	64.0	-0.84	-28.31
C11B1	13.0	6.5	-3.89		C22D1	100	-	-2.96	-29.38
C12E1	-	78.5	2.43	-27.33	C22B1	17.0	5.0		
C12E2	39.5	51.0	1.10	-27.82	C22B2	14.0	5.0		
C12E3	7.0	95.0	3.35	-26.98	C23E1	-	55.5		
C12D1	59.0	1.5	-0.13	-28.18	C23D1	41.5	5.0	-1.37	-28.18
C12D2	100	-	-1.94	-29.32	C23D2	79.5	3.0	-0.77	-28.65
C12B1	-	3.5	-2.50	-22.79	C23D3	100	-	-2.52	-29.60
C12B2	-	8.0	-2.39	-18.94	C23B1	17.9	6.0	-4.07	-21.82
C13E1	-	65.0	0.44	-28.09	C23B2	-	4.5	-3.21	
C13D1	24.5	4.0	-0.67		C24E1	-	65.5	0.01	-2.94
			-0.62	-28.29	C24E2	-	67.5		
C13D2	35.5	4.5	0.25	-28.71	C24D1	34.5	8.0	-2.25	
			0.06		C24D2	84.0	3.0	-2.64	-29.40
C13D3	79.5	3.0	-0.19	-29.75	C24B1	17.5	5.0		
C13C1	29.0	3.5			C25E1	-	61.5	-0.05	-28.09
C13C2	61.5	4.5			C25D1	51.5	5.4		
C13C3	21.2	5.5			C25D2	83.0	4.0		
C13B1	11.0	4.5	-4.18		C26E1	-	82.0	-0.89	-28.67
C13B2	-	4.5	-2.06	-17.26	C26E2	19.0	50.0	-1.59	-28.61
C14E1					C26D1	37.5	5.5	-1.24	-29.04
C14D1	50.0	7.5	-1.90	-29.00	C26D2	89.6	-	-2.46	-28.99
C14D2	100	-	-3.23	-29.45				-2.55	-29.69
C14B1	-	4.0	-4.06	-21.59	C26B1	26.1	5.8	-1.27	-29.56
C14B2	19.0	6.5	-3.90	-22.07	C26B2	14.5	5.6	-3.63	-20.68

ELEMENTAL AND STABLE ISOTOPE ANALYSES FOR LAKE FRYXELL CARBONATES

Sample Nos.	Ca (ppm)	Mg (ppm)	Sr (ppm)	Ba (ppm)	Fe (ppm)	Mn (ppm)	Zn (ppm)	C-13 ‰PDB	O-18 ‰PDB
C7E1	297666	26820	1404	2158	158	856	403	0.66	-29.77
C7D1	347917	9722	2033	2882	197	490	69	-0.13	-19.24
C7D2	288328	13648	2287	3844	258	704	108	-0.77	-29.13
C7D3	331489	11098	1758	2614	213	377	96	0.06	-29.71
C7D4	210986	42789	1962	6322	777	2162	281	-3.73	-26.59
C7B1	38760	42636	1467	5039	1024	2357	947	-3.36	-20.82
C7B2	36849	47078	1347	5426	1156	2204	1321	-2.77	-19.34
C9E1	348574	5441	1247	6518	1271	695	74	-0.72	-28.67
C9E2	355590	13863	3992	7290	288	1500	25	-0.02	-27.86
C9D1	335899	9544	4865	6466	1560	671	126	-0.47	-28.57
C12E1	327214	12850	1170	7113	1097	807	92	2.43	-27.33
C12E2	353707	9661	1043	6901	747	551	132	1.10	-27.82
C12E3	333387	9663	1127	6829	484	424	361	3.35	-26.98
C12D1								-0.13	-28.18
C12D2	323248	2054	1068	7173	335	237	119	-1.94	-29.32
C12B1	91603	21374	2709	3282	3322	1847	366	-2.50	-22.79
C12B2	122576	21222	1427	3659		1819	366	-2.39	-18.94
C14E1									
C14D1	289930	9735	1971	5811	2326	907	214	-1.90	-29.00
C14D2	340306	2218	1081	7020	451	263	114	-3.23	
C14B1	109277	28458	1081	3415	4630	2436	569	-4.06	-21.59
C14B2	24316	17822	2653	3762	2179	2535	149	-3.90	-22.07
C14B3	183161	29542	1768	5367	4558	2363	414	-1.96	-18.26
C14B4	138128	21251	1471	4087	3792	1819	302	-1.81	-17.63
C14B5	117850	30324	1516	6892		2398	586	-1.67	-18.53
C23E1	312124	13559	954	5923	206	725	23		
C23D1	342252	7992	2919	6637	1438	782	160	-1.37	-28.18
C23D2	350101	4039	1616	7343	673	378	51	-0.77	-28.65
C23D3	349920	2163	1082	7503	389	212	54	-2.52	-29.60
C23B1	184450	12687	2505	3416	1453	2193	117	-4.07	-21.82
C23B2	118228	23420	1792	3950	1997	2472	203	-3.21	-19.12
C26E1	349959	15307	964	6830	247	482	210	-0.89	
C26E2	381781	17116	1973	6034	463	328	638	-1.59	-20.74
C26D1	298122	12207	2582	5869	2273	958	239	-1.24	-29.04
C26D2	363199	3634	921	6801	669	239	79	-2.50	-29.69
C26B1	241508	15821	3490	4653	1982	1419	293	-1.27	-29.56
C26B2	174157	13644	1605	2407	1746	1681	197	-3.63	-20.68

GRAIN SIZE ANALYSES FOR THE NON-CARBONATE FRACTIONS OF LAKE FRYXELL SEDIMENTS

UNIT		GRAVEL > -1.0	SAND -1.0 - 1.0	SAND 1.0 - 2.0	SAND 2.0 - 4.0	MUD < 4.0
C9-E	Cum wt%	1.17	5.44	16.81	29.18	100
	wt%	1.17	4.27	11.37	12.37	70.82
C14-E	Cum wt%	0.94	13.54	39.55	64.08	100
	wt%	0.94	12.60	26.01	24.53	35.92
C13-D	Cum wt%	0.23	14.65	50.90	96.95	100
	wt%	0.23	14.42	36.24	46.06	3.05
C13-C	Cum wt%		1.01	3.50	24.05	100
	wt%		1.01	2.39	20.55	75.95
C14-C	Cum wt%	1.01	9.16	31.00	53.88	100
	wt%	1.01	8.15	22.85	22.88	46.12
C13-B	Cum wt%		0.05	0.18	2.98	100
	wt%		0.05	0.13	2.85	97.42
C21-B	Cum wt%		0.01	0.03	0.13	100
	wt%		0.01	0.02	0.10	99.87
C14-A	Cum wt%	1.77	17.39	44.98	63.80	100
	wt%	1.77	15.62	27.59	18.82	36.20
C23-A	Cum wt%		0.03	0.61	60.59	100
	wt%		0.03	0.58	59.98	39.41
Ice cores	Cum wt%		0.97	6.10	71.80	100
	wt%		0.97	5.19	65.70	28.20

APPENDIX V

MINERALOGICAL,ELEMENTAL AND STABLE ISOTOPE ANALYSES OF MARSHALL VALLEY SAMPLES

UNIT	SAMPLE Nos.	MINERALOGY (wt%) aragonite	calcite	Ca (ppm)	Mg (ppm)	Sr (ppm)	C-13 (‰,PDB)	O-18 (‰,PDB)
1A	23	A		124960	11996	3299	2.80	-32.0
	24	A		16820	10688	4195		
2A	1		C	335638	8015	3106	-0.80	-40.1
	2		C	325163	8404	2401	-1.20	-39.9
	8	24	65	372016	6820	3927	0.17	-39.1
	9	39	52	324510	6690	6390	-0.70	-39.0
	12	11	85	339760	10493	2448	-0.40	-38.2
2B	4	27	61	369467	5901	5546		
	7	46	34	309190	5603	9206	3.90	-33.5
	10	20	64	329194	8028	3519	-0.25	-40.2
	17	82	15	291000	4900	12880		
2C	5	57	29	324450	4592	9983		
	6	25	69	319840	5197	5897	0.03	-40.6
	11	29	74	335154	7378	5152	-0.04	-39.1
	13	82	29	329870	4498	9146		
	14	27	65	334700	8293	4096	0.26	-38.9
	16	60	30	320000	4500	7650	1.59	-32.0
2D	15	88		296060	5001	7201		
	18	98		294880	4598	6447	1.74	-40.1
	19	75		219600	10581	4991	1.50	-37.9
	20	gypsum						
3A	33	27	56	336010	9438	3353	-0.95	-40.9
	34	gypsum						
	35	gypsum						
	47		C	316110	10537	2712	-1.16	-39.0
3B	27		C	338270	9373	4109		
	28	?	?					
	29	gypsum						
	41		C	356310	7645	5406	-1.95	-40.7
	36		C	369444	2674	1188	0.06	-39.1
3C	46	A		290570	6920	1384	3.60	-29.0
	42	25	46	281650	8056	2865		
	43	gypsum						
	44	40 + gypsum		237300	1738	5147	1.10	-24.3
	37	A		298450	10526	3133	-0.55	-38.6
	38	gypsum						
	39	40 + gypsum		184490	1852	4039	1.12	-25.6
3D	30	33	54	315895	10478	3159	0.22	-40.0
	31	100		312372	1429	7962	1.53	-41.3
	40	A		295570	2880	6127	-1.62	-40.8
	45	A		385940	930	4618	1.40	-38.9

BIBLIOGRAPHY

Anderton, P.W.; Fenwick, D.K. (1976). *Dry Valleys Antarctica 1973-74.* Hydrological Research: Annual Report No. 37. Ministry of Works and Development. Wellington. 42pp.

Angino, E.E.; Turner, M.D.; Zeller, E.J. (1962a). Reconnaissance geology of Lower Taylor Valley, Victoria Land, Antarctica. *Geological Society of America Bulletin,* Vol. 73. pp.1553-1562.

Angino, E.E.; Armitage, K.B.; Tash, J.C. (1962b). Chemical stratification in Lake Fryxell, Victoria Land, Antarctica. *Science,* Vol. 138. pp.34-36.

Angino, E.E.; Armitage, K.B. (1963). A geochemical study of Lakes Bonney and Vanda, Victoria Land, Antarctica. *Journal of Geology,* Vol. 71. pp.89-95.

Angino, E.E.; Armitage, K.B.; Tash, J.C. (1964). Physiochemical limnology of Lake Bonney, Antarctica. *Limnology and Oceanography,* Vol. 9. pp.207-217.

Armstrong, R.L.; Hamilton, W.; Denton, G.H. (1968). Glaciation in the Taylor Valley, Antarctica, older than 2.7 million years. *Science,* Vol. 159(3811). pp.187-189.

Bathurst, R.G.C. (1975). *Carbonate Sediments and their Diagenesis.* 2nd Ed. Developments in Sedimentology 12. Elsevier. Amsterdam, Oxford, New York. 658pp.

Berner, R.A. (1976). The solubility of calcite and aragonite in seawater at atmospheric pressure and 34.5°/oo salinity. *American Journal of Science,* Vol. 276(6). pp.713-731.

Berner, R.A. (1980). *Early Diagenesis. A Theoretical Approach.* Princeton University Press. Princeton, N.J. 241pp.

Berner, R.A.; Morse, J.W. (1974). Dissolution kinetics of calcium carbonate in seawater: IV. Theory of calcite dissolution. *American Journal of Science,* Vol. 274. pp.108-134.

Berner, R.A.; Wilde, P. (1972). Dissolution kinetics of calcium carbonate in seawater: I. Saturation state parameters for kinetic calculations. *American Journal of Science*, Vol. 272(9). pp.826-839.

Bischoff, J.L.; Fyfe, W.S. (1968). Catalysis, inhibition, and the calcite-aragonite problem: I. The aragonite-calcite transformation. *American Journal of Science*, Vol. 266(2). pp.65-79.

Blatt, H.; Middleton, G.; Murray, R. (1972). *Origin of Sedimentary Rocks*. Prentice-Hall. New Jersey. 634pp.

Boswell, C.R.; Brooks, R.R.; Wilson, A.T. (1967a). Trace element content of Antarctic lakes. *Nature*, Vol. 213. pp.167-168.

Boswell, C.R.; Brooks, R.R.; Wilson, A.T. (1967b). Some trace elements in lakes of McMurdo Oasis, Antarctica. *Geochimica et Cosmochimica Acta*, Vol. 31. pp.731-736.

Brand, U.; Veizer, J. (1980). Chemical diagenesis of a multi-component carbonate system - 1: Trace elements. *Journal of Sedimentary Petrology*, Vol. 50(4). pp.1219-1236.

Broecker, W.S. (1974). *Chemical Oceanography*. Harcourt Brace, New York. 214pp.

Broecker, W.S.; Oversby, V.M. (1971). *Chemical Equilibria in the Earth*. McGraw-Hill, New York. 318pp.

Brownlow, A.H. (1979). *Geochemistry*. Prentice-Hall, Englewood Cliffs. New Jersey. 498pp.

Burns, D.A. (1980). *Aspects of the Carbon and Oxygen Stable Isotope Geochemistry of some New Zealand Cenozoic Calcareous Sediments*. M.Sc. thesis, University of Waikato.

Burton, H.R. (1981). Chemistry, physics and evolution of Antarctic saline lakes. A review. *Hydrobiologia*, Vol. 82. pp.339-362.

Carver, R.E. (Ed.) (1971). *Procedures in Sedimentary Petrology*. Wiley-Interscience. New York. 653pp.

Chapman-Smith, M. (1975). Geological log of DVDP 12, Lake Leon, Taylor Valley. *Dry Valley Drilling Project Bulletin No. 4.* pp.1-70.

Chapman-Smith, M.; Luckman, P.G. (1974). Late Cenozoic glacial sequence cored a New Harbour Victoria Land, Antarctica: (DVDP 8 and 9). *Dry Valley Drilling Project Bulletin No. 4.* pp.120-148.

Chave, K.E. (1952). A solid solution between calcite and dolomite. *Journal of Geology,* Vol. 60(2). pp.190-192.

Chave, K.E. (1954a). Aspects of the biogeochemistry of magnesium 1. Calcareous marine organisms. *Journal of Geology,* Vol. 62. pp.266-283.

Chave, K.E. (1954b). Aspects of the biogeochemistry of magnesium 2. Calcareous sediments and rocks. *Journal of Geology,* Vol. 62. pp.587-599.

Chilingar, G.V.; Bissell, H.J.; Wolf, K.N. (1979). Diagenesis of carbonate sediments and epigenesis (or catagenesis) of limestones. pp.247-422 *In* Larsen, G.; Chilingar, G.V.; (Eds.). *Diagenesis in Sediments and Sedimentary Rocks.* Developments in Sedimentology 25A. Elsevier. Amsterdam-Oxford-New York.

Claridge, G.G.C. (1965). The clay mineralogy and chemistry of some soils from the Ross Dependency, Antarctica. *New Zealand Journal of Geology and Geophysics,* Vol. 8(2). pp.186-220.

Claridge, G.G.C.; Campbell, I.B. (1977). The salts in Antarctic soils, their distribution and relationship to soil processes. *Soil Science,* Vol. 123(6). pp.377-384.

Cole, G.A. (1979). *Textbook of Limnology.* 2nd Ed. Mosby, St Louis. 426pp.

Collinson, J.D. (1978). Lakes. pp.61-79 *In* Reading, H.G.; (Ed.) *Sedimentary Environments and Facies.* Blackwell Scientific Publications.

Craig, H. (1957). Isotopic standards for carbon and oxygen and correction factors for mass-spectrometric analysis of carbon dioxide. *Geochimica et Cosmochimica Acta*, Vol. 12. pp.133-149.

Dansgaard, W. (1964). Stable isotopes in precipitation. *Tellus*, Vol. 16(4). pp.436-468.

Denton, G.H.; Armstrong, R.L.; Stuiver, M. (1970). Late Cenozoic glaciation in Antarctica: The record in the McMurdo Sound Region. *Antarctic Journal of the United States*, Vol. 5. pp.15-21.

Denton, G.H.; Armstrong, R.L.; Stuiver, M. (1971). The late Cenozoic glacial history of Antarctica. pp.267-306. *In* Turekian K.K.; (Ed.). *The Late Cenoizoic Glacial Ages*. Yale University Press, New Haven, Conneticut.

Edmond, J.M.; Gieskes, J.M.T.M. (1970). On the calculation of the degree of saturation of sea water with respect to calcium carbonate under *in situ* conditions. *Geochimica et Cosmochimica Acta*, Vol. 34. pp.1261-1291.

Eugster, H.P.; Hardie, L.A. (1978). Saline lakes. pp.237-293. *In* Lerman, A. (Ed.). *Lakes: Chemistry, Geology, Physics*. Springer-Verlag. New York. Heidelberg. Berlin.

Field, A.B. (1975). *The Geochemistry of Soluble Salts in the Wright and Taylor Valleys, South Victoria Land, Antarctica*. M.Sc. thesis, University of Waikato. 71pp.

Folk, R.L. (1968). *Petrology of Sedimentary Rocks*. Hamphill's. Austin. Texas. 170pp.

Folk, R.L. (1974). The natural history of crystalline calcium carbonate: effect of magnesium content and salinity. *Journal of Sedimentary Petrology*, Vol. 44(1). pp.40-53.

Frost, A.A.; Pearson, R.G. (1961). *Kinetics and Mechanism*. 2nd Ed. Wiley and Sons. New York. London. Sydney. 405pp.

Galehouse, J.S. (1971). Sedimentation analysis. pp.69-94. *In* Carver, R.E.; (Ed.). *Procedures in Sedimentary Petrology.* Wiley-Interscience. New York. London. Sydney. Toronto.

Garrels, R.M.; Christ, C. (1965). *Solutions, Minerals and Equilibrium.* Harper and Rowe. New York. 450pp.

Gat, J.R. (1981). Isotope hydrology of very saline lakes. pp.1-7. *In* Nissenbaum, A.; (Ed.). *Hypersaline Brines and Evaporitic Environmental* Developments in Sedimentology 28. Elsevier. Amsterdam-Oxford-New York.

Griffin, G.M. (1971). Interpretation of X-Ray diffraction data. pp. 541-569. *In* Carver, R.E.; (Ed.). *Procedures in Sedimentary Petrology.* Wiley-Interscience. New York. London. Sydney. Toronton.

Grinsted, M.J. (1977). *A Study of the Relationships between Climate and Stable Isotopes in Tree Rings.* D.Phil. thesis. University of Waikato. 237pp.

Gumbley, J.W. (1975). *A Sedimentological Study of Three Saline Lakes in the Dry Valleys of Victoria Land, Antarctica.* M.Sc. thesis, University of Waikato. 140pp.

Hardie, L.A.; Eugster, H.P. (1970). The evolution of closed basin brines. *Mineralogical Society of America Special Paper No. 3.* pp.273-290.

Hardie, L.A.; Smoot, J.P.; Eugster, H.P. (1978). Saline lakes and their deposits: a sedimentological approach. pp.7-41. *In* Matter, A.; Tucker, M.E., (Eds.). *Modern and Ancient Lake Sediments.* Special Publication Number 2 of the International Association of Sedimentologists. Blackwell Scientific Publications. Oxford. London. Edinburgh. Melbourne.

Haskell, T.R.; Kennett, J.P.; Prebble, W.M.; Smith, G.; Willis, I.A.G. (1965). The geology of the middle and lower Taylor Valley of South Victoria Land, Antarctica. *Transactions of the Royal Society of New Zealand.Geology*, Vol. 2(12). pp.169-186.

Henderson, R.A.; Prebble, W.M.; Hoare, R.A.; Popplewell, K.B.; House, D.A.; Wilson, A.T. (1966). An ablation rate for Lake Fryxell, Victoria Land, Antarctica. *Journal of Glaciology*, Vol. 6(43). pp.129-133.

Hendy, C.H. (in prep.). Lakes of the Antarctic Dry Valleys.

Hendy. C.H.; Wilson, A.T.; Popplewell, K.B.; House, D.A. (1977). Dating of geochemical events in Lake Bonney, Antarctica, and their relation to glacial and climatic changes. *New Zealand Journal of Geology and Geophysics*, Vol. 20(6). pp.1103-1122.

Hendy, C.H.; Healy, T.R.; Rayner, E.M.; Shaw, J.; Wilson, A.T. (1979). Late Pleistocene glacial chronology of the Taylor Valley, Antarctica, and the global climate. *Quaternary Research*, Vol. 11. pp.172-184.

Hoare, R.A.; Popplewell, K.B.; House, D.A.; Henderson, R.A.; Prebble, W.M.; Wilson, A.T. (1965). Solar heating of Lake Fryxell, a permanently ice covered Antarctic lake. *Journal of Geophysical Research*, Vol. 70(6). pp.1555-1558.

Hoefs, J. (1973). *Stable Isotope Geochemistry*. Springer-Verlag, Berlin. 140pp.

Holser, W.T. (1979). Mineralogy of evaporites. pp.211-294. *In* Burns, R.G.; (Ed.). *Marine Minerals: Reviews in Mineralogy*, Vol. 6. Mineralogical Society of America.

House, D.A.; Hoare, R.A.; Popplewell, K.B.; Henderson, R.A.; Prebble, W.M.; Wilson, A.T. (1966). Chemistry in the Antarctic. *Journal of Chemical Education*, Vol. 43(9). pp.502-505.

Hudson, J.D. (1977). Stable isotopes and limestone lithification. *Journal of the Geological Society of London*, Vol. 4. pp.637-660.

Hume, T.M. (1978). *Clay Petrology of Mesozoic to Recent Sediments of Central Western North Island, New Zealand.* D. Phil. thesis. University of Waikato.

Ichikuni, M. (1973). Partition of strontium between calcite and solution: effect of substitution of manganese. *Chemical Geology,* Vol. 11(4). pp.315-319.

Ingle-Smith, D.; Mead, D.G. (1962). The solution of limestone. *Proceedings of the University of Bristol Spelaeological Society,* Vol. 9(3). pp.188-211.

Ingram, R.L. (1971). Sieve Analysis. *In* Carver, R.E. (Ed.). *Procedures in Sedimentary Petrology.* Wiley-Interscience. New York. London. Sydney. Toronto.

Jennrich, R.; Sampson, P. (1981). Stepwise Discriminant Analysis P7M. pp.519-537. *In* Dixon, W.J.; (Chief Ed.). *BMDP Statistical Software 1981.* University of California Press. Berkeley. Los Angeles. London.

Johnsen, S.J.; Dansgaard, W.; Clausen, H.B. Langway, C.C. (1972). Oxygen isotope profiles through Antarctic and Greenland ice sheets. *Nature,* Vol. 235. pp. 429-434.

Jones, L.M.; Faure, G. (1978). A study of strontium isotopes in lakes and surficial deposits of the Ice-Free Valleys, Southern Victoria Land, Antarctica. *Chemical Geology,* Vol. 22. pp.107-120.

Kellog, D.E.; Stuiver, M.; Kellog, T.B.; Denton, G.H. (1980). Non-marine diatoms from late Wisconsin perched deltas in the Taylor Valley, Antarctica. *Paleogeography, Paleoclimatology, Paleoecology,* Vol. 30(1/2). pp.157-189.

Keys, J.R.; Williams, K. (1981). Origin of crystalline, cold desert salts in the McMurdo region, Antarctica. *Geochimica et Cosmochimica Acta,* Vol. 45. pp.2299-2309.

Kinsman, D.J.J. (1969). Interpretation of Sr^{2+} concentrations in carbonate minerals and rocks. *Journal of Sedimentary Petrology*, Vol. 39(2). pp.486-508.

Kinsman, D.J.J. (1971). Diagenetic history of limestones determined from Sr^{2+} distribution. pp.259-263. *In* Bricker, O.P.; (Ed.). *Carbonate Cements*. The John Hopkins University Studies in Geology. No. 19. John Hopkins Press. Baltimore-London.

Koch, G.S.; Link, R.F. (1971). *Statistical Analysis of Geological Data*, Vol. II. Wiley and Sons. New York. 375pp.

Krauskopf, K.B. (1979). *Introduction to Geochemistry 2nd Ed.* McGraw-Hill. New York, N.Y. 617pp.

Larson, T.E.; Buswell, A.M. (1942). Calcium carbonate saturation index and alkalinity interpretations. *Journal of the American Water Works Association*, Vol. 34(11). pp.1667-1684.

Lerman, A. (1979). *Geochemical Processes. Water and Sediment Environments*. Wiley-Interscience. New York. Chichester. Brisbane. Toronto. 481pp.

Li, Y-H.; Takahashi, T.; Broecker, W.S. (1969). Degree of saturation of $CaCO_3$ in the oceans. *Journal of Geophysical Research*, Vol. 74(23). pp.5507-5525.

McCabe, B. (1977). *The Geochemistry of Groundwater Solutions Entering Limestone Caverns*. M.Sc. thesis. University of Waikato.

McCraw, J.D. (1962). Volcanic detritus in Taylor Valley, Victoria Land, Antarctica. *New Zealand Journal of Geology and Geophysics*, Vol. 5(5). pp.740-745.

McCraw, J.D. (1967a). Some surface features of McMurdo Sound region, Victoria Land, Antarctica. *New Zealand Journal of Geology and Geophysics*, Vol. 10(2). pp.394-417.

McCraw, J.D. (1967b). Soils of Taylor Dry Valley, Victoria Land, Antarctica, with notes on soils from other localities in Victoria Land. *New Zealand Journal of Geology and Geophysics*, Vol. 10(2). pp.498-539.

McIntire, W.L. (1963). Trace element partition coefficients - a review of theory and applications to geology. *Geochimica et Cosmochimica Acta*, Vol. 27(12). pp.1209-1264.

McKelvey, B.C. (1976). Cenozoic marine and terrestrial glacial sedimentation in Taylor Valley. *Dry Valley Drilling Project Bulletin No. 7*. pp. 101-104.

McKelvey, B.C.; Webb, P.N. (1959). Geological investigations in South Victoria Land, Antarctica. Part II. Geology of the upper Taylor Glacier region. *New Zealand Journal of Geology and Geophysics*, Vol. 2(4). pp.718-728.

Milliman, J.D. (1974). *Marine Carbonates. Recent Sedimentary Carbonates Part 1*. Springer-Verlag. Berlin. Heidelberg. New York. 375pp.

Morse, J.W.; Berner, R.A. (1979). The chemistry of calcium carbonate in the deep oceans. pp.499-535. *In* Jenne, E.A.; (Ed.). *Chemical Modeling - Speciation, Sorption, Solubility and Kinetics in Aqueous Systems*. American Chemical Society Symposium Series, No. 93.

Müller, G.; Irion, G.; Förstner, U. (1972). Formation and diagenesis of inorganic Ca-Mg carbonates in the lacustrine environment. *Naturwissenschaflen*, Vol. 59. pp. 158-164.

Murray, R.C. (1964). Origin and diagenesis of gypsum and anhydrite. *Journal of Sedimentary Petrology*, Vol. 34(3). pp.512-523.

Murrell, B. (1973). Cenozoic stratigraphy in Lower Taylor Valley, Antarctica. *New Zealand Journal of Geology and Geophysics*, Vol. 16(2). pp.225-242.

Nelson, C.S.; Cochrane, R.H.A. (1970). A rapid X-ray method, for the quantitative determination of selected minerals in fine grained and altered rocks. *Tane*, Vol. 16. pp.151-162.

Nichols, R.L. (1963). Origin of chemical stratification in Lake Vanda, South Victoria Land. *Polar Record*, Vol. 11. pp.751-752.

Owen, B.B.; Brinkley, S.R. (1941). Calculation of the effect of pressure upon ionic equilibria in pure water and in salt solutions. *Chemical Reviews*, Vol. 29. pp.461-474.

Padan, E. (1979). Impact of facultatively anaerobic photoautotrophic metabolism on the ecology of cyanobacteria (Blue-green algae.). pp.1-48. *In* Alexander, M.; (Ed.). *Advances in Microbial Ecology*, Vol. 3. Plenum Press. New York.

Parker, B.C.; Simmons, G.M. (1981). Blue-green algal mats - living stromatolites - from frigid light-limited Antarctic lakes. *Trends in Biochemical Sciences*, Vol. 6. pp.iii-iv.

Parker, B.C.; Simmons, G.M.; Love, F.G.; Wharton, R.A.; Seaburg, K.G. (1981). Modern stromatolites in Antarctic Dry Valley lakes. *BioScience*, Vol. 31(9). pp.656-661.

Pettijohn J.F. (1975). *Sedimentary Rocks. 3rd Ed.* Harper and Rowe. New York, Evanston, San Francisco, London. 628pp.

Péwé, T.L. (1960). Multiple glaciation in the McMurdo Sound region, Antarctica - a progress report. *Journal of Geology*, Vol. 68(5). pp.498-514.

Pingitore, N.E. (1978). The behaviour of Zn^{2+} and Mn^{2+} during carbonate diagenesis: theory and applications. *Journal of Sedimentary Petrology*, Vol. 48(3). pp.799-814.

Plummer, L.N.; Wigley, T.M.L. (1976). The dissolution of calcite in CO_2-saturated solutions of 25°C and 1 atmosphere total pressure. *Geochimica et Cosmochimica Acta*, Vol. 40. pp.191-202.

Pytkowicz, R.M. (1963). $CaCO_3$ and the *in situ* pH. *Deep Sea Research*, Vol. 10. pp633-638.

Pytkowicz, R.M. (1965). Rates of inorganic calcium carbonate precipitation. *Journal of Geology*, Vol. 73(1). pp.196-199.

Pytkowicz, R.M. (1973). Calcium carbonate retention in supersaturated seawater. *American Journal of Science*, Vol. 273(6). pp.515-522.

Pytkowicz, R.M. (1975). Activity coefficients of bicarbonates and carbonates in seawater. *Limnology and Oceanography*, Vo. 20(6). pp.971-975.

Rawley, B.A. (1982). *Diurnal changes in the heterotrophic uptake of glycolate and glucose in two lakes*. M.Sc. thesis. University of Waikato.

Roques, H. (1969). A review of present-day problems in the physical chemistry of carbonates in solution. *Transactions of the Cave Research Group of Great Britain*, Vol. 11(3). pp.139-163.

Scott, R.F. (1905). *The Voyage of the Discovery*, Vol. 2. Smith and Elder. London. 508pp.

Seaburg, K.G.; Parker, B.C.; Wharton, R.A.; Simmons, G.M. (1981). Temperature-growth responses of algal isolates from Antarctic oases. *Journal of Phycology*, Vol. 17. pp.353-360.

Sofer, Z.; Gat, J.R. (1975). The isotopic composition of evaporating brines: effect of the isotopic activity ratio in saline solutions. *Earth and Planetary Science Letters*, Vol. 26(2). pp.179-186.

Standard Methods for the Examination of Water and Wastewater 14th Ed. (1975). American Public Health Association (APHA). New York.

Standard Soil Colour Charts (Revised). (1970). Fujihira Industry Co. Ltd., 11, Honjo 6-Chrome Bunkyo-Ku, Tokyo, Japan.

Stuiver, M.; Denton, G.H.; Hughes, T.J.; Fastook, J.L. (1981). History of the marine ice sheet in West Antarctica during the last glaciation: A working hypothesis. pp.319-436. *In* Denton, G.H.; Hughes, T.J.; (Eds.). *The Last Great Ice Sheets.* Wiley and Sons. New York. 484pp.

Stumm, W.; Morgan, J.J. (1981). *Aquatic Chemistry. An Introduction Emphasizing Chemical Equilibria in Natural Waters. 2nd Ed.* Wiley-Interscience. New York. Chichester. Brisbane. Toronto. 780pp.

Tarutani, T.; Clayton, R.N.; Mayeda, T.K. (1969). The effect of polymorphism and magnesium substitution on oxygen isotope fractionation between calcium carbonate and water. *Geochimica et Cosmochimica Acta,* Vol. 33. pp.987-996.

Taylor, T.G. (1922). The physiography of the McMurdo Sound and Granite Harbour region. *British Antarctic (Terra Nova) Expedition 1910-1913.* Harrison and Sons, London. 246pp.

Thompson, T.G.; Nelson, K.H. (1956). The concentration of brines and deposition of salts from seawater under frigid conditions. *American Journal of Science,* Vol. 254. pp.227-238.

Torii, T.; Yamagata, N.; Nakaya, S.; Murata, S.; Hashomoto, T.; Matsubaya, O.; Sakai, H. (1975). Geochemical aspects of the McMurdo saline lakes with special emphasis on the distribution of nutrient matters. pp.5-29. *In* Torii, T.; (Ed.). *Memoirs of the National Institute of Polar Research. Special Issue No. 4.*

Torii, T.; Yamagata, N. (1981). Limnological studies of saline lakes in the Dry Valleys. pp.141-159. *In* McGinnis, L.D.; (Ed.). *Dry Valley Drilling Project. Antarctic Research Series Volume 33.* American Geophysical Union. Washington.

University of Waikato Antarctic Research Unit (1975) Report No. 4.

Veizer, J.; Demovic, R. (1974). Strontium as a tool in facies analysis. *Journal of Sedimentary Petrology,* Vol. 44(1). pp.93-115.

Vincent, W.F. (1981). Production strategies in Antarctic inland waters: phytoplankton eco-physiology in a permanently ice-covered lake. *Ecology*, Vol. 2(5). pp.1215-1224.

Volfinger, M.; Robert, J-L. (1980). Structural control of the distribution of trace elements between silicates and hydrothermal solutions. *Geochimica et Cosmochimica Acta*, Vol. 44. pp.1455-1461.

Walter, M.R. (Ed.) (1976). *Stromatolites. Developments in Sedimentology 20*. Elsevier. Amsterdam-Oxford-New York. 790pp.

Webb, P.N.; Wrenn, J.H. (1976). Interpretation of foraminiferal assemblages from lower Taylor Valley (DVDP8-12). *Dry Valley Drilling Project. Bulletin No. 7*. pp.105-107.

Wharton, R.A.; Parker, B.C.; Simmons, G.M.; Seaburg, K.G.; Love, F.G. (1982). Biogenic calcite structures forming in Lake Fryxell, Antarctica. *Nature*, Vol. 295(5848). pp.403-405.

White, D.E. (1957). Magmatic, connate and metamorphic waters. *Geological Society of America Bulletin*, Vol. 68(12). pp.1659-1682.

Whitfield, M. (1975). The extension of chemical models for seawater to include trace components at 25^{o}C and 1 atm. pressure. *Geochimica et Cosmochimica Acta*, Vol. 39(11). pp.1545-1557.

Wilson, A.T. (1964). Evidence from chemical diffusion of a climatic change in the McMurdo Dry Valleys 1200 years ago. *Nature*, Vol. 201(4915). pp.176-177.

Wilson, A.T. (1965). Escape of algae from frozen ponds and lakes. *Ecology*, Vol. 46(3). p.376.

Wilson, A.T. (1967). The lakes of the McMurdo Dry Valleys. *Tuatara*, Vol. 15(3). pp.152-164.

Wilson, A.T. (1970). The McMurdo Dry Valleys. pp.21-30. *In* Holdgate, M.W.;(Ed.). *Antarctic Ecology*. Academic Press, London.

Wilson, A.T. (1981). A review of the geochemistry and lake physics of the Antarctic Dry Areas. pp.185-192. *In* McGinnis, L.D.;(Ed.). *Dry Valley Drilling Project. Antarctic Research Series Volume 33.* American Geophysical Union. Washington D.C.

Wilson, A.T.; Wellman, H.W. (1962). Lake Vanda: an Antarctic lake. *Nature,* Vol. 196(4860). pp.1171-1173.

Wilson, A.T.; Hendy, C.H.; Healy, T.R.; Gumbley, J.W.; Field, A.B.; Reynolds, C.P. (1974). Dry Valley lake sediments: a record of Cenozoic events. *Antarctic Journal of the United States,* Vol. 9(4). pp.134-135.

Wolf, K.H.; Chilingar, G.V.; Beales, F.W. (1967). Elemental composition of carbonate skeletons, minerals and sediments. pp.23-149. *In* Chilingar, G.V.; Bissell, H.J.; Fairbridge, R.W.; (Eds.). *Carbonate Rocks. Development in Sedimentology 9B.* Elsevier. Amsterdam, London, New York.

Yamagata, N.; Torii, T.; Murata, S. (1967). Report of the Japanese summer parties in Dry Valleys, Victoria Land, 1963-1965, V, Chemical composition of lake waters. *Antarctic Record,* Vol. 29. pp.53-75.

Yoshida, Y.; Torii, T,; Yusa, Y.; Nakaya, S.; Moriwaki, K. (1975). A limnological study of some lakes in the Antarctic. pp.311-320. *In* Suggate, R.P.; Cresswell, M.M.; (Eds.). *Quaternary Studies.* Royal Society of New Zealand. Wellington, New Zealand.

'ALBERT'

Though skuas they care not of this
Of holes and optimists
To this audacious bird
Philosophy and science come not within its realm
They rule the skies about this zone
Their squawk is always heard
The object of some ridicule
Is this our garrulous friend
Our food they take as theirs
From off our breakfast plate
Bacon, peas or our rice pud
Do suffer equal fate
A ballpoint pen or sample rope
They take most anything
But we suffer this most mindful
Of the humour that they bring.